UNIVERSITY OF LONDON THESIS

Degree PhD Year 2005 Name of Author HART, Paul Edward

COPYRIGHT

This is a thesis accepted for a Higher Degree of the University of London. It is an unpublished typescript and the copyright is held by the author. All persons consulting the thesis must read and abide by the Copyright Declaration below.

COPYRIGHT DECLARATION

I recognise that the copyright of the above-described thesis rests with the author and that no quotation from it or information derived from it may be published without the prior written consent of the author.

LOAN

Theses may not be lent to individuals, but the University Library may lend a copy to approved libraries within the United Kingdom, for consultation solely on the premises of those libraries. Application should be made to: The Theses Section, University of London Library, Senate House, Malet Street, London WC1E 7HU.

REPRODUCTION

University of London theses may not be reproduced without explicit written permission from the University of London Library. Enquiries should be addressed to the Theses Section of the Library. Regulations concerning reproduction vary according to the date of acceptance of the thesis and are listed below as guidelines.

A. Before 1962. Permission granted only upon the prior written consent of the author. (The University Library will provide addresses where possible).

B. 1962 - 1974. In many cases the author has agreed to permit copying upon completion of a Copyright Declaration.

C. 1975 - 1988. Most theses may be copied upon completion of a Copyright Declaration.

D. 1989 onwards. Most theses may be copied.

This thesis comes within category D.

☐ This copy has been deposited in the Library of UCL

☐ This copy has been deposited in the University of London Library, Senate House, Malet Street, London WC1E 7HU.

Human mitochondrial disease: from pathogenesis to therapeutic intervention.

by Dr Paul Edward Hart BSc(Hons) MB BS(Hons) MRCP

A thesis submitted, in fulfilment, for the degree of Doctor of Philosophy.

ADDENDUM:

Chapter 1, Section 1.3.1, page 30, line 5:

proposal of a strand asynchronous asymmetrical model (75 Clayton 1982), which...

should read :

proposal of a strand asynchronous asymmetrical model[75]*, which...*

Chapter 6, Section 6.4.2, page 200, paragraph 3, line 8:

Patients were assessedneurologically, and with MRS and echocardiography at.....

should read:

Patients were treated with 400mg/day Coenzyme Q10 and 2100 IU/day vitamin E and assessed neurologically, and with MRS and echocardiography at.....

ProQuest LLC
789 East Eisenhower Parkway
P.O. Box 1346
Ann Arbor, MI 48106-1346

HUMAN MITOCHONDRIAL DISEASE: FROM PATHOGENESIS TO THERAPEUTIC INTERVENTION.

by

Dr Paul Edward Hart BSc (Hons) MB BS (Hons) MRCP

Department of Clinical Neurosciences
Royal Free Campus
Royal Free and University College Medical School
University of London

A thesis submitted, in fulfillment, for the degree of Doctor of Philosophy

2005

Abstract

The spectrum of diseases caused by mitochondrial dysfunction is very broad and encompasses the archetypal mtDNA mutation diseases, mutations of nuclear genesencoding mitochondrial proteins (including those of the oxidative phosphorylation system), and a variety predominantly neurodegenerativediseases in which the primary cause of mitochondrial dysfunction remains undefined.

The last two decades have seen an explosion in our understanding of the archetypal mitochondrial disorders. Attention has now focused on the nuclear encoded mitochondrial disorders. Furthermore, nuclear factors may be of significance in the pathogenesis of the archetypal disorders associated with mitochondrial DNA mutations. These conditions are typified by their clinical diversity and poor phenotype-genotype correlation. One of several potential explanations for this is that nuclear genes determine the fate of mtDNA mutations, or that secondary mtDNA mutations have a modulating effect upon the expression of the primary mutation.

In this thesis I have sought to address several aspects of the biochemical and clinical features of mitochondrial diseases. In chapter 3 cell cybrids have been used to study the role of the nuclear genome on the biochemical expression of mtDNA mutations in an attempt to understand potential influences on phenotypic expression. An extension of this was the use of xenomitochondrial cybrids to analyse nuclear-mitochondrial interactions and thre function of the respiratory chain. At the biochemical/clinical interface, skeletal muscle from patients with focal dystonia has been used as a model to investigate the role that mitochondrial dysfunction might play in this movement disorder. Finally, the clinical role of therapy for mitochondrial disorders has been investigated in the context of Friedreich's ataxia (FRDA). Existing rating scales have been assessed and new ones developed to lay a firm foundation for evaluating disease-modifying therapies. These have been piloted in a long term intervention trial for FRDA.

Declaration

The author performed all of the experimental work presented in this thesis unless otherwise stated.

In chapter 3 mutation load was ananlysed by fluorescent PCR by Dr T Pulkes and Dr M Hanna, Institue of Neurology, Queen Square, London. The work detailed in chapter 6 represents the efforts of a large group of investigators as listed in that chapter. I was principally involved in the design of the trial and in the clinical evaluation of the subjects.

Acknowledgements

I am eternally grateful to my wife Jacqueline and my daughters, Amelia, Jessica, and Olivia for enduring with me this period of research and writing up. Without their support none of what follows would have been accomplished.

I am indebted to my supervisor, Prof AHV Schapira, for guidance on experimental design and direction, and to Dr JM Cooper for his guidance and advice. I should also like to thank Dr JW Taanman, Dr J Bradley, Dr S Williams, Dr S Tabrizi, Dr J Blake, Dr M Cleeter, Dr M Gu, Dr J Schott, Dr C Turner, and Dr P Koolipara. I should like to thank Dr R Morris for patient statistical advice, and Dr P Simmons for scientific advice and clarification, and Dr J Hobart for his input towards chapter 6. A549 cells were kindly provided to the department by Dr I Holt, and 206 cells by Prof. G. Attardi.

I should like to thank all patients and their families who took part in these studies, and I would like to thank all the Neurologists that referred patients with FRDA.

This period of research was funded by the Wellcome Trust. The trial in chapter 6 was supported by the Ataxia Society, the National Lottery Fund, and by Pharma Nord.

INDEX Page

	Abstract	2
	Declaration	3
	Acknowledgements	4
	Table of Contents	5
	List of Figures	11
	List of Tables	14
	Abbreviations	16

Chapter 1 Introduction

1	Introduction	18
1.1	Mitochondrial function: Biochemistry	19
1.2	The Biochemistry of Oxidative Phosphorylation	23
1.2.1	Complex I	23
1.2.2	Iron sulphur centers	23
1.2.3	Ubiquinone (Coenzyme Q)	24
1.2.4	Complex II	25
1.2.5	Complex III	25
1.2.6	Cytochromes	26
1.2.7	Complex IV	27
1.2.8	Complex V	27
1.3	Mitochondrial DNA	28
1.3.1	Mitochondrial DNA replication	30
1.3.2	Mitochondrial DNA transcription	31
1.3.3	Mitochondrial DNA translation	32
1.3.4	Transfer RNA molecules	35
1.4	Mitochondrial import	39
1.5	Cybrid technology	39

1.6	The genetics of mitochondrial respiratory chain dysfunction	41
1.7	Genetic features of mitochondrial DNA diseases	44
1.7.1	Maternal inheritance	45
1.7.2	Heteroplasmy	47
1.7.3	The threshold effect	47
1.7.4	Mitotic segregation	48
1.7.5	The bottleneck phenomenon	48
1.7.6	Secondary MtDNA mutations	49
1.7.7	Immunological and Environmental factors	50
1.8	Mitochondrial disease	50
1.8.1	The archetypal mitochondrial encephalomyopathies	50
1.8.1.1	Chronic progressive external ophthalmoplegia / Kearns Sayre syndrome	53
1.8.1.2	Mitochondrial encephalomyopathy, lactic acidosis, and stroke-like episodes	54
1.8.1.2.1	Pathogenesis of the A3243G common MELAS mutation	55
1.8.1.3	Myoclonic epilepsy and ragged-red fibres	60
1.8.1.4	Neurogenic muscle weakness, ataxia, and retinitis pigmentosa	62
1.8.1.5	Leigh syndrome	63
1.8.1.6	Mitochondrial DNA depletion syndrome	64
1.8.1.7	Myoneurogastrointestinal encephalopathy	65
1.8.2	The non-encephalomyopathic archetypal mitochondrial disorders	66
1.8.3	Biochemical classification of mitochondrial disease	66
1.9	Pathogenic mechanisms of mtDNA mutations	70
1.10	Models of mitochondrial disease	71
1.10.1	Animal models	75
1.11	Class II non-archetypal secondary OXPHOS defects	79
1.12	Reactive oxygen species and oxidative damage as a pathogenic mechanism in class I and class II mitochondrial disorders	81
1.13	The rele of mitochondrial dysfunction in neurodegeneration	
1.13.1	Friedreich's ataxia	87

1.14 Therapeutic intervention in class I and class II mitochondrial disorders 96

Chapter 2 Materials and Methods

2.1 Materials 101
2.2 Cell Culture 102
2.2.1 Cell lines 102
2.2.2 Cell growth conditions 103
2.2.3 Cell culture maintenance and harvesting 103
2.2.4 Culture conditions for the generation of ρ^0 cell lines 104
2.2.5 Cell freezing and defrosting 104
2.3 Cell fusion methods 105
2.4 Isolation of clones 106
2.5 DNA extraction 106
2.6 Estimation of DNA concentration and purity 106
2.7 Polymerase Chain Reaction (PCR) 107
2.8 Semi-quantitative PCR detection of mtDNA levels 107
2.9 Restriction enzyme digests of DNA 108
2.10 Detection of PCR DNA products 108
2.11 Determination of mutant load 108
2.12 Enzyme Analyses 109
2.12.1 Citrate Synthase 109
2.12.2 NADH-CoQ_1 oxidoreductase (complex I activity) 110
2.12.3 Succinate cytochrome c oxidoreductase (complex II/III) 110
2.12.4 Succinate-ubiquinol oxidoreductase (complex II) 111
2.12.5 Ubiquinol-cytochrome c reductase (complex III) 111
2.12.6 Cytochrome c oxidase (complex IV) 112
2.12.7 Aconitase 113
2.13 Preparation of mitochondrial-enriched fractions (MEFs) 114
2.14 Preparation of brain homogenates 114
2.15 Preparation of muscle homogenates 114

2.16 Preparation of cell homogenates (for aconitase assay) 114
2.17 Protein assay 115
2.18 Immunofluorescence staining of cultured cells 115
2.19 Microscopy and photography 115
2.20 Statistical analysis 115
2.21 Health related quality of life in Friedreich's ataxia 116
2.21.1 Patients 116
2.21.2 Genetic analysis 116
2.21.3 Health status measures 116
2.22 Friedreich's ataxia: evaluation of ICARS and factors influencing clinical progression 118
2.22.1 Patients 118
2.22.2 Genetic analysis 118
2.22.3 Clinical assessments 118
2.22.4 Statistical analysis 119

Chapter 3 Nuclear influences on the biochemical expression of the A3243G mitochondrial DNA mutation

3.1 Introduction 120
3.2 Experimental hypothesis 121
3.3 Experimental design 121
3.4 Results 122
3.5 Discussion 149

Chapter 4 Xenomitochondrial cybrids for the investigation of nuclear-mitochondrial interactions and the development of cellular models of mitochondrial disease

4.1 Experimental hypothesis 155
4.2 Experimental design 156
4.3 Results 157
4.4 Discussion 165

Chapter 5 Spectrophotometric analysis of muscle mitochondrial respiratory chain function in sporadic focal dystonia

5.1 Introduction 167
5.2 Experimental hypothesis 167
5.3 Results 167
5.4 Discussion 172

Chapter 6 Friedreich's ataxia

6.1 Introduction 175
6.2 Health-related quality of life in Friedreich's ataxia 177
6.2.1 Introduction 177
6.2.2 Experimental design 177
6.2.3 Results 178
6.2.4 Discussion 181
6.3 Friedreich's ataxia: Evaluation of the International Cooperative Ataxia Rating Scale (ICARS) and factors influencing clinical progression 183
6.3.1 Experimental design 183
6.3.2 Results 183
6.3.3 Discussion 196
6.4 Antioxidant treatment of patients with Friedreich's ataxia Three year follow up 199
6.4.1 Introduction 199
6.4.2 Experimental design 200
6.4.3 Results 201
6.4.4 Discussion 207

References 209

Appendix 1 270

Publications 292

List of figures

1.1	The five complexes of the mitochondrial respiratory chain are located in the mitochondrial inner membrane	21
1.2	The five complexes of the mitochondrial respiratory chain and their subunit structure	22
1.3	Ubiquinone / Ubiquinol reactions	25
1.4	Map of the human mitochondrial genome, showing the 13 polypeptide-coding genes, and 24 protein synthesis genes	29
1.5	The mitochondrial $tRNA^{Lue(UUR)}$ molecule, showing its nucleotide sequence, amino acid acceptor stem, dihydrouridine loop, TΨC loop, anticodon, and sites of common mutations	38
1.6	Brief phylogeny of the Muridae	74
3.1	Analysis of mtDNA content, by semiquantitative serial dilution PCR for a 630 bp mtDNA fragment and by immunoflourescence for subunit I of COX, of A549 lung ρ^+ and ρ^0 cells	126
3.2	Analysis of mtDNA content, by semiquantitative serial dilution PCR for a 630 bp mtDNA fragment and by immunoflourescence for subunit I of COX, of 206 osteosarcoma ρ^+ and ρ^0 cells	127
3.3	Analysis of mtDNA content, by semiquantitative serial dilution PCR for a 630 bp mtDNA fragment and by immunoflourescence for subunit I of COX, of Myoe (embryonal myoblasts) ρ^+ and ρ^0 cells	128
3.4	Analysis of mtDNA content, by semiquantitative serial dilution PCR for a 630 bp mtDNA fragment and by immunoflourescence for subunit I of COX, of NT2 neuronal ρ^+ and ρ^0 cells	129
3.5	Analysis of mtDNA content, by semiquantitative serial dilution PCR for a 630 bp mtDNA fragment and by immunoflourescence for subunit I of COX, of SHSY-5Y ρ^+ and ρ^0 cells.	130

3.6 Serial dilution semi-quantitative PCR of NT-2 ρ^+ and "ρ^{0}" neuronal cells using primers for the 630 bp MELAS region of mtDNA, and primers for a 1000 bp mtDNA fragment (B) 131
3.7 Relationship between number of cybrid clones with varying levels of A3243G mtDNA in different cell types. 135
3.8 Comparison of A3243G mutant load in 72 cybrids as assessed by semi-quantitative Apa I digest with that as assessed by fluorescent labelled PCR 136
3.9 Influence of A3243G mutant load upon mitochondrial respiratory chain activities in SHSY-5Y cybrids generated by fusion of platelets from all patients. 139
3.10 Influence of A3243G mutant load upon mitochondrial respiratory chain activities in A549 cybrids generated by fusion of platelets from all patients. 140
3.11 Influence of A3243G mutant load upon mitochondrial respiratory chain activities in 206 cybrids generated by fusion of platelets from all patients. 141
3.12 Influence of A3243G mutant load upon mitochondrial respiratory chain activities in IB3 cybrids generated by fusion of platelets from all patients. 142
3.13 Influence of A3243G mutant load upon mitochondrial respiratory chain activities in SHSY-5Y, A549, and 206 cybrids generated by fusion of patients with a severe MELAS phenotype. 143
3.14 Influence of A3243G mutant load upon mitochondrial respiratory chain activities in IB3 and 206 cybrids generated by fusion of patients with a mild MELAS phenotype. 144
3.15 Influence of A3243G mutant load upon aconitase activity in SHSY-5Y, A549, 206, and IB3 cybrids generated by fusion of all patients. 145

3.16	Influence of A3243G mutant load upon aconitase activity in SHSY-5Y, A549, 206 cybrids generated by fusion of patients with a severe MELAS phenotype; and IB3 and 206 cybrids generated by fusion of a patient with a mild MELAS phenotype.	146
4.1	1.2% agarose gel of STOG mouse fibroblast ρ^+ and ρ^0 cells	158
4.2	1.2% agarose gel to show results of primer pairs designed to distinguish human rat and mouse mtDNA	161
4.3	Rat or mouse mtDNA content of xenocybrids clones	163
4.4	Mitochondrial respiratory chain activities of xenocybrids clones	164
5.1	Mitochondrial respiratory chain and aconitase activities in sporadic focal dystonia and control muscle samples	169
6.1	Relationship between the size of the smaller GAA1 repeat and age of onset in 77 FRDA patients	185
6.2	Relationship between patient age at assessment and the distribution of total ICARS score and the four component scores of ICARS	187
6.3	Relationship between patient age and total ICARS scores in groups of FRDA patients with GAA1 repeat sizes in the range >900, 751-900, 600-750, and <600.	191
6.4	Retrospective analysis of disease progression in 77 FRDA patients	192
6.5	Percentage change in 31P MRS heart PCr/ATP and 31P MRS skeletal muscle Vmax in 10 FRDA patients receiving combined coenzyme Q_{10} and vitamin E therapy for 35 months	203
6.6	Percentage change in cardiac fraction shortening in 10 FRDA patients receiving combined coenzyme Q_{10} and vitamin E therapy for 35 months	204
6.7	Percentage change in A) total ICARS score, B) Posture and Gait component of ICARS, and C) Kinetic component of ICARS in 10 FRDA patients receiving combined coenzyme Q_{10} and vitamin E therapy for 35 months	205

6.8 Comparison of the progression of the total ICARS score for 10 FRDA patients treated for 35 months with combined coenzyme Q10 and vitamin E, with cross-sectional data obtained from 75 untreated FRDA patients 206

List of Tables

1.1	Inheritance of genetically determined disorders of oxidative phosphorylation	46
1.2	The classification of mitochondrial disorders	51
1.3	Clinical features of the A8344G MERRF and A3243G MELAS mutations	62
1.4	Nuclear gene defects related to mitochondrial disorders	69
1.5	Comparison of *Mus musculus* and *Ratus norvegicus* mitochondrial translation products	
1.6	Genetic causes of bioenergetic defects in neurodegeneration	80
1.7	Clinical, genetic and neurophysiological parameters in Friedreich's ataxia	89
2.1	Dimensions of four health measures Barthel, General Health Questionaire 12, EuroQol health status, and Short Form 36	117
3.1	A3243G mutation loads as determined by quantitative fluorescence PCR in patient blood and fibroblasts.	133
3.2	Number of clones isolated from fusion between patient mtDNa and various ρ^0 cell lines	134
4.1	Summary of results with primer pairs designed to distinguish rat, mouse and human mtDNA	160
5.1	Dystonia patient and control details: light and electron microscopy findings	170
6.1	Descriptive statistics for the self report Barthel, General health questionnaire 12, EuroQol thermometer, and EuroQol Health State	179
6.2	Descriptive statistics for the eight domains of the Short Form -36 questionnaire	180
6.3	Percentage prevalence of clinical features in Friedriech's ataxia patients not assessed as part of the International Cooperative Ataxia Rating Scale	184
6.4	Relationship between ICARS and ICARS component scores and various disease parameters in 77 Freidrich's ataxia patients	189

6.5 Relationship between various echocardiographic parameters and neurophysiology parameters and GAA1, disease duration, patient age, or clinical severity in 77 FRDA patients 195

Abbreviations

AD	Alzheimer's disease
ADP	adenine diphosphate
ALS	amyotrophic lateral sclerosis
ATP	adenine triphosphate
BI	Barthel Index
BrdU	bromodeoxyuridine
CNS	central nervous system
CPEO	chronic progressive external ophthalmoplegia
ddH_20	double distilled water
DMEM	Dubelco's modified Eagles medium
DMSO	dimethylsulphoxide
DNA	deoxyribonucleic acid
DTNB	5-5'-dithiobis-nitrobenzoic acid
ETC	Electron transport chain
FRDA	Friedreich's ataxia
$FADH_2$	flavin adenine dinucleotide (reduced)
GHQ12	General health questionnaire 12
HD	Huntington's disease
HSP	hereditary spastic paraparesis
ICARS	International Cooperative Ataxia Rating Scale
IF	Immunofluorescence
KSS	Kearns Sayre syndrome
LHON	Leber's hereditary optic neuropathy
LS	Leigh's syndrome
MEFs	Mitochondrial enriched fractions
MELAS	mitochondrial encephalomyopathy, lactic acidosis and stroke-like episodes
MERRF	myoclonic epilepsy and ragged red fibres
MNGIE	myoneural gastrointestinal encephalopathy
MRC	mitochondrial respiratory chain
MRS	magnetic resonance spectroscopy

MtDNA	mitochondrial DNA
NADH	nicotine adenine dinucleotide (reduced)
NARP	neuropathy, ataxia and retinitis pigmentosa
3-NP	3-nitropropionic acid
OXPHOS	oxidative phosphorylation
PBS	phosphate buffered saline
PCR	polymerase chain reaction
PD	Parkinson's disease
PEG	polyethylene glycol
PRP	platelet rich plasma
Q_1	ubiquinone-1
RNA	ribonucleic acid
ROS	reactive oxygen species
RT	room temperature
SOD	superoxide dismutase
SF36	Short Form 36
TBS	tris buffered saline
TCA	tricarboxylic acid cycle
$\Delta\Psi_M$	transmembrane potential
Tris	tris(hydroxymethyl)aminomethane
UV	ultraviolet
WD	Wilson's disease
XLSA/A	X-linked sideroblastic anaemia with anaemia.

1 INTRODUCTION

Our understanding of the role of mitochondria in human disease has expanded exponentially in the last 25 years. Mitochondria were first described in 1856, however it was not until 1946 that Albert Lehninger, Eugene Kennedy and others identified mitochondria as the major site of energy metabolism within the cell. Mitochondrial DNA (mtDNA) was identified in 1963 and the human mtDNA sequence was published in 1981[1]. Subsequently the mtDNA sequence of many other species has been determined, revealing a high degree of conservation between mammals[2].

There is now good evidence that mitochondria are the ancestors of free living, oxygen metabolising (i.e. aerobic) purple bacteria that were engulfed by ancestral eukaryotic anaerobic cells approximately 1.5 billion years ago. They typically measure 2 x 0.5 μm. As a consequence of their endocytic origins mitochondria are enclosed by both a relatively permeable outer membrane, and a relatively impermeable inner membrane. The outer membrane is permeable due to the abundant presence of porin, a transmembrane protein with a large pore. It is this inner membrane folded into numerous cristae that is the site of the mitochondrial respiratory chain. Like bacteria, mitochondria contain their own genome, ribosomes, and tRNAs. However, in order to function fully they rely upon a close symbiotic relationship between the nuclear and mitochondrial genome. The nuclear genome contributes the vast majority of mitochondrial proteins

Initially it was believed that disease caused by mitochondrial dysfunction would prove fatal *in utero*. However, a rapidly expanding number of diseases caused by mutations in mtDNA have been identified, and more recently diseases caused by mutations in nuclear genes have been found to have mitochondrial dysfunction at the centre of their pathogenesis. In a number of instances this is because the responsible mutation lies in a nuclear encoded mitochondrial protein.

Over the last decade mitochondrial biology has expanded into the fields of ageing, oxidative stress, and programmed cell death. These organelles now occupy a cornerstone of human biology.

1.1 MITOCHONDRIAL FUNCTION –BIOCHEMISTRY

Mitochondria are the site of numerous metabolic pathways including the Kreb cycle, fatty acid β oxidation, and amino acid pathways. In fact all pathways of fuel oxidation except glycolysis are located within mitochondria. These organelles are also involved in the cellular homeostasis of calcium, the protection of the cell from damage caused by reactive oxygen species generated during oxidative phosphorylation, and necrosis and apoptosis. These multiple functions are intricately interconnected.

In aerobic organisms, all energy yielding metabolic pathways culminate in oxidative phosphorylation. Five discrete protein-lipid complexes, embedded in the mitochondrial inner membrane, orchestrate this final stage of cellular respiration to generate adenosine triphosphate (ATP) the universal currency of energy (Fig 1.1). The process of oxidative phosphorylation is encompassed by the chemiosmotic theory proposed in 1961[3]. Reduced nicotinamide adenine dinucleotide (NADH) and flavin adenine dinucleotide ($FADH_2$) formed during glycolyisis, fatty acid β oxidation, and the Kreb cycle are oxidised to NAD^+ and FAD. NADH and $FADH_2$ are energy rich molecules because each contains a pair of electrons that have a high transfer potential. The donated electrons are passed through a series of electron donors and electron acceptors that include quinoid structures (flavin mononucleotide, FAD, and ubiquinone (coenzyme Q_{10}), and transition metal proteins (iron-sulphur clusters (Fe-S), hemes, and protein bound copper). Electrons are transferred to molecular oxygen via a chain of enzyme complexes in a series of oxidation/reduction reactions. These are driven by differences in the redox potential between the electron donor and acceptor. The free energy of these reactions is linked to the pumping of protons from the mitochondrial matrix, across the inner mitochondrial membrane, to the intermembrane space. A pH gradient and a transmembrane electrical potential is thus generated. The flow of these protons back to the matrix through complex

V, the final complex of the mitochondrial respiratory chain, is linked to the phosphorylation of adenosine diphosphate (ADP) to ATP [4](Fig 1.2). The transmembrane electrical potential is also used to drive the electrophoretic importation of nuclear DNA encoded proteins across the mitochondrial membranes. The proton gradient also serves to drive the transport of ions across the inner mitochondrial membrane [5].

The ATP generated by this process is used to meet energy demands in the mitochondrial matrix, or is transported to the cytosol in exchange for ADP by the adenine nucleotide translocator (ANT) the most abundant protein of the inner membrane. If OXPHOS is impaired cells become reliant on glycolysis for their supply of ATP. In order to regenerate NAD from NADH, pyruvate is converted to lactate via lactate dehydrogenase. Glycolysis is a far less efficient ATP synthesis pathway than OXPHOS. Catabolism of a single glucose molecule via the glycolytic pathway generates four ATP molecules, whereas catabolism via OXPHOS will generate twenty-six. ATP produced by fatty acid metabolism comes entirely from OXPHOS [6].

Figure 1.1

The five complexes of the mitochondrial respiratory chain are located in the mitochondrial inner membrane. (coutesy of M Cooper)

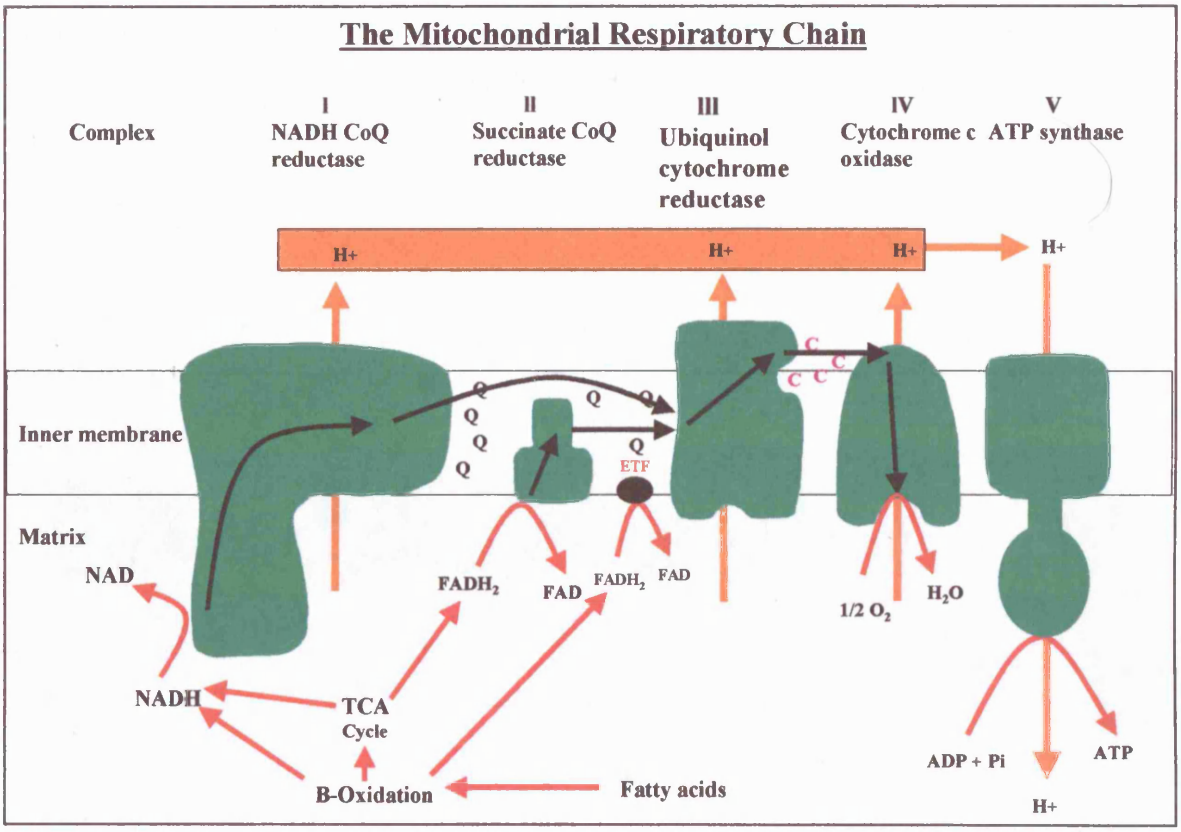

Figure 1.2

The five complexes of the mitochondrial respiratory chain are shown. Nuclear encoded (clear hexagons) and mitochondrial DNA encoded (coloured hexagons) combine to form these multimeric complexes. A proton gradient is generated and the flow of these protons back to the matrix through complex V, the final complex of the mitochondrial respiratory chain, is linked to the phosphorylation of adenosine diphosphate (ADP) to ATP. (CoQ = coenzyme Q; H^+ = protons; cyt c = cytochrome c; e^- = electrons; roman numerals refer to the mitochondrial respiratory chain complexes) (from AHV Schapira with permission)

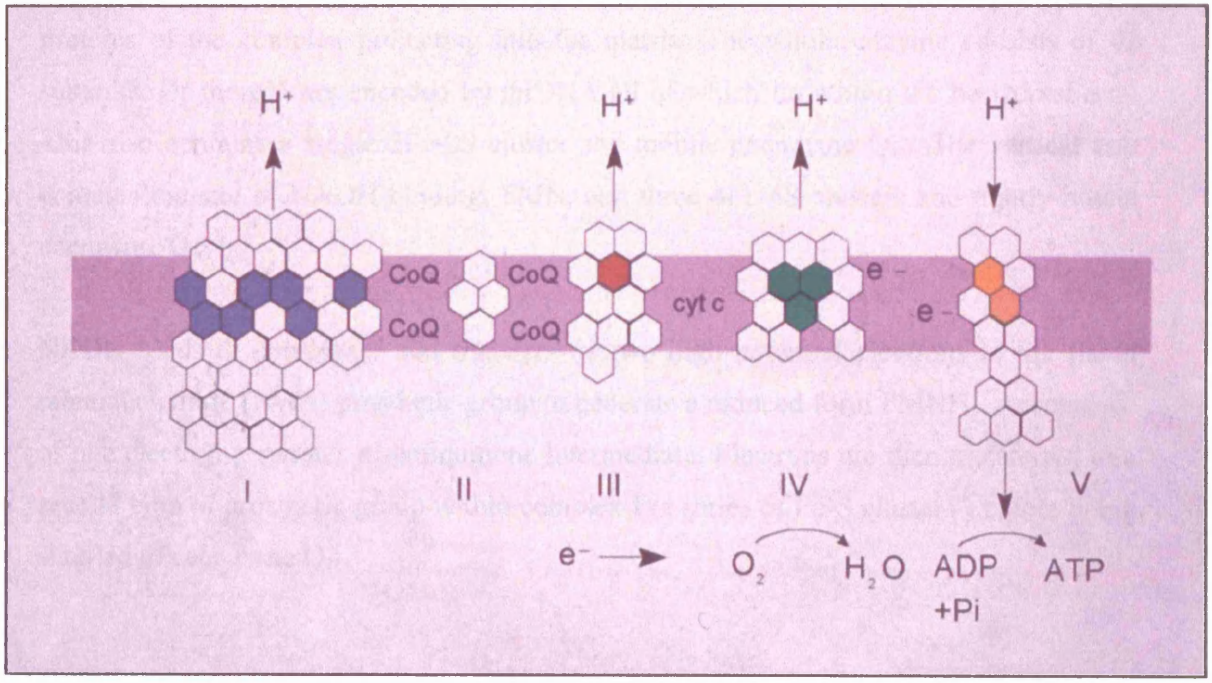

1.2 THE BIOCHEMISTRY OF OXIDATIVE PHOSPHORYLATION

As described above electrons are transferred from NADH to O_2 through the complexes of the mitochondrial respiratory chain. These are complex I (NADH-CoQ reductase), complex III (ubiquinone cytochrome c reductase), and complex IV (cytochrome oxidase). Electrons from $FADH_2$ are transferred through complex II (succinate dehydrogenase ubiquinone oxidoreductase) to complex III.

1.2.1 Complex I: (NADH dehydrogenase ubiquinone oxidoreductase)

This enzyme has two major domains, a hydrophobic horizontal arm buried in the mitochondrial inner membrane, and a vertical arm containing the peripheral membrane proteins of the complex projecting into the matrix. The whole enzyme consists of 42 subunits. Of these 7 are encoded by mtDNA all of which lie within the horizontal arm. This also contains a single 2Fe-2S cluster and mobile coenzyme Q_{10}. The vertical arm contains the site of NADH binding, FMN, and three 4Fe-4S clusters and tightly bound coenzyme Q_{10} [6].

NADH binds to complex I and transfers its two high potential electrons to the flavin mononucleotide (FMN) prosthetic group to generate a reduced form $FMNH_2$. Acceptance of one electron generates a semiquinone intermediate. Electrons are then transferred to a second type of prosthetic group within complex I (a series of Fe-S clusters) before being shuttled to coenzyme Q_{10}.

1.2.2 Iron sulphur clusters

Iron sulphur clusters within iron-sulphur proteins (non heme iron proteins) are critical for a large number of reduction reactions in biological systems. They can exist as several varieties: 1) Fe-S: a single iron atom linked to the sulfhydryl group of four cysteine residues of a protein 2) 2Fe-2S: two iron atoms and two inorganic sulfides, in addition to four cysteine residues 3) 4Fe-4S: four iron atoms, four inorganic sulfides, and four

cysteine residues. The iron atoms in these clusters cycle between the reduced (Fe^{2+}) and oxidised (Fe^{3+}) state. Complex I contains both 2Fe-2S and 4Fe-4S types of Fe-S clusters [6].

1.2.3 Ubiquinone (Coenzyme Q)

Coenzyme Q is found ubiquitously in biological systems. In the mitochondria respiratory chain it serves to carry electrons from complex I to III and II to III, and from the oxidation of fatty acids and branched chain amino acids via the flavin linked dehydrogenases. A long isoprenoid tail containing five carbon units makes this quinone strongly hydrophobic so that it diffuses rapidly within the hydrocarbon core of the mitochondrial inner membrane. The number of isoprene units varies between species, the most common form in mammals if 10 units (coenzyme Q_{10}). Ubiquinone is reduced to a free radical semiquinone anion by the reduction of a single electron. This enzyme bound intermediate is reduced by the acceptance of a second electron to form ubiquinol (QH_2).

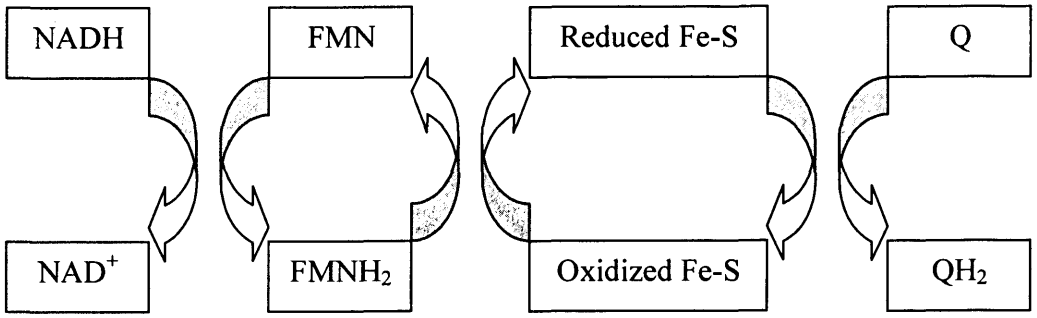

Figure 1.3: Ubiquinone / Ubiquinol reactions.

The flow of two electrons from NADH to QH_2 leads to four protons being pumped across the inner mitochondrial membrane. Coenzyme Q_{10} may also plays a role as an antioxidant and membrane stabiliser [7,8].

1.2.4 Complex II (succinate dehydrogenase ubiquinone oxidoreductase)

In the citric acid cycle succinate is oxidized to fumarate by succinate dehydrogenase with the reduction of FAD to $FADH_2$. This enzyme is part of complex II and, like the other OXPHOS enzymes, resides in the mitochondrial inner membrane. Following the oxidation of $FADH_2$ electrons are transferred to the Fe-S clusters of complex II, and then via coenzyme Q to thecytochrome b of complex III. Complex II consists of four subunits all encoded by nuclear genes. The free energy change of the catalysed reaction is small and therefore this enzyme does not translocate protons.

1.2.5 Complex III (ubiquinone-cytochrome c oxidoreductase)

Complex III is the second of the three proton pumps of the respiratory chain. It catalyses the transfer of electrons from QH_2 to cytochrome *c*, a water-soluble protein loosely associated with the inner membrane. This is linked to the pumping of protons across the inner mitochondrial membrane. Due to its lower thermodynamic driving force the transfer of one electron pumps only two protons, making it half as effective as complex I. Complex III contains cytochromes *b* and c_1, an iron sulphur protein, and 11 polypeptide subunits only one of which is encoded in mtDNA. The prosthetic group of all three of these cytochromes is iron-protoporphyrin IX (i.e. the same heme as found in myoglobin and haemaglobin). QH_2 transfers one of its electrons to the Fe-S cluster of complex III. It then passes to cytochrome c_1 and then cytochrome *c*. The second electron, now residing in a semiquinone ($Q^{\cdot-}$), is transferred through the two heme groups of cytochrome *b*. The different polypeptide microenvironments of each of these creates different electron affinities. The cytochrome *b* pathway enables the complex to efficiently funnel electrons from the two electron carrier QH_2 to the one electron carrier cytochrome *c* [6].

1.2.6 Cytochromes

These are electron transferring proteins that contain a heme prosthetic group. Their iron atoms oscillate between the reduced ferrous (Fe^{2+}) and oxidised ferric (Fe^{3+}) state during electron transfer. Cytochrome *c* has been extremely well characterised since its high water solubility has made it easy to isolate. It consists of 104 amino acids and a covalently attached heme group. It is able to interact with both its oxidase and reductase through the strong electrostatic charges generated by its cluster of lysine side chains around the heme crevice on the face of the protein. Cytochrome *c* is present in all organisms that have mitochondrial respiratory chains. The cytochrome *c* of any species will interact with the cytochrome oxidase of any other species. Cytochrome *c* has remained highly conserved over the 1.5 billion years since the mitochondrial symbiotic relationship began, with 26 of the 104 residues remaining unchanged over this time.

1.2.7 Complex IV (cytochrome *c* oxidase)

Complex IV consists of 13 polypeptide subunits, three encoded by mtDNA. It catalyses the transfer of four electrons from reduced ferrocytochrome *c* to molecular oxygen to form H_2O. Complex IV consists of a protein backbone bound by two copper containing prosthetic groups, and two non-covalently attached heme A groups (a and a3).

Molecular oxygen is an ideal terminal acceptor of electrons, because its high affinity for electrons generates a large thermodynamic driving force for OXPHOS, and in contrast to other strong electron acceptors (e.g. F_2) it reacts very slowly unless catalysed. However, partial reduction leads to the generation of superoxide anions. Complex IV reduces molecular oxygen, via peroxy intermediates, between the Fe^{2+} and Cu^{+} ions of its heme a3-Cu_B centre located in the mitochondrially encoded subunit I. This provides a strong reducing environment designed to prevent the release of partially reduced moieties. Four protons are translocated when a pair of electrons flows through the oxidase [9].

1.2.8 Complex V (ATP synthase)

Complex V phosphorylates ADP via a mechanism that differs from the synthesis of ATP during glycolysis. The latter occurs via high energy intermediates (e.g. 1,3-biphosphoglycerate). Complex V consists of a 378 kDa F1 unit of an $\alpha_3\beta_3\gamma\delta\varepsilon$ subunit composition. This can act as an ATP synthase or an ATP hydrolase. It is attached to and transverses the inner membrane by a F_0 stalk unit that acts as the proton channel. The role of the proton gradient is not to form ATP but to release it from the ATP synthase [10].

ATP and ADP do not cross the inner mitochondrial membrane freely, but rely upon a specific transport protein, adenine nucleotide translocator. The translocase is abundant accounting for 14% of inner mitochondrial membrane proteins.

The main factor regulating the rate of OXPHOS is the level of ADP. This regulation is called respiratory control. The level of ADP also affects the rate of the citric acid cycle.

Therefore the system is designed so that electrons do not flow from fuel molecules to O_2 unless there is a requirement for ATP synthesis [6].

1.3 MITOCHONDRIAL DNA

The human nuclear genome of three billion base pairs contains within it only approximately 30,000 genes. The human mitochondrial genome is small by comparison, consisting of 16,569 base pairs arranged in a covalently closed, double stranded, circular molecule. Cells contain hundreds of mitochondria, and each of these mitochondria contains multiple copies of mtDNA located in the matrix [11].

A diagram of the human mtDNA molecule is shown in figure 1.4. It encodes 13 polypeptides, all of which are subunits of the MRC, 22 tRNAs, and 2 rRNAs [1,12,13]. The two strands of the mtDNA duplex have different base compositions, and this allows the identification of a light (L) and a heavy (H) chain. The H strand contains most information, encoding 12 polypeptides, 2 rRNAs, and 14 tRNAs.

MtDNA has a number of features that distinguish it from nuclear DNA. Some genes overlap, and intergenic sequences are absent or limited to only a few base pairs. In this absence of introns, non-coding regions are limited primarily to the displacement or D-loop which plays a central role in the regulation of replication and transcription. In replicating cells this region contains a triple helix due to the binding of a short DNA strand to the L strand causing displacement of the H strand. Mitochondrial tRNA and rRNA genes are small, and termination codons of most protein genes are generated post transcriptionally [14].

Figure 1.4

Map of the human mitochondrial genome, showing the 13 polypeptide-coding genes, and 24 protein synthesis genes (12S and 16S ribosomal RNAs and 22 transfer RNAs (1-letter amino-acid code). OH = origin of replication of Heavy strand. Numbers refer to base pairs and those in bold print show common mutation sites. (from [11])

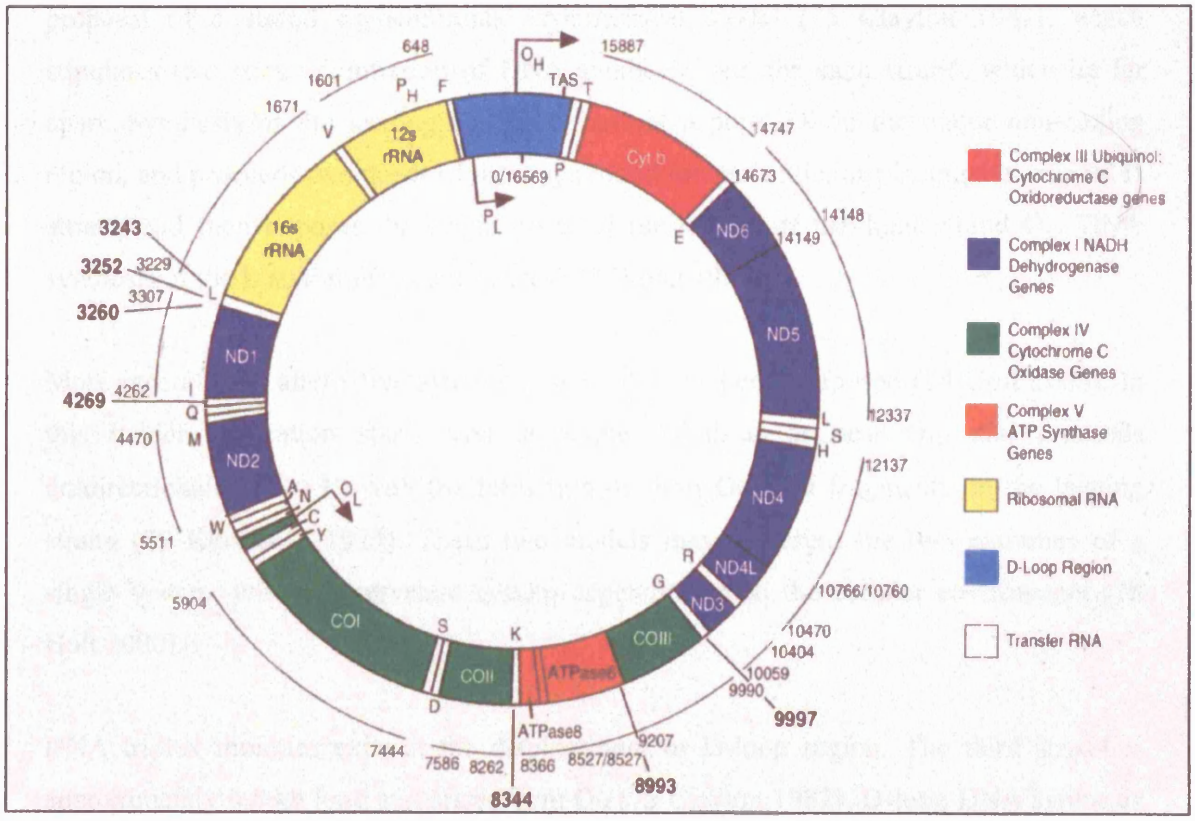

1.3.1 MtDNA replication

Mammalian mtDNA maintenance and propogation is wholly dependent upon nuclear encoded proteins, only a few of which have been identified to date. Replication of mammalian mtDNA has long ben recognized as unusual. The identification of intermediates containing long stretches of partially single stranded DNA led to the proposal of a strand asynchronous asymmetrical model (75 Clayton 1982), which stipulates two sites of initiation of DNA synthesis, one for each strand, which lie far apart. Synthesis of the leading H-strand starts at a point O_H in the major non-coding region, and proceeds two thirds of the way around the molecule, displacing the original H strand, and then exposes the origin point of replication of the light strand O_L. DNA synthesis of the L strand then commences (77 Wong 1985).

More recently, an alternative synchronous model has been proposed (78 Holt 2000). In this model replication starts from a single poion at or near O_H, and proceeds unidirectionally (5'→3') with the formation of short Okazaki fragments on the lagging strand (79 Kurosawa 1975). These two models may represent the two extremes of a single system, with the prevelant system depending upon the cellular environment (78 Holt 2000).

DNA triplex moieties exist at the displacement or D-loop region. The third strand is approximately 0.5 kb long and arises from O_H (75 Clayton 1982). D-loop DNA synthesis appears to be preceded by the formation of an RNA primeroriginating at the L strand promotor (82 Kandg 1997 (81 Gillum1978). D loops are thought to represent aborted replication intermediates, and most if not all are degraded. Termination of leading strand DNA synthesis is poorly understood, but may involve Termination Associated Sequences (TAS) in the major non-coding region (80 Doda 1981). The continuation of H strand synthesis beyond TAS is thought to mark a dedicated replication event.

1.3.2 MtDNA transcription

The light and heavy mtDNA strands each have one major site for the initiation of transcription (IT_L and IT_{H1}) located approximately 150 bp apart within the D-loop. These sites are embedded within a promoter element (HSP and LSP) that, with their upstream *cis*-acting enhancer elements, are critical for transcription. IT_L and IT_{H1} function independently. A second initiation site for H strand transcription (IT_{H2}) located at np 638 in the $tRNA^{Phe}$ gene may exist [15].

Two *trans*-acting proteins are known to be involved in transcription initiation. Mitochondrial transcription factor A (mtTFA) is a 25 kDa protein that confers selectivity on the binding of the second factor, an RNA polymerase, to the HSP and LSP [16]. The major part of mtTFA consists of two DNA binding motifs that bind to the upstream enhancer regions to ensure that transcription proceeds in the correct direction [17]. MtTFA may also induce conformational changes in the DNA that influence the access of RNA polymerase to the DNA [18], and be involved in the maintenance of mtDNA levels. Homozygous mtTFA knock-out mice are non-viable, and heterozygotes exhibit mtDNA depletion, a quantitative defect of mtDNA [19]. A further factor, mtTFB, with similarities to known RNA modifying enzymes, has been identified [20]. Further *trans*-acting factors probably remain to be discovered.

The L strand is transcribed as a single polycistronic precursor [21]. A dual H strand transcription initiation model has been proposed to explain the observation that the rate of transcription of rRNAs is greater than that of the mRNAs encoded on the H strand [15]. This proposes that transcription is initiated infrequently from IT_{H2} resulting in transcription of the whole H strand, whereas IT_{H1} more frequently initiates transcription but is terminated at the 3' end of the 16S rRNA gene. The latter results in transcription of both rRNA genes, plus $tRNA^{Phe}$ and $tRNA^{Val}$. A mitochondrial transcription termination factor (mtTERM) has been identified that has specificity for a tridecamer sequence within the $tRNA^{Leu(UUR)}$ gene, and is the mechanism by which transcription of this shorter transcript is terminated [22]. The DNA binding capacity of mtTERM is mediated by its

three leucine zipper motifs and two basic domains [23]. The exact mechanism of mtTERM is unclear. There is evidence that an additional factor may be necessary for termination activity. MtTERM may also inhibit L strand replication, but its role here is again unclear, because no L strand encoded genes are present downstream of this site [24]. Polyadenylation of mitochondrial mRNAs and rRNAs, by an as yet unidentified enzyme, serves to stabilize the transcripts [25]. This is achieved despite the lack of upstream polyadenylation signals like those found in nuclear mRNAs.

1.3.3 Mitochondrial DNA translation

The majority of mitochondrial genes are separated by tRNA genes, and their secondary structure is believed to provide punctuation marks for the transcription of mtDNA [14]. Excision of tRNAs is achieved by a 5' mtRNaseP and a 3' tRNA precursor processing endonuclease [26]. Some tRNA genes overlap, and may therefore be transcribed in a shortened form, with missing residues added later [27]. Various other tRNA post-transcriptional modifications are required to ensure cloverleaf folding [28], and proper codon recognition [29]. Efficient aminoacylation of tRNAs is dependent upon the 3' addition of CCA by a nuclear encoded ATP(CTP)tRNA specific nucleotidyltransferase (mtCCA) located on chromosome 3p25.1 [30]. Other nuclear encoded enzymes, the aminoacyl tRNA synthetases, are responsible for charging mitochondrial tRNAs and their related amino acids. This group of enzymes catalyses the activation of amino acids and their subsequent linkage to tRNA molecules. At least one enzyme exists for each amino acid, and the reactions with both the tRNA and the amino acid are highly specific [31]. In-built mechanisms ensure a low error rate, for instance the enzyme for isoleucine will hydrolyse valine, which differs by only one methylene group, if it is bound inadvertently. Interaction with the tRNA is via the anticodon itself for some aminoacyl-tRNA synthetases, for others the recognition site resides in the 3' acceptor stem, and for others recognition is via multiple determinants. ATP drives the reaction. Carboxyl group of amino acid is joined to the 3-hydroxyl terminus of the tRNA.

The attachment of amino acids to tRNA molecules achieves two objectives. Firstly, the amino acids by themselves are not able to recognise the mRNA codons, and secondly this reaction activates the carboxyl group of the amino acid thus enabling the otherwise thermodynamically unfavorable reaction of peptide bond formation between the carboxly group of one amono acid and the hydroxyl group of another. The mitochondrial genome contains two $tRNA^{Ser}$ ($tRNA^{Ser(AGY)}$ and $tRNA^{Ser(UCN)}$), and two $tRNA^{Leu}$ ($tRNA^{Leu(CUN)}$ and $tRNA^{Leu(UUR)}$). A single enzyme performs serylation of both $tRNA^{Ser}$ species. This is despite the fact that they share no sequence motifs and differ structurally, with the $tRNA^{Ser(AGY)}$ lacking the entire dihydrouridine loop containing arm [2].

Protein synthesis is initiated by N-formyl methionyl, formed by the post-transcriptional action of methionyl-tRNA transformylase on methionyl-tRNA. Mitochondrial protein synthesis is considered to follow the classical model of protein synthesis as first described for *E.coli*. Thus during the first step this initiato tRNA will bind to the ribosomal P (peptidyl) site, while the other two sites for tRNA molecules, the aminoacyl (A) site and the exit (E) site, remain empty. Protein synthesis then proceeds in an amino to carboxyl direction by the sequential addition of amino acids to the carboxyl end of the growing peptidyl chain. One mitochondrial translation initiation factor has been identified (mtIF-2) on chromosome 2p16-p14 [32]. It belongs to a family of GTPases that are molecular switches capable of alternating between an active (mtIF-2.GTP) and inactive (mtIF-2.GDP) conformation. It promotes the binding of N-formylmethionyl tRNA to the small ribosomal subunit in a GTP and mRNA-dependent reaction [33].

Mitochondrial ribosomes inhabit the matrix, and half of the population is attached to the inner mitochondrial membrane [34]. They differ from ribosomes in the cytosol, but share a number of features with prokaryotic ribosomes. They have a low RNA, and high protein content. There are 29 mitochondrial ribosomal proteins (MRPs) in the small ribosomal subunit, and 48 in the large [35,36]. Some are homologous to those found in E.coli. Others are apparently unique proteins, and some of these have previously been identified as pro-apoptotic proteins (death associated protein-3, and PDCD9), thus implicating mitochondria in cellular apoptotic signaling pathways [37 38]. Some MRPs exist as several

isoforms that may influence the decoding properties of the ribosome. The ribosomal population is therefore heterogeneous [38].

Mitochondrial mRNAs have limited ribosomal binding abilities, lacking the mechanisms used for this in the cytosol and in prokaryotes. Mitochondrial translational efficiency is low and may be a consequence of this [39]. The small ribosomal unit binds mRNA tightly. This involves approximately 400 nucleotides but is a sequence independent process. This may explain why the shortest open reading frames of human mtDNA (ATPase 8 and NDL4) are both part of overlapping genes.

After initiation, elongation begins with the binding of an aminoacyl tRNA to the ribosomal A (aminoacyl) site. Elongation of the mRNA product is facilitated by a number of elongation factors. The genes for several of these have been identified in humans (EF-Tu on chromosome 16p11.2, EF-Ts on chromosome 12q13-q14, EFG1 on chromosome 3q35.1-q26.2 and EFG2 on chromosome 5q13) [40-42]. The process of translation elongation in E.coli is better established, and the human system is believed to be essentially similar. At the ribosomal A site mtEF-Tu forms a ternary complex with the correct amino-acyl-tRNA as determined by the codon. GTP is then hydrolysed, and EF-Tu.GDP leaves the ribosome. EF-Ts, the nucleotide exchange factor, replaces the GTP on EF-Tu to allow elongation to continue. Peptide bond formation is catalysed by the large ribosomal subunit, and the EF-G (like EF-Tu a GTPase), promotes the translocation of the tRNAs at the A and P sites to the P and E sites respectively. The mRNA is moved to expose the next codon to the A site. The deacylated tRNA is released from the site [43].

The initiator moves to the ribosomal E (exit) site before leaving the ribosome. The process is repeated as a new aminoacyl-tRNA binds to the now vacant A site. The whole process is powered by the hydolysis of GTP. Termination of translation requires several release factors (RF) that recognise and bind to stop codons at the A site, resulting in hydrolysis of the bond between the polypeptide chain and the tRNA at the P site. Other RFs serve to release the mRNA. The two ribosomal subunits then dissociate [44]. A single

putative human mitochondrial RF has been identified on chromosome 13q14.1-q14.3 [45,46].

1.3.4 Transfer RNA molecules

tRNAs are small ribonucleic acids, present in all organisms to ensure ribosome-dependent protein biosynthesis. More than 4300 sequences are documented including prokaryotic, eukaryotic-cytosolic, eukaryotic-chloroplastic, and eukaryotic-mitochondrial molecules [47]. It is primarily the canonical tRNAs (bacterial and eukaryotic cytosolic tRNAs) that have been studied in most detail. Current knowledge encompasses structural features (including their cloverleaf secondary structure, conserved sets of primary elements, tertiary interactions, and L-shaped three dimensional structure), and functional aspects (including recognition of aminoacyl tRNA synthetases, translation initiation or elongation factors, and ribosomal proteins). In contrast, mitochondrial tRNAs are structurally and functionally more diverse, and less well understood than the canonical tRNAs [48,49].

The mitochondrial genetic code differs from the standard code in a number of ways. As a result mitochondria need only 22 tRNAs instead of the predicted 32 tRNAs to translate all codons. All known tRNA molecules are single chains of between 73 and 93 ribonucleotides and molecular weight of approximately 25 kD. Other common features are that the 5' end is always phosphorylated and the terminal residue is usually pG. At the 3' end the final residues are CCA, with the relevant amino acid attaching to the 3' hydroxyl group of the terminal Adenosine. Approximately half of the nucleotides are base paired to form double helices. In this way all tRNA sequences can be written in a cloverleaf pattern. This uniform structure allows them all to interact with the same ribosomes, mRNAs and elongation factors. There are five groups of bases that are not base paired. The 3' CCA terminal region, the TΨC (ribothymidine, pseudouricil, cytosine) loop, the DHU loop containing several dihydrouracil residues, the anticodon loop, and an extra arm that contains a variable number of residues. Most bases in non-helical regions participate in unusual hydrogen-bonding interactions, usually between

non-complementary bases. The anticodon loop consists of seven bases that conform to the pattern: - 5' pyrimidine - pyrimidine - X - Y - Z – modified uridine – variable base – 3'. The $tRNA^{Leu(UUR)}$ molecule is shown in figure 1.5.

Each tRNAs contain between 7 and 15 unusual bases. These are formed by enzymatic modification of A U C and G, and include Inosine (I), pseudouridine (Ψ), dihydrouridine (UH_2), ribothymidine (T), and methylated derivatives of Guanosine and Inosine. Methylation inhibits the formation of certain base pairings and thus makes the base available for alternative interactions that may be of importance to the stability of the molecule. Methylation can also alter the hydrophobicity of regions of the tRNA and thereby alter the interaction with synthetases, ribosomal proteins, and folding and other mechanisms. Other modifications can have an effect on codon recognition.

The first tRNA base sequence was established by Holley in 1965 [50]. This was the yeast alanine tRNA, a 76 ribonucleotide chain. The three dimensional structure of yeast $tRNA^{Phe}$ was established in 1974 by x-ray crystallography [51]. They were shown to be "L" shaped structures with the two arms of the "L" formed by two double helix segments. This structure places the CCA terminus at one end of the "L", and the anticodon loop approximately 80 A^0 away at the other end of the "L". This large distance may be functionally important to allow the molecule to accomplish its two separate tasks of recognising both the correct mRNA codon, and the correct aminoacyl tRNA synthetase. The DHU and TΨC loops lie at the corner of the "L".

Codon recognition is achieved by base pairing with the tRNA anticodon. The amino acid in the aminoacyl-tRNA does not play a role in this. Some tRNAs are able to recognise more than one codon. The yeast $tRNA^{Ala}$ investigated by Holley can recognise GCU, GCC, and GCA. Models of various base pairs to determine the distance and angle between the glycosidic bonds. If some steric freedom or "wobble" is allowed certain base pairings are allowed at the third base pair position. These are C:G, A:U, U:A or G, G: U or C, I: U or C or A, (codon:anticodon). The number of codons read by an anticodon is determined by its first base. Those beginning G or C will read 1codon, those beginning U

or G two, and those that start with Inosine, formed by the post transcriptional deamination of adenosine, read three codons. Therefore part of the degeneracy of the genetic code arises from wobble in the pairing of the third position of the codon and the first position of the anticodon.

Mitochondrial tRNAs show a number if differences from cytosolic tRNAs. Cloverleaf folding occurs in all but the tRNA $^{Ser(AGY)}$ group, but exhibits large size variations especially within the T-loops. This aspect of tRNA structure is highly conserved in the canonical tRNAs. Furthermore all mt tRNAs have a variable region restricted to 3 to 5 nucleotides, as opposed to the standard 23 nucleotides variable region in canonical tRNAs [47]. The degree of conservation of nucleotides in the primary sequence also differs greatly from non-mitochondrial tRNAs. These are often nucleotides involved in tertiary folding, implying that mt tRNAs probably have their own set of folding rules.

Figure 1.5

The mitochondrial $tRNA^{Lue(UUR)}$ molecule, showing its nucleotide sequence, amino acid acceptor stem, dihydrouridine loop, TΨC loop, anticodon, and sites of common mutations. (from [115])

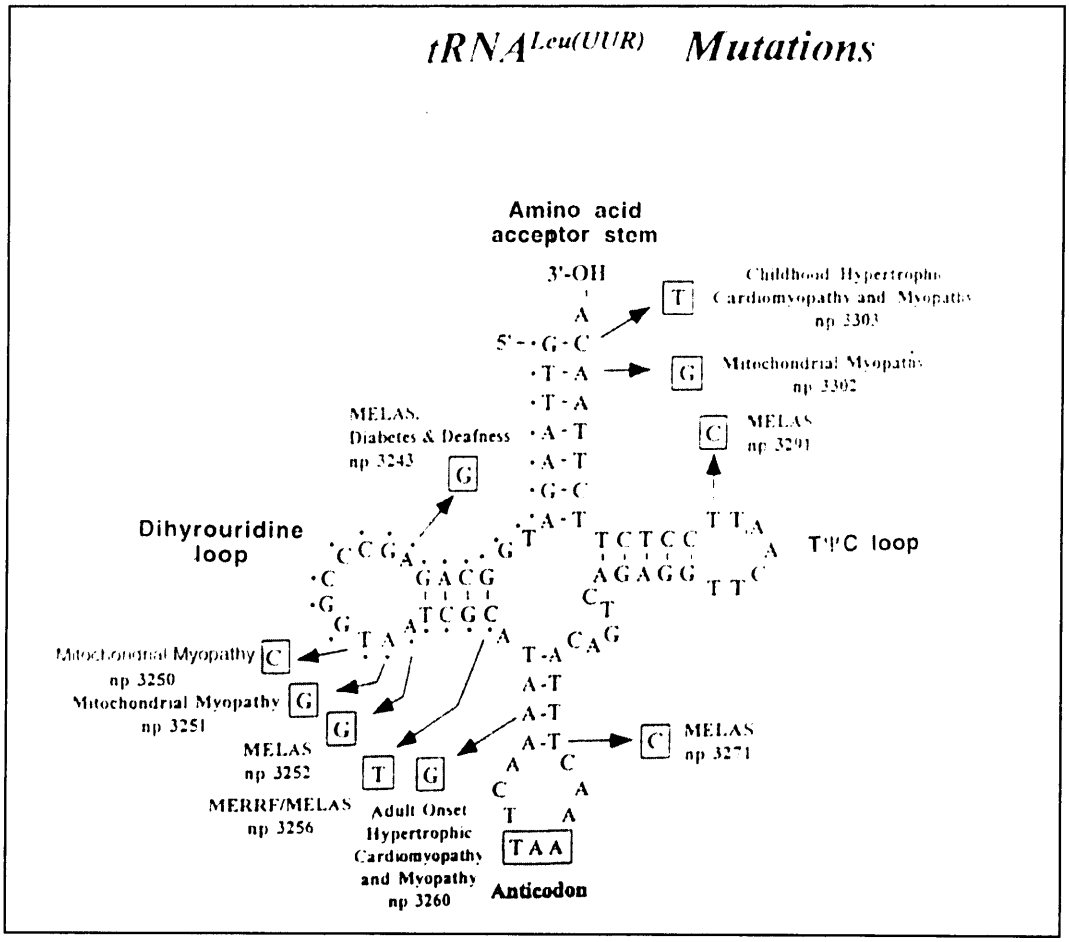

1.4 MITOCHONDRIAL IMPORT

Nuclear genes encode the vast majority of mitochondrial proteins. Therefore, in order to reach their target organelle these nuclear encoded mitochondrial proteins rely upon transport mechanisms to reach their intended target. Protein translocation across and into the mitochondrial membranes involves at least four specialised translocation systems. A single general translocase (the TOM complex) is present in the outer membrane and is responsible for the transfer of all nuclear encoded mitochondrial proteins through the outer membrane [52]. The inner membrane however contains three distinct translocases, each for different classes of preproteins. Some mitochondrial preproteins, transcribed on cytosolic ribosomes, contain an N-terminal mitochondrial targeting sequence. The preprotein interacts with the inner membrane surface and then inserts into the preprotein translocase of the inner membrane (TIM 23 complex). Hydrophobic preproteins with internal targeting signals rely on the TIM 22 complex for insertion into the inner membrane. The OXA translocase controls the insertion of preproteins and mitochondrially encoded proteins from the mitochondrial matrix into the mitochondrial inner membrane [53]. Translocation through the outer and inner membrane is completed by the mitochondrial HSP 70-ATP dependent driving system associated with the TIM complex. The preproteins also undergo proteolytic processing in the mitochondrial matrix. Protein folding is achieved by molecular chaperone systems, mtHSP70, HSP60, and associated co-chaperones [54]. Successful translocation across the inner membrane requires ATP and the presence of the mitochondrial membrane potential. Insertion into the membrane requires the membrane potential only.

1.5 CYBRID TECHNOLOGY

The ability to deplete cells of their mtDNA whilst maintaining their viability has allowed the development of cybrid technology. This has proved a powerful tool in the investigation of mitochondrial disorders. MtDNA replication can be inhibited by ethidium bromide. This intercalates with DNA and at low concentrations (0.1-2μg/ml)

inhibits mtDNA replication without affecting nuclear DNA [55,56]. Dideoxycytosine and azidothymidine also result in depletion of mtDNA levels but achieve this effect by the inhibition of mtDNA polymerase γ [57,58]. Cells lacking mtDNA are termed rho-zero (ρ^0).

Rho-zero yeast cells remains viable if supplemented with a fermentable energy source. Human cells however cannot survive even in a high glucose environment [59]. Pyrimidine synthesis is also deficient in these cells because dihydrooratate dehydrogenase, an enzyme of the pyrimidine synthesis pathway located on the mitochondrial inner membrane requires mitochondrial electron transport for normal function [60]. Uridine supplementation is therefore necessary for cell survival. The addition of pyruvate to the culture medium is also required. The reason for this requirement is uncertain but probably relates to the need for excess cytoplasmic NADH to be oxidised to NAD in order for glycolysis to proceed. This is achieved by the conversion of pyruvate to lactate via lactate dehydrogenase. Additional pyruvate is therefore required to provide sufficient levels for entry into the tricarboxylic acid cycle [61].

The generation of cytoplasts, by the enucleation of mammalian cells provides a source of mitochondrial DNA devoid of nuclear DNA. Their subsequent fusion with ρ^0 cells (containing nuclear DNA but devoid of mitochondrial DNA) to generate cybrids allows the mixing of mtDNA with novel nuclear backgrounds [62-64]. After its initial development this technique also proved applicable to human cells [61]. Repopulated cybrids with functioning mitochondria are able to grow in the absence of uridine and pyruvate [59]. Nuclear markers are also required to exclude the presence of nucleated donor cells, because most enucleation procedures will leave some residual intact nucleated cells [59]. "206" osteosarcoma cells are thmidine kinase deficient and therefore able to survive in the presence of bromodeoxy Uridine since toxic products are not generated. A549 lung carcinoma cell lines are resistant to Geneticin. Alternatively, platelets can be used to provide an easily obtainable, naturally enucleated source of mitochondria [65].

Cybrid technology therefore allows the study of specific mtDNA genotypes containing mutations and nuclear-mitochondrial genomic interactions at the cellular, molecular, and

biochemical level. The persistence of a biochemical defect after transfer of mtDNA to a new nuclear environment is considered proof of a mtDNA aetiology of the defect [66]. If the defect is complemented then a nuclear origin for the defect is implicated. Cybrid technology also allows the generation of clones containing a range of mutant loads from 0 to 100%. This is an important resource in the investigation of molecular mechanisms underlying mtDNA mutations. The persistence of altered protein synthesis and respiratory chain deficiencies after the introduction of mtDNA harbouring the A3243G mutation into 206 ρ^0 cells was the first functional proof of the pathogenicity of this common MELAS mutation. A threshold value of 6% wild type mtDNA, sufficient to restore the normal biochemical parameters, was also established by this technique [67,68]. The same technique revealed that mutant levels above 60% resulted in the synthesis of little or no ND6 complex I subunit, and impaired complex I activity. Clones of similar mutant load showed markedly different levels of O_2 consumption with pyruvate. Mutant levels above 95% showed a consistently reduced complex I, III, and IV activities with a marked generalised reduction in levels of mitochondrial translation products [69]. In a similar way platelet fusion experiments proved the mtDNA genotype containing the common MERRF A8344G mutation to be causal [65].

Cybrid technology was also used to demonstrate the nuclear origin of mtDNA depletion syndromes. Patient fibroblasts with mtDNA levels below 2% and impairment of all respiratory chain enzymes, were enucleated and fused with A549 ρ^0 cells. This led to the restoration of mtDNA levels and MRC function confirming that nuclear genes were responsible for this disorder [70]. The nuclear origin of COX deficient Leigh syndrome was shown in a similar manner [71].

1.6 THE GENETICS OF MITOCHONDRIAL RESPIRATORY CHAIN DYSFUNCTION.

In the 1.5 billion years since the incorporation of mitochondria into eukaryotic cells, a complex symbiotic relationship has developed. Mitochondria are no longer self

supporting. Nuclear genes encode 72 of the 85 subunits that make up the MRC. All other non-respiratory chain proteins within a fully functioning mitochondrion, numbering in excess of 1000, are also nuclear encoded. The human genome contains an estimated 30,000 genes, and thus 3% of the nuclear genome is devoted to the function of a single organelle, the mitochondrion [11]. Therefore, the majority of mitochondrial proteins are encoded by nuclear genes, translated in the cytoplasm usually as precursors with an N-terminal mitochondrial targeting sequence, and then transported across one or both of the mitochondrial membranes. Once inside the mitochondrion they may require cleavage of the targeting sequence and further modification by assembly and other factors [11]. Furthermore, although mtDNA encodes all the tRNAs required for mitochondrial translation, these tRNAs need to be charged by aminoacyl-tRNA synthases that are nuclear encoded. In addition although mtDNA encodes two rRNAs, all the associated mammalian mitochondrial ribosomal proteins are the products of nuclear genes that also require importation to the mitochondrion from the cytosol.

In the short history of mitochondrial medicine innumerable rearrangements and over 130 point mutations have been described [72]. The mutation rate of mtDNA is estimated to be 5 to 100 times that of nuclear DNA, due to the oxidative environment, and poor repair mechanisms of mtDNA [73,74]. However, in children with an isolated or combined OXPHOS enzyme deficiency, a mtDNA mutation is identifiable in only 5-10% of cases [75,76].

MRC dysfunction can be a consequence of mutations within either mitochondrial or nuclear DNA. MtDNA mutations can be either rearrangements or point mutations. Rearrangements are usually deletions, but also include duplications. MtDNA deletions result in the loss of protein coding genes, tRNAs or rRNAs, but can also generate novel fusion products. Point mutations can involve protein coding genes, rRNAs or tRNAs. Of all point mutations a third are located in mtDNA encoded polypeptides (18 in complex I mtDNA subunits, 14 in cytochrome b subunits of complex III, 11 in complex IV subunits, and 5 in complex V all of which lie within the ATPase 6 subunit gene).

The first nuclear gene mutation causing a mitochondrial respiratory chain defect in humans was reported by Bourgeron in 1995 [77]. In two siblings with complex II deficiency presenting as Leigh syndrome, an Arg554Trp substitution was detected in a conserved domain of the nuclear-encoded flavoprotein subunit gene of succinate dehydrogenase (SDH). The mutation was shown to have a deleterious effect on the catalytic activity of SDH (complex II) in an SDH- yeast strain transformed with mutant Fp cDNA.

To date, mutations in nuclear encoded OXPHOS subunits have been identified in complex I subunits (NDUFS4 in four patients with Leigh syndrome (LS), NDUFS7 in two siblings with LS, NDUFS8 in a singleton with LS, and NDUFV1 in two infants with leukodystrophy and myoclonic epilepsy, and three LS patients, NDUFS2 in three families affected by cardiomyopathy and encephalomyopathy, and NDUFS1 in three unrelated LS patients) [78-85]. Mutations in the FP subunit of complex II were responsible for late onset neurodegenerative disease in two sisters with optic atrophy, ataxia, and proximal myopathy [86]. Two families have also been described with mutations of complex II associated with LS [77,87]. Three different families with hereditary paragangliomas have been linked to the PGL1, PGL2, and PGL3 loci. Mutations in SDHD and SDHC are responsible for PGL1 and PGL3 respectively. These are the smallest subunits of complex II and are responsible for anchoring the enzyme to the inner mitochondrial membrane [88,89]. Mutations in the region of SDHD have also been identified in non-familial phaeochromocytoma [90] (Table 1.4). In a few unrelated families a syndrome of muscle coenzyme Q_{10} deficiency causing recurrent myoglobinuria, seizures, ataxia and mental retardation, with ragged red fibres, the histological hallmark of mitochondrial myopathies, and lipid storage in muscle is described [91]. Cases lacking myoglobinuria and with mild myopathic signs are also seen. These are attributed to defects in coenzyme Q_{10} synthesis and respond to coenzyme Q_{10} supplementation [91-94]. To date, mutations in nuclear encoded complex III or IV subunits have not been described.

Our knowledge of the 70 human nuclear genes that encode the subunit building blocks of the OXPHOS system has grown. Mutation identification has focused on those nuclear subunits with a high degree of evolutionary conservation, and established functional

significance. It has subsequently become apparent that most nuclear gene mutations resulting in mitochondrial disease lie not in these genes, but in genes for proteins involved in the regulation of transcription, translation, post-transcriptional modification, mitochondrial signaling, folding and assembly, or the transport of nucleotides and metabolites [72]. Approximately 340 of these genes are known to be involved in mitochondrial maintenance and assembly in *Saccharomyces cerevisiae* [95]. A number of these genes are now identified in humans and those associated with the archetypal mitochondrial encephalomyopathies are discussed under the relevant sections below. Mutations in the dystonia deafness protein, a human homologue of the yeast mitochondrial import protein Tim8p, are responsible for Mohr-Tranebjaerg syndrome [96]. This is the first example of defective mitochondrial import in human disease and is discussed further in Chapter 5. Future efforts using human expressed sequence tag databases and known genes of lower species to identify candidate genes should expand this area of mitochondrial biology.

1.7 GENETIC FEATURES OF MITOCHONDRIAL DNA DISEASES.

Diseases associated with mtDNA mutations are characterised by their diverse manifestations. They have a predilection for the neuromuscular system and can manifest with disease affecting any part of the neuraxis. Their presenting features are often commonly occurring neurological symptoms such as stroke, epilepsy, neuropathy, movement disorders, dementia, ocular disease and deafness. Mitochondrial disorders often cause multi-system disease with endocrine, heamatological, gastrointestinal, hepatic, renal, dermatological, psychiatric, ophthalmological, and cardiovascular manifestations. Age of onset can cover a wide range even for specific disease entities. The relationship between phenotype and genotype is notoriously poor. A single phenotype can invariably result from multiple mtDNA mutations, and a single mutation may result in a wide range of phenotypes. Phenotypic variability may be marked even within a single family. A reported family with the A8344G common myoclonic epilepsy and ragged red fibres (MERRF) mutation illustrates this point. Within the family different

members presented with Leigh syndrome, spinocerebellar degeneration, or atypical Charcot-Marie-Tooth disease. Even within those presenting with a phenotype of spinocerebellar degeneration cases varied from age of onset in late childhood with death aged 73 years, to onset aged 20 years and death at 40. This family illustrated another common finding in mitochondrial disease in that when they were first reported they were classified as an unknown neurological disease of autosomal dominant inheritance. When they were re-reported the ascertainment of oligosymptomatic subclinical cases revealed the maternal pattern of inheritance.

A number of genetic features peculiar to mitochondrial DNA that distinguish it from Mendelian genetics may underlie the clinical diversity of these conditions.

1.7.1 Maternal inheritance

The ovum contains several hundred mitochondria and these, each containing several copies of mtDNA, contribute to the zygote. The sperm in contrast, despite containing mitochondria to power its motility, have been believed to contribute no mtDNA material to their offspring [97]. Paternal mtDNA may be excluded from the zygote simply because sperm mitochondria fail to gain access to the interior of the oocyte. Alternatively, if sperm mitochondria do gain access they may be lost from the zygote due to a dilutional effect. Other mechanisms, including molecular surveillance mechanisms have also been proposed [98]. Therefore, if inheritance is purely maternal, a mother harbouring a mtDNA mutation would pass it on to all her offspring, but only her daughters would pass it on to subsequent generations [99]. Recent evidence however has proposed that paternal mtDNA inheritance does in fact occur. Schwartz and Vissing described a patient with exercise intolerance, lactic acidosis after minimal exertion, and RRFs. MtDNA sequencing revealed a 2 bp deletion in the ND2 gene in 90% of muscle mtDNA, but absent from lymphocyte mtDNA. Sequencing of the parents mtDNA revealed a paternal haplotype that matched the patients muscle mtDNA, but a maternal haplotype that matched the patients lymphocyte mtDNA. The 2 bp deletion was not present in either parent and is assumed to have arisen as a new mutation in the paternal germ line or during

embryogenesis. In embryogenesis metabolic needs are met by glycolysis and there is therefore no selection against mutant mtDNA [100]. Paternal mtDNA transmission has previously been reported only as a very rare event that occurs in crosses of different strains of laboratory mice [101]. Its occurrence in humans has not previously been reported, although detection methods may have been sub optimal.

Alternatively, mitochondrial disease caused by nuclear gene mutations may exhibit X-linked, autosomal dominant or autosomal recessive patterns of inheritance (table 1.1).

Table 1.1 Inheritance of Genetically Determined OXPHOS Disorders

Nuclear Gene Defects	**Inheritance**
Structural OXPHOS genes	AR
Non-structural OXPHOS genes	
Assembly defects	AR
Import defects	XR
nDNA-mtDNA communication	AR
Mitochondrial DNA defects	
Point mutations	Maternal
Single deletions	Sporadic
Multiple deletions	AR / AD
Depletion	AR

1.7.2 Heteroplasmy

Each cell contains two alleles of each nuclear gene, one paternally, and one maternally derived. Each cell however contains several hundred to several thousands mitochondria, each of which contains several mtDNA molecules [102]. Each cell therefore contains several thousand copies of each mtDNA genome. Silent polymorphisms in mtDNA usually affect all mtDNA molecules in a given individual, a state known as homoplasmy. In contrast, pathogenic mtDNA mutations usually affect a proportion of these molecules in each state. They therefore coexist with wild type molecules, a state known as heteroplasmy. The ratio of mutant to wild type can vary from cell to cell, and tissue to tissue. This mutant load can also vary over time if one population expands more rapidly than the other, or if a certain cell with a particularly high or low mutant load proliferates faster than other cells. This segregation may occur as a random event or due to selection advantages of particular cells.

MtDNA pathogenic mutations may exist in the homoplasmic state contrary to the above rule. For some time this has been known to be true for mutations causing Leber's Hereditary Optic Neuropathy [103], but more recently further evidence has accumulated regarding pathogenic homoplasmic mtDNA mutations [104]. A 35 year old woman was described who in ten pregnancies from four partners, had had one therapeutic termination, one live child with Leigh syndrome, and eight infant deaths, usually from cardiac failure and lactic acidosis at a maximum of 85 hours. Three of her siblings had died in early infancy. She herself had a past history of migraine, and a proximal myopathy was evident on examination. Muscle biopsy revealed a uniform decrease in COX activity, instead of the usual mosaic pattern seen as a consequence of heteroplasmic mutations. MtDNA sequencing revealed a C1624T $tRNA^{Val}$ mutation in the highly conserved dihydrouridine loop. The explanation for the mother's relatively asymptomatic survival remains a mystery [104].

1.7.3 The Threshold Effect

MtDNA mutations need to be present above a specific level before biochemical impairment and clinical features occur. This level or threshold varies between mutations and tissue types. In general the threshold is lower for more aerobically dependant tissues. In vitro studies have shown that both the A3243G and A8344G mutations cause a mitochondrial respiratory chain defect and impair intramitochondrial protein synthesis once the level of mutant mtDNA exceeds about 85% [66,105-107]. The extent to which this single factor accounts for phenotypical variation remains to be established. A high level of correlation between mutation load and clinical phenotype has been found in some studies [108-110], but not in others [107,111-114]. Other unidentified factors, environmental or genetic, have also been suggested to determine phenotype via modulation of the primary mtDNA defect [115 116,117].

1.7.4 Mitotic segregation

At cell division wild-type and mutant mtDNA molecules may segregate to the daughter cells unevenly. The level of heteroplasmy can therefore shift between passages of cells. Thus during embryogenesis larger amounts of mutant mtDNA can move into different cell lineages. This process of shift also means that thresholds can be exceeded at any point in time. The tissue distribution of different mtDNA mutations differs. Deletions, unlike point mutations are rarely present in peripheral blood samples. The variable segregation to different cell lineages could be an important factor in determining phenotype. If this theory were correct it would imply that the passing of deletions into all three germ layers would result in the Kearn Sayre syndrome (KSS),segregation into the haematopoietic lineage would cause Pearson marrow-pancreas syndrome, and segregation to muscle alone would result in chronic progressive external ophthalmoplegia (CPEO) [118].

1.7.5 The Bottleneck Phenomenon

A fertilised oocyte contains approximately 100,000 mtDNA molecules [119]. However only about 1000 of these will eventually repopulate the foetus. This dramatic reduction is

thought to take place in early oogenesis and is referred to as the bottleneck. This phenomenon was first observed in Holstein cows when heteroplasmy at position 346 shifted towards homoplasmy within a single generation [120]. Neutral mitochondrial genotypes were shown to segregate in different directions in the offspring of the same female. Heteroplasmy was shown to return to homoplasmy within only two or three generations. Previous insect studies had suggested much slower rates of mtDNA segregation. Fundamental differences are believed to exist in the mechanisms of mitochondrial gene transmission between different taxa. As a consequence of the bottleneck phenomenon the evolution of a polymorphism through generations is difficult to predict.

1.7.6 Secondary MtDNA mutations

There is evidence that secondary mutations, mitochondrial or nuclear, may influence the clinical or biochemical effect of primary mtDNA mutations. For example the A3243G common MELAS mutation has been shown to be 2.7 times more likely to cause stroke-like episodes if an A12308G nucleotide change is also present [121]. This secondary mutation exists as a neutral polymorphism in 16% of the population. Also in vitro studies have shown that the biochemical effects of the A3243G mutation are ameliorated by the presence of a G12300A mutation in the tRNA $Leu^{(CUN)}$ gene [122]. This was identified from a cell line containing 99% A3243G mutant mtDNA and exhibiting a severe defect in mitochondrial respiratory metabolism. A spontaneous derivative was isolated that, whilst still containing 99% mutant mtDNA levels, had reverted to the wild type phenotype as determined by normal respiration, growth characteristics in selective media, mitochondrial protein synthesis, and biogenesis of mitochondrial membrane complexes. The secondary G12300A heteroplasmic mutation within the tRNA $Leu^{(CUN)}$ gene was detected in this clone, and accounted for approximately 10% of its total mtDNA. The secondary mutation was predicted to generate a suppressor tRNA with the ability to decode UUR leucine codons, thus bypassing the deleterious effects of the A3243G tRNA $Leu^{(UUR)}$ mutation.

1.7.7 Immunological and Environmental factors

Evidence also exists for a role of immunological and environmental factors. The effects of ageing on the mitochondrial genome and the fact that some subunits show tissue specificity (such as 2 of the 13 complex IV subunits) may also be of importance in determining phenotypic expression.

1.8 MITOCHONDRIAL DISEASE

As our knowledge of the genetic mechanisms underlying mitochondrial disease has expanded, the need has arisen for a revised classification of these disorders [123,124]. They are now classified as class I (primary), and class II (secondary) OXPHOS defects to incorporate the concept of disease originating from either mitochondrial or nuclear genome defects (see table 1.2) [1,2]. The former represents the archetypal mitochondrial encephalomyopathies. Class II disorders are predominantly neurodegenerative disorders.

1.8.1 THE ARCHETYPAL MITOCHONDRIAL ENCEPHALOMYOPATHIES

The mitochondrial encephalomyopathies are a clinically diverse group of disorders. This diversity combined with their multi-system nature demands a high index of suspicion in order to ensure the detection of these progressive and potentially fatal disorders. The situation is further complicated by the complexities of mtDNA genetics, the limitations of investigation modalities including genetic analysis, uncertainties regarding potential therapeutic agents, and further limitations regarding prognostication.

The incidence of the mitochondrial encephalomyopathies is undoubtedly higher than often appreciated. An epidemiological study in Finland covered a population of 245,201 and identified 615 individuals with any of the symptoms reported to occur in the mitochondrial encephalomyopathy, lactic acidosis and stroke like episodes syndrome (MELAS). 480 of these were analysed for the common A3243G MELAS mtDNA point mutation. A mutation frequency of above 16.3/100,000 of the adult population was

Table 1.2

MITOCHONDRIAL DISORDERS

(Classification according to Leonard + Schapira 2001)

Class I: Primary OXPHOS defects

a. MtDNA mutations

i. large scale deletions, duplications involving protein coding genes and tRNA genes

ii. mutations of protein coding genes e.g. point mutations, small rearrangements.

iii. mutations of tRNA and rRNA genes.

b. Mutations of nuclear encoding OXPHOS subunits

including mutations affecting the gene promoter, mature protein or its mitochondrial targeting sequence.

Class II: Secondary OXPHOS defects

a. Genetic

i. abnormalities of mtDNA induced by nuclear gene defects affecting mtDNA transcription, translation, or replication.

e.g. autosomal dominant or recessive multiple deletions, or mtDNA depletion.

ii. direct damage to mtDNA or defects of mtDNA repair

e.g. frataxin deficiency and oxidative damage in Friedreich's ataxia

iii. defects of the import pathway of nuclear encoded OXPHOSsubunits

e.g. membrane receptors, protein processing, etc

iv. defects of the assembly of OXPHOS

e.g. chaperone mutations, defects of heme synthesis

b. Toxic

i. endogenous

e.g. free radicals including superoxide, nitric oxide, peroxynitrite

ii. exogenous

e.g. 1-methyl-4-phenyl 1,2,3,6 tetrahydropyridine, 3-nitropropionic acid, malonic acid, isoquinolines

established [125]. The high prevalence of the common MELAS mutation in the adult population suggests that mitochondrial disorders constitute one of the largest diagnostic categories of neurogenetic disease. A study in the northeast of England estimated a minimum point prevalence of 7.59/100,000 in those under the age of sixty-five years. 12.48/100,000 either had mtDNA disease or were at risk of developing it. This would make mtDNA disease as common as amyotrophic lateral sclerosis (point prevelance 6:100,000, annual incidence 1:50,000) or Huntington's chorea (point prevelance 5:100,000; annual incidence 0.4:100,000), and more common than Duchenne muscular dystrophy(prevelance 3:100,000, incidence among live born males 20-30:100,000) or myotonic dystrophy (1:8000 live births) [126]. Furthermore, the A3243G mutation has been found in 0.9% of unselected patients with diabetes mellitus (DM), and in 1.6% of those with matrilineal DM [127].

The first report of disease resulting from mitochondrial respiratory chain dysfunction was published in 1962. A 35 year old woman developed severe euthyroid hypermetabolism and a mitochondrial respiratory chain defect resulting in the uncoupling of oxidation and phosphorylation in muscle mitochondria[129]. Further cases were reported [130], and these cases also described heat intolerance, profuse sweating, polyphagia, and polydipsia without polyuria. Muscle weakness was mild. Ragged red fibres (RRFs) were found on skeletal muscle biopsy. This histological change, which came to be the defining feature of mitochondrial myopathies [131], represents the peripheral and intermyofibrillar proliferation and accumulation of structurally abnormal mitochondria (Figure 1.5). RRFs were later noted to be associated with progressive external ophthalmoplegia [132,133] and with other myopathic syndromes lacking ophthalmolplegia. Subsequently, RRFs were also identified in patients with non-myopathic central nervous system manifestations of mitochondrial disease. This realisation led to the introduction of the term "mitochondrial encephalomyopathies". Non-myopathic cases may present with any of a vast range of neurological symptoms including cognitive impairment manifesting as psychomotor retardation or dementia, movement disorders and ataxia, stroke, seizures, retinopathy or deafness, or peripheral neuropathy in various combinations and permutations, leading to the identification of the archetypal encephalomyopathies [134-136].

A number of mitochondrial encephalomyopathy syndromes have subsequently been delineated. Common to all is the phenotypic and genotypic diversity. The correlation between phenotype and genotype is poor and a complete explanation for this remains elusive. In the majority of these conditions, a wide range of potential clinical manifestations are described in addition to the core clinical features, and a wide range of disease causing mutations have been described, in addition to the commonest mutation.

1.8.1.1 Chronic Progressive External Ophthalmoplegia / Kearns Sayre Syndrome (CPEO / KSS)

Chronic progressive external ophthalmoplegia is one of the commonest manifestations of mitochondrial myopathy. Presentation is with slowly progressive ptosis, and multidirectional limitation of eye movements, affecting upgaze maximally. In Kearns Sayre syndrome CPEO is accompanied by pigmentary retinopathy, and one or more of complete heart block, a CSF protein level of above 1 g/l, and ataxia [137].

In 1988 Ian Holt made the seminal discovery of single large scale deletions on mtDNA in patients with mitochondrial myopathies [145]. The following year Zeviani showed that these deletions were consistently associated with KSS [146]. This mtDNA abnormality is detectable in DNA extracted from muscle samples of CPEO/KSS, but blood mtDNA analysis is normal. Deletions lack segments of DNA in the major arc between O_H and O_L and most are flanked by direct sequence repeats [147,148]. These deletions are found in 80% of those with KSS, and 70% of those with CPEO [149]. MtDNA duplications are also occasionally found [149]. Conversely, all patients with single mtDNA deletions and neurological disease have CPEO, with only two exceptions to this rule described [150,151]. Histological examination of muscle reveals RRFs and a mosaic pattern of COX negative fibres. Patients with mtDNA deletions present as sporadic cases [152]. Other CPEO patients show a maternal pattern of inheritance and in these cases mtDNA point mutations are detectable. This is most commonly the A3243G MELAS mutation, although several other point mutations have also been detected [153]. Autosomal dominant and recessive pedigrees

also occur. In contrast to sporadic cases, these are associated with multiple mtDNA deletions that arise secondary to nuclear gene defects [146,154]. Three loci have been associated with adPEO, 4q34-35, chromosome 10q24, and 15q22-q26 [155-158]. Mutations in the genes encoding adenine nucleotide translocator (ANT-1), DNA polymerase γ (Pol γ), and Twinkle have been identified [159-161]. ANT-1 forms a homodimeric inner mitochondrial membrane channel for the exchange of ADP into and ATP out of the mitochondrial matrix. In addition ANT is a component of the mitochondrial permeabiliy transition pore that has a pivotal role in mitochondrially-mediated apoptosis [159]. Twinkle has homology to bacteriophage helicases, and mutations identified to date are believed to alter its dNTPase activity with consequent mitochondrial nucleotide pool imbalance [162]. Mutations of the catalytic unit of POLγ have been identified, but their functional significance is as yet undetermined [158]. This finding suggests that disorders of mtDNA replication can also be responsible for mtDNA deletions. Models for the generation of deletions have been proposed and include "slip-replication" and "illegitimate-elongation" [163,164].

The size of the deletion does not correlate with the clinical phenotype, in the same way that although a wide variety of deletions have been described, each removing a different set of mitochondrial genes, all KSS patients have fundamentally the same phenotype. This is thought to occur brcause mtDNA that remains and is transcribed, will still not be able to be translated due tot the fact that tRNAs, scattered around the genome are also removed by the deletion. Every documented pathogenic mutation in KSS or PEO removes at least 1 tRNA gene. If wild type mtDNA co-exists at a high enough level though, it can compliment this deficiency.

1.8.1.2 Mitochondrial Encephalomyopathy, Lactic Acidosis, and Stroke Like Episodes (MELAS)

In 1984, MELAS was described by Pavlakis as a distinct clinical syndrome within the spectrum of mitochondrial disorders[171]. This original report described two cases and nine other similar cases from the literature. Normal early development was later complicated by stunted growth, the development of focal and generalised seizures, and recurrent

neurological deficits resembling strokes. Additional clinical features have been described in association with the core features of MELAS [172]. The phenotypic consequences of this mutation and the common MERRF mutation have been compared (Table 1.3).

Of all cases meeting the clinical criteria for MELAS, 80 % are positive for an A to G transition at base pair 3243 within the tRNA Leu^{UUR} gene [199,200]. A large number of different mutations have also been found to result in the MELAS phenotype. A G13513A mutation in the ND5 gene was also associated with recurrent focal cortical brain hematomas in a child with MELAS [201]. Conversely, of all cases with the 3243 mutation from an unselected population of 17 patients with mitochondrial myopathy, 50% were found to fulfil the criteria for MELAS at the time of clinical assessment [140]. Theoretically further cases could develop these clinical features with the passage of time. Mutations in protein coding genes (ND5 and COX III) have also been reported in patients with clinically typical MELAS [202-204].

1.8.1.2.1 Pathogenesis of the A3243G common MELAS mutation:

Disease associated mutations have been identified in 20 of the 22 mt tRNA genes, and it seems likely that the two remaining tRNAs ($tRNA^{Arg}$ and $tRNA^{His}$) will be added to this list in the future. Certain tRNAs such as $tRNA^{Leu(UUR)}$, $tRNA^{Lys}$ and $tRNA^{Ile}$ appear to be hot spots for mutations whilst other tRNA genes are less often affected. Most pathogenic mutations affect highly conserved nucleotides whereas most polymorphic mutations affect rather non-conserved nucleotides. However exceptions to this rule do exist. Furthermore, the type of mutation (transition or transversion), the distribution on the secondary structural domains, and their structural effect in stems also fail to completely distinguish polymorphic and disease associated mt tRNA mutations.

Despite the identification of the A3243G common MELAS mutationin in 1990 [199], an accepted explanation of how this mutation causes disease, and in particular how it causes such a diverse spectrum of phenotypes was slow to appear. This hampered the development of therapeutic interventions or preventative strategies which had to rely on

educated guesses alone. A body of literature has focused on the relationship between mutant load, and tissue distribution of mutations and the severity of the clinical phenotype. Whilst there is a lot of evidence to support the threshold theory, it is also apparent that other factors must be involved in the pathway from mutation to disease.

Much of the initial investigations into the mechanism of the A3243G mutation focused on the fact that the mutation lies within the mtDNA binding site for mTERF, a protein factor that promotes termination of transcription at the 16S rRNA / $tRNA^{Leu(UUR)}$ boundary. *In vitro* assays revealed a marked decrease in affinity of purified mTERF for the mutant target sequence. By contrast, in transformants carrying the MELAS mutation, despite severe protein synthesis and respiration defects, RNA transfer hybridisation experiments failed to show any significant change in the steady-state amounts of the two rRNA species encoded upstream of the termination site, and of the mRNAs encoded downstream [68,574]. In addition the reduction in labelling of the various mitochondrial translation products in defective transformants is not correlated to their UIUR-encoded leucine content, thus arguing against an effect of the MELAS mutation on the function or stability of the $tRNA^{Leu(UUR)}$ [575]. Altered RNA processing has also been implicated in the pathogenesis of the A3243G mutation, after the identification of the accumulation of a novel RNA transcripts, termed RNA 19, in immortalised cell lines and patient tissue samples. This abnormal transcript corresponds to 16S rRNA plus $tRNA^{Leu(UUR)}$ plus subunit 1 of the NADH-coenzyme Q-oxidoreductase gene [576].

Cybrid analysis has been a cornerstone of this field of research. This in vitro scenario has many potential limitations. Studies in osteosarcoma and lung carcinoma cell lines have suggested that the mutant tRNA is functionally deficient and thus less able to decode Leu UUR codons. Impaired aminoacylation [711,581], low levels of base modification within the D-stem [712], and low steady state levels in some cell lines[122] but not others[713] have all been observed. This loss of function mechanism would be consistent with the observed threshold effect that results in impaired MRC function and loss of mitochondrial protein synthesis.

Other cybrid studies, predominantly those using Hela cells, have given conflicting results. Despite lower levels of the mutant tRNA aminoacylation is minimally affected [577]. The mutant tRNA lacks the wobble base U hypermodification. This feature normally confers specificity of codon recognition, and without it phenylalanine UUY codons may also be translated by $tRNA^{Leu(UUR)}$. This mechanism would confer a gain of function that would result in an impairment of mitochondrial protein synthesis.

The picture is complicated further by studies in patient derived lymphoblastoid cell lines that have shown no effect of the mutation on $tRNA^{Leu(UUR)}$ levels or the level of mitochondrial protein synthesis. There was however reduction of the relative amounts of incorporation of leucine into some mitochondrial translation products [578]. The inference was that the mutant tRNA may be mischarged with incorrect amino acids or that the affinity of the mutant tRNA for the codon is impaired allowing other tRNAs to incorporate the wrong amino acid at UUR codons. In this setting mutant levels as low as 70% significantly reduced complex IV activity. Gain of function mechanisms would explain the presence of the disease in patients with mutant levels below the threshold levels found in cybrid studies. Other potential gain of function mechanisms have been proposed, and include a role for precursor-like RNA molecules that are believed to accumulate in mutant cells and interfere with ribosome function [122,579].

In vivo protein synthesis studies may clarify the picture but are currently lacking. However, it may be that these apparently conflicting views are in fact both correct. Studies in A549 cells support the loss of function hypothesis. A heteroplasmic anticodon mutation within $tRNA^{Leu(CUN)}$ generates a novel tRNA capable of reading UUR. This suppresses the protein synthesis defect and respiratory impairment of cells with high A3243G mutant loads [122]. This phenotype suppression effect is transmitted along with the "suppressor mtDNA" to successive generations [580]. In the 143B nuclear background abnormal translation products are present at mutant loads below the threshold levels normally accepted to cause total loss of mitochondrial translation [69]. As in lymphoblasts respiratory deficiency occurs at levels at which protein synthesis appears normal [69,581]. Despite proteins appearing to be synthesised at normal rates, the proteins generated may

not be totally normal. Low but functionally significant levels of amino acid misincorporation have been reported [580]. High mutant A3243G levels have also been associated with as yet unidentified structural modification of $tRNA^{Leu(CUN)}$ [122]. This may represent a compensatory or partial suppressor mechanism allowing a proportion of $tRNA^{Leu(CUN)}$ to read UUR codons.

The question will always remains as to whether all of these in vitro changes represent primary or secondary effects of the mutation. Cybrid studies utilise immortalised, usually tumour derived, cell lines. The nuclear material of these cells is not normal with high rates of aneuploidy that vary even within a single cell line and within a single culture.

In vivo studies of mutant $tRNA^{Leu(UUR)}$ levels and aminoacylation efficiency in muscle biopsies from A3243G patients have shown defects of both in most patients. In some however, one parameter was low and the other normal, and in one patient no abnormality was apparent. Four different patterns were therefore seen. The patients studied however all had similar phenotypes at the far end of the spectrum of disease associated with this pathogenic mtDNA mutation [582].

The role of nuclear genes, mitochondrial haplotype, developmental background, and epigenetic factors remains unestablished. The primary effect of the mutation on tRNA function has also not been fully explored. Potential mechanisms of interest include the level of expression of other tRNAs, such as $tRNA^{Phe}$. Incorrect modification of normally aminoacylated mutant $tRNA^{Leu(UUR)}$ may result in frequent misreading of the Phe codon. The Leu(UUR) and Phe tRNAs would then compete for the UUY codon and the generation of abnormal translation products would then depend upon the relative levels of these two tRNAs. $TRNA^{Phe}$ synthesis is almost entirely dependent upon not the full length overlapping H strand, but the rRNA transcription unit, the termination of which is inhibited by the 3243 mutation [583]. In a different background aminoacylation of the mutant tRNA may be the limiting factor. The relationship between mutant load and phenotype would therefore differ due to this loss of function mechanism. Recent studies have focused on wobble modification deficiency in mutant tRNAs in patients with

mitochondrial diseases. Mt $tRNA^{Leu(UUR)}$ containing the A3243G mutation has previously been shown to be deficient in a normal taurine containing modification (taum5U;5-taurinomethyluridine) at the anticodon wobble position. This is believed to result in a UUG codon specific translational defect (A5). This has been demonstrated in cybrid cells with different nuclear backgrounds as well as from patient tissues (A1). Correlation with clinical phenotype has also been shown by comparing $tRNA^{Leu(UUR)}$ mutations known to cause a MELAS phenotype and those causing milder disease (A2).

Nuclear factors may influence the expression of mtDNA mutations. In yeast, a mutation in the initiation codon of the mitochondrial COX III was suppressed by a reduction in the level of cytoplasmic ribosomal protein S18 [584]. This effect was believed to be mediated by changes in cytoplasmic translation accuracy or by products that affect mitochondrial protein synthesis. Suppression of mutated tRNA function has also been reported. Again in yeast, a mutated $tRNA^{Asn}$ causing impaired maturation could be compensated for by the presence of additional copies of the mitochondrial Ef-Tu and aspartyl-tRNA synthetase [585]. In humans, a secondary mutation in $tRNA^{Leu(CUN)}$ has been shown to suppress the effects of the archetypal MELAS A3243G $tRNA^{Leu(UUR)}$ mutation. This occurs because the secondary mutation enables the $tRNA^{Leu(CUN)}$ to recognise UUR codons [122]. Recently a G5703A mutation that causes a severe mitochondrial protein defect and a reduction in the steady state levels of $tRNA^{Asn}$, has been shown to generate revertant lines due to presumed nuclear gene factors. These revertant clones contained homoplasmic levels of the mutation, but did not exhibit the biochemical defects and had normal OXPHOS activity. When the mitochondria were transferred to a novel nuclear background the original defective phenotype was restored [586].

The effect of mtRNA mutations on the pattern of mitochondrial proteins at a broader level has been assessed using comparative proteomics as a tool to evaluate several hundred mitochondrial proteins. In cybrid cell lines carrying the A3243G MELAS or the A8344G MERRF mutations, large quantitative decreases were apparent for COX Va and COX VIa, two nuclear encoded subunits of cytochrome c oxidase. This finding opens yet

another avenue through which to explore the pathogenic mechanisms of mitochondrial tRNA mutations.

1.8.1.3 Myoclonic Epilepsy and Ragged-Red Fibres (MERRF)

The syndrome of myoclonic epilepsy and red ragged fibres (MERRF) was first described in 1980 [135], although the association between progressive myoclonic epilepsy and ragged red fibres had been described seven years previously [205]. Subsequently the role of mtDNA mutations in the pathogenesis of MERRF was documented [206]. The core clinical features are of myoclonus, ataxia, and seizures.

The most commonly detected mutation, found in approximately 80% of cases fulfilling the clinical criteria for MERRF, is at position 8344 within the tRNA Lys, and was first reported by Shoffner in 1990 [206]. The relationship between mutant load and phenotype has revealed a positive correlation in some reports [140,206,210] but not others [211]. Other mutations within the same tRNA gene (T8356C and G8363C) are also described in association with MERRF [209,212]. Insertion of a C nucleotide at position 7472 in the tRNA Serine UCN gene results in a syndrome of hearing loss, ataxia, and myoclonus that is very similar to MERRF [213]. MERRF has also been reported in patients harbouring multiple mtDNA deletions [166], and overlap syndromes with features of both MERRF and MELAS have been reported for the T7572C and T8356C tRNA Serine$^{(UCN)}$ mutations.

MELAS and MERRF are thus both phenotypically highly variable, in terms of age of onset, organs involved and severity of symptoms [115,200,211]. Both mutations in vitro cause mitochondrial respiratory chain defects, and impaired intramitochondrial protein synthesis, above a specific threshold of about 85% [210,216]. It is generally accepted that variation in the percentage mutation load is the principle factor responsible for the varied clinical presentation of mtDNA defects [216,217] however previous studies have only found a weak correlation between the mutation load and the clinical phenotype [107,110,112-114]. This may be explained by intercellular heteroplasmy but secondary factors as discussed above may also be aetiologically significant.

Analysis of 245 individuals with the A3243G of A8344G mutation showed a strong correlation between the frequency of the more common clinical features and mutant load in muscle however no relationship with mutant load in blood was shown [186]. Thus percentage mutant mitochondrial DNA in muscle has been proposed, but not yet widely accepted, as a useful prognostic indicator.

The relationship between maternal mutation load and the frequency of clinically affected offspring has also been examined in an attempt to guide genetic counseling [218]. These studies concluded that the higher the level of mutant load in mother's blood the higher the frequency of affected offspring, and at any one level of mutant load, the number of affected offspring was found to be always greater for the A3243G mutation than for the A8344G MERRF mutation. These two mutations both involve tRNA genes and have similar effects on respiratory chain function in vivo [136]. The reason for different inheritance patterns is therefore unclear. Mothers with A3243G have a high (>25%) frequency of affected offspring what ever their mutant load. Women with less than 40% A8344G have a relatively low frequency of having an affected child [218]. Prospective studies are required to provide sufficient information for predictive genetic counselling purposes.

Table 1.3

Clinical features of the A8344G MERRF and A3243G MELAS mutations (from [186])

Clinical feature	A3243G	A8344G
Recurrent stroke	48 %	1 %
CPEO	28	6
Diabetes mellitus	15	3
Pigmentary retinopathy	15	0
Deafness	44	39
Dementia	27	25
Epilepsy	50	43
Myopathy	53	70
Short stature	15	13
Lipomata	1	8
Optic atrophy	1	13
Neuropathy	5	24
Ataxia	24	50
Myoclonus	8	61

1.8.1.4 Neurogenic Muscle Weakness, Ataxia, and Retinitis Pigmentosa (NARP)

First described by Holt et al in 1990, the key features are peripheral neuropathy, ataxia, retinitis pigmentosa, seizures and dementia [219]. Inheritance is maternal. The commonest mutation is a T to G transversion at nucleotide position 8993. This causes a change from the highly conserved leucine to arginine within subunit 6 of the mitochondrial F_0F_1 ATP synthase. This mutation has also been identified in several cases of maternally inherited Leigh syndrome (MILS) [220], and both LS and MILS have been reported within the same

family [221]. A T8993C transition replacing leucine with proline has been reported in one NARP/MILS family [222] and also in one patient with LS [223]. Both of these mutations involve a conserved charged region of ATP synthase which is associated with the proton channel of this enzyme complex [224]. These changes may interfere with the utilisation of the electrochemical gradient to produce ATP [10].

Patients with NARP usually have above 80% mutant mtDNA levels. With mutant mtDNA levels below 75% patients usually suffer from pigmentary retinopathy alone, or suffer migraines, or are asymptomatic [225]. This illustrates the good correlation between mutant load and disease severity that is not present in the majority of the other mitochondrial encephalomyopathies.

1.8.1.5 Leigh Syndrome (LS)

This subacute necrotising encephalomyelopathy was first described in 1951 [228]. Its characteristic neuropathology is of bilateral symmetrical focal necrotic lesions within the thalamus, extending into the pons, inferior olives and spinal cord. The clinical features of LS are of psychomotor retardation, hypotonia, failure to thrive, respiratory abnormalities, oculomotor disturbances, optic atrophy, seizures and lactic acidosis. Biochemical abnormalities include defects of oxidative phosphorylation (in particular complex I [229] or complex IV [230], and deficiency of the pyruvate dehydrogenase complex [231] and biotinidase deficiency [232]. Ragged-Red fibres are absent.

The majority of LS cases are believed to result from nuclear gene defects [233,234]. This has been confirmed for cases of LS with deficiency of the PDH complex [233], complex I [80], and II [77]. The majority of children with complex IV deficient LS harbour mutations in the surfeit-1 housekeeping gene [235,236]. This gene is involved in the complex process of complex IV assembly [237-239]. Mutations in other complex IV assembly genes have been identified. These include SCO2 (*S*ynthesis of *C*ytochrome *O*xidase gene) mutations in three unrelated infants with fatal cardio-encephalomyopathy and isolated complex IV deficiency [240]. All were compound heterozygotes and all had an E140K mutation on one

allele. SCO 10 (heme A farnesyltransferase) mutations have been identified in complex IV deficient patients with LS and DeToni-Fanconi-Debre syndrome [241]. This enzyme catalyses the first step in the conversion of protoheme to the heme A prosthetic groups of cytochrome oxidase. SCO1 mutations have also recently been reported in a single family with multiple cases of neonatal ketoacidotic coma and isolated COX deficiency [242]. Deficiency of heat shock protein (Hsp) 60, a mitochondrial matrix protein involved in the assembly and folding of polypeptides into many complex mitochondrial enzymes, is also known to result in multiple mitochondrial inner membrane enzyme deficiencies, and a fatal systemic mitochondria disease [243,244]. The underlying genetic defect is not established.

The BCS1 gene is involved in complex III assembly, and mutations within this gene have been detected in six patients from 4 unrelated families with neonatal proximal tubulopathy and hepatopathy [245]. This gene may be a frequent cause of complex III deficiency.

Nuclear gene defects are also presumed to be causal for cases of LS with biotinidase deficiency. Mutations in the E1α subunit of PDH have been identified in X-linked and sporadic cases. Up to 20% of LS patients have the T to G, or T to C, mtDNA mutation at position 8993 within the ATPase 6 gene of complex V [234]. Mutant loads are above 90%, and lower levels of this mutation are associated with the neurogenic muscle weakness, ataxia, and retinitis pigmentosa (NARP) syndrome. High levels of the A3243G MELAS mutation and the A8344G MERRF mutation have also been reported in LS [234]. Other mtDNA mutations described include G1644T within the tRNA Val gene [246], and deletions [247] and depletion of mtDNA levels [248]. The ATPase 6 mutations T8851C and T9176C are also associated with bilateral striatal necrosis and with maternally inherited LS [249,250].

1.8.1.6 Mitochondrial DNA Depletion Syndrome

This quantitative disorder of mtDNA was first described in 1991 [251]. More than 30 cases of this severe (up to 99%) tissue specific reduction in total mtDNA copy number have now been described [252], and this syndrome thus represents a relatively common cause of lactic acidosis in infancy. Clinical heterogeneity is marked, but typically neonatal or infantile fatal lactic acidosis is associated with severe hypotonia, and progressive liver failure. Seizures, ophthalmoplegia, Fanconi syndrome, congestive cardiac failure, and cataracts are also described. The clinical course is often rapidly fatal with death before the first year.

There has been no evidence of maternal transmission. Some cases are sporadic, and some autosomal families are also described. In vitro complementation studies concluded a nuclear gene defect to be responsible for this syndrome [70]. This syndrome is both clinically and genetically heterogeneous. Mutations in the deoxyguanosine kinase gene (DGUOK - chromosome 2p), and mitochondrial thymidine kinase gene (TK - chromosome 16q) have been identified in kindreds of Druze Israeli descent [254,255]. Both of these enzymes are responsible for the salvage of nucleotides within mitochondria. There is no *de novo* synthesis of nucleotides within mitochondria, and their only other source is from the import of cytosolic nucleotides. In non replicating cells cytosolic dNTP synthesis is down regulated, forcing mitochondria to rely on these nucleotide scavenging pathways.

Depletion of mtDNA can also be secondary, occuring in inclusion body myositis, or iatrogenic, as occurs in patients receiving nucleoside analogues. MtDNA is also reported in Alpers' syndrome and Navajo hepatopathy [256,257], but it is unclear whether it represents a primary or secondary event in these conditions.

1.8.1.7 Myoneurogastrointestinal Encephalopathy (MNGIE)

This recessively inherited syndrome was first described in 1987 [258] and the term MNGIE was proposed in 1994 [259]. Diagnostic criteria include peripheral neuropathy, CPEO, gastrointestinal dysmotility, in combination with histological features, namely RRFs,

increased SDH staining or ultrastructurally abnormal mitochondria [259]. A variety of oxidative phosphorylation enzyme defects have been reported in these patients including isolated partial complex IV defects and combined enzyme defects. Molecular defects are usually of multiple mtDNA deletions. MtDNA depletion is also described [260]. Homozygous and compound heterozygous mutations within the thymidine phosphorylase gene (chromosome 22q13.32-ter) have been identified [261]. The mechanism by which these mutations result in multiple deletions is uncertain.

1.8.2 THE NON-ENCEPHALOMYOPATHIC ARCHETYPAL MITOCHONDRIAL DISORDERS:

Leber Hereditary Optic Neuropathy (LHON) is a maternally inherited bilateral acute or subacute painless optic neuropathy. 90% of patients present before the age of 45, with mean age of onset of 23 years. 85% of patients are male. The majority of cases result in severe and permanent visual loss. Acuity may deteriorate to less than 6/60 over a period of a few weeks [262].

Three mtDNA point mutations, all lying within the complex I genes, account for the vast majority of cases. The G11778A mutation in the ND4 gene is found in 50-70% of LHON cases, the G3460A mutation in ND1 in 15-25%. A mutation at nucleotide 14484, within the ND6 gene, is associated with a better prognosis with some visual recovery in 70% of those affected [263]. The mutations are detectable in blood, and are often homoplasmic, in contrast to the point mutations found in the other mitochondrial encephalomyopathies.

Complex I deficiency has been demonstrated in the muscle and platelets of some patients [265,266]. Only 15% of females carrying one of the primary mutations are clinically affected. This led to the hypothesis of an X-linked susceptibility locus [267], but linkage analysis has not supported this [268].

Pearson marrow-pancreas syndrome was described in four unrelated children in 1979. These infants presented with refractory sideroblastic anaemia, vacuolation of erythroid and myeloid precursors within the marrow, and exocrine pancreatic failure [295]. All reported cases harbour mtDNA rearrangements (deletion, duplication, or both) [296]. Cases are usually sporadic, although maternal inheritance has been reported [297]. Mortality in Pearson syndrome is high. Occasional cases show spontaneous improvement of the anaemia, reflecting the clearance of mutant mtDNA from rapidly dividing haematopoietic tissue. In slowly dividing tissues however mutant mtDNA may accumulate. In this way multisystem features, including KSS, may gradually develop [298]. The spectrum of mtDNA re-arrangements is similar in both KSS and Pearson syndrome, suggesting that they may both be part of the same disease entity although KSS is less clinically severe. There is no correlation between the type, size, or location of the mtDNA arrangements and clinical course.

1.8.3 BIOCHEMICAL CLASSIFICATION OF MITOCHONDRIAL DISEASE

Mitochondrial respiratory chain activity can be analysed in any tissue, but most commonly muscle or platelets. Whole, fresh or frozen muscle samples can be used, or mitochondrial preparations can be fractionated from tissue samples. Analysis can be performed by polarography or spectrophotometric methodologies. In this way deficiencies of each of the mitochondrial respiratory chain complexes can be identified. Complex I deficiency is associated with a wide spectrum of mitochondrial disorders, most commonly as LS [234]. It is probably the commonest respiratory chain defect associated with MELAS and MERRF, and occurs in isolation or with complex III and/or IV defects [310-312]. Complex I deficiency has also been found in CPEO and mtDNA deletions [313]. The deleted region in these cases encompassed only complex I genes and the intervening tRNAs. These are the only examples where the deleted mtDNA genes correspond exactly with the biochemical defect. LHON is also associated with complex I defects.

Complex II deficiencies are less common, but again are associated with a wide clinical spectrum. Complex III deficiency is usually not an isolated defect [314]. Complex IV defects may result from mutations of mtDNA encoded subunits, or from mutations of assembly genes (Table 1.4). The clinical spectrum is again diverse, and includes LS, benign and fatal infantile myopathies and cardiomyopathies, adult onset myopathies, MNGIE, MERRF, and MELAS.

Table 1.4

NUCLEAR GENE DEFECTS RELATED TO MITOCHONDRIAL DISORDERS

1 Structural components of RC complexes

Protein	Function	Phenotype
NDUFS4	CxI	Atypical LS
NDUFS8	CxI	LS
NDUFV1	CxI	LS, leukodystrophy, myoclonus
NDUFS1	CxI	LS
NDUFS7	CxI	LS
Flavoprotein	CxII	LS
SDHD, SDHC	Cx II	Hereditary paraganglioma
CoQ10 synthesis	Cx I II III	Ataxia, myopathy, epilepsy

2 Factors controlling OXPHOS or mtDNA metabolism

Protein	Function	Phenotype
SURF1	COX assembly	LS
SCO1	COX assembly, Copper metabolism	IE
SCO2	COX assembly, Copper metabolism	Infantile CM
COX 10	COX assembly, heme A synthesis	IE
BCS1	Complex III assembly	IE, tubulopathy, hepatopathy
ANT1	Nucleotide pool	adPEO
Twinkle	Helicase	adPEO
Thy phos	Nucleoside pool	MNGIE

3 Mt proteins indirectly related to OXPHOS

Protein	Function	Phenotype
Tim 8/9	transporter	X dystonia deafness
ABC7	iron exporter	X ataxia/ sidero anaemia
Frataxin	iron storage	Friedreich's ataxia
Paraplegin	metalloprotease	HSP
OPA1	dynamin-related protein	AD Optic Atrophy

1.9 PATHOGENIC MECHANISMS OF MtDNA MUTATIONS

The pathogenesis of mitochondrial DNA mutations is only partly explained by the rules of mitochondrial genetics. The influence of heteroplasmy, the bottleneck effect, threshold, and mitotic segregation on the phenotypic consequences of mtDNA genotypes has been discussed above. However, despite these theories, the poor genotype-phenotype correlation typical of the mitochondrial encephalomyopathies remains to a great extent unexplained.

Mutations in tRNA genes are usually associated with multisystem disease. In cases of isolated myopathy a family history is usually lacking, the inference being that the mutations arise spontaneously. In most patients the mtDNA mutation is also detectable in blood and fibroblasts suggesting that the phenotype is a consequence of "skewed heteroplasmy" with preferential accumulation of the mutation in skeletal muscle [315].

As the spectrum of mitochondrial disorders widens other phenotype-genotype correlations have proved invalid. Protein coding gene mutations, as in LHON and NARP/MILS, were thought to always cause multisystem, maternally inherited, disease and to be inconsistently accompanied by lactic acidosis and never associated with RRFs [284]. The evaluation of patients with exercise intolerance, with or without myalgia and myoglobinuria due to ND4, ND1, cytochrome b, COX III, and COX I mutations disproved these rules [316-321].

Our understanding of the phenotypic consequences of mtDNA mutations will be enhanced by the recent development of several animal models of mitochondrial disease (see chapter 4). Until now reliance has been on the use of cybrid cell technology. Human cell lines are depleted of mtDNA using a variety of agents. These mtDNA-less (ρ^0) cells can then be repopulated with heteroplasmic mtDNA to generate clones of varying degrees of heteroplasmy. This in vitro system has a number of potential limitations. Cybrid cells require a high percentage of A3243G mutant mtDNA to be present before OXPHOS is impeded. *In vivo* studies suggest a much lower threshold effect. Calf muscle magnetic resonance spectroscopy from an oligosymptomatic patient revealed markedly

decreased maximal ATP production despite the fact that the mutant load was very low in muscle [322]. Proton MRS has shown elevated lactate in the brain of A3243G carriers, and that the relationship to the proportion of mutant mtDNA was linear as opposed to the exponential pattern usually seen for the threshold effect [323].

1.10 MODELS OF MITOCHONDRIAL DISEASE

The pathogenesis of mitochondrial disease remains obscure. There is still little understanding of the causes of clinical heterogeneity and progression of symptoms, and this lack of knowledge has hindered the development of directed therapies. The quest for a greater understanding of the pathogenesis of human mitochondrial diseases and the desire for systems in which to evaluate potential therapeutic agents have stimulated attempts to develop both *in vivo* and *in vitro* models of mitochondrial diseases. A number of strategies have been developed based on cellular and animal models.

Primary myoblast or fibroblast cultures, established from muscle or skin biopsies of patients with mitochondrial disease, have been used as cellular models of mitochondrial disease [587]. Transformed cell lines rendered ρ^0, transmitochondrial hybrids (cybrids), and xenocybrids have also been employed to this end. The latter is a technique unique to mitochondrial biology. Cloning provides cell lines of varying mutant load. The lifespan of these cell lines in culture is limited, but they have been used for the investigation of transcription, translation, threshold effects, and segregation of mtDNA mutations [106]. Cell lines devoid of mtDNA (ρ^0 cells) can be generated in a number of ways. From these ρ^0 cells transmitochondrial cybrids can be generated by fusion with platelets or enucleated cells. This technique allows the study of the effect of different levels of mutant mtDNA on transcription, translation, and respiratory chain function in a constant nuclear background.

The generation of inter-specific (xenomitochondrial) cybrids, as first suggested by Kenyon and Moraes [588], has provided both an alternative approach to generating OXPHOS defects in mouse cells, and also provided opportunities to explore cross-species

nuclear-mitochondrial interactions. MtDNA divergence is about 5-13 times more rapid than in nuclear DNA (nDNA) [589]. Therefore as species evolve a general incompatibility between nuclear and mitochondrial encoded gene products would be expected. This is predicted to occur between pairs of even recently diverged taxa [590]. The complete mtDNA sequence for mouse, rat, and a number of non-human apes have been determined (Bibb 1981) [591], and provides a very clear picture of the evolution of mtDNA in these species. Despite a relatively high number of sequence variations, once non-coding and synonymous mutations are ignored, a high level of functional homology is revealed [591]. Even between human and orang-utan this homology exceeds 95%. The co-evolution of the nuclear and mitochondrial genomes in vertebrates, and how these interactions evolved to optimise OXPHOS are poorly understood.

Prior to the work on Kenyon and Moraes the maintenance of mitochondrial genomes in interspecies somatic hybrids had been dependent upon the presence of a complete set of cognate chromosomes [592-594 595]. It has subsequently been shown that OXPHOS function in human ρ^0 cell lines can be restored by the insertion of mtDNA from other humanoid primates including the common chimpanzee (*Pan troglodytes*), pigmy chimpanzee (*Pan paniscus*), and gorilla (*Gorilla gorilla*). These results suggest that in primates mitochondrial nuclear compatibility had been preserved over approximately 5-12 million years (myr). MtDNA from orang-utan (*Pongo pygmaeus*) however, a species that diverged from other humanoids 12-18 million years ago, is unable to functionally replace human mtDNA implying an increase in failed mitochondrial nuclear interactions at this degree of evolutionary distance. The critical nNDA-mtDNA interactions that have been affected in unsuccessful xenomitochondrial cybrids are not known. Potential candidates include primate promotor recognition by the nuclear-coded human mitochondrial RNA polymerase [596]. Further studies on human-chimpanzee or human-gorilla xenocybrids revealed a 20-30% reduction in oxygen consumption and a 40% decrease in complex I activity, attributable to defective interactions between nDNA and mtDNA encoded complex I subunits [597]. These cybrids also exhibited an increased sensitivity to programmed cell death when treated with complex I inhibitors [324].

Transmitochondrial mouse cells have been created using *mus musculus* ρ^0 cells and mtDNA from *rattus norvegicus* or *mus spretus* [589]. Evolutionary distances are controversial but believed to be 10-12 myr and 1 myr respectively [598]. Both fusions generated viable cybrids. The mouse-mouse xenocybrid product exhibited normal OXPHOS function. The mouse-rat xenocybrid showed normal replication, transcription, and translation (as determined by S^{35} methionine labelling) but complex I activity was 46%, complex III 37%, and complex IV 78% of control values. The maximal rate of respiration, analysed polarographically, was 12-31% of control and *mus spretus-mus musculus* xenocybrids. It is anticipated that the generation of other mouse xenocybrids with less severe OXPHOS phenotypes will provide models of a broader spectrum of human mtDNA diseases.

The retention of both species of mtDNA in mouse-rat and mouse-hamster xenocybrids has also been reported. However it is not known whether both species of mtDNA are expressed or whether one set is selectively repressed [599]. The uniparental loss of mtDNA has been shown to occur in parallel with chromosomal loss [595,600-602]. Human cells will preferentially replicate defective human mtDNA over foreign normal primate mtDNA suggesting that mtDNA determinants for trans-acting factors may be of greater significance than OXPHOS functionality [603].

MRC defects of primate xenocybrids differ from those of mouse-rodent xenocybrids, both in terms of which complexes are affected, and the evolutionary distance that can be tolerated. These findings provide new insights into the interactions of nuclear DNA and mitochondrial DNA by showing that predictions regarding viability and phenotype of xenomitochondrial cells do not correlate strictly with evolutionary divergence or the overall number of amino acid or nucleotide differences and will vary depending on the species used. By comparative studies of the species used it will be possible to gain important insights into the nuclear mitochondrial interactions that determine efficient mitochondrial function, and may provide useful mouse models of human mtDNA disease.

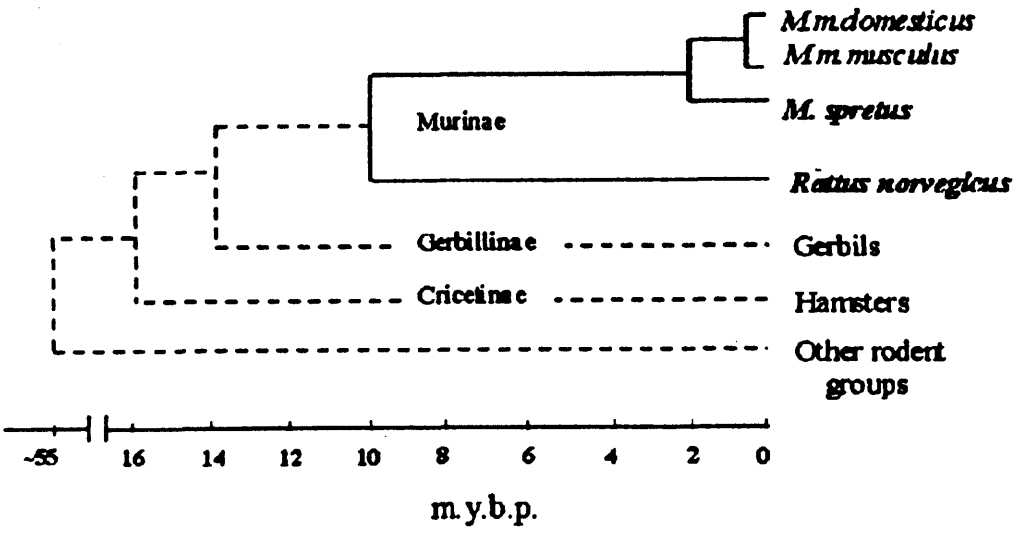

Figure 1.6 Brief phylogeny of the Muridae showing divergence times estimated from molecular studies. Time is shown by the scale below the phenogram and expressed as millions of years before present (m.y.b.p.). (from [589]).

mt gene product	Identity	Number of amino acids		No. of amino acid differences
		Rat	Mouse	
NAD1	90%	318	315	32
NAD2	74	345	345	88
COXI	97	514	514	14
COXII	99	227	227	3
ATP8	79	67	67	14
ATP6	95	226	226	12
COXIII	97	261	261	9
NAD3	87	115	114	15
NAD4L	86	98	97	14
NAD4	87	459	459	59
NAD5	78	610	607	133
NAD6	80	172	172	34
Cytochrome b	93	380	381	26

Table 1.5 Comparison of *M. musculus* and *R. novegicus* mitochondrial translation products.

1.10.1 Animal Models

The high cellular mtDNA copy number and the lack of demonstrated mechanisms of recombination have presented technical barriers to the generation of mtDNA "knockout" mice or animal models of mtDNA mutations. Several mechanisms have been explored to overcome this [604]. Some approaches may be limited by the lack of available mtDNA mutants in cultured mouse cells.

Using available vectors the stable introduction of mutant mtDNA into the mitochondria of mammalian cells is problematic. Attempts have been made to use a transfection approach using a DNA construct linked to a mitochondrial target peptide leader sequence [504,605]. Commonly used vectors are retroviruses that require active DNA replication to enable their insertion into genomic DNA. This technique is therefore precluded in myoblasts, which like neurons cease DNA synthesis before fusion [606]. An alternative approach was developed using transformed cybrid technology to generate a mouse model of mitochondrial disease, termed mito-mouse [607]. Synaptosomes were isolated from healthy aged mouse brains and fused with ρ^0 cells. Aging tissue accumulates mtDNA deletions [608], and these are referred to as low abundance rearranged molecules or "sublimons". The resultant cybrids containing such deletions were identified, and these cells were enucleated and electro-fused with zygotes before implantation into pseudopregnant female mice. Previously mtDNA had been shown to be eliminated from zygotes, depending upon its tissue origin, inter or intra species barriers, and whether it is implanted into sperm or oocytes [609]. These findings implied the existence of imprinting factors [610]. The mtDNA deletion was passed not only into somatic cells but also into the germ line, a rare event for human pathologically rearranged mtDNA other than partial duplications. It accumulated in successive generations, and when a threshold of 90% was reached mitochondrial dysfunction become apparent in various tissues.

In humans, the presence of deleted or partially duplicated mtDNA above a threshold of 50% causes multisystem disease of variable phenotype. The phenotype is determined by both the tissue distribution of the rearranged mtDNA, and the type of rearranged

molecule present, and probably other, as yet unidentified, factors. Duplications tend to cause more widespread disease. Red ragged fibres and weakness are almost always present. Mito-mouse exhibited no RRFs, there was a mosaicism of respiratory impairment in cardiac and skeletal muscle, and death occurred at 200 days due to renal failure and anaemia, rare manifestations of disease in humans. Furthermore, in contrast to human mtDNA disease, the mouse levels of mutant mtDNA showed little variation between different tissues. In addition to the deleted mtDNA, partially duplicated mtDNA molecules were detectable in the mice. It was deduced that in early development donor deleted mtDNA must have recombined with wild type mtDNA to generate these partially duplicated species. Inter molecular recombination of this type has not been observed in human cybrids heteroplasmic for deleted mtDNA. Mito-mouse has therefore provided a disease model for human mtDNA rearrangement diseases. However the dissimilarities from human mtDNA biology, also rather than detracting from this model, serve to provide us with new insights into a number of aspects of mtDNA biology, including the maintenance of mtDNA during development, tissue expression, and transmission.

An A2379T mutation within the 16S rRNA mtDNA gene confers resistance to chloramphenicol (CAP) in mouse 3T3 cells. The introduction of this "(CAP)-resistant" mtDNA mutation into mouse embryonic stem cells has provided another animal model of mtDNA disease. Embryonic stem cells were obtained, and CAP-sensitive mtDNAs selected against. Chimeric mice were then generated by fusing these cells with enucleated CAP-resistant 3T3 mouse cells. The resulting cell lines had a mutant load of 90% and reduced cytochrome oxidase activity [611]. Chimeric heteroplasmic (transmitochondrial) mice were generated by the injection of these cells into blastocysts. The mutant mtDNA load in tissues analysed varied from 0% to 50% [611,612]. The mice developed cataracts, retinopathy, cardiomyopathy and myopathy [612,613]. Parallels can be drawn to human mitochondrial disease because sensorineural deafness may also result from mutations of rRNA genes, the A3243G MELAS mutation results in a similar translational defect, and the NARP T8993G ATPase6 mutation causes a similar alteration in retinal function [611,613]. The variable segregation of wild and mutant type mtDNA into different tissues also mirrors human mtDNA disease [611]. The lack of a technique for site directed

mutagenesis of the mitochondrial genome means that this method may be of use in the generation of mouse mutants for different mtDNA mutations. Severe combined immunodeficiency (SCID) mice have been used to generate animal models of human mtDNA disease. Myoblasts obtained from patients with NARP and MERRF are able to regenerate and express their mtDNA after injection into the tibialis anterior muscle of SCID mice [614].

Three different classes of nuclear DNA encoded mitochondrial gene mutations have been reported in the mouse. These include mutations in a biosynthetic apparatus gene (Tfam), mutations in the mitochondrial bioenergetics genes ANT1 and UCP1-3, and mutations in the mitochondrial antioxidant genes GPx1 and SOD2 (MnSOD). Knockout gene technology has been used to generate mouse models of mitochondrial disease due to nuclear DNA defects. Mitochondrial transcription factor A (mtTFA) is a nuclear-encoded protein that binds upstream of the light and heavy chain mtDNA promoters, promotes transcription and may also regulate mtDNA replication [615]. Knockout of the mouse homologue *Tfam* causes severe mtDNA depletion and embryonic lethality in the homozygous state. Mitochondria are enlarged, of abnormal morphology, and are deficient in COX but not SDH. Heterozygous mice have a 34% reduction in mtDNA copy number, a 22% reduction in mitochondrial transcripts, and a partial reduction of the COI protein in heart but not in liver [19]. Tissues vary in their sensitivity to changes in the levels of mtTFA. A gene-dosage effect may therefore contribute to tissue-specific differences in respiratory chain capacity in humans [19]. A similar model has been developed with Tfam inactivation confined to cardiac and skeletal muscle [616]. This caused postnatal lethality due to dilated cardiomyopathy. Cardiac conduction defects were also present. There was a reduction of complexes I and IV, but not II. Tfam inactivation in the pancreatic β cells has been used to examine the importance of mtDNA depletion in diabetes [617].

Inactivation of the mouse nDNA adenine nucleotide translocase (ANT1) gene provides a model of mtDNA multiple deletion syndrome [159,294], but also provides insight into the role of depleting cellular ATP, inhibition of the electron transport chain, and increasing

mitochondrial ROS production in the pathophysiology of mitochondrial disease [159]. ANT1 mutants exhibit exercise intolerance and cardiac hypertrophy, a dramatic proliferation of mitochondria, and the presence of ragged-red muscle fibers [294]. There are elevated levels of serum lactate, alanine, succinate, and citrate, consistent with inhibition of the TCA cycle and the ETC [294]. Inhibition of ETC causes electrons to be redirected to O_2 to generate $O_2^{\cdot-}$. There is increased production of reactive oxygen species (ROS) in the ANT1 deficient mice, with a six to eight-fold increase in levels of hydrogen peroxide (H_20_2). The respiratory defect is complete in skeletal muscle, and partial in cardiac muscle. The levels of antioxidant defence enzymes induced are consequently higher in skeletal muscle than the heart, and the accumulation of mtDNA damage is lower in skeletal muscle [329]. The ANT1 -/- mouse therefore provides a model of AD-PEO, but one important difference is that ANT1 mutations in human are dominant, but in mice are recessive.

Mutations in the genes for superoxide dismutase (SOD), an enzyme that reduces superoxide anions generated during the OXPHOS process to H_20_2, result in reduced ATP synthesis and increased oxidative stress [618]. There are three genes for SOD and their effects have been examined in knockout mice [486]. Inactivation of SOD2 gene causes the most deleterious phenotype, with cardiomyopathy, lactic acidosis and hepatic fat accumulation [619]. Biochemical analysis revealed severe deficiencies in MRC complexes I and II and the tricarboxylic acid cycle enzymes. A severe inhibition of ATP synthesis and the accumulation of oxidative mtDNA damage result [485,486,620]. The SOD mimetic and synthetic antioxidant manganese 5, 10, 15, 20-tetrakis (4-benzoic acid) porphyrin (MnTBAP) may prevent the development of cardiomyopathy and the accumulation of lipid in the liver [620]. Therefore, the SOD2 knockout mice constitute a good model to examine the efficacy of antioxidants and to study the mechanisms of oxidative damage that may be associated with mitochondrial disease.

Glutathione peroxidase 1 deficient mice have increased levels of mitochondrial H_2O_2 production. Their phenotype is determined by the inter-tissue (high expression in liver, brain, and renal cortex) and intra-cellular (cytosol and mitochondria of liver and kidney,

and cytosol of heart) distribution of GPx1. GPx1 mice have chronic growth retardation, increased H_2O_2 production in the liver, but this has only a mild deleterious effect on respiration [621].

Uncoupling proteins (UCP) increase the mitochondrial inner membrane permeability to protons. This short circuits the $\Delta\psi$ (membrane potential) and activates the ETC to rapidly burn brown fat to generate heat. Mice lacking either UCP2 or 3 (the more widely expressed isoforms) exhibit increased mitochondrial ROS production [622,623]. Mitochondrial function was assayed by determining the resistance of mice to infection with *toxoplasma gondii*

1.11 CLASS II NON-ARCHETYPAL SECONDARY OXPHOS DEFECTS

A growing number of neurodegenerative disorders without overt primary OXPHOS defects are now linked to mutations in mitochondrial proteins that are indirectly linked to the processes of cellular respiration and energy production. The breadth of mitochondrial disorders is therefore expanding to include more common neurological disorders. It may be that mitochondrial biology underlies an even greater number of disorders both neurological and others. (Table 1.5)

OXPHOS defects have consequences beyond impairment of ATP production. In vitro drug induced complex I deficiency results in alterations in cellular respiration, growth, free radical production, lipid peroxidation, mitochondrial membrane potential, and apoptosis. The degree of complex I inhibition correlates with the extent of these defects [324]. Mechanisms of free radical production and oxidative damage have been proposed in the pathogenesis of both the class I archetypal mitochondrial encephalomyopathies and the class II neurodegenerative conditions.

Table 1.6

Genetic causes of bioenergetic defects in neurodegenerative diseases

Diseases with nuclear DNA-encoded mitochondrial defects

Friedreich's ataxia

Wilson's disease

Hereditary spastic paraparesis

Deafness-dystonia

Leigh's disease

Diseases with nuclear DNA mutations with secondary mitochondrial dysfunction

Huntington's disease

Cerebellar degenerations

Diseases with mitochondrial DNA-encoded mitochondrial defects e.g.

LHON

KSS/CPEO

MELAS

MERRF

Leigh's disease

Diseases with some evidence of mitochondrial dysfunction

Amyotrophic lateral sclerosis

Parkinson's disease

Alzheimer's disease

Progressive supranuclear palsy

1.12 Reactive Oxygen Species and Oxidative damage as a pathogenic mechanism in class I and class II mitochondrial disorders.

Over 85% of the oxygen used by a cell is consumed by its mitochondria [325,326]. If free electrons are released during this process, or if the oxygen is incompletely processed, oxygen radicals are generated that are damaging to lipids, protein, and DNA. Mitochondria have therefore evolved a number of ROS scavenging mechanisms both enzymatic and non-enzymatic. Their capacity is however usually exceeded by the rate of production of ROS [327,328]. The degree of damage to mtDNA is inversely proportional to the levels of these antioxidant defences [329].

The major ROS are superoxide ($O_2^{\cdot-}$), hydrogen peroxide (H_2O_2), and the hydroxyl radical ($OH^{\cdot}$). Superoxide is formed by the transfer of a free electron to molecular oxygen. This reaction occurs at a number of specific sites within the electron transport chain. Production is maximal from complex I and III. Superoxide is highly reactive and diffuses poorly throughout the cell. Damage is therefore maximal at the site of production, the mitochondrial inner membrane. The mitochondrial scavenging enzyme manganese superoxide dismutase converts superoxide to H_2O_2, which is, by contrast, highly diffusible. H_2O_2 in turn is converted to H_2O by glutathione peroxidase. This reaction requires reduced glutathione as a coenzyme. However, in the presence of reduced transition metals, H_2O_2 reacts via the Fenton reaction to generate $OH^{\cdot}$ a highly reactive ROS that lacks any known scavenging mechanism.. This will react with virtually any molecule in close proximity.

Other important radicals include nitric oxide (NO) and peroxynitrite ($ONOO^-$). These can be produced endogenously by mitochondrial NO synthetase [330-332]. NO can have both beneficial and detrimental effects, with its influence on the mitochondrial permeability transition pore being dependent on the prevailing NO concentration [333]. Mitochondrial NO decays via ubiquinol oxidation, reversible binding to cytochrome c oxidase, and by interaction with superoxide resulting in the formation of $ONOO^-$ [334]. Peroxynitrite causes modification of proteins by nitration of tyrosine residues to form dityrosine, and oxidizes

tryptophan to cysteine [335]. These effects culminate in mitochondrial swelling, depolarization, calcium release, and permeability transition [336].

Mitochondria thus play the role of both assailant and victim in ROS induced cellular damage. These roles have been proposed to be of pathological significance in a number of archetypal mitochondrial encephalomyopathies and other neurodegenerative conditions, and are thought to result in a vicious cycle of cellular damage. In this way an initial MRC defect causes generation of ROS, which, by induction of secondary mtDNA mutations further exacerbates the ROS production rate and MRC defect.

Oxidative stress causes greater damage to mtDNA than nuclear DNA due to the lack of histones, repair mechanisms, non-coding sequences from mtDNA, and due to its location near the site of ROS production [337]. However in patients with pathogenic mtDNA mutations PCR based techniques failed to show an increased level of mtDNA deletions in muscle arguing against this vicious cycle theory [338]. ROS production and oxidative damage are increased in MELAS and MERRF fibroblasts [339]. Hydroxyl radical damage of mtDNA is reported in MELAS and can be accelerated by specific genotypes [340]. ROS associated telomere shortening has been reported in both MELAS and LHON [341]. These hypotheses have been strengthened by the findings in xenomitochondrial cybrids, where the degree of complex I deficiency correlates with the rates of cellular respiration and growth, ROS production, lipid peroxidation and other markers of ROS induced damage [324]. Partial MRC deficiencies may therefore precipitate cellular degeneration via ROS related pathways.

1.13 The role of mitochondrial dysfunction in neurodegeneration

Mitochondrial dysfunction has been implicated in the pathogenesis of a range of neurodegenerative conditions. Hereditary spastic paraparesis (HSP) is a clinically and genetically heterogeneous group of disorders. Incidence is estimated at 1:10000 [342,343]. It occurs as complicated and pure forms and can be inherited as autosomal recessive or

dominant, or X-linked traits [344]. The unifying feature is of progressive spasticity and less evident weakness of the lower limbs. Seven loci for AD HSP, three autosomal recessive loci and two X chromosome loci have been identified. Chromosome 16 linked families with AR complicated and pure HSP (SPG7), have been found to harbour mutations in the gene encoding paraplegin a protein of 795 amino acids [346]. Muscle biopsies from these patients revealed typical mitochondrial pathology [346,347]. Paraplegin shows high sequence homology to three yeast proteins (Afg3p, Ymelp, and Rcalp), suggesting that it also is a mitochondrial ATP-dependent zinc metalloprotease of the triple 'A' protease family (*A*TPases *a*ssociated with a variety of cellular *a*ctivities). These proteins act as chaperones and are involved in the ATP dependent degradation of mitochondrial translation products. AD HSP Linked to 2p (SPG4) is caused by mutations in spastin. This is also a member of the AAA family [348], but does not localize to the mitochondrion. Evidence of mitochondrial dysfunction has been reported in HSP patients not linked to chromosome 16 [349,350]. Spastic paraparesis secondary to the ingestion of chick peas (lathyrism) is also linked to mitochondrial dysfunction [351].

Hepato-lenticular degeneration (Wilson's disease WD) is an autosomal recessive disorder that causes the accumulation of copper, maximal in the brain and liver. It affects approximately 1:30,000, and is the consequence of mutations in the ATP7B gene on chromosome 13. The WD protein localizes to mitochondria [352]. The ATPase is expressed predominantly in the liver and transports copper into the hepatocyte secretory pathway for subsequent incorporation into caeruloplasmin and excretion into bile [353]. This is the only significant pathway for copper removal. Mitochondrial morphology is abnormal in WD [357]. Impaired activities of mitochondrial respiratory chain complex I, II/III, IV and aconitase are found in WD liver [358]. The level of oxidative stress has been shown to correlate negatively with the copper concentration [359]. Copper is an important component of complex IV, and it may act as a substitute for iron in redox reactions resulting in the generation of free radicals [360,361].

Dystonia is a disorder of movement caused by sustained involuntary muscle contractions affecting one or more body sites. This frequently causes twisting and repetitive

movements, or abnormal postures [631,632]. The prevalence of dystonia is not accurately known, and estimates vary between 127 to 329 per million [633,634]. The aetiology of dystonia remains uncertain in the majority of cases. Furthermore in those cases with an identified gene, the pathogenic mechanisms remain to be elucidated. Mitochondrial dysfunction, either as a primary or secondary phenomenon, has been implicated by a number of studies.

Among the many clinical manifestations of the primary mitochondrial diseases, disorders of movement, especially dystonia, occur at a greater frequency than expected. In 85 consecutive patients with mitochondrial myopathy 10.5% had a movement disorder, which included dystonia, chorea, Parkinsonism and myoclonus [142]. In a number of families with Leber's hereditary optic neuropoathy (LHON) dystonia is also present. A missense mutation in the mtDNA encoded ND6 complex I subunit gene was identified in one family [272]. Cells from patients containing this G14459A mutation showed a 55% reduction in complex I activity [669]. In a Dutch family a heteroplasmic A11696G in the ND4 gene, and a homoplasmic T14596A mutation in ND6 were identified. Biochemical analysis of a muscle biopsy revealed a severe deficiency of complex I [271].

Further support for the role of mitochondrial dysfunction in the aetiology of dystonia came with the identification of the causative gene for Mohr-Tranebjaerg syndrome/X-linked deafness-dystonia-optic atrophy syndrome [670]. This condition is characterised by X-linked recessive sensorineural hearing loss, dystonia, dementia, psychotic features and optic atrophy. The DFN1/MTS locus was linked to Xq21.3-22 [673] and a mutation identified in a novel gene DDP (deafness-dystonia peptide) [670]. The DDP gene generates a 1167 bp cDNA which encodes a 97 amino acid, 11kDa polypeptide, named DDP1 [96]. This protein is homologous to a family of yeast proteins known as the 'Tiny Tims', which are part of a complex of proteins known as inner membrane translocases. Via yeast homolgy studies the DDP1 protein was identified as TIMM8a [675]. TIMM8a assembles with TIMM13 in a 70kDa complex in the mitochondrial intermembrane space. This complex is responsible for the import, at low membrane potentials, of Tim23 an essential component of the import machinery for matrix-targeted proteins. Impairment of this mechanism would therefore lead to a significant reduction of many mitochondrial functions [677].

Mitochondrial involvement in the pathogenesis of dystonia is further supported by studies of the systemic administration of subacute doses of 3NP, a mitochondrial toxin, in cebus apella monkeys. This led to the developed of dyskinesia at 5-6 weeks after discontinuation of 3NP. After this time period chorea lessened as dystonia worsened in severity and intensity [678]. Biochemical evidence of mitochondrial dysfunction in primary dystonia first came in 1992 [679]. Decreased complex I activity was demonstrated in the platelets of patients with focal (37% mean reduction), and segmental or generalised (62% mean reduction) primary dystonia. In a separate study a complex I defect was confirmed in platelets from patients with sporadic focal dystonia (mean reduction 21%). However for patients with generalised dystonia (linked or unlinked to chromosome 9q34) the difference from controls was not significant [680]. Biochemical analysis of cybrids from these patients with sporadic focal dystonia, showed that the defect was complemented in mixed and clonal cybrid lines [681] suggesting that the complex I defect in dystonia is caused by a nuclear mutation or a circulating toxin.

Huntington's disease (HD) is caused by an expanded CAG repeat on chromosome 4p. This causes a polyglutamine repeat in the N-terminal region of the widely expressed Huntingtin protein. Roles in glutamate homeostasis, endocytosis and vesicle trafficking have been proposed for Huntingtin [369,370]. Post mortem, in vivo and in vitro studies have implicated mitochondria in the pathogenesis of HD. OXPHOS defects of complexes II, III, and to a lesser extent complex IV, have been reported in HD caudate nucleus [371,372]. Huntingtin does not localize to mitochondria, and OXPHOS function is normal in cybrid studies [373]. Mitochondrial dysfunction is thought to be a secondary consequence of excitotoxicity mechanisms and/or oxidative stress. Other evidence pointing to a disturbance of cellular energy metabolism includes the findings of elevated lactate levels in the occipital cortex and basal ganglia [374], abnormalities on muscle ^{31}P MR spectroscopy [375], and that mitochondrial toxins can create animal models of HD [376,377]. Studies of transgenic HD mice also implicate secondary mitochondrial dysfunction as a consequence of the gene mutation [378,379].

1-methyl-4-phenyl-1,2,3,6-tetrahydropyridine (MPTP), a contaminant of synthetic opiates, led to an outbreak of young-onset parkinsonism [380]. MPTP is metabolized to

MPP^+ a complex I inhibitor [381]. In the substantia nigra of patients with idiopathic Parkinson's disease there is a 30-40% decrease in complex I activity [382], and reduced immunohistochemical subunit staining for complex I, with sparing of the other MRC complexes [383]. Cybrid studies imply a mtDNA-encoded defect [384,385]. Both the susceptibility to MPP^+ and free radical production are increased, and mitochondrial calcium buffering is impaired [386]. The 11778 mtDNA mutation has been associated with multisystem degeneration, parkinsonism, and a complex I defect [387]. MtDNA mutations have however not been identified in idiopathic PD, implying that the bioenergetic defect may be the result of unidentified mtDNA mutations or polymorphisms, or the interaction of genetic and environmental factors [388].

Alzheimer's disease (AD) postmortem tissues show complex IV defects [389]. Immunostaining shows reduced subunit levels maximal for mtDNA encoded subunits [390]. The biochemical defect persists in cybrids generated from AD platelets. Results are conflicting however and a study of cybrids generated from synaptosomes and platelets failed to find a MRC defect [391]. Initial results suggesting a mtDNA mutation to be responsible for the defect, were withdrawn when a nuclear pseudogene was later found to be responsible for this spurious result [392]. Further mtDNA polymorphisms of proposed aetiological significance have been reported [393].Oxidative damage to mtDNA is increased threefold in AD post-mortem tissue [394]. Other parameters of oxidative damage also imply that this is an important mechanism in the pathogenesis of AD.

The role of mitochondrial dysfunction in sporadic amyotrophic lateral sclerosis is supported by a large body of literature. Mitochondria are histologically abnormal in liver and anterior horn cells [395,396]. In skeletal muscle complex I activity is reduced by 50% [397], and mitochondrial volume and calcium concentrations are increased [398]. There is also evidence of increased oxidative damage [399]. A COX subunit I mutation has been reported in an individual with sporadic ALS [400]Mutations in copper-zinc superoxide dismutase (SOD) are found in a proportion of patients with familial ALS [401]. These mutations have been shown to impair mitochondrial function in vivo [402], and transgenic studies show mitochondrial morphological changes to be an early feature preceding motor weakness and loss of motor neurons [403].

1.13.1 Friedreich's ataxia:

This ataxic disorder was first described by Nicholaus Friedreich in a series of five papers published between 1863 and 1877 [404-408]. He reported nine members of three families who had onset in puberty of ataxia, dysarthria, sensory loss, muscle weakness, scoliosis, foot deformity, and cardiac symptoms. Areflexia was only described in the final two reports, but was later adopted as one of the clinical diagnostic criteria. In the intervening 133 years until the elucidation of the molecular mechanism of FRDA there was much debate about the clinical features and the phenotypic spectrum of this disorder [409].

FRDA is now recognised as the commonest inherited ataxia. Prevalence studies performed after the introduction of genetic testing have suggested that it is commoner than previously recognised with values up to 1:29,000 [410]. Carrier prevalence is estimated at between 1:60 to 1:90 [411]. The disease is rare in Asia and Africa. Autosomal recessive inheritance was established by segregation analysis [409], although this had also been suggested by the high rate of consanguinity [412]. Due to the high carrier frequency pseudo-dominant inheritance had also been reported [413,414].

Prior to the introduction of genetic testing various diagnostic criteria were proposed to enable natural history studies and the investigations of molecular mechanisms [409,415]. Subsequently a number of these have proved invalid, most noticeably with the recognition of onset over the age of 25 years (late-onset Friedreich's ataxia – LOFA), and the preservation of lower limb reflexes (Friedreich's ataxia with retained reflexes – FARR). These patient groups, and others such as the Acadian form of FRDA and Acadian spastic ataxia have all been found to be due to the same genetic mutation [416-424]. Other atypical forms include the presentation of FRDA as a pure spastic paraparesis [425,426]. Presentation as a pure sensory ataxia or as chorea is also recognised [427,428].

The core clinical features of gait and lower limb ataxia are reported in virtually 100% of all reported studies. The frequency of other features varies depending on: 1) whether the patients were identified by clinical or genetic criteria 2) potential racial variations, 3) the range of age and disease duration in the patients studied and 4) the

criteria used to define the presence of certain features. The latter are illustrated by variations between studies in the criteria used to define for example diabetes (defined by patient history, blood glucose values, or oral glucose tolerance tests), cardiomyopathy (defined by ECG alone in some studies, and by echocardiography in others), impaired visual and auditory acuity, and skeletal abnormalities including scoliosis and pes cavus (Table 1.6).

There is a paucity of natural history data for FRDA, a common feature of slowly progressive disorders. Onset ranges from 1.5 years to 51 in reported series. Loss of ambulation has been reported to occur at a mean of 15.5 ± 7.4 years after disease onset but ranges between 3 and 44 years. Death is most commonly as a consequence of cardiomyopathy and is at a mean age of 37.5 ± 14.4 years [429]. Retrospective analysis of disease progression has reported a mean time to wheelchair confinement of 11 years [429].

Pathological studies of FRDA report changes maximal in dorsal root ganglia, dorsal columns, corticospinal tracts, and heart. Macroscopically the spinal cord is atrophic with the posterior and lateral columns particularly affected [430]. Changes within the nervous system are thought to be the consequence of a dying back process from the periphery affecting the longest and largest myelinated fibres that show changes of an axonopathy [431,432]. Demyelination is seen in the dorsal columns. The cerebellar cortex shows only mild neuronal loss [433], but the dentate nucleus, and Clarke's column in the cord show marked changes. The cerebellar, and occipital cortex, show reduced phospholipids levels in the absence of neuronal loss [434]. A hypertrophic cardiomyopathy develops in a significant proportion of patients. Studies of the cardiac phenotype report variable left ventricular hypertrophy (concentric, asymmetric, or both, left ventricular outflow tract obstruction, and thickening of the papillary muscles [435,436]. The presence of cardiac hypertrophy is non concordant with the presence of ECG abnormalities or the neurological features of the condition. The mechanism of cardiac hypertrophy is unclear. Histology reveals cellular hypertrophy, diffuse fibrosis, and focal myocardial necrosis [437]. The susceptibility of the heart in FRDA may be a reflection of the relatively high cardiac expression of frataxin [438], and the low antioxidant defences of cardiac tissue [329].

Table 1.7

Clinical, genetic, and neurophysiological parameters in Friedreich's ataxia, according to the studies of Harding 1981, Durr 1996, Dalatycki 1999, and Hart 2003 (unpublished data) [409,418,439]. Ages are given in years,other values are percentages of total patient group. (NA= not available)

	Harding 1981	Durr 1996	Dalatycki 1999	Hart 2003
Number of patients (families)	115 (90)	140 (114)	51 (43)	77 (67)
Definition of case	clinical	genetic	genetic	genetic
Mean age (range)	32.3±13.8 (10-73)	31±13 (7-77)	NA	24.1±10 (10-57)
Mean age onset (range)	10.52±7.4 (1.5-27)	15.5±8 (2-51)	10.5±6.4 (1-26)	11.75±6.3 (2-27)
Onset to w/c confinement	NA	10.8± 6	10.1± 4.4	11.2
Mean GAA repeat (range)	NA	630±230 (120-1700)	739±191 (300-1345)	730±225 (130-1080)
Gait ataxia	100	100	100	100[e]
Limb ataxia	99	99	100	100
Dysarthria	97	91	95	95[f]
LL reflexes	0.9	12	2	13
extensor plantars	89	79	74	87
Impaired vibration	73	78	88	56

Impaired visual acuity	18	13	NA	3[d]
Sphincter disturbance	NA	23	41	45[g]
Pes cavus	55	55	74	64
Scoliosis	79	60	78	76
cardiomyopathy	66[a]	63	65	47[h]
Diabetes mellitus	10[b]	32	8	5[c]
Median NCV	52.2±7.63 (n=22)	NA	NA	50.6±3.45
Peroneal NCV	44.96±7.2 (n=22)	NA	NA	40.5±7.4
At least 1 SAP absent	92 (n=26)	NA	NA	83

a cardiomyopathy defined by ECG alone
b 10% of patients known to be diabetic. No other patients found to have glycosuria
c patients known to be diabetic, including one unknown case detected on random serum glucose and HbA1c analysis
d patients previously investigated for optic atrophy
e Gait ataxia defined as unable to walk more than 4 steps in tandem
f any modification of fluency or suggestion of slurring.
g Minimum criteria: patients reporting mild urinary hesitancy, urgency or retention < once per month
h Defined as an interventricular septal thickness of greater than 11 mm.

Clinical parameters also correlate with the repeat length size. The size of GAA1 accounts for between 33 and 73% of the variation in the age of onset in various studies. GAA2 accounts for les than 20% of this variability [418,419,440,441]. Indeed GAA1 correlated better than GAA2 for several disease parameters and complications, including cardiomyopathy, in all studies [418,419,439,441,442] except one [423]. Diabetes mellitus by contrast correlated in only one study [441].

Further variation may result from other factors. The GAA repeat length may vary in a tissue specific pattern due to mitotic instability, and peripheral blood samples may be a poor indicator of repeat lengths in pathologically affected tissues. GAA1 has been shown to differ in different brain regions [443] and in various tissues [443-446]. Cis acting factors may also influence the phenotype. Potential mechanisms would include effects upon the stability of the trihelix structure by sequence alterations within or flanking the GAA expansion [447]. Other genetic or environmental factors may also exert an influence on the phenotype. This is illustrated by the finding that the age of onset in sibs correlates strongly regardless of the degree of difference between their repeat lengths [440,448].

Our level of understanding of mitochondrial involvement in FRDA is perhaps greater than for any other neurodegenerative condition. Subsequently mitochondrially targeted therapies have been trialed in FRDA. This issue, and in particular the measurement of the efficacy of potential therapies for FRDA are the subject of chapter 6. At this point the clinical and molecular features of FRDA and the evidence to date for therapeutic benefit will be discussed.

In 1988 the FRDA gene was mapped to chromosome 9 [449]. The gene was linked to 9q13-21.1 in 1990 and cloned in 1996 [450,451]. 95% of cases are now known to be the result of a homozygous GAA triplet repeat expansions in intron 1 of the FRDA gene on chromosome 9 [452]. This is a unique trinucleotide repeat disorder in that its inheritance is autosomal recessive, its location is intronic, and it involves a GAA trinucleotide. The repeat length is normal individuals is 6 to 34, but is expanded in patients and carriers to between 67 and 1700 [418,453]. The remaining 5% of patients are compound heterozygotes harbouring an expanded repeat on one allele and a point mutation on the other. Twenty-three different point mutations are described to date

and include missense, frameshift, splice site, initiation codon, and nonsense mutations. The former are found only in the C-terminal suggesting that functional domains reside in this part of the protein [454]. The location of these mutations in highly or poorly conserved amino acids correlates with the severity of the phenotype and the presence of atypical features [455-458]. No cases resulting from homozygous point mutations have been described, although the population incidence of such individuals has been calculated to be $1:100x10^6$ [459]. Clinically typical FRDA may occur in individuals in the absence of linkage to chromosome 9 suggesting that a second locus may exist [460].

The FRDA gene contains seven exons (1-5a, 5b, and the non-coding exon 6) within 80 kb of nuclear DNA. Transcription most commonly generates a 1.3 kb product representing exons 1 to 5a [452]. This is translated into a 210 amino acid protein named frataxin. Alternative splicing, with the transcription of exon 5b instead of 5a, generates a 171 amino acid protein of uncertain significance [452]. Frataxin and mRNA levels are maximal in tissues of high mitochondrial content (heart, pancreas, liver and skeletal muscle) [438]. Not all of these exhibit obvious clinical involvement in FRDA. Within the CNS mRNA levels are highest in the cord, low in the cerebellum, and very low in the cerebral cortex [452]. Frataxin appears to play a role in development; its homozygous knockout is embryonically lethal [461]. Frataxin mRNA levels are high in fetal spinal cord, dorsal root ganglion, heart, liver, skeletal muscle, and skin [462,463]. Lymphocytes from patients with homozygous expansions contain low levels of frataxin, and this level, and that of the mRNA, are inversely related to the size of the smaller repeat [438,464,465]. The block is thought to occur at the level of transcript elongation [465], and the mechanism for this is believed to be through the formation of unusual DNA structures, such as DNA triplexes, by the GAA/TTC repeats [466]. Several point mutations (I145F, G130V) appear to alter the secondary structure of the protein and thus influence mitochondrial uptake or cleavage [467].

The function of frataxin is incompletely understood. The amino acid sequence shows no strong homology to any proteins of known function. It has however been shown to contain an N-terminal mitochondrial targeting sequence in it's first 55 amino acids and a sequence of highly conserved amino acids in exons 4 and 5a [468]. The predicted mitochondrial location was confirmed when tagged expressed frataxin was shown to

co-localise with mitochondrial markers in HeLa and COS cells [463,469,470]. An inner membrane and a matrix location within the mitochondrion have both been proposed [438,471]. X-ray crystallography studies reveal similarities to ferritin, a site for protein-protein interaction, and the ability to bind one molecule of iron [468]. An oligomer structure may be required for this latter attribute. Point mutations in the protein core cause more severe phenotypes than those within the ferritin-like anionic patch, or flat external protein interaction surface.

Repeat lengths are unstable. Paternal transmission is associated with a reduction in repeat length, an effect that increases with increasing paternal age. Maternal transmission can cause an increase or decrease in repeat length, and expansions are greater with increasing maternal age [445]. The repeat length is less in an individual's sperm than in their blood, suggesting post-zygotic mechanisms. Repeat length can vary between and within tissues, somatic mozaicism has been demonstrated in different CNS tissues [443]. The effects of these factors on frataxin levels and clinical phenotype are uncertain.

A number of models of FRDA have aided our understanding of the pathogenesis of FRDA. Ataxia with vitamin E deficiency (AVED), caused by mutations in the α tocopherol transfer protein on chromosome 8, causes a phenocopy of FRDA. This fact provided the first evidence that an increased susceptibility to oxidative stress could be involved in the pathogenesis of FRDA[472]. The yeast homologue of frataxin (yfh1p) was identified as a suppressor which rescued a mutant yeast strain unable to grow on iron limited medium [469]. Loss of the yeast frataxin homologue (YFH1) causes poor growth on non-fermentable substrates, a two-fold increase in cellular and a ten-fold increase in mitochondrial iron content, defects of complexes I, IV, and V of the MRC, reduced mtDNA levels, and increased susceptibility to hydrogen peroxide induced oxidative stress [460,469,473]. However, these findings may simply be a consequence of excess cellular iron causing oxidative damage by promoting the conversion of H_2O_2 to the hydroxyl radical. Analysis of patient tissues has also shown iron deposits in the hearts of some but not all patients [433,474]. Post-mortem human cardiac and skeletal muscle shows reduced activity of aconitase, an enzyme particularly susceptible to free radical damage [475], and this may be further evidence of increased oxidative damage in

FRDA [474,476]. Cardiac muscle also exhibited severe defects of complexes I and II/III with a milder defect detectable in skeletal muscle [474,476]. These four enzymes all contain iron-sulphur centers. Magnetic resonance imaging has shown increased iron content in the dentate nucleus of the cerebellum [477], and iron levels are mildly increased in FRDA fibroblasts [478]. Yeast, mouse, and human studies suggest that frataxin assembles as multimers of approximately 60 subunits and binds over 3000 atoms of iron [479,480]. Frataxin may therefore have roles in the storage, uptake or efflux, or bioavailability of mitochondrial iron. A mitochondrial ferritin has been identified that may also serve this role but it has a severely limited tissue distribution [481]. Despite this evidence there is to date no evidence of MRC defects in cells cultured from FRDA patients [482]. The role of oxidative damage in the pathogenesis of FRDA is supported by the finding of elevated levels of urinary 8 hydroxy 2' deoxyguanosine, a surrogate markers of oxidative damage [483], reduced blood free glutathione levels [350], and elevated plasma malondialdehyde, a marker of lipid peroxidation [484]. The 2-6 fold elevations of urinary 8OH2'dG, shown in a study of 33 FRDA patients, was not related to GAA1 size or disease duration. The level of plasma DHBA (dihydroxybenzoic acid) a marker of hydroxyl radical attack was not elevated in this group of FRDA patients. MRC defects may be secondary to loss of mtDNA which itself may be the result of increased oxidative damage. MtDNA deficiency has been shown to be present but to a degree insufficient to explain the biochemical defect seen [485]. The pattern of biochemical defect is similar to that seen in response to oxidative stress, as occurs in the manganese SOD knockout transgenic mouse [486], and in Huntington's disease [372].

Evidence suggests a role for frataxin in mitochondrial iron-sulphur (Fe-S) centre synthesis. Loss of this function will affect the assembly of MRC complexes and many other intra and extra-mitochondrial proteins. Reduced MRC and aconitase function would lead to increased mitochondrial iron. Further evidence comes from phylogenic profiles that describe the distribution of genes within multiple genomes. This technique relies upon the fact that genes of similar function are often located in close proximity within the genome. These studies have revealed that Frataxin, or its homologues, are closely located to the numerous proteins already known to be involved pathways of iron-sulphur (Fe-S) centre assembly [487-489]. Furthermore, similarities exist between FRDA and the X-linked sideroblastic anaemia with ataxia

syndrome (XLSA/A), a condition as described above, caused by mutations in hABC7, another Fe-S cluster synthesis protein [367].

^{31}Phosphorous magnetic resonance spectroscopy (^{31}P MRS) provides an in vivo technique for the measurement of high-energy phosphorous compounds (phosphocreatine (PCr) and ATP). The rate of PCr recovery following exercise (Vmax) in skeletal muscle is a measure of the efficiency of OXPHOS. In cardiac muscle the PCr/ATP ratio is a good measure of energy availability [490]. This technique reveals abnormalities in FRDA heart and skeletal muscle, the latter correlating to the GAA repeat size [490-492].

The addition of iron chelators to the culture medium in the YFH1 model prevents iron accumulation and improves MRC activities, but aconitase activity remains low [493]. Frataxin also shows homology with the cyaY protein of γ-purple bacteria. Its knockout in E.coli had no effect on viability, iron content, or susceptibility to oxidative stress [494]. FRDA knockout mice die in utero. In mouse embryo studies frataxin expression increases from day 10 to 14 [462,463]. Conditional knockouts have been generated using a cre recombinase transgene under the control of muscle creatine kinase (MCK) or neurone specific enolase (NSE). This causes tissue specific deletion of exon 4 flanked by loxP sites. These mice died prematurely with features similar to FRDA [495]. Cardiac muscle showed abnormal mitochondria, reduced SDH staining, and impaired complex I, II/III, and aconitase activities a pattern similar to that found in human tissues. Skeletal muscle was unaffected. Iron deposition was seen in MCK mice only, and at a later stage than the bioenergetic defects. Similarly, the mutation of several yeast proteins involved in the synthesis of iron-sulphur clusters also results in late secondary mitochondrial iron accumulation [496]. Knock-in techniques have been used to generate double heterozygous knock-in mice, or knock-in/knock-out mice. Frataxin levels were reduced to 75% in the former, and 30% in the latter but the mice were clinically normal up to one year, and increased cardiac iron levels and fibrosis were found in only one mouse [497]. Lower frataxin levels may be necessary for phenotypic consequences.

The precise relationship between frataxin levels, impaired MRC function, oxidative stress, and anti oxidant defence levels in FRDA remains incompletely understood.

1.14 Therapeutic intervention in Class I and Class II mitochondrial disorders.

The evidence of disturbed bioenergetics in both the archetypal mitochondrial encephalomyopathies and other neurodegenerative disorders has provided therapeutic avenues for exploration.

The treatment of the archetypal encephalomyopathies includes the specific treatment of disease complications. This includes the use of beta-blockers for the treatment of cardiomyopathy, the avoidance of aminoglycoside antibiotics, and pacemakers for cardiac conduction defects. Various pharmacological agents have been trialed in these disorders but hard evidence of efficacy is lacking. This includes the use of quinone derivatives, vitamins B_1, B_{12}, C and K_3, metabolic supplements (succinate, creatine, and carnitine), dichloroacetate, and corticosteroids (for review see [498]). Antioxidants appear to delay clinical progression in various mouse models of mitochondrial disease [499]. A further target for therapeutic intervention has been the apoptotic pathway, in view of the pivotal role of mitochondria within it [500]. Drugs, such as cyclosporin A, that inhibit the mitochondrial permeability transition pore have been proposed but not yet evaluated in mitochondrial disorders or models [501]. Gene therapy to enable the expression of mtDNA protein encoding genes within the nucleus have succeeded in yeast models [502] but failed in mammalian cells in vitro [503]. To date the only success has been with the delivery of self-replicating plasmids to isolated mitochondria [504]. Mechanisms have been identified within yeast for the transport of tRNAs into mitochondria [505] and these may provide pathways for the delivery of gene therapy. Other potential therapies have been designed to alter the level of heteroplasmy in favour of wild type molecules. These techniques include the selective inhibition of the replication of mutant molecules by sequence specific peptide nucleic acids [506]; the use of oligomycin to inhibit mitochondrial ATP synthesis thus leading to an increase in wild type mtDNA [507]; and the use of bupivicaine or concentric exercise to induce the proliferation of satellite cells that usually contain lower levels of mutant mtDNA [508]. Effective patient therapies remain elusive.

Mitochondrially targeted therapies have also been employed in the class II disorders. Administration of vitamin E to AD patients has been shown to slow the rate of progression [509], and vitamin E and C to reduce the risk of AD [510]. Coenzyme Q_{10}, an important antioxidant in mitochondrial and lipid membranes [511,512] and a MRC enhancer, has been shown to increase ATP production in vitro [513]. It has shown benefit in animal models of mitochondrial disease and transgenic ALS mice [514,515]. Two clinical trials have suggested benefit from coenzyme Q_{10} therapy in Parkinson's disease [516,517]. Creatine and phosphocreatine have important roles in brain energy metabolism and the maintenance of membrane potentials [518]. Creatine increases brain energy stores and compensates for an energetic defect, and has also been shown to stabilise the transition pore and to promote glutamate reuptake [519]. Benefit has been shown in 3-nitropropionic acid and MPTP induced neurotoxic models of mitochondrial disease, and in transgenic ALS and HD mice [520-523].

A wide range of agents has been proposed for the treatment of FRDA and other ataxic disorders. These include phosphatidylcholine, acetazolamide, serotonin and carbidopa, amantadine, lecithin and linoleic acid, choline chloride, gamma vinyl GABA [524-532]. These trials were highly variable in their design and the outcome measures utilised. Their unifying feature was that they assessed small numbers of patients for short periods of time and showed no, or equivocal, benefit. Modern therapeutic trials, designed in response to the evidence of mitochondrial iron accumulation, oxidative damage, and MRC abnormalities, therapeutic strategies have been developed for FRDA. Iron chelation restores mitochondrial iron levels and prevents MRC dysfunction in the yeast model [493]. In vivo use has been problematic because desferrioxamine the most commonly used iron chelator is relatively hydrophilic with poor permeability across the plasma membrane [533,534]. In vitro studies have shown that desferrioxamine can protect respiratory chain complex II activity and lipids from oxidation by iron, but reduces aconitase activity. Iron chelators may therefore simply displace the toxic effects of ferrous iron rather than protect against it [535]. Other iron chelators that are able to mobilise mitochondrial iron stores have been developed and include 2-pyridylcarboxyaldehyde isonicotinoyl hydrazone (PCIH) [534]. Iron chelation therapy has not yet been evaluated in FRDA and several potential problems exist with this proposed method of treatment. Serum ferritin and iron levels are normal in FRDA [536] and iron accumulation may be only a

secondary event in the pathogenesis of FRDA [495]. Despite this the reduction of mitochondrial iron levels may still help prevent secondary oxidative damage, however other physiological consequences may ensue since iron still needs to be available for roles such as it's incorporation into iron-sulphur centers.

Antioxidant agents employed in the treatment of FRDA include idebenone [483,537,538], coenzyme Q_{10} and vitamin E [539], N-acetyl cysteine and selenium (http://internaf.org/ataxia/nacupd.html).

Coenzyme Q_{10} (2,3,dimethoxy-5-methyl-6-decaprenil-1,4-benzoquinone) is a naturally occurring antioxidant [540,541]. In 1957 it was isolated from beef heart mitochondria [542]. It is a lipid of the quinonic group. Its name is derived from the fact that it has 10 isoprenoid units in its sidechain. Due to its ubiquitous distribution it is also referred to as ubiquinone. It acts as an electron carrier in the MRC and therefore part of its mechanism of action may be to enhance cellular ATP synthesis. Although Q_{10} is at high concentrations within mitochondria it does not saturate enzymes that it interacts with. Changes in its availability can therefore directly affect the respiratory rate [543]. An average daily diet contains 5 mg. After ingestion it is readily taken up into blood [544], brain [515], heart and liver. Idebenone, a short chain analogue of coenzyme Q_{10} is well tolerated, and is known to cross the blood brain barrier [545].

Vitamin E was discovered in 1922 as a factor required to prevent reproductive failure in rats. It is a naturally occurring lipid soluble anti-oxidant. Its concentration is maximal in the mitochondria. Its structure was elucidated in 1937. It consists of tocopherols (α, β, γ and δ), the former being the most metabolically active form, and tocotrienols that have an unsaturated side chain. Vitamin E is involved in intercepting the production of secondary radicals from lipid hydroperoxide. It achieves this in conjunction with the actions of glutathione and selenium. Vitamin E donates hydrogen from its phenolic group to the peroxyl radical, so reducing it to hydroperoxide and forming the poorly reactive tocopheryl radical. In rats, oral administration of vitamin E increases tissue levels, in particular those of heart, skeletal muscle, and brain [546]. It has been used with varying results in cardiovascular disease, Parkinsons disease, and malignancies [547-549]. In AVED, vitamin E therapy can

lead to a mild improvement in cerebellar ataxia especially in those patients in the early stages of the disease [550].

Vitamin E and coenzyme Q_{10} may act synergistically. Q_{10} regenerates α-tocopherol, the active form of vitamin E, by reducing the α-tocopheryl radical [551]. In addition, vitamin E has been shown in vitro to reduce the formation of the bisemiquinone10 radical, thus increasing the lipophilicity of Q_{10} [552].

Following the in vitro demonstration that in control heart homoigenates, idebenone protects against Fe^{2+} induced complex II deficiency and lipoperoxidation, the effect of idebenone (5 mg/kg/day for 4 to 9 months) was assessed in three FRDA patients. The in vitro studies had also shown that iron chelators and antioxidants worsen some of the biochemical defects, and that the protective effects of idebenone were dependent upon the presence of succinate to reduce it. The in vivo studies revealed a substantial decreases in cardiac septal thickness, and left ventricular wall thickness in the three patients. Left ventricular mass index was reduced by 20% to 30%, and the shortening fraction was substantially improved. In one patient left ventricular outflow tract obstruction decreased from 40 to 10 mmHg pressure gradient, allowing the discontinuation of beta blocker therapy. Intra-rater variability of echocardiographic findings was not addressed in this small study. There were subjective reports of improved hand strength and fine movements, but no objective evidence of improvement in ataxia. Subsequently the same group have reported the results of an open trial of the same treatment in 40 FRDA patients. After 6 months treatment a 20% reduction in left ventricular mass was seen 48% of patients. Six patients had a reduced shortening fraction pre-treatment, and in 5 this improved [553,554].

Idebenone, used for 8 weeks at a dose of 5 mg/kg/day in 8 patients, has also been shown to significantly reduce, by 20%, the levels of 8OH2'dG (a marker of oxidative damage to DNA) [483] but in another study, only a small non significant reduction in MDA (a product of lipid peroxidation) was seen [484].

A placebo controlled cross over trial of idebenone (120 mg tds) in 9 ambulant FRDA patients showed no echocardiographic changes. Treatment blocks were 6 weeks long

with a three-week wash out period. 31P MRS and clinical parameters, as assessed by the international clinical ataxia rating scale (ICARS) [555] also showed no significant change [538].

Our own experience with the combined therapy of Coenzyme Q10 (400 mg/day) and vitamin E (2100 IU/day) in 10 patients with FRDA is discussed in detail in chapter 6. In summary, after 3 months treatment ^{31}P MRS showed an increase of 178% in the PCr:ATP ratio of cardiac muscle, and a 139% increase in the skeletal muscle maximum rate of ATP production. The effect was related to GAA1 length for the latter but not the former. Furthermore these increases were greater in pre-hypertrophic hearts. Four years follow up has now been completed and these effects are maintained.

A recent open-labelled trial of one years treatment with idebenone in 9 FRDA patients aged 11-19 used ICARS, echocardiography, and neurophysiology to evaluate response. There was a significant reduction in ICARS score at 3 months. Cardiac parameters did not change [539].

Future therapeutic trials in FRDA may make use of antioxidants or other agents coupled to the triphenylphosphonium cation, which facilitates mitochondrial targeting of the agent. In this way intra-mitochondrial vitamin E levels can be increased 80 fold [556]. Potentials for gene therapy are also being explored, and may utilise drugs that interfere with the "sticky DNA" structures that are thought to be the cause of the transcription blockade that occurs in FRDA. Gene therapy would need to overcome a large number of hurdles before being a therapeutic option in FRDA. Not least of these would be the systemic manifestations of frataxin deficiency.

Therapeutic trials in FRDA are also hampered by the lack of natural history data, making it difficult to evaluate treatments that may only serve to slow down the rate of disease progression. Furthermore, there is a dearth of information regarding the suitability of the vast range of measurement tools that have been proposed for the evaluation of ataxia it treatment trials. These issues and the results of our own trial of combined Co Q_{10} and vitamin E therapy in FRDA are the subject of chapter 6.

CHAPTER 2

MATERIALS AND METHODS

2.1 Materials

The following equipment was used unless otherwise stated.

Tissue culture and human tissue handling equipment

ICN-Flow Automatic CO_2 Incubator model 320 (ICN-Flow Ltd, High Wycombe, Bucks, UK); Gelaire (ICN-Flow) for tissue culture; Class 1 ICN Flow hood.

Centrifuges

Beckman GPR bench-top centrifuge with GH-3.7 horizantal rotor (Beckman Ltd, High Wycombe, Bucks, UK), Kontron T-124 high speed centrifuge with 8.24 8x50ml fixed angle rotor (Kontron Instruments, Watford, Herts, UK), Biofuge 13 with 18x1.5ml fixed angle rotor (Haraeus, Germany), Fresco Microentrifuge (Heraeus).

Electrophoresis equipment

Biorad 200/2.0 constant voltage power packs (BioRad Lab. Ltd., Hemel Hempstead, Herts, UK), BRL horizontal system for agarose gel electrophoresis (Bethseda Res Lab, Life Tech Inc., Gaithsburg, MD20887, USA) UV transilluminator (GRI Ltd., Dunmow. Essex, UK) and Polaroid camera.

Cell and Tissue homogenisers

Uni-form 5ml and 10ml glass/Teflon homogeniser (Jecons Ltd., Leighton Buzzard, Bedfordshire, UK), 5ml glass homogeniser and Glass-Col stirrer (CamLab Ltd., Cambridge, UK)

Spectrophotometers

Hitachi U-3210 (Hitachi Scientific Instrumants, Wokingham, Berks, UK) and Kontron Uvikon 940 (Kontron Instruments, Watford, Herts, UK) split beam spectrophotometers.

Microscopy and photography

Zeiss axiophot fluorescence microscope with FITC and rhodamine filters (Carl Zeiss Microscope Division, Oberkochen, Germany), Kodak ektachrome 400 for immunofluorescence.

Chemicals

Unless otherwise stated all chemicals were purchased from Sigma, Poole, Dorset, UK or Merck Ltd, Dagenham, Essex, UK.

2.2 Cell Culture

2.2.1 Cell lines

Myoblasts

Primary myoblast cultures were set up from 16 week old foetal skeletal muscle with ethical approval of Imperial College Medical School Ethics Committee.

A549 B2 Neo ρ^0 cells

These cells were a gift from Dr Ian Holt, Ninewells Hospital Dundee. A549 cells are an immortal cell line derived from a human male lung carcinoma. Depletion of mtDNA had been achieved by prolonged exposure to ethidium bromide at 50 ng/ml [557]. This cell line had also been transfected with a gene conferring resistance to G418.

206 ρ^0 cells

These cells were a gift from Dr G Attardi (CalTech, San Francisco, USA). This is an immortal cell line derived from the osteosarcoma line 143B.TK and rendered ρ^0 by the same technique as described for A549 cells. These cells are resistant to bromodeoxyuridine (BrdU).

NT2 cells (Ntera2/D1) (Stratagene, UK)

NT2 cells are neuronal precursor stem cells derived from a human teratocarcinoma. Following treatment with retinoic acid these cells form post-mitotic mature neurones (hNT neurones) [558,559].

SHSY-5Y cells

SHSY-5Y are a human neuroblastoma cell line that can be differentiated with retinoic acid to produce a neuronal phenotype. This phenotype involves both morphological changes such as growth arrest and neuritic sprouting as well as biochemical changes such as the production of dopamine receptors [560].

IB3RN cells (ECACC)

The IB3RN cell line is an SV40 transformed normal male human fibroblast line resistant to geneticin (G418)

STOG ρ^0 cells

STOG mouse fibroblasts cells were a kind gift from Dr P Simons, Dept of Anatomy, Royal Free Campus, UCL medical School. They were rendered ρ^0 by prolonged exposure to ethidium bromide. They are derived from Sim-1 cells (Sandos Inbred Mice) [561]

2.2.2 Cell growth conditions

All chemicals and plates were obtained from Life Technologies Ltd (Paisley, UK) except DMSO, pyruvate and BrdU which were from Sigma chemicals Co. (Poole, UK).

2.2.3 Cell culture maintenance and harvesting

Unless otherwise stated cells were grown on 10 cm plastic culture dishes. Myoblasts were grown in 10 cm pre coated plates (Sarstedt).

Fibroblasts, STOG, A549, IB3RN and NT2 cells were grown in standard growth medium, consisting of Dulbeco's modified Eagles medium (DMEM) containing glucose (4.5g/litre) and glutamine (5mM), penicillin 50units/ml, streptomycin 50mg/l, 10% (v/v) fetal calf serum, 0.2mM uridine and 1mM sodium pyruvate. Myoblasts were grown in standard medium but with 20% (v/v) fetal calf serum. SHSY-5Y cells were grown in standard growth medium except that a 50:50 mix of Eagle's modified essential medium and Ham's F12 replaced the DMEM, with 15% (v/v) fetal calf serum, and 1% non-essential amino acids. Selection medium was made using the above ingredients, but omitting uridine and pyruvate, and using dialysed fetal calf serum (Labtech international). Growth medium was changed twice weekly. Cells were washed whenever medium was changed with sterile phosphate buffered saline (PBS, Sigma UK), consisting of 137mM NaCl, 2.7mM KCl, 10mM Na_2HPO_4, and 1.8mM KH_2PO_4 pH 7.4. When cells reached confluency they were subcultured by harvesting. To harvest, cells were first washed twice with PBS, then 1ml of 10% (v/v) trypsin (2.5%) in Versene was added for 1-2 minutes at 37^0C until the cells were easily dislodged by gently tapping the plate. Trypsin was inactivated by the addition of 5 mls of fresh standard growth medium. Cells were then split onto 2-6 fresh plates, depending on their anticipated rate of growth, and total volume of medium on each plate was made up to 10 mls. Unless stated otherwise cells were grown at 37^0C and 8% CO_2.

Foetal myoblasts were cultured by placing the foetal limb in a bacterial petri dish, covering it with fungizone solution (5ml PBS, 0.1ml penicillin 50units/ml, streptomycin 50mg/l, and 0.5 ml Fungizone250μg/ml), and removing the skin. The muscle was isolated and minced with scissors. Erythrocytes were washed away with

small volumes of PBS. The muscle was transferred to a 10ml of enzyme solution (Hams F10 with 2% L-glutamine and 1% penicillin 50units/ml, streptomycin 50mg/l, plus 0.1% (w/v) collagenase type I, 0.1% (w/v) bovine serum albumin, 0.15-0.2% (w/v) trypsin in DMEM. The enzyme solution was filter sterilized through a 0.2 millipore filter. The muscle in enzyme solution was incubated at 37^0C for 15 minutes with constant agitation. The enzyme solution was then neutralized with an equal volume of growth medium. The solution was trituated in a 10ml pipette for 1 minute to generate a smooth cell suspension. The solution was filtered through a sterile 40μm cell strainer (Fulcon). The filtrate was centrifuged at 350g/1000 rpm for 10 minutes at room temperature. The supernatant was removed and the pellet was resuspended in 10ml of culture medium. The digestion process was repeated a further two times. The combined supernatants were placed onto 35 mm tissue culture dishes precoated with 0.1% gelatin. The dishes were incubated at 37^0C and 5% CO_2. The medium was changed every three to four days [562].

2.2.4 Culture conditions for the generation of ρ^0 cell lines

Cells were grown in the presence of ethidium bromide (EtBr) (Sigma chemicals) at a final concentration of 5, 0.5, 0.05, 0.04, 0.025, 0.01, or 0.005 μg/ml, or in the presence of dideoxycytidine (ddC) (Sigma chemicals) at a final concentration of 1, 2, or 3 μM. The ethidium bromide or ddC were refreshed with each change of culture medium.

2.2.5 Cell freezing and defrosting

A confluent plate of cells was harvested and centrifuged at 350g for 10 mins at RT. The pellet was resuspended in sterile freezing medium. Freezing medium consisted of 90% growth medium and 10% DMSO filter sterilised for all cells except NT2 and SHSY5Y for which 90% fetal calf serum and 10% DMSO was used. All cells were frozen in 1ml cryotubes and frozen slowly in polystyrene boxes at -70^0C overnight before long term storage in liquid nitrogen.

Frozen cells were defrosted by rapidly thawing the vial in a water bath at 37^0C. The contents of the vial were added to 10mls of pre-warmed growth medium and then centrifuged at 350g for 10 minutes. The supernatant was removed and the resultant

pellet was resuspended in 10mls of fresh medium. The following day cells were washed with PBS and fed with fresh medium.

2.3 Cell fusion methods

Enucleations, and construction of A3243G/ρ^0 and control cybrids.

Fibroblasts for enucleation were grown until nearly confluent on collagen coated 2cm plastic discs cut from the bottom of 10cm culture dishes. These were sterilised by 15 mins of exposure to UV light and then coated with 0.1% gelatin. The discs with fibroblasts attached were inverted in sterile centrifuge tubes containing 5mls of pre-warmed DMEM containing 10μg/ml of cytochalasin B. Centrifugation at 12000g for 20 mins achieved enucleation of >50% of fibroblasts as judged by direct visualisation under light microscopy. The cytoplasts (enucleated fibroblasts) were incubated with $3x10^5$ ρ^0 cells for 3 hours at 37^0C. Fusion was then achieved by agitating the cells upon their coverslips for 1 minute in polyethylene glycol (PEG) 50%w/v and DMSO (10%w/v) in DMEM. Coverslips were then washed three times in DMEM / 10%DMSO with a final wash in standard growth medium. 24 hours later cells were plated at very low density in selection medium. Growing colonies were identified and isolated 3-6 weeks later.

Platelet fusions

30 ml of venous blood was taken using a 19G butterfly and no tourniquet. The blood was mixed with 3ml of 3.8% (w/v) tri-sodium citrate to prevent clotting. The platelet rich plasma (PRP) was separated by centrifugation at 200g for 20 mins. The supernatant containing PRP was taken off and prostaglandin I_2 (fc 3.5nM) added to prevent platelet aggregation. The PRP was then centrifuged at 1000g for 30 mins. The resultant PRP pellet was then resuspended in 15mls of modified Tyrodes buffer (see appendix) centrifuged at 1000g for 10 minutes. This Tyrodes wash was repeated twice more.

ρ^0 cells were prepared for fusion by harvesting, counting using a haemocytometer, and resuspending in Ca^{2+} free DMEM to a concentration on $5x10^5$ cells /ml. 2 mls of this was added to the PRP pellet, and the mixture then centrifuged at 200g for 5 mins. The supernatant was aspirated and the pellet containing platelets and ρ^0 cells was resuspended in 100μl of PEG/DMEM mixture (5g PEG 1500 in 4ml Ca^{2+} free DMEM

and 1ml DMSO). The suspension was incubated for exactly 1 minute by agitation by pipetting. 10 ml of standard growth medium was then added and cells transferred to a 10cm culture dish. The next day cells were washed 3 times with PBS to remove debris and fed with standard growth medium. 24 hours later medium was replaced by selection growth medium. Growing colonies were identified and isolated 3-6 weeks later.

2.4 Isolation of clones

Two different techniques were used. 1) Plastic rings were cut from the tops of 0.5ml eppendorfs and autoclaved. Growth medium was removed from the culture duishes containing mature colonies, and two PBS washes were performed. The sterile plastic rings were dipped in UV sterilised high vacuum silicone grease and then placed so as to surround the individual clones. 100µl of trypsin was added to each well and the clone harvested with 100µl of standard growth medium. The cells were them transferred to 35mm culture dishes for further growth and grown in non-selection medium from this point onwards. 2) Sterile 100µl pipette tips were used to draw up 50µl of growth medium followed by 50µl of air so as to leave the bottom half of the tip empty, with medium above this air space. The tip could then be used to scrape over an individual colony, causing the cells of the colony to impact into the air space of the tip. The medium in the upper part of the tip could then be used to flush out the cells onto a fresh 35mm culture dish for further growth. Cells were grown in non-selection medium from this point onwards.

2.5 DNA extraction

DNA was extracted from 1-10x10^6 cells or 2-5mls of whole blood using the Nucleon 1 DNA extraction kit (Scotlab, UK) according to the manufacturer's instructions. The extracted DNA was stored in 50µl sterile TE at –20^0C. The yield was approximately 5µg DNA per 10^6 cells.

2.6 Estimation of DNA concentration and purity

5µl of DNA solution was added to 995µl ddH_2O in a 1ml silica quartz cuvette and mixed by inversion. The solution was scanned by measuring the absorbance pattern between 210nm and 310nm. The DNA concentration (µg/µl) was calculated assuming

that a 1mg/ml DNA solution has an absorbance of 20 at 260nm (Maniatis). The purity of DNA was accepted when the A_{260}/A_{280} ratio was between 1.7 and 2.0.

2.7 Polymerase Chain Reaction (PCR)

DNA primers, dATP, dGTP, dCTP, dTTP, Taq polymerase, polymerase buffer, and $MgCl_2$ were obtained from Perkin-Elmer Ltd (Bucks, UK). The standard PCR mixture, total volume 50µl, contained DNA (1 µg), forward and reverse primers (25 pmol, see relevant chapters for primer sequences), 0.2mM of each dNTP, 1.5mM $MgCl_2$, and 5 units of Taq polymerase, and polymerase buffer (20mM Tris-HCl, 100mM KCl pH7.5). The reaction was either carried out in 0.5 ml eppendorf tubes, with sterile paraffin overlayed, or in 0.3ml thin walled PCR tubes using a Perkin-Elmer 2400 thermal cycler.

Standard reaction conditions were an initial denaturation of 94^0C for 4 mins. Taq polymerase was added at 72^0C if the reaction required a "hot start". This was followed by 1 minute of denaturation at 94^0C, 1 minute of primer annealing (see relevant chapters for annealing temperatures), and 1 minute of primer extension at 72^0C repeated for 25-35 cycles. Finally the reaction was completed with 10mins of extension at 72^0C. Variations of these standard conditions were used, and are described in the relevant chapters.

2.8 Semi-quantitative PCR detection of mtDNA levels

PCR amplification of a 630bp fragment of mtDNA (2928-3558bp) was performed. Standard PCR conditions were used (section 2.7) with an annealing temperature of 60^0C. The forward primer at nt 2928mtDNA:5'-CCT AGG GAT AAC AGC GCA AT-3' and the reverse primer at nt 3558mtDNA:5'-TAG AAG AGC GAT GGT GAG AG-3' were used to amplify the mtDNA fragment. The PCR products were visualised on a 1.2% agarose gel. Comparisons were made with normal controls and a standard curve constructed with a dilution series of cellular DNA starting with 50µg. Known ρ^0 cell lines were also used as positive controls. This allowed for a semi-quantitative analysis of mtDNA levels.

A 1kb PCR was also performed on occasions to exclude the presence of a nuclear pseudogene mimicking the persistence of mtDNA after attempted depletion. The forward primer at nt 8765 mtDNA:5'-CCA CAA CTA ACC TCC TCG GA and the

reverse primer at nt 9765 mtDNA:5'-TGA AGG GAG ACT CGA AGT AC were used to amplify the mtDNA fragment, using standard PCR conditions and an annealing temperature of 59^0C.

2.9 Restriction enzyme digests of DNA

All enzymes and buffers were obtained from Promega (Chilworth Science Park, Southampton). Conditions for individual restriction digests are given in the relevant chapters.

2.10 Detection of PCR DNA products

All PCR reaction products and restriction digest products were separated on agarose gels using the BRL horizontal system for agarose gel electrophoresis (Bethseda Res Lab., Life Technologies Inc.). 0.8-1.2% (w/v) agarose gels (Sigma) were prepared in 1xTAE buffer containing 1μg/ml ethidium bromide. To facilitate loading onto the gel, PCR products, restriction digest products, and DNA size markers (Smartladder (containing fragments of 200bp to 10 kb, Eurogentec, Belgium), or 1kb ladder were all diluted in 6x loading buffer (Promega UK Ltd, Hants). Electrophoresis was performed in 1xTAE buffer at 40-100 Volts for 1-3 hours. The sample was visualised using an ultraviolet transilluminator and then photographed with a Polaroid camera.

2.11 Determination of mutant load

Apa I digest

1μl of ApaI restriction enzyme (Promega, Chilworth Science Park, Southampton), was added to 2.3 μl of restriction enzyme buffer and 20μl of sample. The mixture was incubated at 37^0C for 1 hour. The products of the reaction were run on an agarsoe gel.

Polymerase chain reaction with fluorescent dUTPs

1μl of fluorescently labelled deoxynucleotides (dUTPs) (R6G 1X 3nmol; ABI PRISM) that had been diluted 5 times in water, was added prior to the last cycle of the PCR. The PCR products were purified and subjected to restriction fragment length polymorphism analysis.

Automated capillary electrophoresis (ABI PRISM® 373A, Perkin Elmer) was used for the quantitation of the heteroplasmic proportions for the specific mtDNA mutation in

different patient samples. The digested sample was precipitated using 4 volumes of ethanol per volume pf product. The pellet was mixed with 0.5 loading dye, 2μl of water and 0.5μl of GeneScan-400HD size standard that contains 21 DNA fragments ranging in size from 50 to 400 bp. The run was executed with the ABI PRISM® 373A Data Collection Software (version 1.2). The capillary was filled with the Performance Optimized Polymer 4 (POP4) that achieves size separation of DNA fragments.

After completion of the run (approximately 40 minutes per sample), analysis was accomplished with the GeneScan® Analysis software (version 3.0) that uses the size standard to determine the size of unknown DNA fragments. The GeneScan Analysis software calculates the size of the unknown DNA sample fragments by generating a calibration or sizing curve based upon the migration times of the fragments in the standard. The unknown fragments are mapped onto the curve and converted from migration times to sizes.

Calculation of the percentage of heteroplasmy was achieved by dividing the peak area to data point ratio of the undigested product over the sum of the peak areas to data point ratios of the digested and undigested products.

2.12 Enzyme Analyses

All assays were performed on either Hitachi U3210 or Kontron 940 dual-beam spectrophotometers at 30^0C in a final volume of 1 ml. Each enzyme was assayed in triplicate and values accepted if they were within 15% of each other. All chemicals were from Sigma Chemical Company and Boehringer Mannheim.

2.12.1 Citrate Synthase (CS)

CS is a mitochondrial matrix enzyme which was used as an indicator of mitochondrial mass in preparations as it has not known to be altered in disease states (Cooper JM personal communication). Respiratory chain activities were expressed as CS ratios to correct for variation in the purity of mitochondrial preparations or to correct for variation in the mitochondrial mass in tissue homogenates. The assay is based on the method of Coore et al 1971 [563]. The enzyme catalyses the condensation of acetyl-CoA and oxaloacetate to form citrate, producing CoA whose free thiol group combines with the 5-5'-dithiobis-nitrobenzoic acid (DTNB), resulting in an increase in the absorbance at 412nm.

Two cuvettes were set up containing: 100mM Tris-HCl buffer pH8.0, 200 μM Acetyl-CoA, 200 μM DTNB, 0.1% (v/v) Triton-X-100 and sample in a final volume of 1ml. The reaction was initiated by the addition of 100μM oxaloacetate and the increase in absorbance at 412nm measured. Citrate synthase activity was calculated using the molar extinction coefficient of 13.6 x 10^3 for the DTNB-CoA-SH complex and activity expressed as nmol/min/mg protein.

2.12.2 NADH-CoQ_1 oxidoreductase (complex I activity)

The method of Ragan (1987) was used to measure the rotenone sensitive CoQ_1 dependant oxidation of NADH at 340nm [564]. CoQ_1 was a gift from Eisai Chemical Co, Japan. A dilution of stock CoQ_1 was made in ethanol and its absorbance at 275 nm noted. Complete reduction of quinone to quinol was achieved by addition of excess sodium borohydride to the reference cuvette. The resultant absorbance change was used to calculate the CoQ_1 concentration using a molar extinction coefficient of $2.25x10^3$ [565].

Two identical cuvettes were set up containing 20mM potassium phosphate buffer pH7.2 with 8mM $MgCl_2$, 150μM NADH, 1mM KCN, 2.5 mg/ml BSA and sample. The reaction was initiated in the test cuvette by adding 50 μM CoQ_1. The rate of NADH oxidation was monitored by the change in absorbance at 340nm. After 10 minutes 10 μM rotenone was added to the test cuvette and the rotenone insensitive rate measured for a further 10 minutes. The complex I activity was defined as the rotenone sensitive rate (i.e. the total rate minus the rotenone insensitive rate). Calculation of activity used a molar extinction coefficient of $6.81x10^3$ for NADH to allow for the contribution of reduced CoQ_1 to the absorbance at 340nm. Enzyme activity was expressed as a ratio with citrate synthase (CS)

2.12.3 Succinate cytochrome c oxidoreductase (complex II/III)

This assay, based on the method of King [566], determines the combined activity of complex II and III. It detects the antimycin A sensitive, succinate dependent, reduction of cytochrome c at 55nm.

0.1M potassium phosphate buffer pH 7.4, 0.3mM potassium (K_2) EDTA, and 0.1mM cytochrome c were added to two identical cuvettes. Into two eppendorfs was placed 1mM KCN, 20mM succinate and sample. These were incubated at 30^0C for 5 minutes

to fully activate the enzyme. The contents of the eppendorfs were then added to the cuvettes to initiate the reaction. The change in absorbance at 550nm was monitored. After 10 minutes 20 μM antimycin A was added. The complex II/III activity was calculated as the rate which was sensitive to antimycin A using the molar extinction coefficient of cytochrome c ($19.2x10^3$). Enzyme activity was expressed as a ratio with citrate synthase (CS).

2.12.4 Succinate-ubiquinol oxidoreductase (complex II)

This assay, based on the method of Hatefi et al [567], measures, at 660nm, the reduction a dye, 6,6-dichlorophenolindophenol (DCPIP) in the presence of succinate and ubiquinone-2 (CoQ_2). Enzyme activity is taken as the rate inhibited by 2-thenoyltrifluoroacetone (TTFA).

Two identical cuvettes were prepared containing 50mM potassium phosphate buffer pH7.4, 0.1mM K_2-EDTA, 20mM sodium succinate, 74 μM DCPIP, 1mM KCN, 10μM rotenone and sample. 50μM of ubiquinol-2 was added to initiate the reaction. After 10 minutes 1mM TTFA was added to inhibit the reaction. Activity was calculated using the molar extinction coefficient of DCPIP ($2.1x10^3$). Enzyme activity was expressed as a ratio with citrate synthase (CS).

2.12.5 Ubiquinol-cytochrome c reductase (complex III)

This assay is based on the method of Birch-Machin et al [568]. Ubiquinol-cytochrome c reductase catalyses the oxidation of ubiquinol and the reduction of cytochrome c. This is measured at 550nm. The concentrations of ubiquinone-2 and cytochrome c influence the reaction rate. Their concentrations are therefore established prior to enzyme assay. To determine the cytochrome c concentration 15 μM of cytochrome c in ddH_2O (final volume 1 ml) was added to two identical cuvettes. A few granules of ascorbate were added to the reference cuvette thus reducing the cytochrome c. The absorbance change was noted and the cytochrome c concentration calculated (extinction coefficient19.2mM).

Ubiquinol-2 was prepared from ubiquinone –2 (10mM) in ethanol acidified to pH2 with HCl. After addition of ddH_2O to a final volume of 1ml, a few granules of sodium borohydride were added to reduce quinone to quinol. The quinol was extracted into 3ml of diethylether:cyclohexane (2:1 v/v) and the upper phase collected. 1ml of 2M NaCl was added and the upper diethylether phase collected. This was evaporated to

dryness under a stream of nitrogen gas. The resultant residue was dissolved in 1ml of ethanol, acidified to pH2 with HCl and alliquoted and stored at -20^0C under nitrogen gas to prevent oxidation.

To 10µl of ubiquinol-2 was added 10µl of 5M KOH and 980µl of ethanol. The subsequent oxidation of ubiquinol-2 to ubiquinone-2 led to an absorbance change at 275nm from which the concentration of ubiquinol-2 was determined using the extinction coefficient of 12.25mM.

The rate of non-enzymatic reduction of cytochrome c, influenced by the concentrations of ubiquinone-2 and ubiquinol-2, that occurs in this reaction was determined and subtracted from the observed sample rate. Identical cuvettes were set up with all reaction ingredients (see below) except ubiquinol and sample. Ubiquinol-2 was then added to the test cuvette and the rate of absorbance change at 550nm noted. The non-enzymatic activity was calculated as below.

To assay complex III activity the reaction contained 35mM potassium phosphate buffer pH7.2, 1mM K_2 EDTA, 5mM $MgCl_2$, 2mM KCN, 5µM rotenone and 15µM cytochrome c. 15µM ubiquinol-2 was added to the test cuvette to initiate the reaction which was followed at 550nm for 5 minutes.

Calculation of the pseudo first-order rate constant (k) is performed by extrapolation of the absorbance back to time=0 and determination of the change in absorbance at various time points up to two minutes. The non-enzymatic rate was calculated in the same way and subtracted from the sample rate. K/min/ml was calculated by: {ln0.288-ln(0.288-change in absorbance at time t) x 1000/sample volume(µl) x dilution factor}, where 0.288 represents the absorbance of fully reduced cytochrome c. The k/ml values for five time points were plotted against time and the gradient of the line was calculatedusing linear regression analysis (k/min/ml). Results were expressed as a ratio with citrate synthase (CS).

2.12.6 Cytochrome c oxidase (complex IV)

This assay is based on the method of Wharton et al [569] and monitors the oxidation of reduced cytochrome c at 550nm.

Reduced cytochrome c was prepared from 100 mls of a 1% (w/v) solution of horse heart cytochrome c in 10mM potassium phosphate buffer. This was reduced by adding an excess (13mg) of ascorbate. Complete reduction was confirmed by spectrophotometry at 550nm, using two cuvettes containing 50µl of the cytochrome c

solution and 950µl of 10mM potassium phosphate buffer. 10µl of freshly made saturated ascorbate solution was added to the sample cuvette. A positive change in absorbance would indicate that the cytochrome c solution could be further reduced by the addition of ascorbate, and was therefore not yet fully reduced. When fully reduced, removal of the ascorbate from the cytochrome c solution was achieved by dialysis, using size 1 dialysis tubing (Medicell International Ltd., London) and dialysing against 5litres of 10mM potassium phosphate buffer pH7.0 at 4^0C overnight. To confirm complete removal of ascorbate, oxidised cytochrome c was added to a sample of the dialysed reduced cytochrome c. No change in absorbance implied complete removal of ascorbate.

The concentration of reduced cytochrome c was calculated by placing 100µl of 100mM potassium phosphate buffer pH7.0, 850µl ddH_2O, and 50µl of reduced cytochrome c in two identical cuvettes. 10µl of 0.1M K^+ Ferricyanide was added to the reference cuvette to oxidise the reduced cytochrome c. The change in absorbance was noted and the concentration calculated by: 0.96/Absx50=volume of stock cytochrome c solution required for 50µM solution (where 50µM cytochrome c produces an absorbance of 0.96).

The enzyme assay was performed by adding 10mM potassium phosphate buffer and and 50µM cytochrome c to two identical cuvettes. 10µl of 100mM K^+ Ferricyanide was added to the reference cuvette to oxidise the cytochrome c. The initial absorbance was noted (0.96=50 µM cytochrome c) and the reaction initiated by the addition of sample to the test cuvette. The reaction was followed at 550nm. The pseudo first-order constant k was calculated as for the complex III assay. Complex IV activity (k/min/ml) was expressed as a ratio with citrate synthase (CS).

2.12.7 Aconitase

Aconitase catalyses the isomerisation of citrate to isocitrate. With the reduction of NADP this product then forms α-ketoglutarate. This assay measures this reduction of NADP at 340nm. Into two identical cuvettes are added 50mM Tris-HCl pH7.4, 0.4mM NADP, 5mM sodium citrate, 0.6mM $MgCl_{2,\ 1\%}$ (v/v) Triton X-100 and 2 units of isocitrate dehydrogenase. Sample was added to the test cuvette only, and both cuvettes were pre-incubated at 30^0C for 30 minutes. The absorbance change at 340nm was then followed for 15 minutes. Aconitase activity was calculated using the molar extinction coefficient for NADP ($6.22x10^3$).

2.13 Preparation of mitochondrial-enriched fractions (MEFs)

MEFs were prepared from twenty confluent 10cm plates of cells based on the method of Ragan et al [564]. Harvested cells were washed three times in PBS and the resultant pellet frozen at -70^0C overnight. The pellets were thawed and resuspended in 2ml of ice-cold homogenisation buffer (see appendix). Each sample was homogenised on ice using a Potter homogeniser for 20 strokes at 1000 rpm. The sample was spun at 1500g for 10 minutes at 4^0C. The resultant post-nuclear supernatant (PNS) was collected into a fresh tube on ice. Homogenisation of the residual pellet in a further 2ml of homogenisation buffer and subsequent centrifugation was performed twice more. The combined PNS (6 mls) was subjected to a further centrifugation and any resudual pellet discarded. The final PNS was centrifuged at 10,000g for 12 minutes at 4^0C on a Kontron Centrikon T-124. A small brown pellet, the mitochondrial enriched fraction, was generated. This was resuspended in 200-800µl of ice-cold homogenisation buffer, snap frozen in liquid nitrogen and stored at -70^0C for a maximum of five days before assaying. All samples were freeze thawed in liquid nitrogen three times before assaying to maximise the mitochondrial enzyme activities.

2.14 Preparation of brain homogenates

Brain samples were stored at -70^0C. Aliquots were removed, put in liquid nitrogen and weighed. Homogenisation was performed in nine volumes of ice-cold homogenisation buffer using a 5ml glass/Teflon homogeniser. Samples were freeze-thawed as above prior to immediate assaying.

2.15 Preparation of muscle homogenates

Muscle samples were stored at -70^0C. Aliquots were removed, put in liquid nitrogen and weighed. Homogenisation was performed in ice-cold homogenisation buffer using a glass/glass homogeniser. Samples were freeze-thawed as above prior to immediate assaying.

2.16 Preparation of cell homogenates (for aconitase assay)

Three confluent plates of cells were harvested using a cell scraper (Lifetech Ltd). Cells were washed three times in PBS and the pellet was then resuspended in 1ml of ice-cold homogenisation buffer. Assays were performed immediately.

2.17 Protein assay

All protein assays were performed using the Pierce-Warriner BCA™ Protein assay reagent. This system uses the reaction of protein with Cu^{2+} in an alkaline environment to form Cu^{1+} which is then detected by the reagent bicinchoninic acid (BCA). The purple reaction product of BCA and Cu^{1+} is water-soluble and exhibits a strong absorbance at 562nm. For each assay a set of protein standards, made to cover the range of protein concentrations expected for the samples being tested, was made using bovine serum albumin (BSA) in the same diluent as the samples. The assay was performed according to the manufacturers instructions. The protocol requiring thirty minutes incubation at room temperature was used. Each assay was performed in triplicate.

2.18 Immunofluorescence staining of cultured cells

Cultured cells were seeded onto coverslips. Coverslips were washed three times im PBS, and then fixed in pre-warmed 4% paraformaldehyde in PBS for 20 minutes. After a further three washes in PBS coverslips were immersed in methanol at -20^0C for 15 minutes. After a further three washes in PBS coverslips were blocked with 10% normal goat serum in PBSfor 30 minutes at 37^0C in a humidified atmosphere. Cells were then incubated with the primary antibody for 2 hours at 37^0C, then washed, then incubated with goat anti-mouse IgG Alexa® 488 (molecular probes, Inc.) for 1 hour at 37^0C. After a final three washes in PBS coverslips were mounted on glass slides in Citifluor/PBS/glycerol (Agar) supplemented with 1 μg/ml of DAPI (Sigma).

2.19 Microscopy and photography

All microscopy for immunofluorescent staining of cultured cells was performed using a Zeiss axiophot microscope (Carl Zeiss microscope division, Oberkochen, Germany) with Kodak EPH p1600 (ASA 3200) film.

2.20 Statistical analysis

Statistical analysis of all enzyme activity data was performed using the Mann-Whitney U test via Instat statistical software for enzyme assay data.

2.21 Health-Related Quality of Life in Friedreich's Ataxia

2.21.1 Patients

Fifty-six patients with clinically defined FRDA, and with confirmed homozygosity for the GAA intronic repeat expansions in the FRDA gene were recruited via the Ataxia Society. The patients had contacted us in response to an advertisement placed in the Ataxia Society magazine asking for volunteers for a therapeutic trial.

2.21.2 Genetic Analysis

Prior to recruitment into this study, the diagnosis of FRDA was confirmed in all patients by the detection of the GAA repeat expansion within our own laboratory [539].

2.21.3 Health status measures

A single questionnaire containing demographic questions and the four health status measures were sent by post to these 56 patients. The four health status measures used were the Barthel Index, General Health questionnaire, Euroqol, and short form 36. Questionnaires were sent out at t=0 and resent to non-respondents at 6 weeks, and again at 6 weeks after that. Only patients over the age of 18 were sent the questionnaire since these health measures have not previously been validated for use in children.

The SF-36 contains eight domains and a single question about perceived changes in health change over the preceding month. A scoring algorithm converts the raw scores onto a scale from 0 (poor health) to 100 (good health). Two summary scales, the Physical Component Summary Score (PCS) and the Mental Component Summary Score (MCS) can be derived. Scores above 50 imply better health than the mean of the general population and scores below 50 imply worse health. There is one further unscaled item in the SF-36 asking respondents about health change over the past year. Findings can be compared with normative data obtained in the UK [570,571].

Euroqol was developed by a multidisciplinary group of researchers from 5 European countries. It requests one of three possible responses of no problem, some problems, unable or extreme problems to questions regarding mobility, self-care, usual activities, pain/discomfort, and anxiety/depression (table 6.1). A single overall score is also gained by the Euroqol thermometer, a simple visual analogue scale. The items that comprise the Barthel Index and the GHQ 12 are also listed in table 2.1.

EuroQol Health State	SF-36
Mobility (1 item)	Physical functioning (10 items)
Self care (1 item)	Social functioning (2 items)
Usual activity (1 item)	Role limitations due to physical problems (4 items)
Pain/discomfort (1 item)	Role limitations due to emotional problems (3 items)
Anxiety/depression (1 item)	Mental health (5 items)
	Energy/vitality (4 items)
	Pain (2 items)
	General health perception (5 items)

Barthel	GHQ 12
Bathing (1 item)	Concentration (1 item)
Transfer (1 item)	Worry (1 item)
Dressing (1 item)	Playing a useful part in things (1 item)
Feeding (1 item)	Making decisions (1 item)
Mobility (1 item)	Under strain (1 item)
Stairs (1 item)	Overcoming difficulties (1 item)
Toilet use (1 item)	Enjoying normal activities (1 item)
Grooming (1 item)	Facing up to problems (1 item)
Bladder (1 item)	Unhappy and depressed (1 item)
Bowels (1 item)	Self confidence (1 item)
	Worthlessness (1 item)
	Happiness (1 item)

Table 2.1

Dimensions of four health measures: Barthel, General Health Questionnaire 12, EuroQol Health State and Short Form 36. Numbers in brackets show the number of items in each category.

2.22 Friedreich's ataxia: Evaluation of ICARS and Factors Influencing Clinical Progression.

2.22.1 Patients.

Patients were recruited via Ataxia UK and by direct referral from consultant Neurologists. All assessments and investigations were performed with the approval of the Royal Free Hospital Ethics committee.

2.22.2 Genetic Analysis.

Genetic analysis was performed as in 2.21.2

2.22.3 Clinical Assessments

Patients were examined and assessed using ICARS on a total of 209 occasions. Examinations were recorded onto videotape. Ten patients were entered into a pilot open labelled study following their initial assessments [539], and a further 3 patients were added to the pilot study following several assessments. The remaining 64 patients were assessed on two or three occasions and 50 patients were entered into a double-blind, randomised, placebo-controlled treatment trial of combined vitamin E and coenzyme Q_{10}. The same examiner (PEH) performed all assessments. At selected assessments patients also underwent studies to evaluate the symptoms associated with cardiac (Dr J Joshi, National Amyloidosis centre, Royal Free Hospital), neurophysiology (Dr M Al-Khayatt, Department of Neurosciences, Royal Free Hospital), speech, swallowing and upper and lower limb co-ordination as part of the therapeutic trial.

Activities of daily living (ADL) were scored using a 0 to 36 point scale modified from standard scales [572]. A maximum of four points from normal to severe disability was assigned to speech, swallowing, cutting food and handling utensils, dressing, personal hygiene, falling, walking, quality of sitting position, and bladder function.

Retrospective analysis of disease progression was achieved using a patient questionnaire and interview. This ascertained five disease stages (0-4) as defined by the age at which the patient first: 0) had difficulty walking, 1) always required aid while walking outside, 2) used a wheelchair, 3) had to use a wheelchair all the time when outside, and 4) had to use a wheelchair all the time when outside or inside.

Complete 2D echocardiography and Doppler studies were performed using GE Vingmed System V performance ultrasound machine with wide band width 2.5mHz centre frequency probe with coded harmonics. Left ventricular wall thickness was measured from the anterior and posterior walls from short axis cuts at the mitral level, papillary muscle and apex, and corrected for body surface area in children.

Nerve conduction studies were performed with a Medelec Saphire 112ME and evoked potential using a Digitimer D200. Limb temperatures were maintained at room temperature. Sensory action potentials (SAP) and sensory nerve conduction velocities (SNCV) were determined in the right median, ulnar, radial and sural nerves. Motor studies were performed on the right median and common peroneal nerves by placing surface electrodes on the right abductor policis brevis and extensor digitorum brevis muscle respectively. Somatosensory evoked potentials (SSEP) were analysed on the right median nerve. Latencies to Erbs point (N9), cervical region (N13) and parietal cortex (N20) were calculated.

The presence of diabetes mellitus or impaired glucose tolerance was ascertained by patient history and by random plasma glucose and HbA1c analysis. Optic neuropathy and scoliosis were defined by patient history alone.

2.22.4 Statistical analysis

Single and multiple linear regression analyses were performed using SPSS.

Retrospective analysis of disease progression was analysed between groups via weighted means at subsequent timepoints with the weights based on estimated survival curves as described by Zilber et al 1994 [573]. Due to censored observations at intermediate stages the method was slightly modified. Each survival curve was bounded by the survival curve of the following stage. Group comparisons were done with a closed test procedure of *F* tests in repeated measurement ANOVAs (analysis of variance).

CHAPTER 3

NUCLEAR INFLUENCES ON THE BIOCHEMICAL EXPRESSION OF THE A3243G MITOCHONDRIAL DNA MUTATION.

3.1 Introduction

Phenotypic variability is a key feature of the archetypal mitochondrial disorders. Patients can present at a wide range of ages with mild or severe disease. Patients may have an isolated slowly progressive non-disabling myopathy, or present with a severe multi-system disorder that proves rapidly fatal.

Mutation load is generally accepted as a key factor underlying this phenotypic variability. However as previously discussed (section 1.8.1.2) a number of studies have failed to confirm a threshold effect and alternative mechanisms have been suggested to determine the phenotypic consequences of mtDNA point mutations. Both nuclear and secondary mtDNA factors have been suggested and the experiments in this chapter were designed to explore this hypothesis.

Four aspects have been addressed in this experimentation.

- does the nuclear background of the recipient cell influence the level of A3243G mtDNA that can be established in cybrids,
- what is the effect of mutant mtDNA level on MRC function,
- what is the effect of mutant mtDNA levels on reactive oxygen species injury in cybrid clones,
- what influence does nuclear background have on these preceeding two issues.

To study this mtDNA from patients with severe and mild A3243G associated phenotypes was fused with a variety of nuclear backgrounds, and resultant cybrids were analysed for mutant load, MRC function, and oxidative damage.

3.2 Experimental Hypothesis

The phenotypic variability associated with the A3243G common MELAS pathogenic mtDNA mutation is influenced by its nuclear environment and mtDNA genotype.

3.3 Experimental Design

The experiment was designed in two parts. Part A of the experiment was designed to test the integrity of the experimental techniques used in part B, and is described in full below. Part B forms the core part of the experiment and involves the fusion of different A3243G containing mtDNA with different nuclear backgrounds. The effect on the MRC function and aconitase activity of the resultant cybrids of varying mutant load would allow analysis of the effect of nuclear or mitochondrial background upon the expression of the A3243G mutation.

Part A: The generation of cybrid clones containing nuclear and mitochondrial DNA of different origins relies on the generation of ρ^0 cells that lack mtDNA. The introduction of foreign mtDNA to these cells then allows their survival in culture conditions that select for cells with intact MRC function. In order to rely upon this technique it must first be established to what extent ρ^0 cells are truly devoid of mtDNA, whether small amounts of native mtDNA persist and whether these have the potential to repopulate their parent cells. After fusion of platelets or enucleated fibriblasts with ρ^0 cells, prolonged culture is necessary for clones to become established. There is therefore a hypothetical concern that during this prolonged culture, ρ^0 cells with levels of native mtDNA below the level of detection may be able to repopulate themselves with self mtDNA. These cells would then be able to survive the selection process designed to ensure that only ρ^0 cells that have successfully fused with patient mtDNA proliferate. Therefore in this part of the experimentation the mtDNA content of ρ^0 cells was tested using semiquantative PCR and immunoflourescnece, and these were repeated after the cells had been cultured for a further 28 days (the average duration of the cybrid selection process) in culture medium free of the mtDNA depleting agent (ethidium bromide or ddC).

Part B: To investigate the potential contribution of the nuclear DNA and mtDNA background to the biochemical expression of mtDNA mutations we identified patients who harboured the A3243G common MELAS mtDNA mutation, but who had markedly different phenotypes. Patient platelets or enucleated fibroblasts were fused with a variety of ρ^0 cell lines, thus introducing patient mtDNA into a variety of nuclear backgrounds. Neuronal (SHSY-5Y) and embryonal myoblast (Myo^e) ρ^0 cell lines were generated *de novo* to provide a more physiological *in vitro* representation of the tissues most commonly affected *in vivo*. Fibroblast (IB3), lung (A549), and osteosarcoma (206) ρ^0 cell lines were also used. In this way the following sets of cybrids would be generated.

	A549 Lung	206 Osteosarcoma	SHSY-5Y Neuronal	IB3 Fibroblast	Myo Myoblast
Patient 1	1L	1OST	1N	1F	1M
Patient 2	2L	2OST	2N	2F	2M
Controls	C3	COST	CN	CF	CM

Clones covering a range of mutant loads were isolated and respiratory chain complex, aconitase and citrate synthase activities were analysed spectrophotometrically. Analysis of the biochemical function of these cell lines would allow the determination of the effect of different mtDNA molecules within the same nuclear background (i.e. 1 versus 2 versus Controls), and the effect of different nuclear backgrounds on the same mtDNA molecule (i.e. L versus OST versus N versus F versus M).

3.4 RESULTS

The generation of ρ^0 cell lines.

Lung A549ρ^0 cells were provided by Dr I Holt (Dunn Human Nutrition Unit, University of Cambridge) and osteosarcoma 206 ρ^0 cells were provided by Prof G Attardi (CalTech, California). Neuronal (SHSY-5Y and NT2), fibroblast (IB3) and embryonal myoblast (myo^e) ρ^0 were generated using standard mtDNA depleting

agents (ethidium bromide 0.005 – 5 μg/ml or dideoxycytidine ddC 1-10μM, section 2.2.4) for up to 120 days.

To determine if the cells had mtDNA depletion DNA extracted from the various cells was amplified to generate a 630 bp mtDNA specific product and semi-quantified using serial dilutions of the DNA template and the products analysed using agarose electorphoresis (section 2.8). To help exclude the presence of a nuclear pseudogene a 1kb PCR was also performed on some samples (section 2.8) In addition immunofluorescence using anti COX 1 antibodies was used to assess the relative loss of mtDNA encoded proteins (section 2.18).

Semi-quantitative PCR of A549 ρ^0 cells confirmed the absence of a 630bp mtDNA product even at the highest DNA template concentration of 50 ng and therefore demonstrated that they were ρ^0 (Figure 3.1A). Growth of the cells for a further 28 days in medium lacking ethidium Bromide (EtBr) gave rise to a faint 630 bp band at the highest DNA concentration after PCR amplification (figure 3B). This would imply mtDNA levels less than 0.1% of those of wild type ρ^+cells. Immunofluorescence using an antibody to a mtDNA encoded subunit (COX I) gave rise to clear cytosolic punctate pattern of staining in normal cells, most intense around the nucleus (figure 3.1C arrow). Immunoflourescence (IF) for A549 cells after EtBr treatment showed a loss of this punctate pattern (fig 3.1d arrow) confirming the loss of mtDNA demonstrated by PCR. 28 days after removal of EtBr COX I staining showed minimal punctate staining in some cells (fig 3.1E arrow) in keeping with the PCR results.

206 ρ^0 cells appeared to have significant levels of mtDNA as judged by semi-quantitative PCR (Figure 3.2 A) being perhaps 10% residual mtDNA levels compared to ρ^+cells. Paradoxically, after removal of EtBr for 28 further days of culture, mtDNA levels appeared to have reduced to 1% (fig 3.2B). IF results (figure 3.2 C-E) showed that ρ^0 cells had lost the punctate pattern of staining seen in ρ^+cells and that there was no significant change in the staining of ρ^0 cells after 28 days free from the effects of EtBr. The punctate staining evident in fig 3.2C was essentially absent in the ρ^0 cells at t=0 (fig 3.2D arrow). This suggested the ρ^0 cells had a lack of functional mtDNA in contradiction to the PCR findings.

Embryonal myoblasts were confirmed to be ρ^0 by PCR (fig 3.3A) and to not accumulate mtDNA after 28 days of culture in the absence of ddC (Fig 3.3B). Of note, the ρ^+cells showed mtDNA detectable to 4 serial dilutions, but at 28 days later, after no change in their culture conditions, mtDNA was only detectable to two serial dilutions. One could infer that mtDNA cell content varies greatly as a normal phenomenon, or perhaps more probably that the technique employed (semi-quantitative PCR) has limitations. Immunoflourescence with COX I antibody of embryonal myoblasts showed punctate staining (fig 3.3C) but in a less intense pattern than that seen in other cell types. ρ^0 cells lacked the punctate staining of the ρ^+cells cells, and had a different morphology (fig 3.3D arrow). At 28 days after removal of the mtDNA depleting agent, there are no discernable changes to the IF pattern (fig 3.3E arrow).

MtDNA was undetectable by PCR in the SHSY-5Y ρ^0 cells (fig 3.5 A) and remained so after 28 days in the absence of ethidium bromide (figure 3.5). IF studies again showed punctate staining in the ρ^+ cells (fig 3.5C), and absence of this pattern of staining in the ρ^0 cells (fig 3.5D arrow) and no reaccumulation of staining after removal of EtBr (fig 3.5E arrow).

NT2 cells, after prolonged exposed to maximal concentrations of EtBr or ddC, or both, failed to achieve ρ^0 status (fig 3.4 A). MtDNA content was reduced to approximately 1% of normal, but complete irradication of mtDNA from these cells was not achieved. The PCR product could be the result of a nuclear pseudogene but this potential explanation was excluded by performing a second PCR for a 1 kb fragment of a different part of the mtDNA molecule (fig 3.6). There was no evidence of an increase in mtDNA levels after removal of EtBr from the culture medium as judged by the PCR based technique, althought there was perhaps some increase in staining on immunoflourecence (fig 3.4 E).

A549, embryonal myoblasts, and SHSY5Y cells were therefore all shown to be suitable for use in platelet fusion experiments. It was apparent that NT-2 cells could

not be used for cybrid generation because, despite prolonged exposure to mtDNA depleting agent both singly and in combination, they failed to reach ρ^0 status. Due to the failure of NT-2 cells to reach ρ^0 status, IB3 cells (fibroblasts) were substituted after being confirmed ρ^0 (data not shown). 206 cells were also shown to contain residual mtDNA, but after further treatment true ρ^0 status was regained (data not shown) and these cells were used for cybrid generation. Neither PCR techniques nor IF studies provided any clear evidence of the re-accumulation of mtDNA levels after the removal of mtDNA depleting agents from the culture medium.

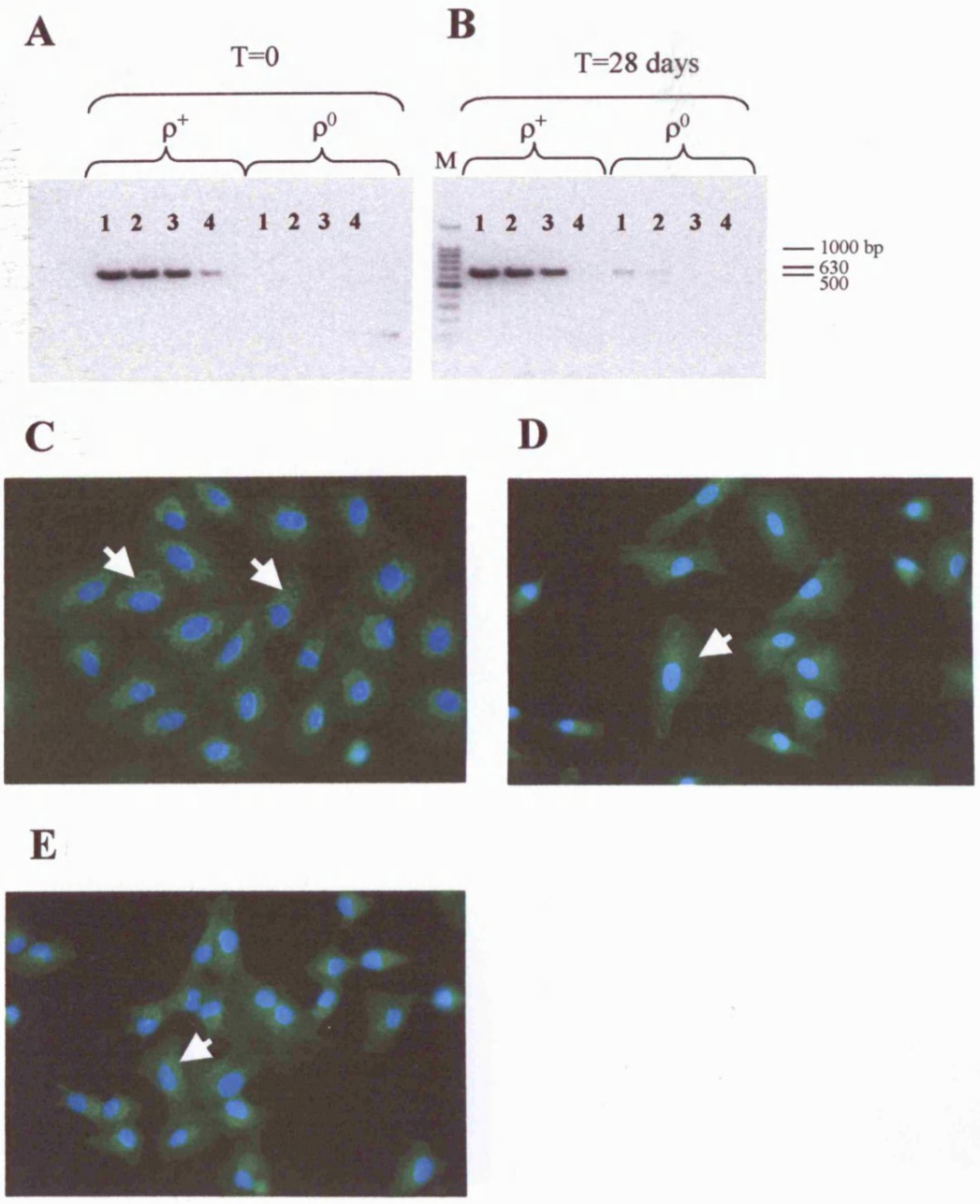

Figure 3.1 Analysis of mtDNA and COX I in A549 ρ+ and ρ^0 cells.

Semiquantitative PCR of a 630bp mtDNA fragment using serial dilution of cellular DNA,(lanes 1 to 5: 50, 5, 0.5,0.05 and 0.005ng DNA). (A) A549 ρ+ and A549 ρ^0 cells immediately following ethidium bromide treatment. (B) A549 ρ+ and A549 ρ^0 cells after 28 days growth in the absence of ethidium bromide. M is a 100bp ladder.

Immunoflourescence of subunit I of COX in (C) A549 ρ+ showing clear punctate mitochondrial staining (arrow), (D) ρ^0 cells after ethidium bromide treatment where mitochondrial staining is absent (arrow) and (E) ρ^0 cells 28 days after the removal of ethidium bromide showing a slight increase in mitochondrial staining (arrow).

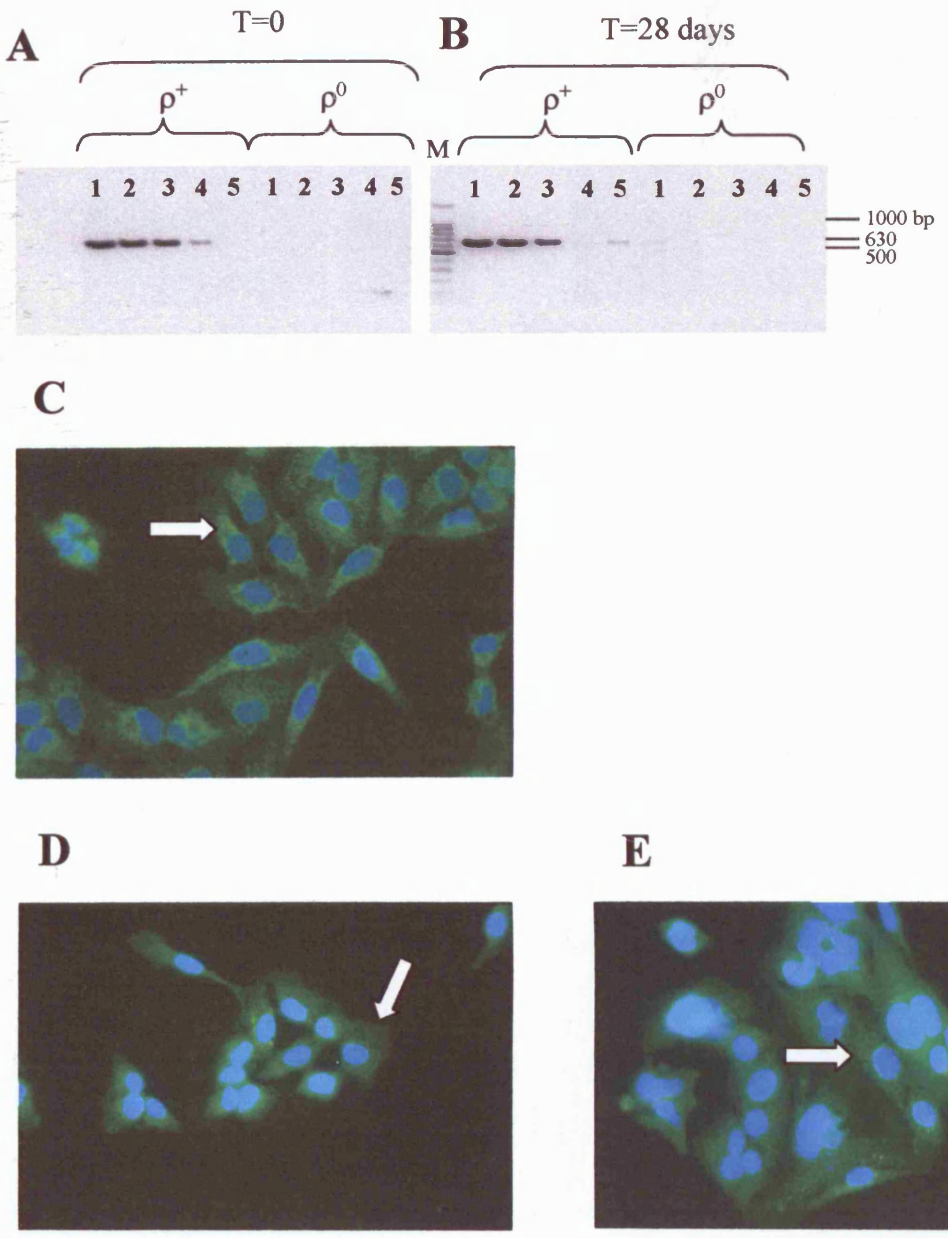

Figure 3.2 Analysis of mtDNA and COX I in 206 osteosarcoma ρ+ and ρ^0 cells.

Semiquantitative PCR of a 630bp mtDNA fragment using serial dilution of cellular DNA,(lanes 1 to 4, 50, 5, 0.5,0.05 and 0.005ng DNA). (A) 206 ρ+ and 206 ρ^0 cells immediately following ethidium bromide treatment. (B) 206 ρ+ and 206 ρ^0 cells after 28 days growth in the absence of ethidium bromide. M is a 100bp ladder.

Immunoflourescence of subunit I of COX in (C) 206 ρ+ showing clear punctate mitochondrial staining (arrow), (D) ρ^0 cells after ethidium bromide treatment where mitochondrial staining is absent (arrow) and (E) ρ^0 cells 28 days after the removal of ethidium bromide showing a slight increase in mitochondrial staining (arrow).

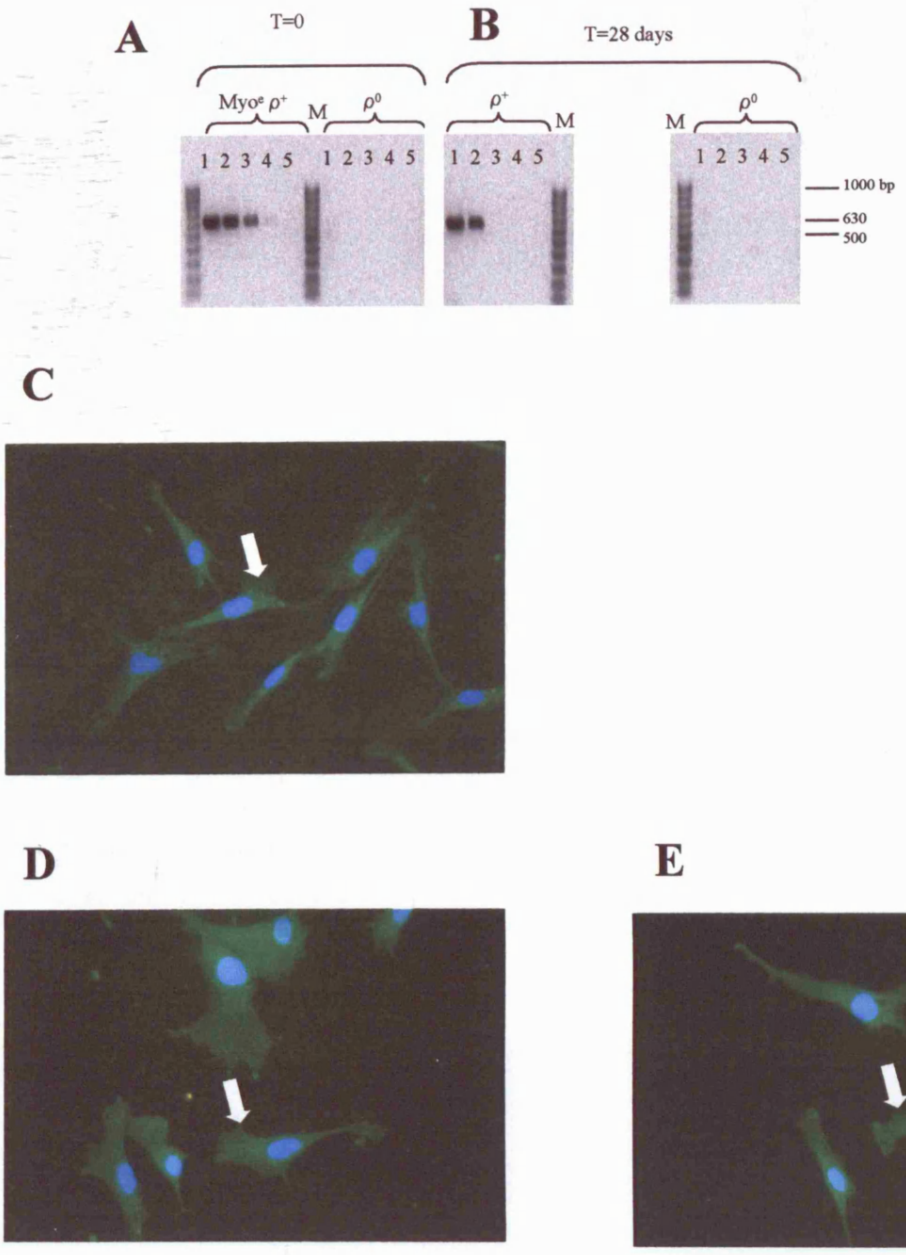

Figure 3.3 Analysis of mtDNA and COX I in embryonal myoblasts (Myo^e) ρ+ and ρ^0 cells.

Semiquantitative PCR of a 630bp mtDNA fragment using serial dilution of cellular DNA,(lanes 1 to 5, 50, 5, 0.5,0.05 and 0.005ng DNA). (A) Myo^e ρ+ and Myo^e ρ^0 cells immediately following ethidium bromide treatment. (B) Myo^e ρ+ and Myo^e ρ^0 cells after 28 days growth in the absence of ethidium bromide. M is a 100bp ladder.

Immunoflourescence of subunit I of COX in (C) Myo^e ρ+ showing clear punctate mitochondrial staining (arrow), (D) Myo^e ρ^0 cells after ethidium bromide treatment where mitochondrial staining is absent (arrow) and (E) Myo^e ρ^0 cells 28 days after the removal of ethidium bromide showing a slight increase in mitochondrial staining (arrow).

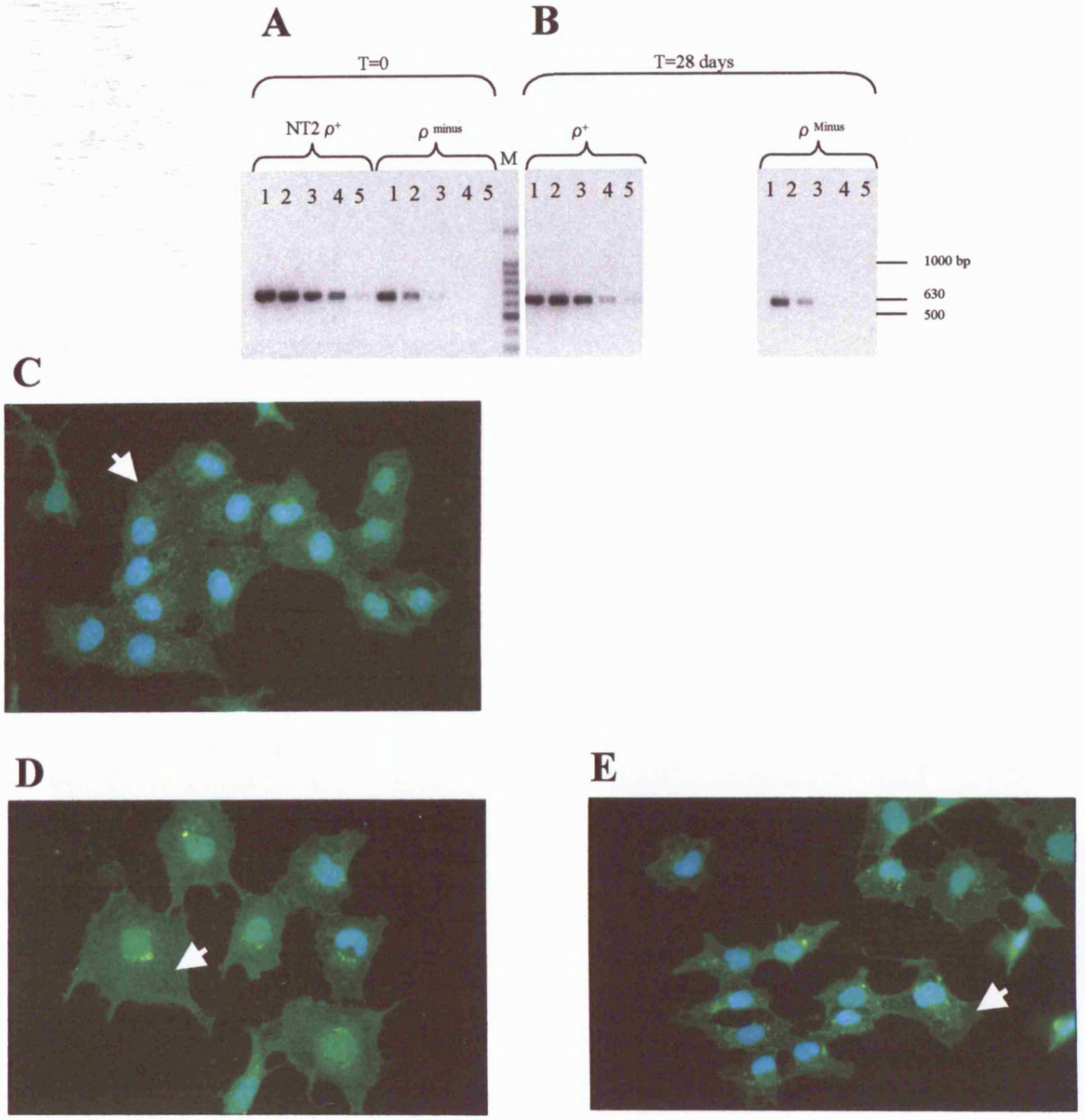

Figure 3.4 Analysis of mtDNA and COX I in NT2 neuronal ρ+ and ρ^0 cells.

Semiquantitative PCR of a 630bp mtDNA fragment using serial dilution of cellular DNA,(lanes 1 to 5: 50, 5, 0.5,0.05 and 0.005ng DNA). (A) NT2 ρ+ and A549 ρ minus cells immediately following ethidium bromide treatment. (B) NT2 ρ+ and NT2 ρ minus cells after 28 days growth in the absence of ethidium bromide. M is a 100bp ladder.

Immunoflourescence of subunit I of COX in (C) NT2 ρ+ showing clear punctate mitochondrial staining (arrow), (D) ρ minus cells after ethidium bromide treatment where mitochondrial staining is absent (arrow) and (E) ρ minus cells 28 days after the removal of ethidium bromide showing an increase in mitochondrial staining (arrow).

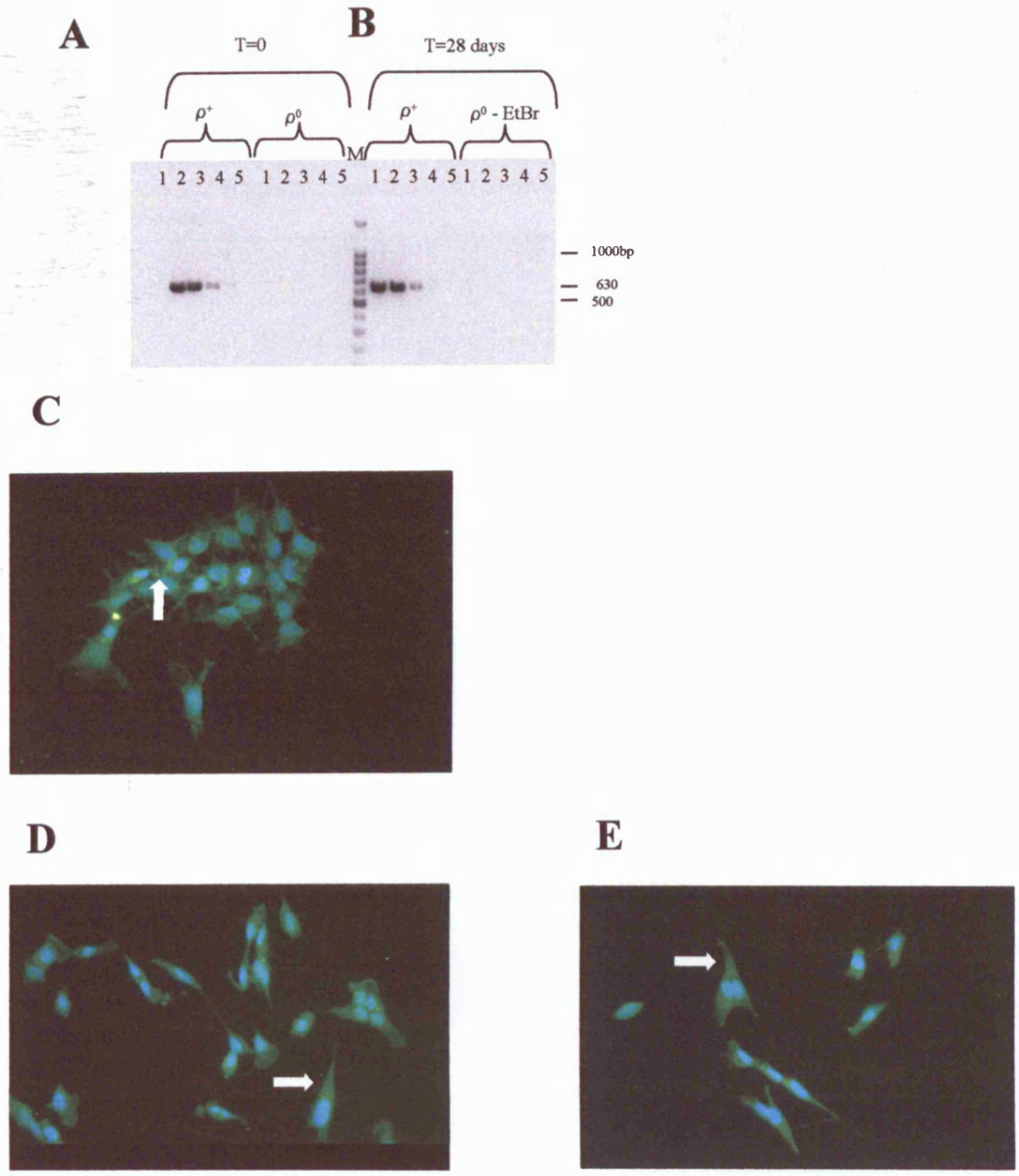

Figure 3.5 Analysis of mtDNA and COX I in SHSY-5Yρ+ and ρ^0 cells.

Semiquantitative PCR of a 630bp mtDNA fragment using serial dilution of cellular DNA,(lanes 1 to 5, 50, 5, 0.5,0.05 and 0.005ng DNA). (A) SHSY-5Y ρ+ and SHSY-5Y ρ^0 cells immediately following ethidium bromide treatment. (B) SHSY-5Y ρ+ and SHSY-5Y ρ^0 cells after 28 days growth in the absence of ethidium bromide. M is a 100bp ladder.

Immunoflourescence of subunit I of COX in (C) SHSY-5Y ρ+ showing clear punctate mitochondrial staining (arrow), (D) SHSY-5Y ρ^0 cells after ethidium bromide treatment where mitochondrial staining is absent (arrow) and (E) SHSY-5Y ρ^0 cells 28 days after the removal of ethidium bromide showing no reaccumulation of punctate staining(arrow).

Figure 3.6 Analysis of mtDNA content of NT-2 ρ^+ and "ρ^0" neuronal cells

Semi-quantitative PCR of NT-2 ρ^+ and "ρ^0" neuronal cells using primers for a 630 bp mtDNA (A), and a 1000 bp mtDNA fragment (B) to exclude a nuclear pseudogene being responsible form the result in A. Serial dilutions of cellular DNA (lanes 1to 5: 50, 5, 0.5, 0.05, and 0.005 ng DNA). M is a 100 bp ladder.

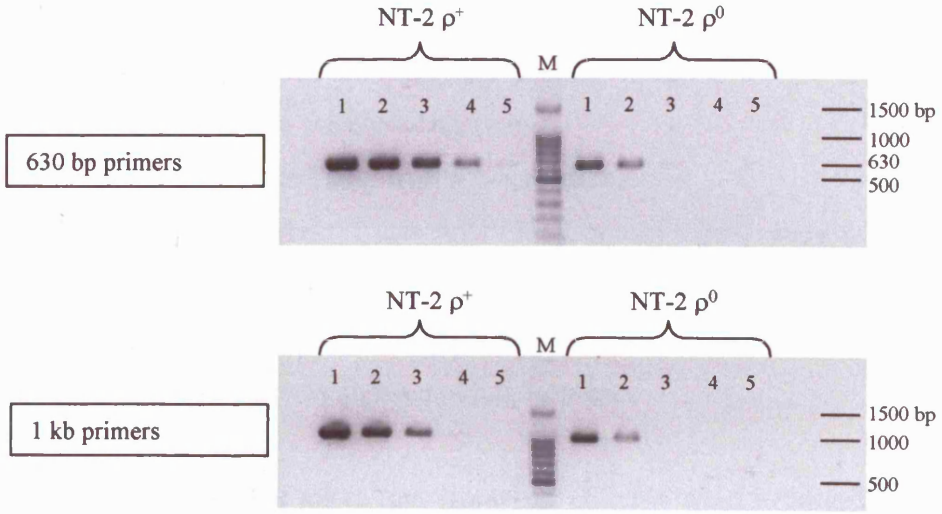

Generation of Cybrids containing mtDNA from A3243G mutant patients and controls.

Patient details:

All patients were confirmed A3243G positive.

EF was a 62 year old man who had presented 12 years previously with a pure myopathy. He had not developed central nervous system disease.

RS was a 44 year old man with a 2 year history of stroke like episodes, cognitive decline, seizures, and lactic acidosis.

KK was an 18 year old man diagnosed with MELAS at the age of 8 years. He had short stature, mental retardation, lactic acidosis, and seizures. He died of his illness 1 year after participating in this study.

YK was the mother of KK. She was positive in blood for the A3243G mutation but was asymptomatic at the age of 46 years.

CH was a middle-aged lady with a severe phenotype.

BB (52 year old female) and AW (58 year old male) were used as age and sex matched healthy controls

RS, KK, and CH therefore represented a severe phenotype, EF exhibited a mild phenotype, and YK was an asymptomatic carrier.

Blood samples were taken and fibroblast cultures were established for each patient and the proportion of the A3243G mutation quantitated using fluorescent PCR analysis as described in section 2.11. Mutation loads are shown in table 3.1 (data not available for patient CH). These show that the two patients with severe phenotypes had high mutant load in both tissues tested. KK had a much earlier age of onset than RS, but had slightly lower mutant loads, some of which (fibroblasts 60%) are some way below the normal expected threshold levels of 80-90%. The asymptomatic patient YK had low levels in both tissues, whereas in patient EF fibroblast mutant levels were significantly greater than those in blood.

Patient	Phenotype	Blood %	Fibroblasts %
RS	severe	77	80
EF	mild	7	48
KK	severe	72	60
YK	asymptomatic	8	22

Table 3.1
A3243G mutation loads as determined by quantitative fluorescence PCR in blood and fibroblasts in patients RS EF KK and YK

Fusion of platelets and fibroblasts with ρ^0 cells

Platelets and fibroblasts from patients RS EF YK KK and controls were fused with SHSY-5Y, A549, 206, IB3 and embryonal myoblast ρ^0 cells (section 2.3) as shown in table 3.2. All colonies of cells growing in selection medium were harvested by ring cloning or picking techniques as described (section 2.4). The number of cybrid lines generated for each cell type are represented in Table 3.2.

As regards fusions using A549, 206, SHSY-5Y, and IB3, cybrids were obtained from all attempted fusions except the RS/IB3. Embryonal myoblasts appear to generate cybrids poorly using this technique, only being successful for the fusion with patient RS, and failing to generate cybrids at all for all other attempted fusions. The failure of some experiments to generate cybrids does not appear to be dependent upon the technique used, because IB3/RS used enucleated fibroblasts whereas myoblast fusions were all performed using patient platelets. Platelet fusions from patient CH were a gift from Dr Mei Gu and data relating to number of clones obtained is not available.

Patient	Rho-zero cell line				
	A549	206	SHSH-5Y	IB3	Myo
RS	23	15	52	0	9
EF	23	29	20	14	0
YK			15		0
KK			22		0

Table 3.2 Number of clones isolated from platelet (clear boxes) and enucleated fibroblast (light grey boxes) fusions between patients and various ρ^0 cell lines. (Dark grey boxes refer to fusions not performed).

Distribution of mutant load in cybrids

DNA was extracted from all cybrids generated, the 630 bp region surrounding the A3243G mutation was amplified by PCR, the product digested with ApaI, and separated on ethidium bromide agarose gels (section 2.11). The ratio of 630 bp to 315 bp was assessed to determine mutant load, and these were classified according to whether they contained 0%, <50%, >50%, or 100% mutant mtDNA. The distribution of the clones between these mutant load groups is shown in figure 3.7.

Combining the data from clones from the same cell type from all five patients (fig 3.7A), shows variation in the distribution of mutant mtDNA content in generated cybrids. The majority of SHSY-5Y clones had lower mutant loads, indeed 60% of these clones contind only wild type mtDNA. 206 and IB3 cybrids had greater than 50% mutant load in all cybrids. Myoblasts most commonly generated clones containing greater than 50% and A549 cybrids most commonly less than 50%. Only a few clones contained 100% mutant load and this only occurred in SHSY-5Y and 206 cells.

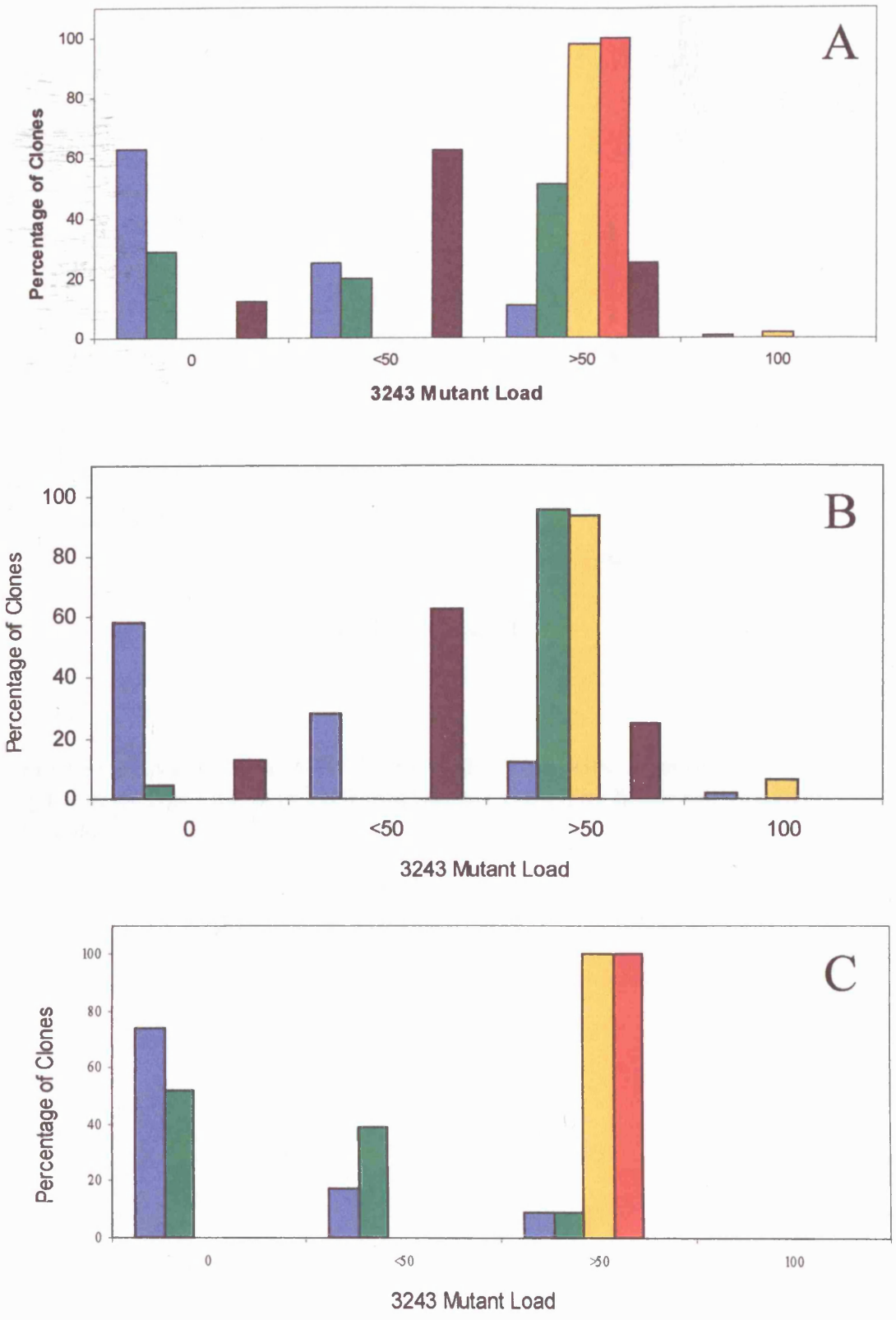

Figure 3.7. Relationship between number of cybrid clones with varying levels of A3243G mtDNA in different cell types ; SHSY5Y (blue), A549 (green), 206 (yellow), IB3 (red) and myoblasts (black). A – cybrids from all patients studied; B – from patients with severe phenotype (RS, KK); C – patients with mild phenotype (EF, YK).

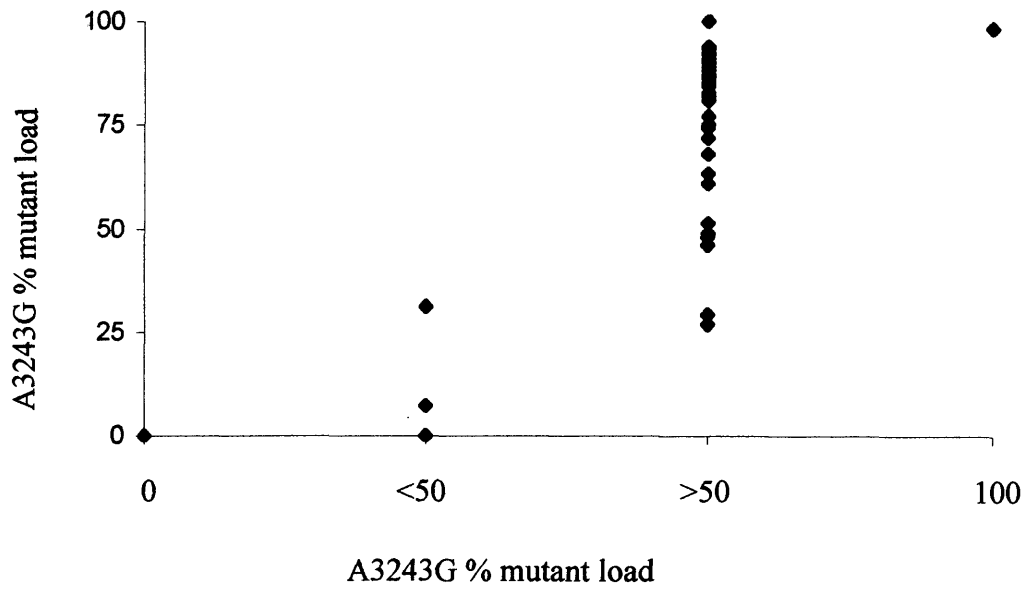

Fig 3.8 Comparison of A3243G mutant load in 72 cybrids as assessed by semi-quantitative Apa I digest (x axis) with that as assessed by fluorescent labelled PCR (y axis)

When categorized according to phenotype severity of the donor mtDNA (fig 3.7 B+C) the same pattern was seen in both groups for SHSY5Y and 206 cells. However a different pattern was seen in A549 cells. When mtDNA was derived from patients of a severe phenotype, clones had a higher mutant load than when mtDNA was derived fom those of a mild phenotpye.

Mild phenotype patients failed to generate any clones of 100% mutant load. However, this did occur when the donor mtDNA was derived from severe phenotype patients, but the absolute number of these clones was very small. Myoblast fusions only succeded when fused with severe phenotype mtDNA. However all of these were derived from fusion with a single severe phenotpye patient, and failed to succeed with the second severe phenotype patient. This would imply technical factors underlay this finding rather than it being attributable to mitochondrial or nuclear genetic factors.

For each cybrid generated that contained >50% mutant load as judged by the ApaI digest technique (section 2.11) mutation load was determined with greater accuracy by fluorescent labelled PCR as described (section 2.11). This was kindly performed by Dr Teeraton Pulkes, Institute of Neurology, London. The accuracy of the initial estimation of mutant load by visual inspection of ApaI digests was assessed with reference to the more accurate value obtained by the fluorescent labeled PCR technique (fig 3.8). This scatter plot shows a good degree of correlation between the two techniques. Only 2.5% of clones were misclassified by the ApaI digest technique.

Mitochondrial Enzyme and Aconitase Activities

Spectrophotometry for complexes I, II/III, IV, CS, and Aconitase:

Cybrid clones with 0% or greater than 50% mutant load were selected, grown to a suitable number for mitochondrial enrichment and spectrophotometric analysis performed as described (section 2.12-2.13 and 2.16).

Analysis of spectrophotometric data:

Complex I, II/III, and IV activities, expressed as CS ratios, and aconitase activities per mg protein were plotted against mutant mtDNA load. Clones containing between 0%

and 50% mutant mtDNA were not analysed further since it was felt that any potential threshold effect was unlikely to fall within this range of heteroplasmy. The number of clones subjected to spectrophotometric analysis (i.e. both the number containing 0% and the number containing mutant mtDNA) is shown in table 3.X. Clones containing 0% mutant mtDNA (i.e. 100% wild type mtDNA) were used as internal controls. Where these were not generated by the fusion experiment, control fusions generated from age-matched healthy control individuals were used.

As the number of clones derived for each patient in each cell type was not sufficient for the enelysis to be performed for each patient individually the data was pooled. First of all the activities were expressed for each cell line, combining the data from all patients, and secondly the clones were combined into two groups, those from patients with severe and those from patients with a mild MELAS phenotype.

The spectrophotometric data is shown graphically in figures 3.9-3.16.

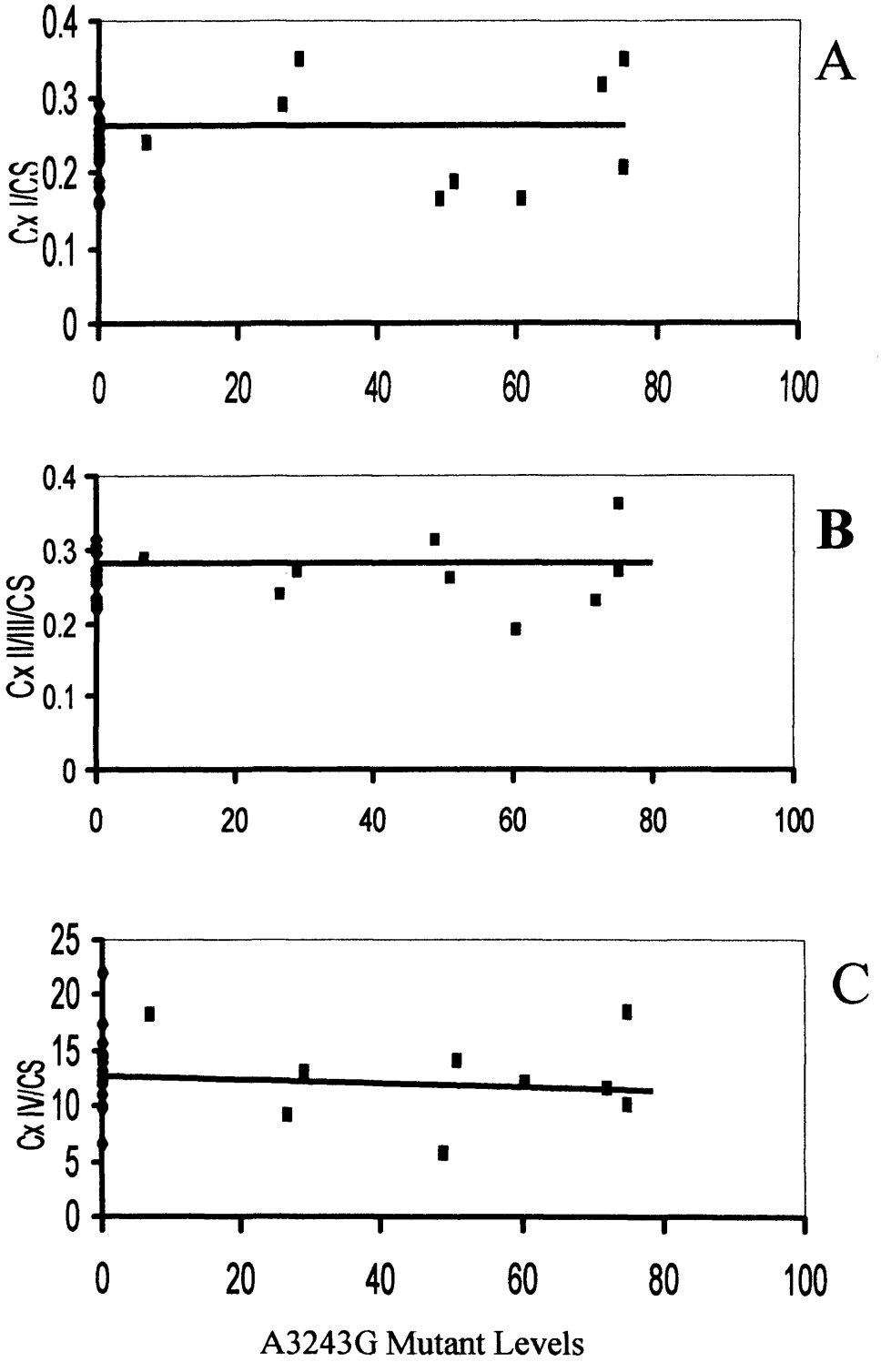

Figure 3.9 Influence of A3243G mutant load upon mitochondrial respiratory chain activities in SHSY-5Y cybrids generated by fusion of platelets from all patients. Clones containing mutant mtDNA (blue squares) and those containing wild type mtDNA (blue diamonds) are shown. The latter act as controls. Citrate synthase ratios with ; A NADH CoQ1 reductase B Succinate cytochrome c reductase, C cytochrome oxidase

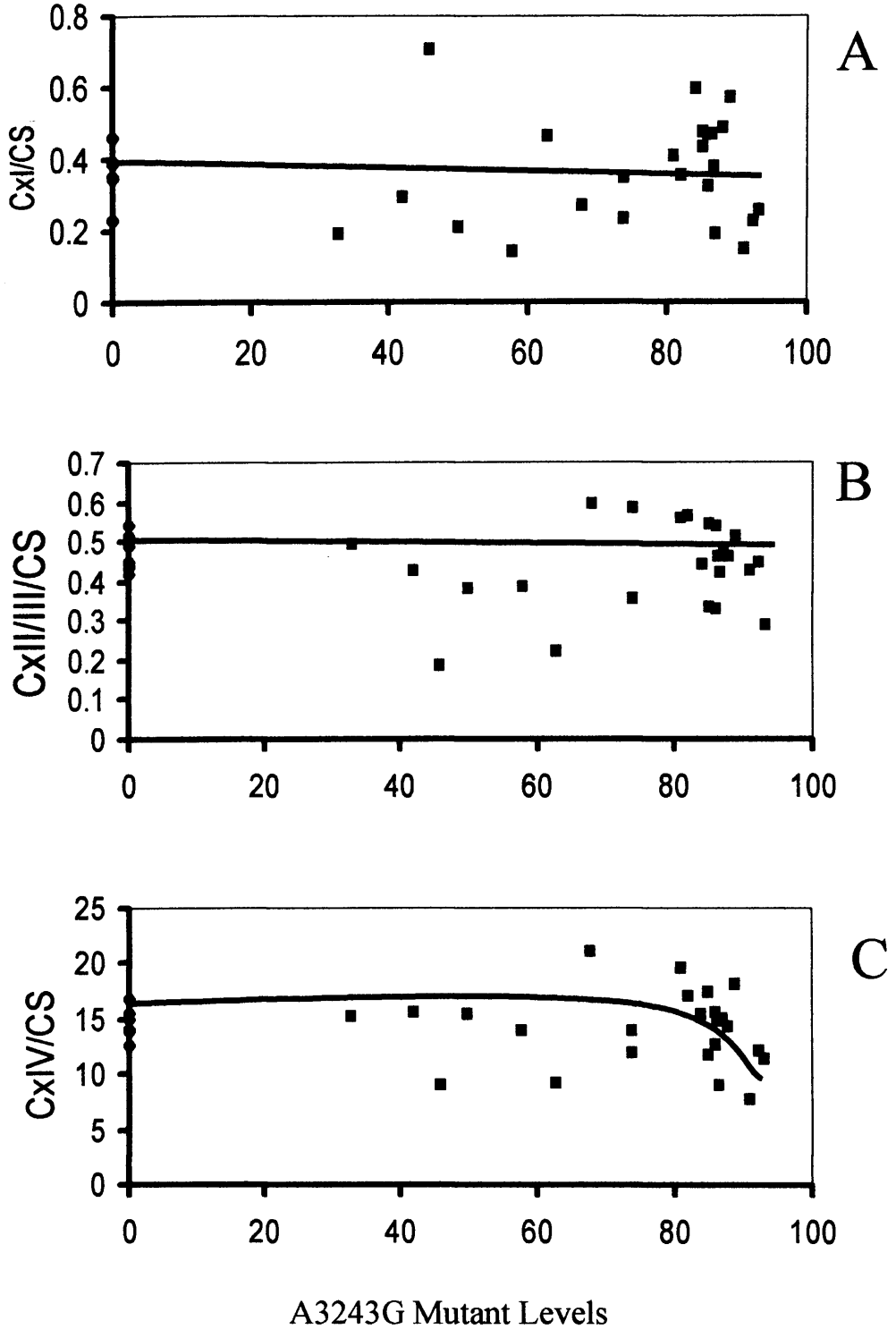

Figure 3.10 Influence of A3243G mutant load upon mitochondrial respiratory chain activities in A549 cybrids generated by fusion of platelets from all patients. Clones containing mutant mtDNA (blue squares) and those containing wild type mtDNA (blue diamonds) are shown. The latter act as controls. Citrate synthase ratios with ; A NADH CoQ1 reductase B Succinate cytochrome c reductase, C cytochrome oxidase

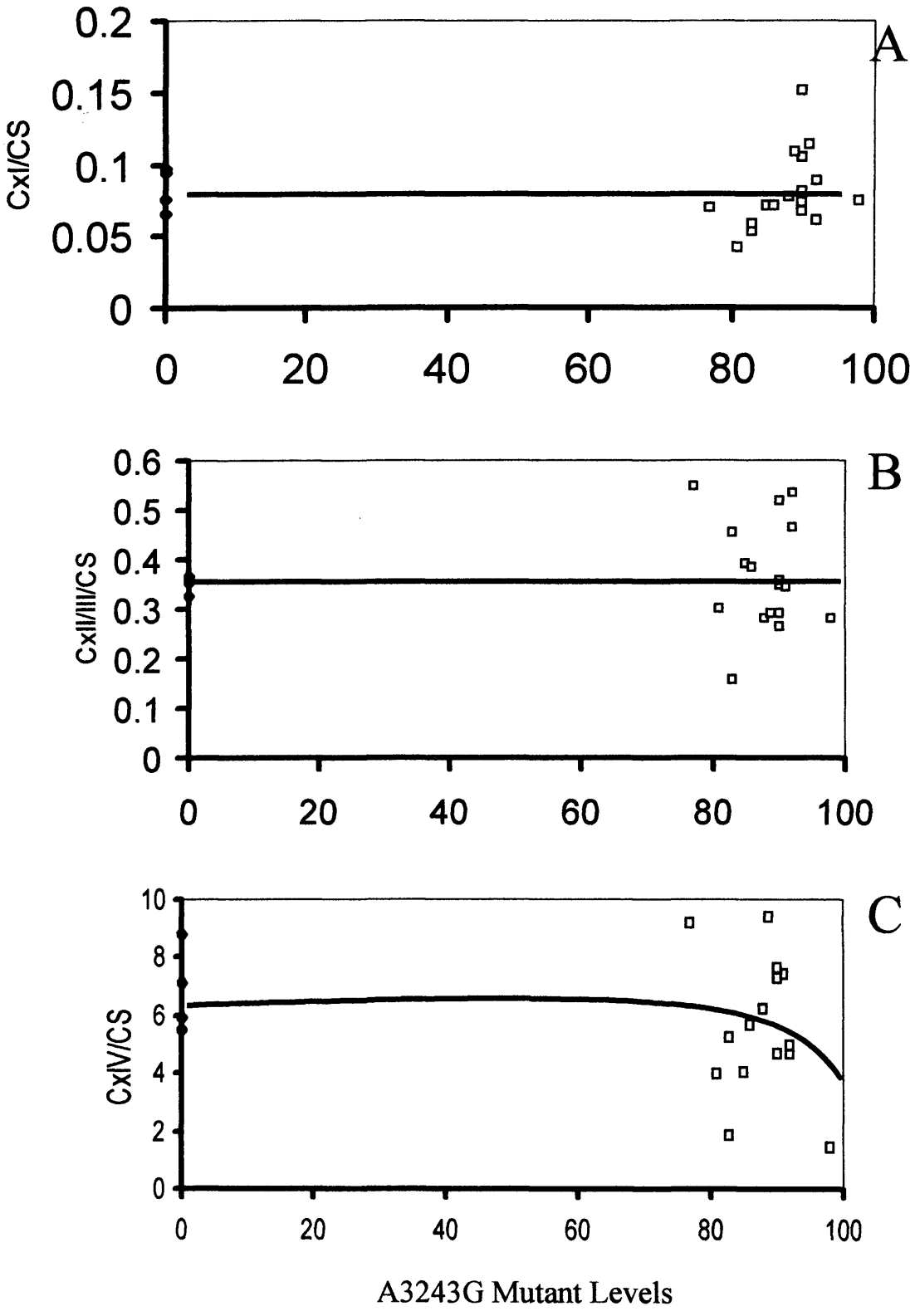

Figure 3.11 Influence of A3243G mutant load upon mitochondrial respiratory chain activities in 206 cybrids generated by fusion of platelets from all patients. Clones containing mutant mtDNA (blue squares) and those containing wild type mtDNA (blue diamonds) are shown. The latter act as controls. Citrate synthase ratios with ; A NADH CoQ1 reductase B Succinate cytochrome c reductase, C cytochrome oxidase

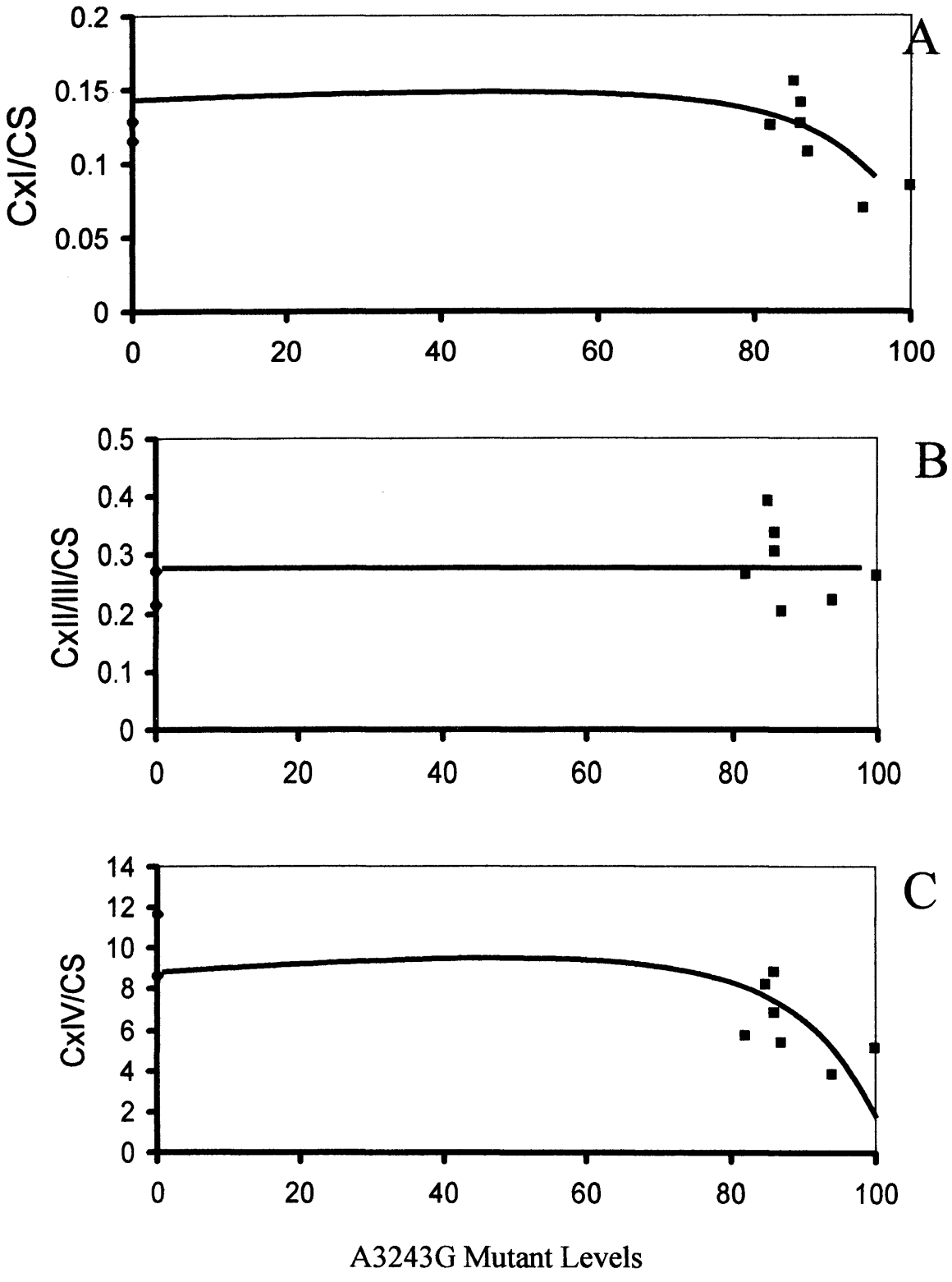

Figure 3.12 Influence of A3243G mutant load upon mitochondrial respiratory chain activities in IB3 cybrids generated by fusion of platelets from all patients. Clones containing mutant mtDNA (blue squares) and those containing wild type mtDNA (blue diamonds) are shown. The latter act as controls. Citrate synthase ratios with ; A NADH CoQ1 reductase B Succinate cytochrome c reductase, C cytochrome oxidase

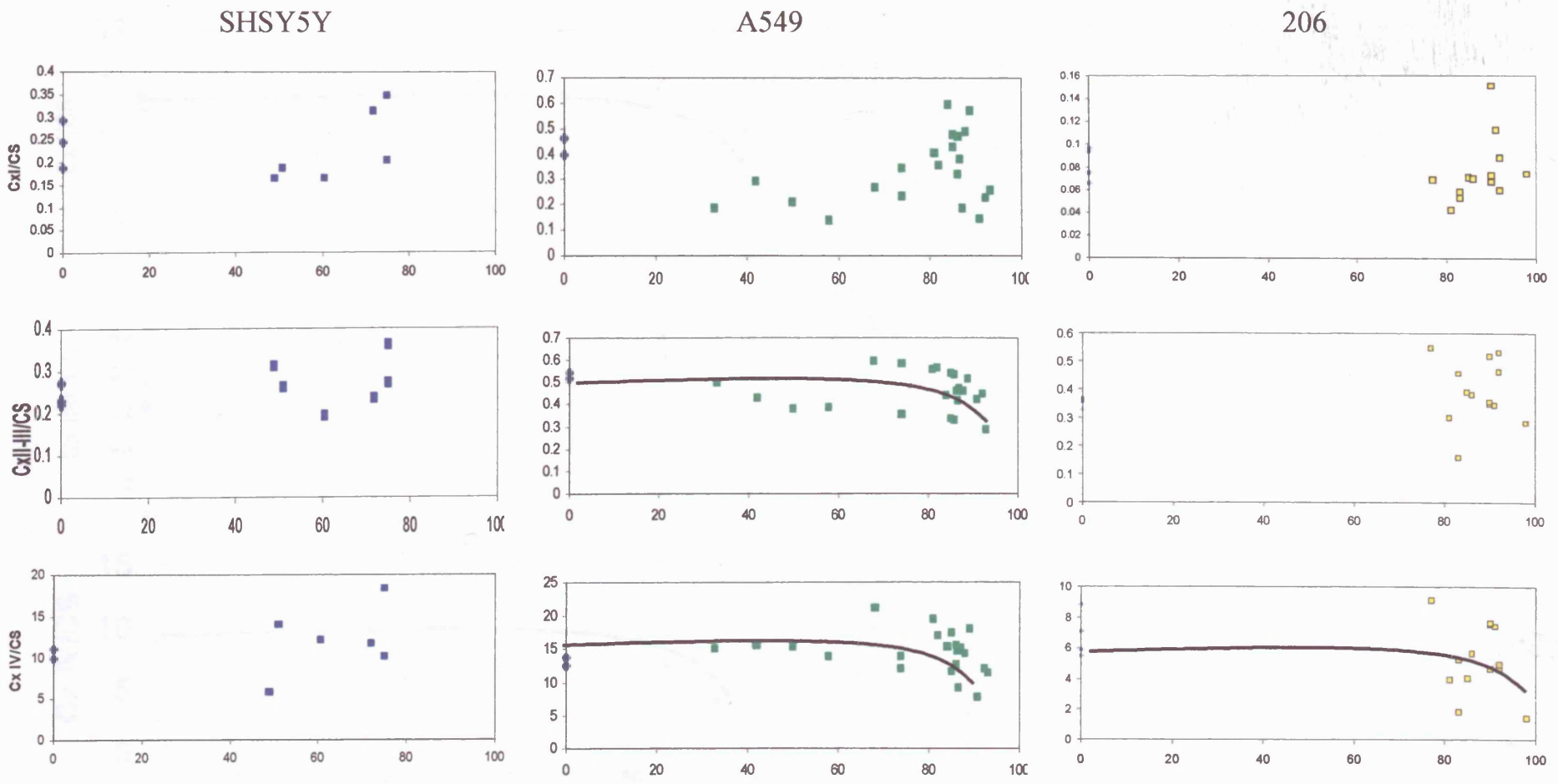

Figure 3.13 Influence of A3243G mutant load upon mitochondrial respiratory chain activities in SHSY5Y, A549 and 206 cybrids generated by fusion of patients with a severe MELAS phenotype (RS, KK, CH). Data represents; CXI / CS - NADH CoQ1 reductase; CX II/III / CS - Succinate cytochrome c reductase, CX IV / CS - cytochrome oxidase

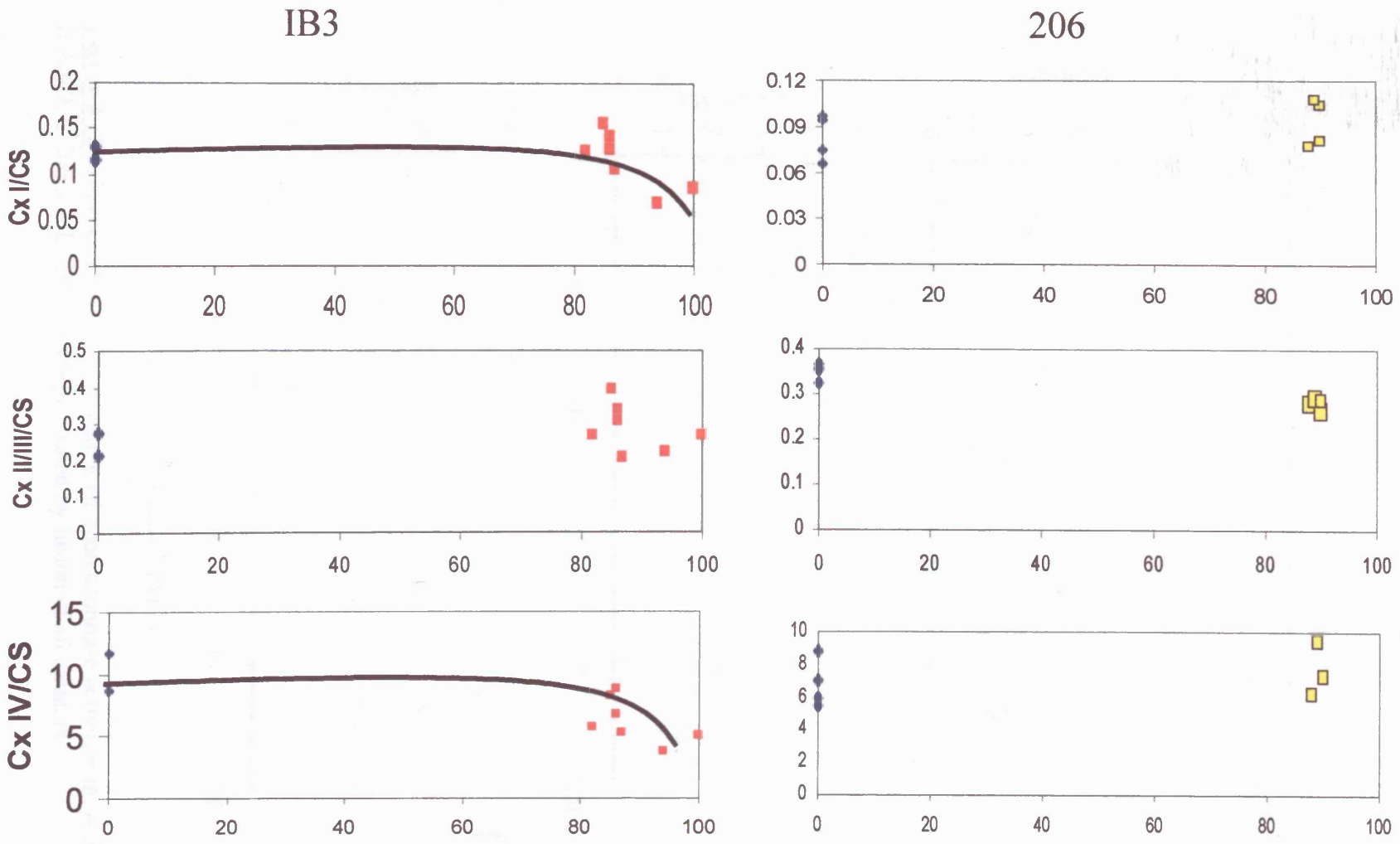

Figure 3.14 Influence of A3243G mutant load upon mitochondrial respiratory chain activities in IB3 and 206 cybrids generated by fusion of a patient with a mild MELAS phenotype (EF). Data represents; CXI / CS - NADH CoQ1 reductase; CX II/III / CS - Succinate cytochrome c reductase, CX IV / CS - cytochrome oxidase

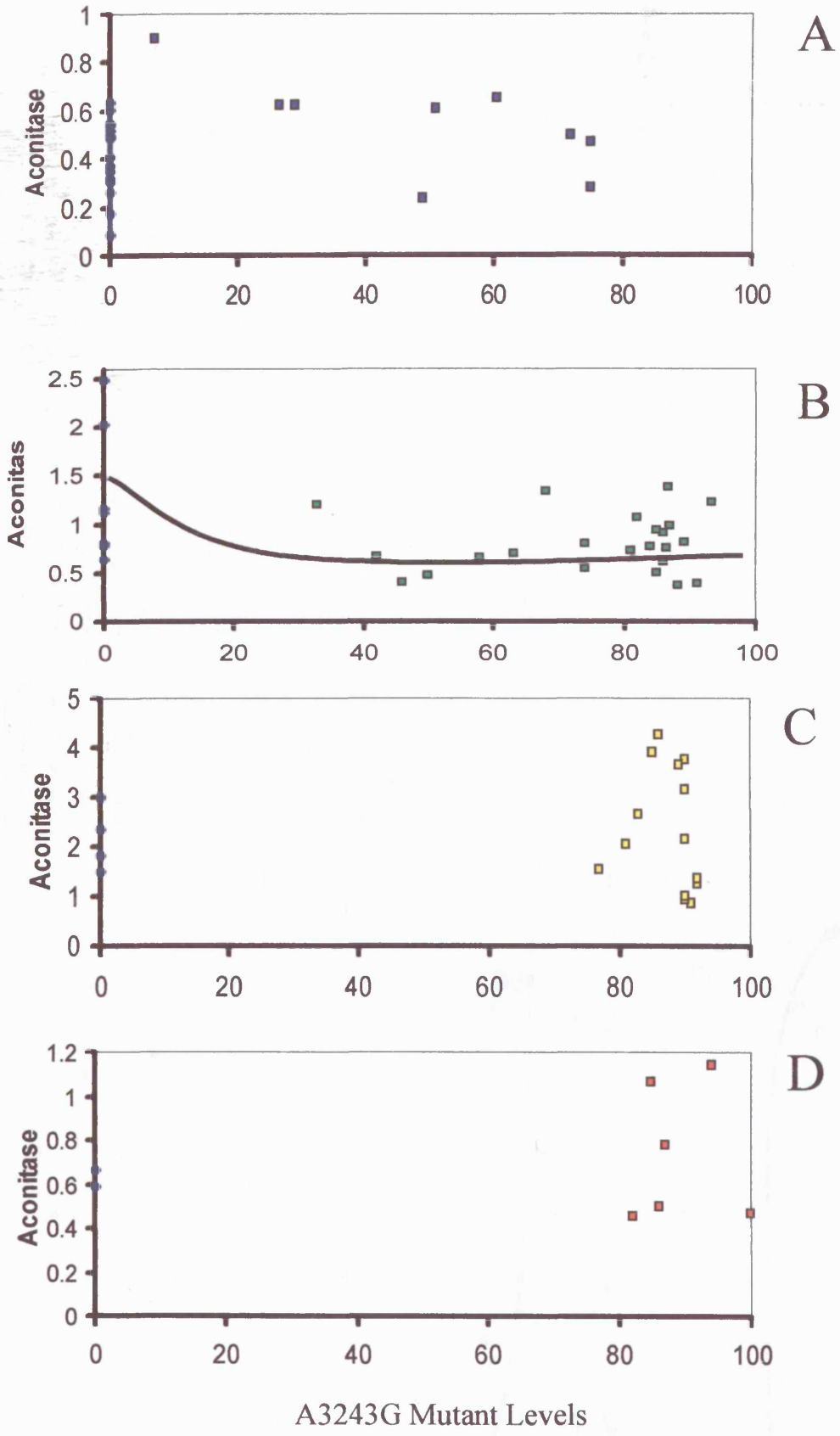

Figure 3.15 Influence of A3243G mutant load upon aconitase activities in; A SHSY5Y ; B A549; C 206 and D IB3 cybrids generated by fusion of all patients.

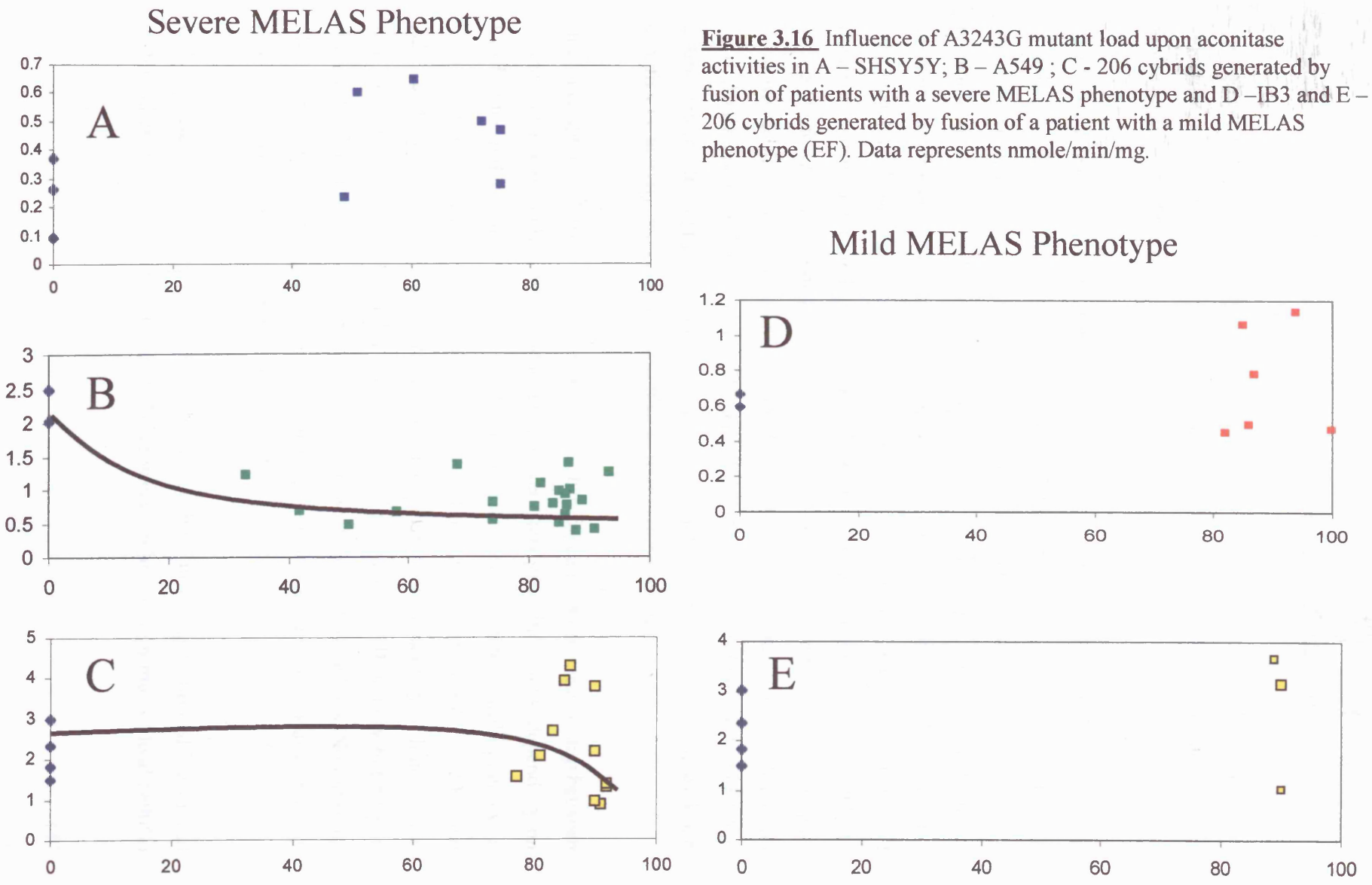

Figure 3.16 Influence of A3243G mutant load upon aconitase activities in A – SHSY5Y; B – A549 ; C - 206 cybrids generated by fusion of patients with a severe MELAS phenotype and D –IB3 and E – 206 cybrids generated by fusion of a patient with a mild MELAS phenotype (EF). Data represents nmole/min/mg.

Relationship between A3243G mutant load, nuclear background, and MRC dysfunction

To understand the relationship between mutant load and MRC activity in the different cell types the CS ratio for complexes I, II/III, and IV for each clone from all patients were plotted against mutant load.

SHSY-5Y clones contained mutant mtDNA up to a level of 76%. Up to this level complex I, II/III, and IV showed no decline in activity (fig 3.9). Of course a threshold effect above this level could not be excluded. In A549 cells there was a good range of mutant loads obtained, with a maximum mutant load of 94% (fig 3.10). These exhibited a reduced complex IV activity at above approximately 85% mutant mtDNA. No such trend was apparent for complex I and II/III, however the wide spread of activity at low mutant clones may mask a threshold effect. 206 cells (fig 3.11) had mutant loads from 76% to 98% and showed a reduction of complex IV activity above 90% mutant load , but again there was a significant spread in the data. No clear trend was seen for complex I and II/III. Analysing all patient clones in IB3 cells (fig 3.12), mutant load ranged from 82% to 100%, and results suggested a threshold of approximately 90% for both complex I and complex IV activity. No decline in complex II/III activity was seen.

In an attempt to understand the effect of mtDNA haplotype upon the relationship between mutant load and nuclear background clones were analysed in groups depending on whether the mtDNA had been derived from a patient with a severe or mild phenotype. Only sufficient clones were available to perform this analysis in SHSY-5Y, 206, and A549 cell lines (figure 3.13). There was a reduced complex IV activity at high mutant load in A549 and 206 cells, and a similar decline in complex II/III activity but only in A549 cells. The threshold level was approximately 85% in all of these lines. No threshold effect was demonstrable in SHSY-5Y cells but again, in this group no cybrids containing greater than 80% mutant mtDNA were obtained.

Only sufficient clones were available to perform analysis in IB3 and 206 cell lines fused with mild phenotype patients (fig 3.14). There was a decline at high mutant load (>90%)

for complex I and complex IV activity in IB3 cells. In 206 cells despite the analysis of clones containing 90% A3243G mtDNA no clear biochemical defecit was seen. In particular no decline in complex IV activity was seen as in the fusions generated with severe phenotype patients (fig 3.13). Again of course a threshold level may exist in 206 cells at a level of mutant load above that of the maximum cybrid mutant load generated by these fusion experiments.

Relationship between A3243G mutant load, cell type, and oxidative damage

In A549 cells, when the data was pooled for all patients studied, aconitase activity showed a reduction at low mutant levels (fig 3.15B) but no such pattern in any of the other cell lines, some of which did not generate clones of mutant load above 80% (eg SHSY-5Y cells - fig 3.15A), whilst others included clones up to 93% or 100% (eg 206 cells fig 3.15C and IB3 cells fig 3.15D respectively).

In an attempt to understand the effect of mtDNA haplotype upon the relationship between mutant load and nuclear background, clones were analysed in groups depending on whether thee mtDNA had been derived from a patient with a severe or mild phenotype. A Aconitase activity in A549 cells fused with mtDNA from severe phenotype patients (fig 3.16 B) was below control levels in all cybrids irrespective of mutant load. In this set of cybrids the lowest mutant load assayed was 32%. This might imply a very low threshold for ROS cell injury in this setting. Fusions between 206 cells and severe phenotype patients also showed a threshold effect for aconitase activity but at a more traditional level of 80-90%. The other cybrid sets (severe patients in SHSY-5Y, mild patients in IB3, and mild patients in 206) did not demonstrate a threshold effect, in some cases this was perhaps due to the lack of high mutant load cybrids for analysis (fig 3.16A), whereas in other cybrid sets high mutant load clones were available for analysis, but there was a wide spread of aconitase activities in clones of similar mutant load (fig 3.16 D and E)

3.6 DISCUSSION

Knowledge of pathological mtDNA mutations has expanded at a rapid rate over the past fifteen years. However our understanding of the pathophysiological consequences of these mutations has not progressed at an equivalent rate. For instance, as discussed in section 1.8.1.2) although many explanations have been proposed for the mechanism underlying the clinical variability seen with the A3243G mutation, none have been universally accepted. Mt DNA factors have been proposed that may modify the effect of the A3243G mutation. The clearest example of this to date is seen with tRNA suppressor mutations [122]. Nuclear genotype factors, environmental and epigenetic factors have also been proposed, and their interaction with the threshold effect explored [720].

The initial part of this experimentation, part A, addressed the robustness of the methods employed in generating cybrids. Results from immunofluorescent (IF) and PCR based studies showed no evidence of re-accumulation of mtDNA in ρ^0 cells once free of the influence of the agent initially used to deplete their mtDNA levels, suggesting that this is not a potential cofounding factor when analyzing the results of cybrid studies. Interpretation of IF photomicrographs is qualitative. Dilutional PCR studies can be considered semi-quantitative, and results supported the conclusions drawn from the IF studies. The results from part A also illustrate that diferent cell lines required different agents in order to successfully render them ρ^0. A549, 206, and embryonal myoblasts all became ρ^0 in the presence of ethidium bromide. In contrast some cell lines were resistant to the effects of ethidium bromide, requiring exposure to ddC in order to render them ρ^0. Furthermore, some cell lines never became ρ^0 despite prolonged exposure to maximal concentrations of ethidium bromide, or ddC, alone or in combination. This was the case for the NT2 neuronal cell line (figure 3.6). Maximal doses of these agents were used. At higher doses cells failed to proliferate or died. The apparent failure to attain ρ^0 status as determined by PCR may have been due to the presence of a nuclear pseudogene. This possible explanation was refuted by the second PCR for a non-overlapping 1 kilobase mtDNA fragment (figure 3.6). Of note, the successful generation of ρ^0 NT2 cells has been reported after the use of ethidium bromide as a mtDNA depleting agent [721]. Why we were

not able to reduplicate this is unclear. Also, why cell lines should differ in their susceptibility to mtDNA depleting agents is unclear but may relate to their ability to metabolise or remove the agent. There is some suggestion that this observation mirrors the clinical findings of variable tissue susceptibility to the effects of nucleoside analogue drugs used to treat the human immunodeficiency virus, for which neuronal toxicity is a major dose-limiting factor.

Cybrid studies have suggested that a variety of factors may promote the non-random segregation of mutant and wild-type mtDNA in different tissues [186, 714, 715, 716, 717]. Using 206 cells Dunbar et al [714] generated cybrids that had either a stable mitochondrial genotype or showed an increase in the proportion of mutant mtDNA. Other cell lines however showed a shift to wild type mtDNA, suggesting that the nuclear genetic background of the recipient cell line can influence the segregation of mutant and wild-type mtDNA. Variability of mutant load has also been seen at the single cell level [718]. NT2 cells have shown mitotic segregation towards increasing levels of mutant A3243G mtDNA [722]. This rapid segregation was frequently followed by complete loss of mtDNA. These findings suggest that pathological mtDNA mutations are particularly deleterious in specific cell types, and may explain some of the tissue-specific aspects of mtDNA diseases. Sudden and dramatic changes in heteroplasmy level have also been shown after growth of clones in selective medium [723]. In one instance this was associated with a gain of chromosome 9 [724]. It was proposed that mtDNA exists in nucleoids containing many copies of the genome. These nucleoids may themselves be heteroplasmic, and can be reorganized under nuclear genetic controlresulting in shifts of heteroplasmy level.

Non-random segregation of mutant and wild-type mtDNA was also evident in the experiments described above as shown by the range of mutant loads found in the cybrids generated. The varying effect of different nuclear backgrounds was also evident in the success rate of fusion experiments. With ρ^0 myoblasts only platelets from patient RS generated clones successfully. EF produced clones after fusion with IB3 ρ^0 but RS did not. All other fusions between all patients and all other ρ^0 cell lines were successful. The reasons for this are unclear. If it is a real phenomenon it may represent incompatibility

between different mtDNA molecules and different nuclear backgrounds. It is unlikely to be a factor confined to the A3243G mutation itself, because neither wild type nor mutant mtDNA containing clones were generated. It could of course be related to technical failings in those particular fusion experiments, and thus be an arefactaul finding. To test this further, the fusions could be repeated a number of times to see if they consistently fail to generate viable clones.

The varied effect of different nuclear backgrounds was also evident, as shown in figure 3.7, in the range of mutant mtDNA levels tolerated in the cell lines. In fig 3.7A, IB3 and 206 cells appear to allow higher mutant loads than SHSY-5Y or myoblasts. When comparing fusions using mtDNA from patients with a severe phenotype with those using mtDNA from patients with a mild phenotype the spread of mutant loads was similar in both cases for SHSY-5Y and 206 cells. In contrast, significant variation was seen for fusions with A549 ρ^0 cells, mtDNA from severe phenotype patients giving cybrids of much higher mutant load. This would imply that mtDNA factors also influence the resultant mutant load in cybrids. MtDNA sequencing might shed further light upon these findings.

Of course, these findings might be influenced by the fact that the donor mtDNA used in different fusion experiments contained differing levels of mutant mtDNA. For example Patient YK (mild phenotype) platelets contained only 8% A3243G mutant mtDNA, whereas the level in her son KK (severe phenotype) was 72%. The fact that the spread of mutant load in SHSY-5Y cybrids for fusions generated from severe or mild phenotype patient was very similar would argue against the donor mutant mtDNA level being a significant factor in determining the mutant mtDNA level in cybrids.

A number of other potential confounding factors should be considered. Not all fusion experiments were performed on the same day and therefore conditions might vary. It has already been mentioned that some fusions were performed with patient platelets and others with enucleated patient's fibroblasts. This was due to the difficulties in repeatedly obtaining platelet samples from patients. This factor might also influence the fusion

process. Mutant loads varied between patients and between fibroblasts and platelets of a single patient. Furthermore the results of mutant loads presented are from the products of a single fusion experiment for each patient cell line cross. The data would be more robust if the fusions were repeated a number of times. Limitations aside these variations may provide evidence that both nuclear DNA and secondary mtDNA influence the ability of cells to accept foreign mtDNA, and their ability to tolerate a given level of mutant mtDNA. This may be a reflection of both the metabolic demands of the cell line, and the ability of its MRC machinery to generate ATP. This latter factor would be determined by the efficiency of the multitude of interactions between the nucleus of the ρ^0 cell line and the introduced mtDNA, both mutant and wild type.

The spectrophotometric experiments presented were designed to investigate the relationship between mutant load, MRC activity, aconitase activity (a marker of ROS injury), and nuclear background. The concept of a threshold level of mutant mtDNA, above which MRC activity and other biochemical parameters are affected adversely, is often discussed and accepted. It has been demonstrated in osteosarcoma cells [69] and A549 cells [711]. When A3243G levels reach 70-90% a mild defect in complex I has been reported; above 90% oxygen consumption falls dramatically, and there is a quantitative effect on mitochondrial protein synthesis and an abnormal pattern of translation products most clearly affecting ND6 [69].

However, a number of unexplained inconsistencies exist. In vivo the A3243G mutation appears to have a lower threshold level than the A8344G mutation, but in vitro the reverse is often true [186, 719]. Threshold levels vary between tissues, potentially related to varying energy demands. Brain exhibits a low threshold level, and unusually, shows a linear relationship between the level of heteroplasmy and defects of oxidative phosphorylation [323]. In some cybrid lines mitochondrial protein synthesis activity is preserved despite high mutant load and severe mitochondrial dysfunction [581]. The steady state level of tRNALeu(UUR) and its degree of aminoacylation also vary depending upon the nuclear background studied [580].

The results described above support the hypothesis that both the nuclear DNA background and the mtDNA haplotype influence the biochemical phenotype of the A3243G mutation. Patterns of MRC dysfunction varied between cell lines and also varied depending upon the source of the donor mtDNA (ie from severe or mild penotype patient). Threshold effects were apparent in some cell lines and for some MRC complexes but not in others.

There were of course some limitations in the data. High mutant load clones were not generated from all fusion experiments; enzyme activities showed some spread of data amongst clones of similar mutant load; data from patients had to be combined into severe or mild phenotype groups because numbers of clones generated from single patients were too small to allow meaningful analysis.

The pattern of aconitase activity also varied between cell lines. A549 cells fused with mtDNA from severe phenotype patients (fig 3.16 B) showed low aconitase levels at all mutant loads. This might suggest a high degree of ROS injury even at low mutant levels. The reliability of the control data would need confirmation in future studies. In 206 cells fused with mtDNA from severe phenotype patients a threshold effect for aconitase activity was present at the more common 80-90% level. Aconitase thresholds were not demonstrable in other cybrids.

In summary, the data presented goes some way to support the hypothesis that both the nuclear DNA background and the mtDNA haplotype influence the biochemical expression of the A3243G mtDNA mutation. Repeated attempts at the fusions would strengthen the data regarding the range of mutant loads permissible within different nuclear backgrounds. However, the experimentation as presented was labour intensive, and simply undertaking more upon more fusions, might be too cumbersome an experimental design. Different methodologies should be explored to investigate genotype-phenotpye correlation in the mitochondrial encephalomyopathies, a core feature of these intriguing disorders that still remains to be fully explained pathophysiologically. Not until the fundamental secrets of these disorders are unlocked can rational therapeutic

approaches be planned. Improved understanding of the basic molecular mechanisms will also be of relevance to the rapidly growing number of conditions and pathologies in which mitochondrial dysfunction is now implicated.

Chapter 4

The use of xenomitochondrial cybrids to investigate nuclear -mitochondrial interactions and the development of cell models of mitochondrial disease.

4.1 Experimental hypothesis

Nuclear DNA and mtDNA work together in a complex symbiotic relationship to produce an efficient mitochondrion able to meet the energy requiremtns of the cell and to fulfill the other functions of mitochondria. These interactions occur at a number of levels. The most obvious is the nuclear and mitochondrially encoded subunits of the mitochondrial respiratory chain, but also includes nuclear encoded factors responsible for the import of mitochondrially targeted proteins, and mitochondrial transcription and translation factors. In chapter 3 I explored the relevance of these nuclear mitochondrial interactions in determining the phenotypic manifestation of the A3243G mutation. To explore these interactions further, but at a different level I utilized the technique of xenomitochondrial cybrids. This technique generates cybrids by fusing nuclear and mtDNA from different species. The entire mitochondrial genomes of human, rat, mouse, and a number of non-human primates, amongst other species, are established. I investigated the potential viability and biochemical consequences of human-mouse-rat xenomitochondrial cybrids. The resultant xenocybrids also provide useful models of MRC deficiency.

As discussed in depth in chapter 1, literature already exists on the phlyogenetic relationships of mtDNA from various species, and also on the ability of nuclear and mtDNA to interact adequately or otherwise across these varying phlogenetic distances. The experiments described below use xenomitochondrial cybrids to explore the development of cellular models of human mitochondrial disease, and to provide further insights into the complexities of nuclear mitochondrial interactions.

4.2 Experimental Design

Mouse fibroblast (STOG) cells were depleted of their mtDNA by the addition of ethidium bromide to the culture medium as described (section 2.2.4). Their ρ^0 status was confirmed by PCR methods as described (section 2.8). Platelets isolated from rat or human blood were then fused with these mouse ρ^0 cells (section 2.3). Resultant cybrids were isolated and the origin of their nuclear and mitochondrial DNA was confirmed by PCR techniques as described (section 2.5). Clones were grown to sufficient quantity to allow the isolation of the mitochondrial fraction, and spectrophotometric analysis of these samples was performed as described (section 2.12)

4.3 Results:

Mouse fibroblasts (STOG) a gift from Dr Paul Simons, Dept of Anatomy, Royal Free Campus, Royal Free and University College Medical School, University College London, were cultured as described (section 2.2). They were grown in the presence of ethidium bromide (5μg/ml) for 30 days (section 2.2.4) and the level of mtDNA determined semi-quantitatively by PCR amplification (section 2.8). DNA extracted from untreated STOG fibroblasts showed a clear band at 300 bp, and the intensity of the band could be seen at 0.005μg DNA template. After 30 days of ethidium bromide treatment a 300 bp product was not detectable even using 50 μg DNA template. (see figure 4.1).

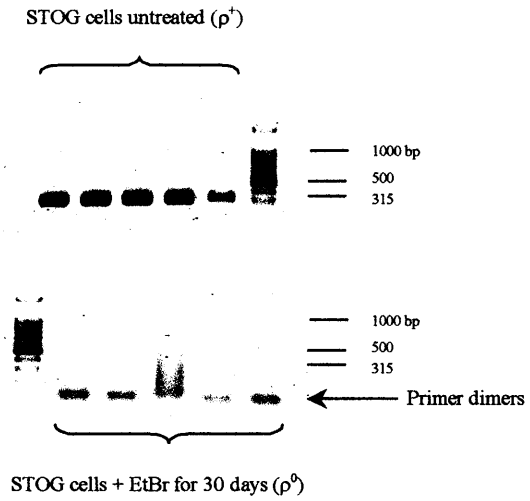

Figure 4.1
1.2% agarose gel of 315kb semi-quantitative mtDNA PCR of STOG ρ^+ cells before (upper) and after (lower) 30 days culture in 5μg/ml Ethidium Bromide. The five lanes represent 1:10 serial dilutions of template DNA (50ng, 5ng, 0.5ng, 0.05ng, 0.005ng) from left to right.

Human platelets were freshly prepared and fused with STOG ρ^0 cells on four occasions (section 2.3). On all occasions they failed to generate any viable clones. However fusion with *mus musculus* or *ratus norvegicus* platelets both generated similar numbers of viable clones. DNA was extracted from cybrids in a standard way (section 2.5). A number of primer pairs were designed by automated (DNAstar, Lasergene 98 – Primer select software) and manual techniques to distinguish human, mouse, and rat mtDNA:

primer pair 1	f1 (9559..9578) 5'-GAA CAG GCA TCA CCC CGC TA
	r1 (9847..9868) 5'CGG ATG AAG CAG ATA GTG AGG A
primer pair 2	f2 (3315..3335) 5'-ACC CTA GCA GAA ACA AAC CGG
	r2 (4107..4129) 5'-CAG GAG GAT AAT TAT TGA GGC TG
primer pair 3	f3 (3356..3376) 5'-GGC TTT AAC GTC GAA TAC GCC
	r3 (4209..4229) 5'-TAG TGG AAT GGG GCT AGT CCA
primer pair 4	f4 (2829..2848) 5'-GCA AAG GCC CCA ACA ACG AA
	r4 (3266..3243) 5'-GTC AGG CGG GGA TTA ATA GTC AGA
primer pair 5	f5 (12520..12540) 5'-GAT TCC ACC CCC TCA CGA CTA
	r5 (12875..12855) 5'-GAG GGC GAG GCT TCC GAT TAC

Standard PCR conditions were used with an annealing temperature of 60^0C. The origin of mtDNA contained within *mus musculus / mus musculus* (MM) and *mus musculus / ratus norvegicus* (RM) clones was assessed using pcr pimer pair 2 and Bam H1 restriction enzyme digestion. The five pairs of primers designed were tested for their specificity for rat, mouse and human mtDNA. DNA was extracted from human ρ^+ cells (H), mouse STOG ρ^+ cells ($M\rho^+$), mouse blood (Mb), and rat blood (Rb). The pcr products were run on a 1.2% agarose gel (figure 4.2). Results of these reactions, summarised in table 4.1,

show that only primer pair 2 with BamH1 digest was able to clearly distinguish between human, rat, and mouse mtDNA.

Primers	H	Mρ$^+$	Mb	Rb
1	0	+	+	(+)
2	0	+	+	+
2+digest		cut	cut	no
3	0	0	+	+
3+digest			no	no
4	0	0	+	+
5	+ (500)	+(380)	+(380)	0

Table 4.1 Summary of the results of PCR with primer pairs 1 to 5 (+/- BamH1 digest) performed on human ρ$^+$ cells (H), mouse STOG ρ$^+$ cells (Mρ$^+$), mouse blood (Mb), and rat blood (Rb). 0 = no PCR product, + = PCR product obtained, (+) = faint PCR product obtained, (xxx) = size of PCR product in base pairs. RE digest results show whether a PCR product was cut by BamH1 (cut) or not (no).

Figure 4.2 Primer design for distinguishing human/mouse/rat mtDNA
Polymerase chain reaction products for primer pairs 1,2,3,4,and 5, and BamH1 digest products for primer pairs 2 and 3. Samples A=human ρ^+ cells, B=mouse ρ^+ cells, C=mouse blood, D=rat blood, E=water blank.

Of the five *Mus musculus / mus musculus* (MM) clones grown up and analysed all contained only mouse mtDNA as assessed by PCR. All these clones after PCR with primer pair 2 and BamH1 digest generated a 565 and 250 bp fragment (figure 4.3). Similarly, of the ten *mus musculus / ratus norvegicus* (RM) clones grown up and analysed all contained only rat mtDNA (see figure 4.3), generating a single product of 815 bp after the same PCR and digest. This PCR also excludes, within the levels of detection of the PCR, the coexistence of both mouse and rat mtDNA in any of the clones

Individual clones were grown up until sufficient quantity (20 confluent 10 cm plates) was obtained for extraction of the mitochondrial fraction and subsequent spectrophotometric analysis of the mitochondrial respiratory chain complexes I,II, III, II/III, IV and CS (section 2.12). Data was analysed using Mann-Whitney U test as described in section 2.20. This revealed a significant reduction in complex I activity (34% of control mouse/mouse cybrids), complex III activity (60% of control mouse/mouse cybrids), and complex IV activity (43% of control mouse/mouse cybrids), and no significant difference in complex II activity figure 4.4).

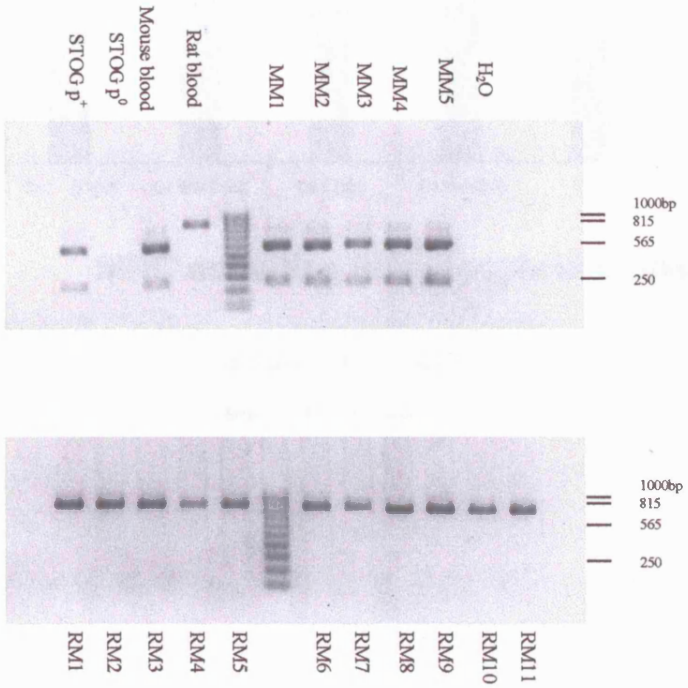

Figure 4.3

Rat or mouse mtDNA content of cybrids obtained by fusing mouse or rat platelets with STOG ρ^0 mouse fibroblasts to generate mouse-mouse (MM) and rat-mouse (RM) clones. PCR performed using pair 2 primers and subsequent BamH1 restriction enzyme digest.

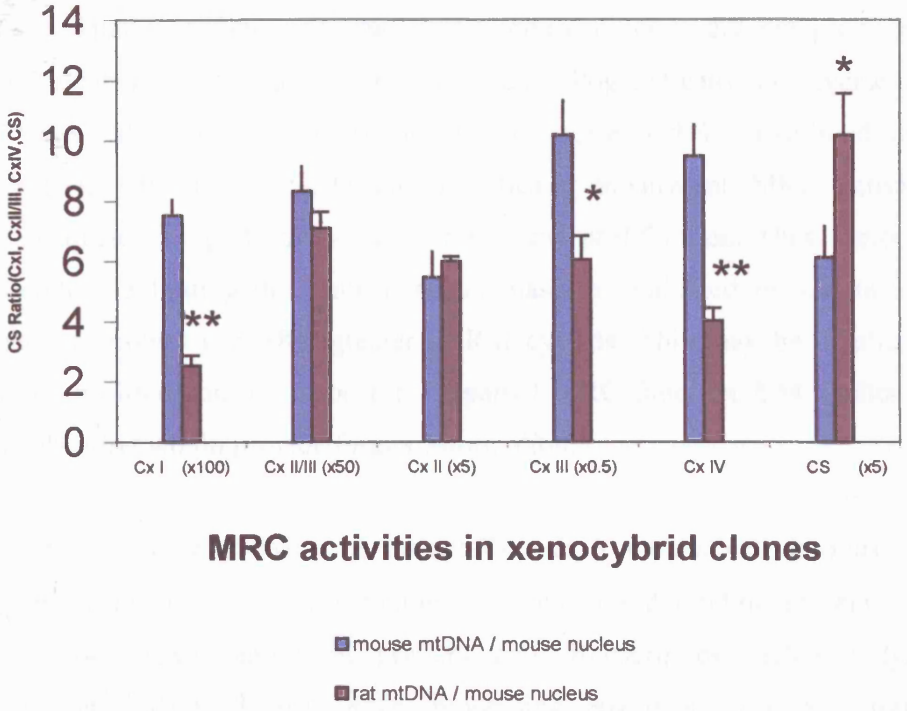

Figure 4.4
Mitochondrial respiratory chain activities expressed as citrate synthase (CS) ratios for complex I (CxI), complex II/III (Cx II/III), and complex IV (CxIV), and CS activities in xenocybrid clones. Ratios are mean + SEM values for mouse/mouse (n=5) and rat/mouse (n=9) xenocybrids. For Cx II and Cx III mouse n=4 and rat n=3. Statistical sinificance by Mann-Whitney U teat: *p,0.05, **p<0.001.

4.4 Discussion:

The introduction of rat mtDNA into a mouse nuclear background was able to generate viable clones. Human mtDNA introduced into mouse ρ^0 cells did not produce viable cybrids, presumably because the two genomes are phyllogenetically too diverse to allow adequate "cross-talk". The rat-mouse xenomitochondrial cybrids exhibited impaired respiratory chain function. Despite this significant impairment MRC activity was obviously adequate enough to allow cell survival and proliferation. These defects were present despite the finding that mitochondrial mass as evaluated by citrate synthase activity per mg protein was 38% greater in RM cybrids. This may be a reflection of mitochondrial proliferation in response to impaired MRC function. EM studies of RM cybrid mitochondria would provide further information.

The maintenance and expression of rat mtDNA in a mouse cell implies that the machinery of replication (DNA polymerase γ, single-strand binding proteins, RNases required for producing replication primers etc), transcription (RNA polymerase, transcription termination factors, RNA processing enzymes, etc), and translation (initiation and elongation factors, aminoacyl tRNA synthetases, ribosomal proteins, etc.) are still able to function sufficiently to permit cell survival despite the mtDNA nucleotide changes present in the foreign mitochondria. However, the partial defects in respiratory chain complexes detected in these experiments would imply that assembly of functional OXPHOS complexes is sensitive to such changes, and whilst still able to function, they do so with reduced efficiency. Transcription and translation studies and the use of two-dimensional denaturing gels to assess subunit structure would be of interest to further investigate the efficiency of interactions between these two genomes from different species.

Other studies have shown that the presence of less then 2% of self mtDNA results in cellular respiration at 40% of parental lines. With time in culture the levels of self mtDNA rise, and when at 10% normal respiratory function is restored. This pattern is similar to that seen in studies of the threshold effect of some pathogenic mtDNA

mutations, when similar levels of wild type mtDNA (6-15%) can complement enzymatic defects [68,624,625]. Despite this increase in the level of self mtDNA with the passage of time in culture, a complete replacement by mouse mtDNA does not occur. This may be because once normal respiratory function is restored the selection advantage in favour of self mtDNA is lost. A similar phenomenon is described in human cells with an ATP6 gene mutation [626]. Native mtDNA was not detectable in rat-mouse cybrids although the potential for accumulation exists during the period between PCR based ascertainment of mtDNA content and growing up of sufficient quantities of cells for spectrophotometry.

Functional incompatibilities appear to be species specific. This may be influenced by variable rates of evolutionary change [627,628]. The rate of substitution in mitochondrial encoded proteins in mammals is at least one order of magnitude greater than it is in fish [629]. The mtDNA mutation rate of rodents has been estimated at 4.8 – 9.7% per Myr, and in humans at 2% per Myr [597,630]. This factor is probably the key influence on the compatibility of the interactions between mtDNA and nuclear DNA from different species. Xenomitochondrial cybrids could be generated across different species barriers because this technology provides a useful addition to the tools available for the exploration of nuclear-mitochondrial interactions, and adds to the currently available models of human mitochondrial disease.

CHAPTER 5

THE ROLE OF MITOCHONDRIAL RESPIRATORY CHAIN FUNCTION IN SPORADIC FOCAL DYSTONIA.

5.1 Introduction

The evidence to implicate mitochondria in the pathogenesis of a range of non-archetypal predominantly neurodegenerative conditions is described in detail in chapter 1. In this chapter the role of mitochondrial dysfunction in dystonia is explored further. This potential pathogenic link has been proposed for a number of reasons that include the fact that dystonia may occur in patients with LHON, and that the gene responsible for Mohr-Tranebjaerg syndrome has been discovered to be a mitochondrial transport protein. However it remains to be established whether mitochondrial dysfunction underlies other forms of dystonia? As described below this experiment used skeletal muscle obtained from patients with sporadic focal dystonia to look for evidence of mitochondrial dysfunction.

5.2 Experimental hypothesis

Mitochondrial dysfunction is involved in the pathophysiology of sporadic focal dystonia, and this biochemical defect would be detectable in the muscle of affected individuals.

5.3 Results

Ten patients with a diagnosis of sporadic focal dystonia and undergoing selective denervation of the sternocleidomastoid muscle for treatment of their spasmodic torticollis were identified. In all patients the sternocledomastoid muscle was biopsied at the time of surgery. Control samples were obtained from 4 patients undergoing a variety of cranio-cervical surgical procedures. In three controls the splenius muscle was sampled, and in one the paraspinal muscle. All patient and control details are summarized in table 5.1. All

patients (but no controls) had previously been treated with botulinum toxin to the affected muscle.

Muscle samples from the 10 patients and 4 age-matched controls were frozen in liquid nitrogen at the time of collection. An aliquot was then removed and homogenised (section 2.15). Spectrophotometric analysis was undertaken of complex I, II/III, and IV of the mitochondrial respiratory chain, citrate synthase and aconitase as described above (section 2.12). Protein estimations were performed (section 2.17). The activities from patients and controls were expressed as citrate synthase ratios and compared using the Mann-Whitney U test (section 2.20).

All muscle samples underwent blinded histological and electron-microscopic evaluation. Ethical approval was obtained from the Ethics committees of the Royal Free Hospital and the National Hospital for Neurology and Neurosurgery.

The mean activities for complexes II/III, IV, and aconitase were lower in patients than in controls. Statistical significance however was not reached for any of these biochemical parameters (figure 5.1). Histology and electron microscopy examination (table 5.1), performed by Professor Landon, Institute of Neurology, showed abnormalities in three of four controls, and six of the 10 patients. The unexpected findings in the control samples were of RRFs in all three cases. These findings were suggestive of a mitochondrial myopathy in the controls. EM findings were not available for all patients. Two controls showed large peripheral collections of excess abnormal mitochondria. These mitochondria had abnormal christae and paracrystalline inclusions. The histological abnormalities in the patient samples were more suggestive of denervation secondary to botulinum toxin therapy. RRFs were found in patient 9, SDH changes (RRF equivalents) in patient 3, and occasional COX negative fibres in patient 8.

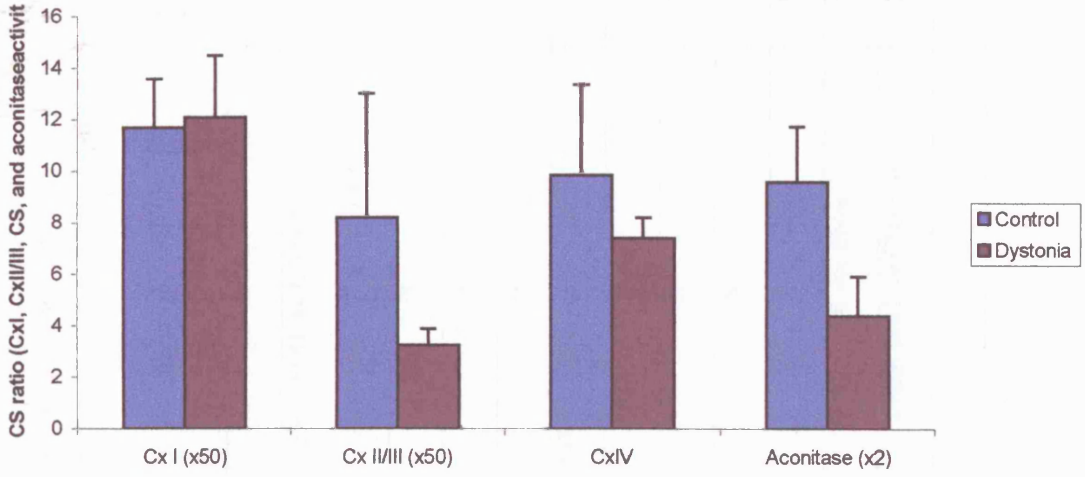

Figure 5.1
Mitochondrial Respiratory Chain (Complexes I, II/III, and IV) expressed as citrate synthase ratios and aconitase activites for sporadic focal dystonia patients (n=10) vs Controls (n=4),. Values shown are mean activities with standard error bars.

Table 5.1 i Patient and Control details, light and electron microscopy findings

Patient / Control Details					Light Microscopy								
Patient / Control	Age	Disease Duration	Muscle biopsied	Diagnosis	VFS	I A+A	II A+A	Cent Nuc	Con Tissue	I / II propn	Ox stains	Gomori	L/G/ADA /P/AP
C1	58	na	sp	bi	0					↑ I			
C2	66	na	sp	csm	30-100	0	0	0	0	N	occ RRFs SDH+ve COXintense or -ve		
C3	80	na	ps	ocf	0	0	+	0	+	↑ I	numerous RRF occ COX-ve	N	N
C4	52	na	sp	pt	0	0	0	0	0	N	N	N	N
P1	57	25 yrs	scm	st	20-90	+	+	+	0	N	N	N	N
P2	53	5	scm	st	+	0	+	0	0	↑ I	N	2RRF	N
P3	54	20	scm	st	to140	+	0	0	0	↑ I	7 SDH +ve (RR equivalents) COX-ve		N
P4	28	2	scm	ptcd	20-80	+	0	0	0	↑ II	N	N	
P5	60	12	scm	st	30-120	0	+	+	+	↑ I	N	N	N
P6	61	3	scm	st	0	+	+	+	0	↑ I	N	N	cores
P7	47	11	scm	st	+	+	+	0	0	↑ I	N	N	cores
P8	42	16	scm	st	0	0	0	0	0	↑ I	occ COX –ve fibres	N	N
P9	30		scm	c+gd	to120	+	+	0	+	N	2 RRF SDH+ve COX+ve	N	N
P10	39		scm	st									

Table5.1 ii Patient and Control details, light and electron microscopy findings

Patient / Control Details					Light Microscopy	Electron Microscopy
Patient / Control	Age	Disease Duration	Muscle biopsied	Diagnosis	Conclusion	Conclusion
C1	58		sp	bi	Abnormal numerous RRF usually COX-ve	Abn mt, abn christae + crystalline inclusions
C2	66		sp	csm	mitochondrial myopathy	
C3	80		ps	ocf	Numerous RRFs usually COX-ve. Myopathic	widespread abnormalities, excess abn mt
C4	52		sp	pt	Normal	
P1	57		scm	st	Probably normal	
P2	53		scm	st	Denervation ? 2^0 to Bot. toxin. 2RRF COX-ve	
P3	54		scm	st	Prob normal scm finding ?relevance of SDH change	
P4	28		scm	st	Mod type II atrophy. No evidence of mt myopathy	
P5	60		scm	st		
P6	61		scm	st	Recent denervation ?Bot. toxin effect	
P7	47		scm	st	1 small area of inflammatory infiltrate. Some myopathic changes. Denervatiojn cx reinnervation	
P8	42		scm	st	Normal	
P9	30		scm	c+gd	Normal	
P10	39		scm	st		

Table 5.1 Patient and Control details, light and electron microscopy findings

Muscle biopsied: sp=splenius, ps=paraspinal, scm=sternocleidomastoid.

Diagnosis: bi=basilar invagination, csm=cervical spondylotic myelopathy, ocf= occipital cervical fusion for Rheumatoid arthritis, pt=pineal tumour, st=spasmodic torticollis, ptcd=post traumatic cervical dystonia, c+gd=cervical and generalized dystonia.

VFS=variation in fibre size (expressed in μm), IA+A=type I fibre atrophy and angulation, IIA+A= type II atrophy and angulation, Cent Nuc=central nuclei (+=present or 0=absent), Con tissue= connective tissue (+=increased or 0=normal), I/II propn= fibre type proportions, ox=oxidative, L/G/ADA/P/AP=lipid, glycogen, adenine deaminase, phosphorylase, acid phosphatase. RRF=Ragged red fibre, COX=cytochrome oxidase, SDH=succinate dehydrogenase.

5.4 Discussion

Several strains of evidence exist to implicate mitochondria in the pathogenesis of dystonia. This study found no evidence of a mitochondrial defect in muscle from patients with sporadic focal dystonia.

The small number of patients and controls limited the analysis. This reflects the difficulties in obtaining muscle samples from dystonic patients. Surgical therapies are rarely performed in this patient group. The advent of more effective medical therapies, mainly botulinum toxin, compounds this problem. Other limitations include the fact that scm was analysed for patients and neck extensor muscles for controls. A significant concern is the quality of the control samples. Three of the four controls had histochemical mitochondrial changes in their muscle biopsies. Whether these are pathological or physiological is uncertain. Although differences in the biochemical and histological properties of different muscle groups are recognized [682], there is no literature on mitochondrial function in normal neck muscles.

Furthermore, the dystonias are a heterogeneous group of disorders. It is known that similar phenotypes can result from different genetic mutations. It is therefore possible that our group of patients could have had a number of different conditions, and hence different pathogeneses. Eight of the ten patients had a diagnostic label of spasmodic

torticollis. Of the other two, one was diagnosed with cervical and generalized dystonia, and the other with post-traumatic dystonia. These may well be different disease entities. A future study could analyse samples from genetically defined homogeneous groups of patients. Drug effects may also affect results, and exposure to botulinum toxin prior to muscle biopsy may have biochemical and histological consequences. This chemical denervation may mask biochemical defects.

Platelets are a more easily accessible tissue allowing greater numbers of patients to be studied. However they may not necessarily be representative of biochemical changes within the basal ganglia. The complex I defect found in Parkinson's disease platelets is however also present in the substantia nigra [683]. Previous reports have shown that platelets from patients with sporadic dystonia have a 21% complex I deficiency [680], a defect that is corrected when platelets are fused with ρ^0 cells [681]. This finding could have three potential explanations: i) the platelet defect was the consequence of a heteroplasmic mtDNA mutation, and after generation of the cybrids the mutation load fell below the threshold required to cause a biochemical defect; ii) the defect could be caused by a nuclear gene defect, and fusion with a new nuclear environment complements that defect; iii) an endogenous or exogenous toxin circulating in blood or bone marrow may induce the complex I defect in platelets.

Muscle may not be the ideal tissue in which to analyse mitochondrial function in this patient group. Neuronal tissue may be of greater interest but would prove difficult to obtain. The archetypal mitochondrial encephalomyopathies are renowned for their tissue specific clinical and biochemical manifestations. Little is known about mitochondrial respiratory chain function in the basal ganglia of dystonic patients. Pathological specimens would be required or biochemical information could be gleaned from magnetic resonance spectroscopy.

This is the first study to assess MRC function in dystonic muscle. No significant disturbance on MRC was found. It is of note that whilst none of our patients biochemical parameters were significantly reduced, the values for complex I activity was the least reduced from the control values. The absence from muscle of a complex I defect as found in platelets would support the previously proposed hypothesis of a

circulating toxin being responsible for the complex I defect found in patient platelets. However, this theory would require a circulating toxin to damage platelets in the circulation or bone marrow, to cross the blood brain barrier and cause mitochondrial dysfunction in the basal ganglia, but yet leave mitochondrial function in myocytes intact. This seems unlikely. Future studies of this nature should involve larger numbers of patients, with more uniformly defined disease entities. Controls should be better matched for age and muscle biopsied, since the current control data adversely affects the validity of the findings of this study.

CHAPTER 6

FRIEDREICH'S ATAXIA: ASSESSING PATIENTS AND EVALUATING THERAPIES.

6.1 Introduction:

A number of potential therapies now exist for FRDA. Several other therapeutic agents are likely to become available as our understanding of the pathogenesis of this condition improves. The size of their treatment effect is difficult to predict. They may either worsen the disease, have no effect, slow disease progression, halt disease progression, or potentially reverse, partially or wholly, already established disability. The outcome will depend on whether the agents protect cells from further damage or are able to repair already damaged cells.

The effective assessment of the diverse clinical presentations associated with FRDA is central to the evaluation of these novel therapies. This requires the evaluation and validation of disease measures, which may be patient-orientated, clinically based, or employ surrogate markers of disease activity. Trials in FRDA are further complicated by the relative rarity of the disease, its chronicity, and the potentially small size of any treatment effect. In common with other chronic conditions, the slowness of progression makes prospective studies problematic. Treatment trials for rare conditions are complicated by the small number of patients available. Large placebo controlled trials may therefore not be feasible. One substitute is the use of historical controls to predict the expected rate of disease progression. A detailed understanding of the natural history of FRDA and the factors that influence disease progression is therefore necessary. Retrospective analysis of disease progression and survival have shown a median time from disease onset to wheelchair confinement in FRDA of 11 years, and a 75% survival for more than 34 years after disease onset [429].

Historically, the use of ataxia scales followed on from the success of scales for basal ganglia disorders and has involved a variety of different scales. The Inherited Ataxia Clinical Rating Scale (IACRS) was published in 1980 [684]. These scales and a variety of novel or modified scales have been used to assess ataxic patient groups and

determine the efficacy of therapeutic trials but their validity has not been rigorously tested [526].

More recently the International Co-operative Ataxia Ratings Scale (ICARS) [555] has been developed for the evaluation of potential pharmacological therapies for ataxia. ICARS is a 100 point scale that consists of four components, posture and gait, kinetic, speech, and oculomotor and uses arbitrary, non-linear, subjective, semi-quantitative scales in an attempt to assign a value of the severity of the ataxia for an individual patient. ICARS has been used to assess patients with FRDA [685] [539] and AVED [550]. To date, despite its use in a number of therapyeutic trials there has been no systematic validation of the usefulness of ICARS as a measurement tool for FRDA or any other ataxic disorder [686].

Perhaps more significantly the degree of disability and the impact of FRDA as assessed from the patients' perspective are poorly understood and poorly documented. FRDA clearly exerts a considerable, although as yet unquantified, impact on general levels of functioning and well being. In virtually all patients with FRDA the disability includes impaired mobility, swallowing, speech and thus communication, while in a significant population of patients cardiac disease, scoliosis, impairment of vision and hearing, and diabetes may impact further on the burden of disability.

The measurement of functioning and well-being from the patient's perspective has become central to the assessment of health and the evaluation of treatment regimes. Consequently, measures variably referred to as health status, quality of life, or health related quality of life instruments are advocated when attempting to assess the outcome of health-care interventions. These measures are often not disease specific and encompass physical, psychological, and social function. While the value of these measures in certain neurological disease is now well established [687] the general use of such measures in neurology has lagged behind that in other medical specialties. Indeed, there is currently no disease specific measure for ataxia, nor have any of the non-specific measures been evaluated in this group of conditions.

6.2 Health-Related Quality of Life in Friedreich's Ataxia

6.2.1 Introduction:

The ability of four generic health status measures to assess 56 patients homozygous for the FRDA repeat expansion was evaluated. The 36-item Short Form Health Survey (SF-36), the self-report Barthel Index (BI), The General Health Questionnaire (GHQ 12), and the EuroQol were used. These health care measures are well established and validated. The SF-36 is perhaps the best known measure, developed from the Rand Corporation's Health Insurance Experiment and the subsequent Medical Outcomes Study [570]. Its brevity allows for rapid and easy completion [688] yet it covers a core set of domains of functioning and well-being. The Barthel Index is already recommended for use in elderly populations, rehabilitation and stroke patients. Goldberg's general health_questionnaire (GHQ) is the most commonly used international scale of general psychiatric morbidity. Developed in London 30 to 40 years ago, it was designed to detect anxiety and depression. Since it includes psychosomatic items it may measure physical health status in addition to psychiatric morbidity. Its use has been validated in over fifty studies. The Euroqol is widely used internationally, and provides a standardized non-disease specific survey instrument for describing health related quality of life.

6.2.2 Experimental Design

Four generic health status measures (SF-36, BI, GHQ 12, and EuroQol) were sent to 56 patients homozygous for the FRDA repeat expansion. The questionnaires were resent to those patients who had not responded by six weeks. Methodologies relating to patients, genetic analysis, and health status measures are as detailed in section 2.22.1 – 2.21.3. The questionnaires are included in appendix 2.

This work was performed in conjunction with Dr JM Cooper and Dr J Bradley of the Department of Clinical Neurosciences, Royal Free Campus, Royal Free and University College Medical School, University of London, who helped with the distribution of questionnaires, and Dr JC Hobart of the Department of Clinical Neurology and Neurorehabilitation, Neurological Outcome Measures Unit, Institute

of Neurology, Queen Square, London, who assisted with the statistical analysis of the replies.

6.2.3 Results:

Of the 56 patients sent the questionnaire, 54 responded immediately, and only 3.6% needed the questionnaire resent at 6 weeks. The ages of the 56 patients ranged from 18 to 57 years (mean 31.0 ± 8.6). 57% were female, and 95% Caucasian. Age of onset ranged from 2 to 30 years, and averaged 13.7 years ±6.4. Disease duration varied from 4 to 38 years with an average of 18.1 years ±8.4. We questioned patients about their employment status, and of the 56, 41% were in employment, 26% retired due to their ataxia, 2% retired for other reasons, 18% unemployed, and 13% were students. 64% of our patients were educated beyond the minimum school leaving age, and 25% of our cohort had a degree or equivalent qualification. As regards marital status, 59% were single, 21% married, 5% divorced, and 14% living with a partner. Regarding mobility, bearing in mind the average disease duration of 18.1 years, 14% walked unaided, 30% walked with an aid, and 55% were wheelchair users.

Descriptive statistics for the self-report Barthel (BI), GHQ 12, EuroQol thermometer, and EuroQol Helath state are shown in table 6.1, and those for the eight domains of the SF-36 questionnaire in table 6.2. Mean scores were near the mid-point of the possible scale-range for role limitation physical, general health perceptions and vitality of the SF-36, and for the GHQ 12 suggesting that the distribution of the scores on these instruments is near normal and likely to detect change. Standard deviation was high, implying variability and thus the ability to detect change and discriminate between individuals, for all measures except the GHQ 12. Standard deviation was particularly high for role limitation physical and emotional of the SF-36. Floor and ceiling effects describe the percentage of patients scoring the maximum and minimum scores respectively. They represent the extent to which the measured range of an attribute is restricted and should ideally be below 15%. This was exceeded in all components of the SF-36 except general health perceptions, vitality, and mental health. Floor and ceiling effects were of desirable levels for BI, GHQ 12, Euroqol thermometer, and Euroqol health state. Skewness is a measure of how normal a

distribution of scores is. A positive value indicates that scores cluster to the left of the mean, and a significant positive result was obtained for SF-36 physical function, and the GHQ 12. Sizeable negative skew values were obtained for all other measures except the SF-36 vitality.

	Barthel Index	GHQ 12	EuroQol thermometer	Euroqol Health State
N	47	51	55	45
Missing data	16%	9%	1.8%	19.6%
Scale range (midpoint)	0-20(10)	12-48(30)	0-100(50)	-0.594-1.00
Score range	2-20	12-40	20-95	-0.09-1.00
Mean (sd)	13.5(4.7)	25.0(6.1)	64.3(19.1)	0.53(0.3)
Floor %	0	0	0	0
Ceiling %	8.5	2.0	0	2.2
Skewness	-0.580	0.678	-0.748	-0.902

Table 6.1

Descriptive statistics for the self-report Barthel, GHQ 12, EuroQol thermometer, and EuroQol Health state.

		Range		Score			
Dimension	**N (missing data %)**	**Scale**	**Score**	**Mean (sd)**	**Floor %**	**Ceiling %**	**Skew**
Physical function	54(3.6)	0-100	0-90	21.7 (23.7)	20.4	0	1.401
Role limitations-physical	55(1.8)	0-100	0-100	50.9 (42.5	27.3	36.4	0.059
Bodily pain	56(0)	0-100	22-100	78.3 (22.6)	0	39.3	-0.814
General health perceptions	55(1.8)	0-100	5-100	46.8 (23.4)	0	1.8	0.217
Vitality	55(1.8)	0-100	0-85	49.8 (22.3)	1.8	0	-0.0474
Social functioning	56(0)	0-100	0-100	71.4 (27.3)	1.8	28.6	-0.885
Role limitations-emotional	53(5.4)	0-100	0-100	73.0 (37.6)	15.1	58.5	-1.056
Mental health	55(1.8)	0-100	24-100	67.2 (21.3)	0	1.8	-0.404

Table 6.2

Descriptive statistics for the eight domains of the SF-36 questionnaire.

6.2.4 Discussion:

The use of health instruments in neurology is well established. This is particularly true for the evaluation of outcomes after head injury [689] stroke, epilepsy, Parkinsons disease, motor neurone disease, spinal injury, and multiple sclerosis [690]. These health measures may be generic or disease-specific. General measures of health status allow comparison with other patient groups. Disease specific measures are more sensitive to change than generic measures, but may be too narrowly focused and thus fail to capture broader outcome measures. Generic and disease specific scores, and utility measures can be used simultaneously. No disease specific measures exist for the evaluation of ataxia, and no literature on the use of generic measures in this group of conditions could be found despite an extensive literature search.

The SF-36 covers facets of life that one would assume to be relevant to patients with ataxia. These are the ability to perform work and daily activities, and physical and social functioning. The reliability, validity, and responsiveness of the SF-36 have been previously well established [691]. It has previously been used in a number of neurological disorders [692-694]. Our results show that the impact of FRDA is significant. Three components of the SF-36 score showed a significant percentage of patients exhibiting maximum poor health scores. This floor effect was significant for physical function, physical role limitations, and emotional role limitations. All other parameters had negligible floor effects and the validity of the score and its usefulness in assessing change are therefore not compromised. Four components of the scale (physical role limitations, bodily pain, social functioning, and emotional role limitations) showed significant ceiling effects, suggesting that a sizeable percentage of our FRDA group reported no disability for these parameters. However two of these (physical role limitations and emotional role limitations) also had significant floor effects showing the group to be spread across the whole range with significant percentages at either extreme.

The three potential responses to the five items of the Euroqol health state questionnaire are combined to give a five-digit response set (eg 13212). Therefore 243 (3^5) potential health states exist within this measure. The Euroqol thermometer, a simple visual analogue scale, provides a single overall score. This is a supplementary

self-assessed measure of overall health status rather than a valuation of utility. The Barthel Index assesses ten clinically relevant items of physical dependence in personal activities of daily living. These are bathing, transferring, dressing, feeding, mobility, stairs, toilet use, grooming, bladder, and bowel function. The general health questionnaire concentrates on broad components of psychiatric morbidity. GHQ 12 is the shortest version of the general health questionnaire, but is as efficient as the 30-item version. The self report Barthel Index, GHQ 12, Euroqol thermometer, and Euroqol Health State exhibited no floor effect and ceiling effects were likewise negligible. However data was missing from 16% of the Barthel Index and almost 20% of the Euroqol health state.

This study documents for the first time the substantial impact that Friedreich's ataxia has on the health status of patients. It has, as might be expected, particularly severe impact on physical functioning, but is also severely deleterious on emotional aspects of health status, social functioning, and mental health.

Further studies will evaluate the impact on health status over time, and the impact on the health status of care givers which has been shown to be an important factor in Alzheimers disease [695], and motor neurone disease [696]. Treatments offering benefit to the patients might also benefit carers. The health status of carers also has implications for support services and charitable organisations. Further studies are underway to design a quality of life measure specific for FRDA.

The impact of FRDA on patients has until now consisted only of descriptive studies of the clinical features of the condition and data on parameters such as age of onset, wheelchair use, and age of death. This study has provided the first large-scale evaluation of the self-reported health status of patients with FRDA, and clearly describes the human impact of the disease. The findings show these measures to provide a meaningful and valid picture of the impact of Friedreich's ataxia on the daily lives of those living with it. The data obtained will enhance our understanding of FRDA, and will be of use in the analysis of future trials that use quality of life as a primary outcome variable, allowing another dimension to the evaluation of the efficacy of potential therapeutic interventions.

6.3 Friedreich's ataxia: Evaluation of ICARS and Factors Influencing Clinical Progression.

6.3.1 Experimental Design

77 patients, homozygous for the FRDA repeat expansion, from 67 different pedigrees were assessed clinically using ICARS as the scoring system. They also underwent echocardiography and neurophysiological evaluation. Methodologies concerning patients, genetic analysis, clinical assessment and statistical analysis are detailed in sections 2.22.1 – 2.22.4

6.3.2 Results

The data is summarised in table 6.3. There were similar numbers of males (37) and females (40), with a broad range of disease onset (2 - 27 years of age). In the vast majority gait ataxia was the presenting feature. Other features bringing patients to medical attention included pes cavus (2 patients), scoliosis (1), upper limb incoordination (2), family history of FRDA in asymptomatic individuals (1), and sphincter disturbance (1). The average time from symptom onset to diagnosis was 4.5 ± 3.9 years, ranging from 4 years prior to the onset of symptoms in the sibling of an affected patient, to 17 years after symptom onset. In those at the upper end of this range disease onset tended to have been prior to the introduction of genetic testing. At the time of assessment the patients were between 10 - 57.7 years of age and disease duration ranged between 1.7 - 39.7 years. The size of the smallest GAA repeat (GAA1) ranged between 130-1080. There was an inverse relationship between GAA1 and age of onset (figure 6.1). In the 62 patients questioned the ADL scores ranged between 2 - 26 (mean 13.6 ± 5.2).

		Clinical Feature	Percent	Clinical Feature	Percent	Clinical Feature	Percent
Number of patients Number of families	77 67	Retained LL reflexes	8 [a]	Dysphagia	60	Absent SSEPs [$]	
Male : Female	37 : 40	Extensor plantars	94	Sphincter disturbance	39 [c]	N9 N13	74 61
Mean age (range)	24.3 ± 10 (10 - 57.7)	Severely impaired vibration	56	Severely impaired vision	3 [d]	N20	37
Mean age of onset (range)	11.9 ± 6.3 (2 - 27)	Scoliosis	68	Square wave jerks [#]	5	Absent SAP [$]	
Mean disease duration (range)	12.4 ± 7.8 (1.7 - 39.7)	Pes cavus[#]	62	Fixation instability [#]	16	Radial Ulnar Median (F2)	50 80 63
Mean GAA1 size (range)	725 ± 229 (130 - 1080)	Diabetes mellitus	5 [b]	LVH by echo	42[e]	Sural	83

Table 6.3. Percentage prevalence of clinical features in Friedreich's ataxia patients not assessed as part of the ICARS.

a. Defined as individuals with knee or ankle deep tendon reflexes
b. Diabetes was determined by a requirement for insulin or a raised random glucose or HbA1c level.
c. Minimum criteria: patients reporting mild urinary hesitancy, urgency or retention < once per month
d. Patients previously investigated for optic atrophy,
e. LVH defined by an intra ventricular septal thickness > 11mm
n=63, $ n = 54

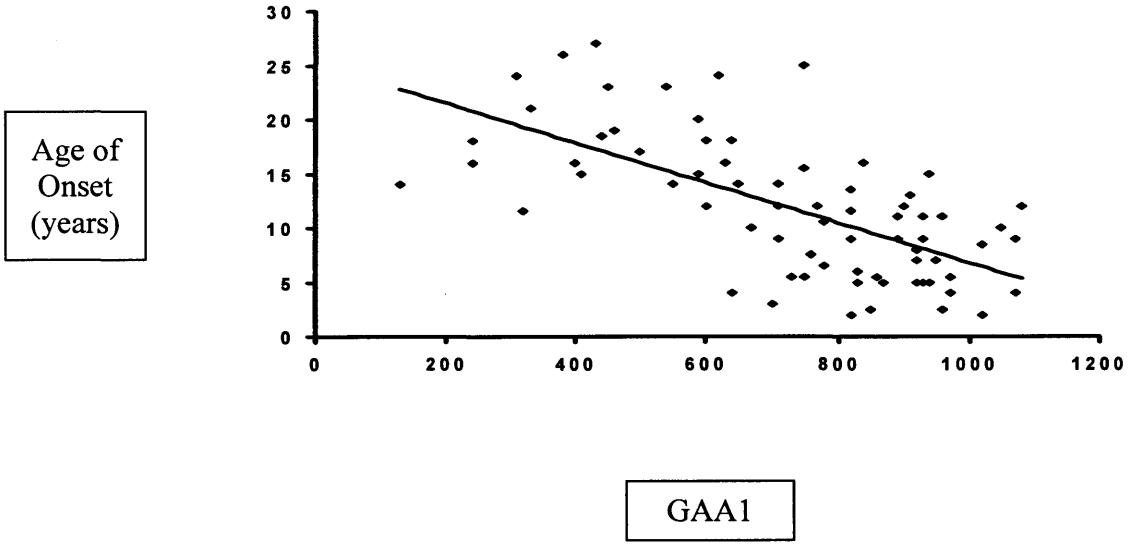

Figure 6.1

Relationship between the size of the smaller GAA repeat (GAA1) and age of onset in 77 FRDA patients. Gradient 0.0184 years / GAA, correlation coefficient, $R=0.666$, $p<0.001$.

Atypical clinical presentations included three cases of onset over the age of 25 years, and six cases with some preservation of lower limb (LL) deep tendon reflexes and a further 6 patients in whom some of the upper limb reflexes were still present. These patients tended to have a slightly older disease onset, and a shorter GAA1 repeat size than the remaining patients, but similar ICARS scores. The differences did not reach statistical significance.

The prevalence of clinical features generally mirrored that of previous studies [697]. However, dysphagia, rarely commented on in previous studies, was reported by 60% of these patients in whom it was graded as moderate (choking more than once a month, 40%) or more severe (20% of patients). Sphincter disturbance was reported by 39%, where it was moderate (moderate hesitance, urgency, or retention once a month, or urinary incontinence less than once a month, %) or more severe (% of patients). Skeletal abnormalities were common. Pes cavus was present in 62%, and scoliosis in 68%, with 31% of those with scoliosis requiring corrective surgery. Only 5% of patients were known to be diabetic, with one further patient having a raised HbA1c level.

The clinical features of the patients as indicated by the total ICARS score (scale range 0-100) was quite diverse with a score ranging between 23 and 95 (mean 52.7 ±17.1). Analysis of how the total ICARS and four component scores changed with increasing patient age demonstrated that all scores fell on the scale with no floor or ceiling effects with the exception of posture and gait scores which increasingly reached a maximum above the age of 23.9 years (Figure 6.2).

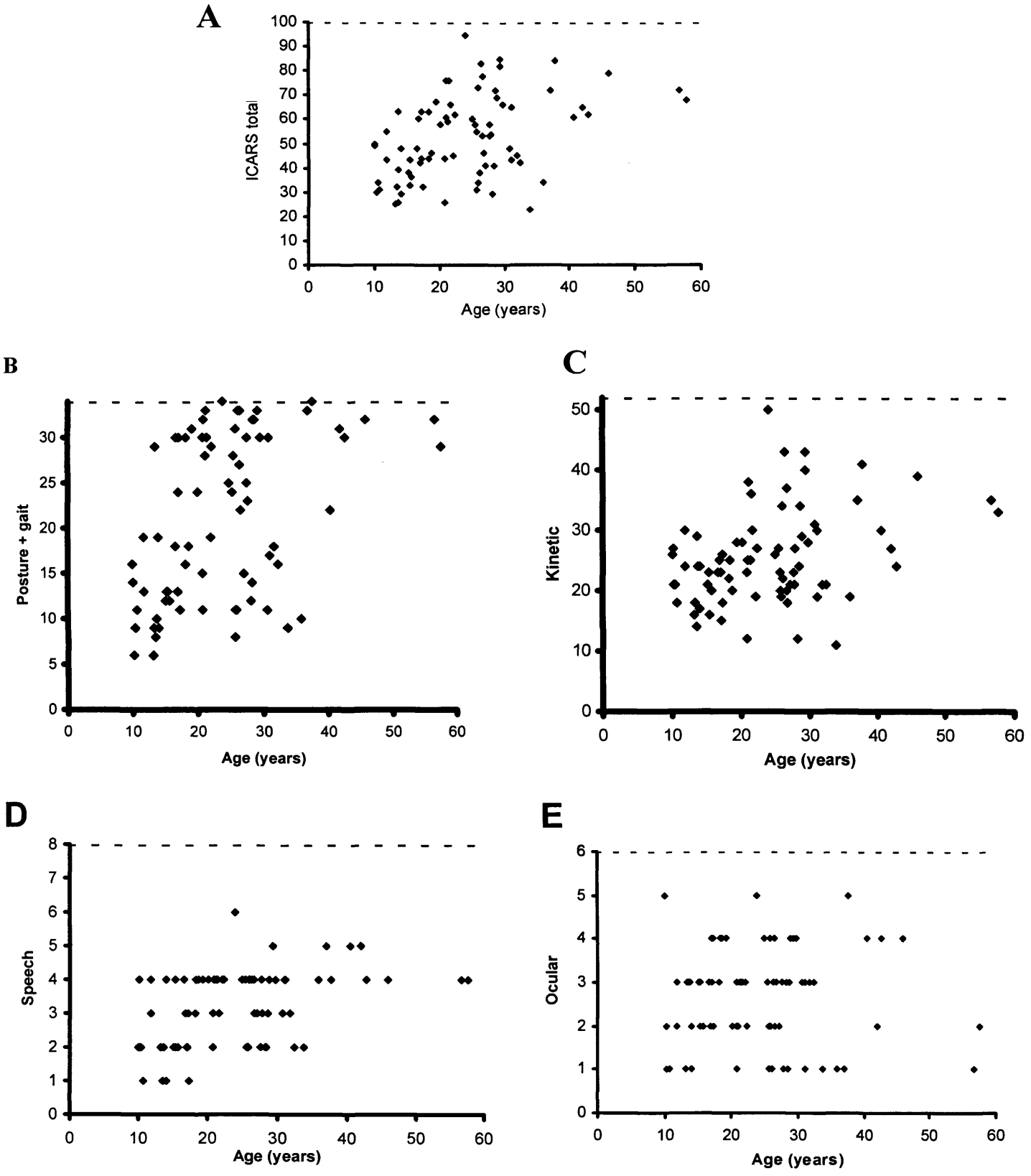

Figure 6.2

Relationship between patient age at assessment and the distribution of total ICARS score (A), and the four component scores of ICARS; posture and gait (B), kinetic (C), speech (D), and ocular (E), in 77 patients with FRDA.

To determine if there was any relationship between clinical progression and GAA1 size, patient age and disease duration the total ICARS and the four individual component scores were correlated with these parameters using single or multiple linear regression analyses (Table 6.4). The most significant correlation was between total ICARS, GAA1 and patient age with 49% of the variation in total ICARS score being attributable to these two combined variables. ICARS component scores were variably related to repeat length, disease duration, and age. Ocular scores, determined by the presence or absence of nystagmus, hypo or hypermetric saccades, and saccadic intrusion of pursuit movements, failed to correlate with these disease parameters (Table 6.4).

Dependent Variable		Independent Variable: GAA1 (number)	Disease Duration (years)	Age (years)	GAA1 / Duration	GAA1 / Age
Total	grad	0.021	1.34	0.71	0.027/1.43	0.05/1.29
	R^2	0.077*	0.366**	0.170**	0.489**	0.490**
Kinetic	grad	0.009	0.576	0.28	0.012/0.617	0.021/0.525
	R^2	0.072*	0.318**	0.123*	0.431**	0.393**
Ocular	grad	NS	NS	NS	NS	NS
	R^2	0.012	0.021	0.00	0.037	0.015
Posture + gait	grad	0.011	0.682	0.386	0.014/0.731	0.027/0.698
	R^2	0.080*	0.343**	0.181**	0.468**	0.517**
Speech	grad	NS	0.064	0.048	0.0/0.065	0.001/0.062
	R^2	0.001	0.212**	0.191**	0.212**	0.239**

Table 6.4

Relationship between ICARS and ICARS component scores and various disease parameters. Gradients (grad) relate to the changes in clinical score per unit of the independent variable, unless the relationship was not significant (NS). Correlation coefficients (R^2 values) for 77 FRDA patients when correlated with various disease parameters. Single and multiple linear regression analyses were performed using SSPS. * = $p < 0.05$, ** = $p < 0.001$

Visualisation of the combined influence of increasing age and GAA1 size on total ICARS scores was achieved by dividing the 77 patients into 4 groups according to the size of their GAA1 (<600, 600-750, 751-900 and >900 GAA), to give approximately equal numbers of patients in each group (Figure 6.3). The linear regression analysis for these groups showed a correlation indicating a progression of; 0.87, 0.54, 1.85 and 2.26 ICARS points per year in the <600, 600-750, 751-900 and >900 groups respectively.

Retrospective analysis of disease progression was determined in the 4 patient groups. This identified a graded progression between the different stages in proportion to the size of GAA1 size. The mean time from onset of walking difficulties to wheelchair confinement for outdoor use was 17.9, 14.9, 10.3, and 9.5 years in the <600, 600-750, 751-900 and >900 GAA groups respectively (figure 6.4). The value for the patient group as a whole was 11.2 years.

The ocular subscore of ICARS is a cumulative score of gaze-evoked nystagmus, abnormalities of ocular pursuit, and dysmetria of the saccade. Pursuit movements were slightly fragmented in 40%, and clearly fragmented in 33% of patients. Nystagmus was present in only 6% of patients, and in these patients only a few non-sustained beats were seen. Saccades were hypermetric in 70%, and hypometric in 19% of patients. Further evaluation of parameters not included in ICARS revealed fixation instability in the primary position in 16%, square wave jerks in 5% of patients and reduced saccadic velocity in 24%, (but only clearly so in 5%) of all patients.

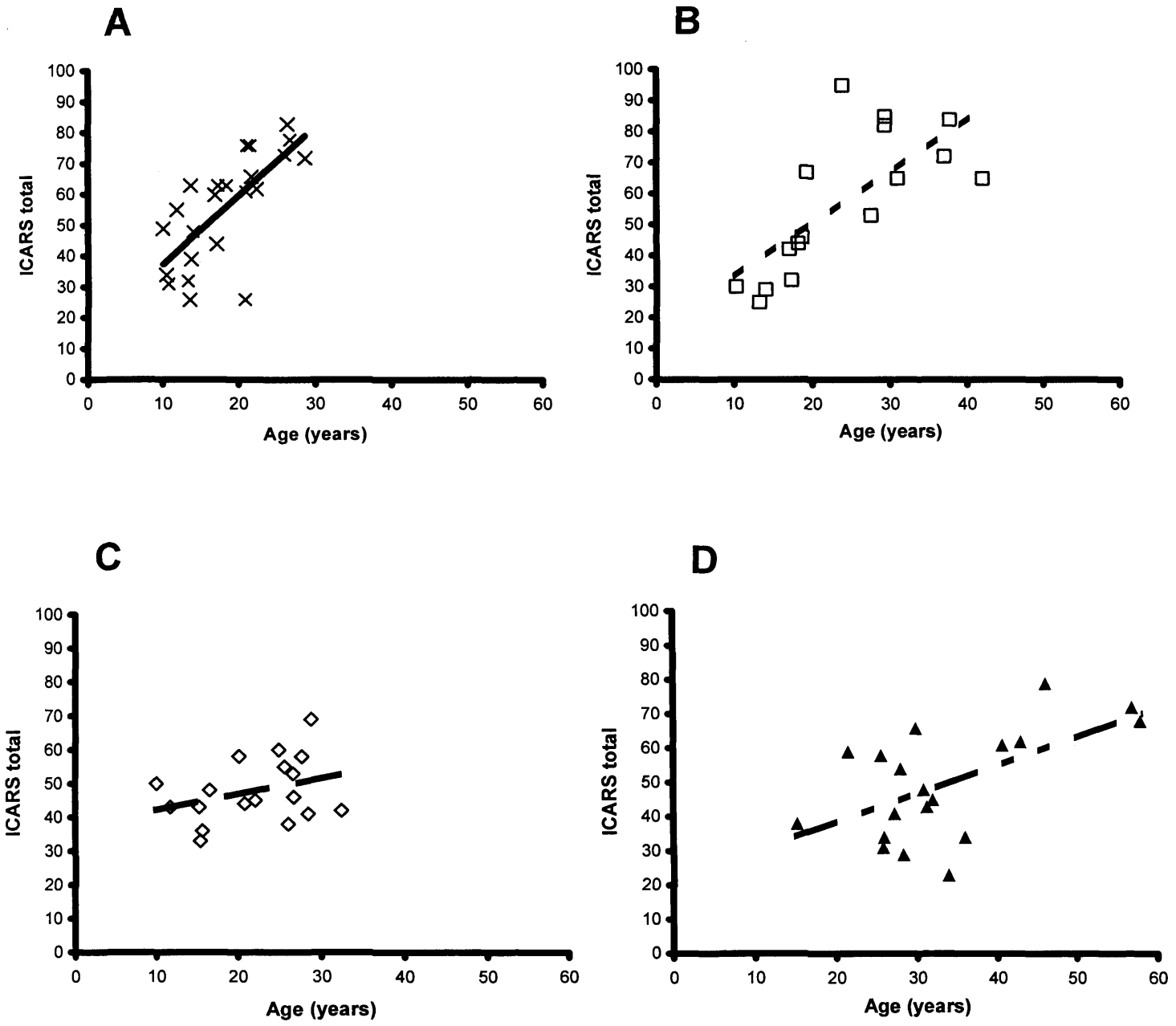

Figure 6.3

Relationship between patient age and total ICARS score in groups of patients with GAA1 repeat sizes in the range; A: >900 GAA (X, n=23), solid line, gradient = 2.26, R^2=0.51 p <0.001 B: 751-900 GAA (open square, n=16), dotted line, gradient = 1.85, R^2=0.58 p <0.001 C: 600-750 GAA (open diamond, n=18), long dashed line, gradient = 0.54, R^2=0.167 p =0.09 D: <600 GAA (closed triangle, n=20) dashed-dotted line, gradient = 0.87, R^2=0.328 p =0.06 E: represents the linear regression lines for each patient group taken from graphs A-D.

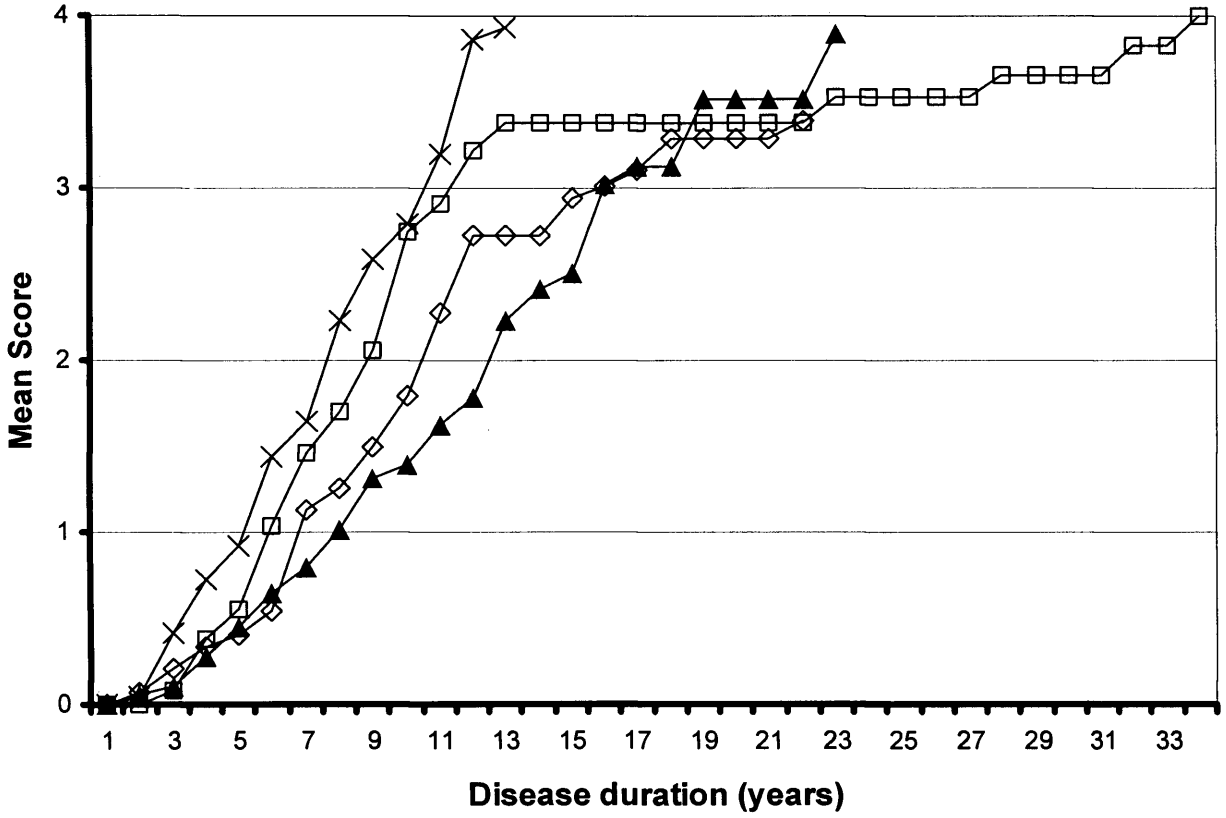

Figure 6.4

Retrospective analysis of disease progression in 77 patients with FRDA according to GAA1 size, expressed as mean disease scores against disease duration. The patient groups and symbols used are as for figure 6.3.

Electrocardiography revealed one patient to be in fast atrial fibrillation while all others were in sinus rhythm. Hypertrophic changes were identified in 42% of patients using echocardiography criteria (IVS >11mm). Additional findings were coarctation of the aorta requiring stenting in one patient, prominent papillary muscles in 5 patients, and systolic apical cavity obliteration in 2 patients. As a group the fraction shortening was 32.6 ± 5.2%, (normal values 28-37%) suggesting there was normal heart function in the majority of patients.

LVDd and LVDs demonstrated a significant positive correlation with disease duration, patient age and ICARS score (Table 6.5), but an inverse correlation with GAA1 size. This suggested LV dilation increased with increasing age, disease duration and clinical severity, but larger GAA1 sizes were associated with decreasing LV dilation. Fraction shortening showed an inverse correlation with disease duration and clinical score (table 6.5) suggesting heart function deteriorated with disease progression. PWd correlated poorly with the disease parameters analysed. However, IVS demonstrated a significant decline with increasing age suggesting less hypertrophy as the patients aged, and a near significant increase with GAA1 size suggesting more severe hypertrophy with larger genetic abnormalities (Table 6.5).

Neurophysiological evaluation was performed in 54 patients. Sural, radial, ulnar and median F2 nerve action potentials were undetectable in 83, 50, 80, and 63% of the patients respectively. The patients with undetectable SAP had larger GAA1 repeat sizes and higher clinical scores (ICARS) (table 6.5), but did not show significant differences between age or disease duration. In those patients where it was detectable the mean sensory action potentials were severely decreased to 1.5 ± 0.83μV (control 5 -30μV), 3.18 ± 1.67μV (control 21 - 80μV), 1.62 ± 0.97μV (control 15 - 50μV) and 1.97 ± 0.94μV (control 16 - 65μV) in the sural, radial, ulnar and median (F2) nerves respectively.

The mean conduction velocities for sural, radial, ulnar and median nerves were respectively 39.3 ± 3.1 m/s (control 46.5 ± 4.0m/s), 48.9 ± 5.3 m/s (control 63 ± 6.0m/s), 44.1 ± 6.35 m/s (control 57 ± 5.0m/s), and 49 ± 5.4 m/s (control 56.9 ± 4.0m/s). Somatosensory evoked potentials were undetectable at N9, N13 and N20 in

74, 61 and 37% of the patients respectively. In those with detectable responses, the latencies were similar to normal at N9, N13 with latencies of: 9.88 ± 1.05 msec (normal 9.83 ± 2.11msec), 13.9 ± 2.4 msec (normal 13.55 ± 2.14msec) but longer at N20 with a latency of 26.7 ± 5.8 msec (normal 19.27 ± 2.22msec). In the patients with measurable SSEPs there were no significant correlations between the SSEP values and other disease parameters (GAA1 size, patient age, disease duration or ICARS score). In those patients with undetectable SSEPs the ICARS scores were significantly higher and the GAA1 repeat sizes tended to be larger, although these were not statistically significant (Table 6.5). Mean motor conduction velocity were slightly decreased to 50.6 ± 3.5 m/s (normal 56.7 ± 3.8 m/s) for the median nerve and 40.5 ± 7.4 m/s (normal 49.9 ± 5.9 m/s) for the common peroneal.

Correlation of the detectable neurophysiology results with GAA1 size, patient age, disease duration and ICARS score revealed the following significant correlations: Mdndml, mfwave and cmapw all showed a significant positive correlation with disease duration, age and clinical severity; Cpdml a positive correlation with clinical severity; Cmapa a significant inverse correlation with genetic severity and age and Cmapk a significant inverse correlation with genetic severity (Table 6.5).

		GAA	Duration	Age	ICARS
LVDd	grad	-0.009	0.280	0.282	0.068
	R2	0.163**	0.183**	0.306**	0.052*
LVDs	grad	-0.0058	0.28	0.231	0.09
	R2	0.075*	0.204**	0.230**	0.104**
FS	grad	NS	-0.211	NS	-0.102
	R2	0.001	0.099**	0.032	0.113**
IVS	grad	NS	NS	-0.047	NS
	R2	0.049	0.017	0.063*	0.002
mdndml	grad	NS	0.026	0.02	0.012
	R2	0.003	0.135**	0.125**	0.177**
cmapw	grad	-0.015	0.6	0.496	NS
	R2	0.134**	0.243**	0.265**	0.014
Mfwave	grad	NS	0.143	0.118	0.084
	R2	0.025	0.128**	0.138**	0.254**
cpdml	grad	NS	NS	NS	0.04
	R2	0.057	0.014	0.005	0.15**
Cmapa	grad	-0.0039	NS	-0.039	NS
	R2	0.172**	0.004	0.172**	0.039
Cmapk	grad	-0.0035	NS	NS	NS
	R2	0.163**	0.004	0.056	0.04

Table 6.5

Relationship between various echocardiographic and neurophysiological parameters and genetic abnormality (GAA1), disease duration, patient age or clinical severity (ICARS). Gradients (grad) relate to the changes in clinical score per unit of the independent variable, unless the relationship was not significant (NS). Correlation coefficients (R^2 values) for 77 FRDA patients when correlated with various disease parameters. Linear regression analyses were performed using SSPS. * = $p < 0.05$, ** = $p < 0.01$

LVDd= left ventricular diameter in diastole; LVDs= left ventricular diameter in systole; FS=fraction shortening; IVS= interventricular shortening; mdndml= median distal motor latency; cmapw= median compound motor action potential at the wrist; Mfwave= median f wave; cpdml= common peroneal distal motor latenct; Cmapa= common peroneal compound motor action potential at the ankle; Cmapk= common peroneal compound motor action potential at the knee.

6.3.3 Discussion

The understanding of the genetic and biochemical features of FRDA has markedly increased over the last decade. Although this knowledge has enabled the trial of a number of therapeutic interventions, analysis of their influence upon disease progression has been limited by the absence of a validated assessment protocol.

The prevalence of the clinical features observed in this cohort of FRDA patients is broadly in keeping with those of previous reports. However, fewer patients were found to be diabetic than previously reported while dysphagia and sphincter disturbance appears as a common complaint in FRDA. These differences are most likely to be due to case selection or differences in the criteria used to define the various clinical features. The recognition of these disease complications is important for the long term care of patients with FRDA.

Various surrogate markers have been used to assess therapeutic effects of treatment regimes including ^{31}PMRS [490] and markers of oxidative stress [483], but ultimately clinical parameters and patient orientated outcome measures are required to confirm any benefits.

In this study neither the total ICARS score nor its component scores showed any significant floor effect, but the posture and gait score reached a ceiling at a relatively early age (23 years), with 17% of patients in this cohort, scoring above the 95th centile, and 2 patients scoring maximum points. This score makes up 34% of the total ICARS score; consequently this component of the ICARS score is of limited use in patients with relatively advanced disease.

Total ICARS scores correlated well with parameters associated with disease progression including age, disease duration and GAA1 size. Analysis of the ICARS component scores demonstrated that kinetic, and posture and gait scores correlated well with these disease parameters, while the speech component correlated to an intermediate level. The assessment of speech in ICARS is highly subjective, is limited to the analysis of only one specific phrase, and relies upon the subjective

interpretation of fluency and intelligibility. More detailed speech analyses may be required to give results that correlate more closely with disease progression.

Of the ICARS component scores, oculomotor parameters correlated extremely poorly with disease parameters. A number of studies have investigated the prevalence of ocular and oculomotor manifestations of FRDA [698,699]. However, the relationship between oculomotor manifestations, disease duration and progression, and the use of ocular parameters to assess treatment effects has, to date, been left largely unexplored. While some ocular features, including square wave jerks, were absent from the ICARS they involved relatively small numbers of patients. The absence of any progression of the ocular defects with disease progression or GAA1 size may indicate that the evaluation of ocular involvement is either too crude and may require a more sensitive protocol, or that there is no progression of these symptoms.

In common with other scales, ICARS is not a continuous scale and often the steps between points are relatively large with some patients falling between values. Many of the clinical symptoms associated with FRDA are not evaluated in the ICARS score. Included in this list are; cardiological and neurophysiological features, loss of reflexes, vibration sense, skeletal abnormalities, diabetes, swallowing problems, sphincter abnormalities and some ocular signs including blindness. These may make up a significant component of any treatment effect and need to be assessed separately.

The rate of clinical progression, as assessed by either ICARS or the retrospective clinical data, was shown to be dependent upon the size of the GAA1. This clearly links the severity of the primary cause of the disease with the rate of clinical progression. Previous observations have shown that the residual level of frataxin is inversely related to the size of GAA1 [439]. Consequently the larger GAA1 alleles lead to lower frataxin levels and a more aggressive disease. This understanding and quantification of varying rates of disease progression will be of value in measuring potential treatment effects.

The patients involved in this study may not be a random representation of the whole FRDA population. Patients with severe disability or advanced cardiac disease may have been prevented from participating in our study due to mobility difficulties or

because they are less inclined to volunteer for assessment. Only patients over the age of 10 were accepted for assessment, therefore potentially skewing our patient population. However, the confounding aspects of child development and an ability to participate in certain assessments may mean the assessment of children may require a modified approach. This will be most evident with therapies that are disease modifying rather than curative where it will be preferable to treat patients either early on in the disease or in pre-symptomatic individuals, many of these patients will fall into the younger age group.

In conclusion we have been able to demonstrate that ICARS is a valid and useful tool to assess the clinical symptoms and progression of FRDA. Using cross sectional ICARS data we have clearly shown that disease progression is predominantly determined by the size of the genetic abnormality (GAA1). Consequently it is particularly important to consider this in the design of long-term therapies and especially for those therapies aimed at modifying disease progression. Posture and gait scores reached a maximum relatively early in the course of the disease making it less suitable for patients with a more advanced disease. In addition there are a number of features not assessed properly by ICARS and therefore require additional assessments. As with many clinical scales the subjectivity involved adds to the variability of the scores and this may be particularly evident in the kinetic components. This can be addressed by using additional tests less prone to subjectivity. Whether electrophysiological or echocardiographic parameters provide good measures of treatment response remains uncertain and may need more long-term follow-up. Further work was completed and continues, assessing quantitative measures of ataxia in these patients. These include tests of upper and lower limb dexterity, timed walks, peg board tests and tests of dysarthria. These, and their comparison with ICARS will be the subject of future publications.

6.4 Antioxidant treatment of Patients with Friedreich's ataxia: 3 year follow up.

6.4.1 Introduction

The identification of the FRDA gene product frataxin as a nuclear encoded mitochondrially targeted protein [438,463,469,470], and the finding of mitochondrial iron accumulation, increased sensitivity to oxidative stress, deficits of respiratory chain complex activities and *in vivo* impairment of cardiac and skeletal muscle tissue energy metabolism in patients with FRDA, has paved the way for the development of rational therapeutic interventions. Consequently these findings have suggested that patients with FRDA may benefit from antioxidant, mitochondrial enhancement, or iron chelation therapy. These findings have also provided surrogate disease markers that can be utilised, in parallel with clinical and patient orientated outcome measures, to monitor the response to novel therapeutic agents. We therefore undertook a pilot study to determine any clinical and bioenergetic benefits of long-term vitamin E and coenzyme Q_{10} therapy in patients with Friedreich's ataxia. We followed 10 patients with genetically defined Friedreich's ataxia after 1, 2 and 3 years on the same therapy and determined the effect upon; the clinical progression of the disease using ICARS and echocardiography; and on the mitochondrial bioenergetics of the heart and skeletal muscle using ^{31}P-MRS.

In vivo phosphorous magnetic resonance spectroscopy (^{31}P-MRS) is a non-invasive technique that detects phosphorous containing compounds and cytosolic pH, and can thus be used to assess tissue oxidative metabolism. The major detectable compounds are ATP, phosphocreatine (PCr) and inorganic phosphate (Pi). Free (metabolically active) ADP, the major regulator of oxidative phosphorylation, can be calculated from the MRS data using the creatine kinase equilibrium equation [700]. Cardiac ^{31}P-MRS enables the *in vivo* measurement of the PCr to ATP ratio. This has been shown by ^{31}P-MRS and conventional biochemistry to be a good measure of the energetic state of cardiac muscle [701,702]. Cardiac PCr to ATP ratio has previously been shown to be significnalty reduced in FRDA patients with and without cardiac hypertrophy [703]. Skeletal muscle provides an ideal tissue in which to assess *in vivo* mitochondrial ATP production rate using ^{31}P-MRS.

It can be studied at rest, during exercise, and during the recovery phase [704]. During incremental exercise there is a progressive reduction of PCr as it is hydrolysed via the creatine kinase reaction in order to buffer the ATP concentration. As soon as the exercise is stopped the PCr concentration begins to return to its pre-exercise levels, as PCr is re-synthesised from ATP. ATP production during recovery from exercise is entirely due to oxidative phosphorylation [704], thus PCr re-synthesis rate reflects the mitochondrial rate of ATP production. Mean muscle Vmax in FRDA patients has been shown to be reduced to 34% of the normal mean and is strongly dependent upon the size of GAA1 [490,539].

6.4.2 Experimental Design:

Acknowledgements: this work was performed in conjunction with others. Dr J Crilley performed all echocardiography; Dr R Lodi and Dr B Rajagopalan performed all MRS studies in conjunction with Drs DJ Taylor, Dr A Blamire, Dr D manners, and Dr P Styles all of the MRC Biochemical and Clinical Magnetic Resonance Unit, Department of Biochemistry, University of Oxford and Oxford Radcliffe Hospital, Oxford, UK. Genetic analysis was performed by Dr J Bradley. All clinical evaluations were performed by myself. The trial was orchestrated by Dr JM Cooper and Prof AHV Schapira. Funding for the trial was provided by the Ataxia Society. All drugs were provided by Pharma Nord.

Subjects – Ten FRDA patients (5 males, age range 16-40 years, mean ± SD 28 ± 6 years) were studied. At zero months their MRS data were compared to 10 healthy volunteers for the calf skeletal muscle (5 males, age range 22-41, mean ± SD 28 ± 5 years) and 10 different healthy volunteers for the cardiac muscle ^{31}P-MRS (5 males, age range 16-40 years, mean ± SD 28 ± 6 years). The diagnosis of FRDA was confirmed by detection of a GAA repeat expansion in the first intron of both alleles of the frataxin gene [474]. The GAA expansion was in the range 290 tom900 repeats for the shorter of the two alleles. Patients were assessedneurologically, and with MRS and echocardiography at 0,3,6,11,23,and 35 months. Informed consent was obtrained from all patients and volunteers. The trial was conducted with the ethical approval of the Central Oxford and Royal Free Hospital Ethics Committees.

^{31}P-MRS – Patients laid prone in the magnet and standard spin-echo MRI were used to position the heart in the centre of the magnet. Cardiac ^{31}P spectra were acquired using a 7 cm circular surface coil placed below the chest. Data were acquired using a slice selective 1-dimensional spectroscopic image imaging technique that separately localises signal from the chest wall and myocardium [705]. Skeletal muscle ^{31}P-MRS spectra were obtained from the right calf muscle at rest, during an aerobic incremental exercise of plantar flexion and the following recovery phase [706]. Relative concentrations of inorganic phosphate (Pi), PCr and ATP were obtained. The maximum rate of mitochondrial ATP synthesis (Vmax) was calculated [707].

Echocardiography – 2D and M-mode imaging from parasternal and apical windows was performed at the above time points using Sonos-5500 (Hewlett Packard, Bracknell, United kingdom). Images were recorded on optical disk for subsequent analysis. Standard M-mode measurements were made using established criteria [708].

Clinical evaluations – were performed at 0, 6, 11, 18, 23, and 35 months, using ICARS as described above.

Statistical analysis – Individual tests were taken as abnormal when they fell outside the normal range. In view of the low number of subjects, non-parametric tests were used. The Mann-Whitney U-test was used to compareindependent groups and the Wilcoxon's matched pair test to compare dependent groups (i.e. data collected from FRDA patients before and during therapy). Statistical significance was taken as $p < 0.05$. Correlation coefficients were calculated by linear regression.

6.4.3 Results:

After 6 months therapy cardiac PCr to ATP ratios increased by more than 50% in the FRDA patients as a group. Cardiac PCr to ATP ratio did not increase in two patients, both of whom had LVH, but one of these was the only patient with a normal cardiac PCr to ATP ratio before therapy. There was a greater degree of PCr/ATP recovery in the 4

FRDA patients without cardiac hypertrophy (+70%) than in the 5 patients with LVH (+37%). Skeletal muscle Vmax increased for the group by 34% after 6 months therapy, and was unchanged in only 2 patients. At 35 months cardiac and skeletal muscle energy metabolism as judged by 31P-MRS showed a sustained improvement (figure 6.5).

Echocardiography data suggests the fraction shortening at the 35 month time point for the patients as a whole was significantly increased relative to the pre-therapy data (figure 6.6). The total ICARS score and posture and gait, and kinetic component did not differ significantly from the pre-treatment group values (figure 6.7). Comparison of the progression of the patients' clinical scores with cross-sectional data suggested the clinical scores for 8 patients were better than predicted while 2 patients scores declined as expected (figure 6.8).

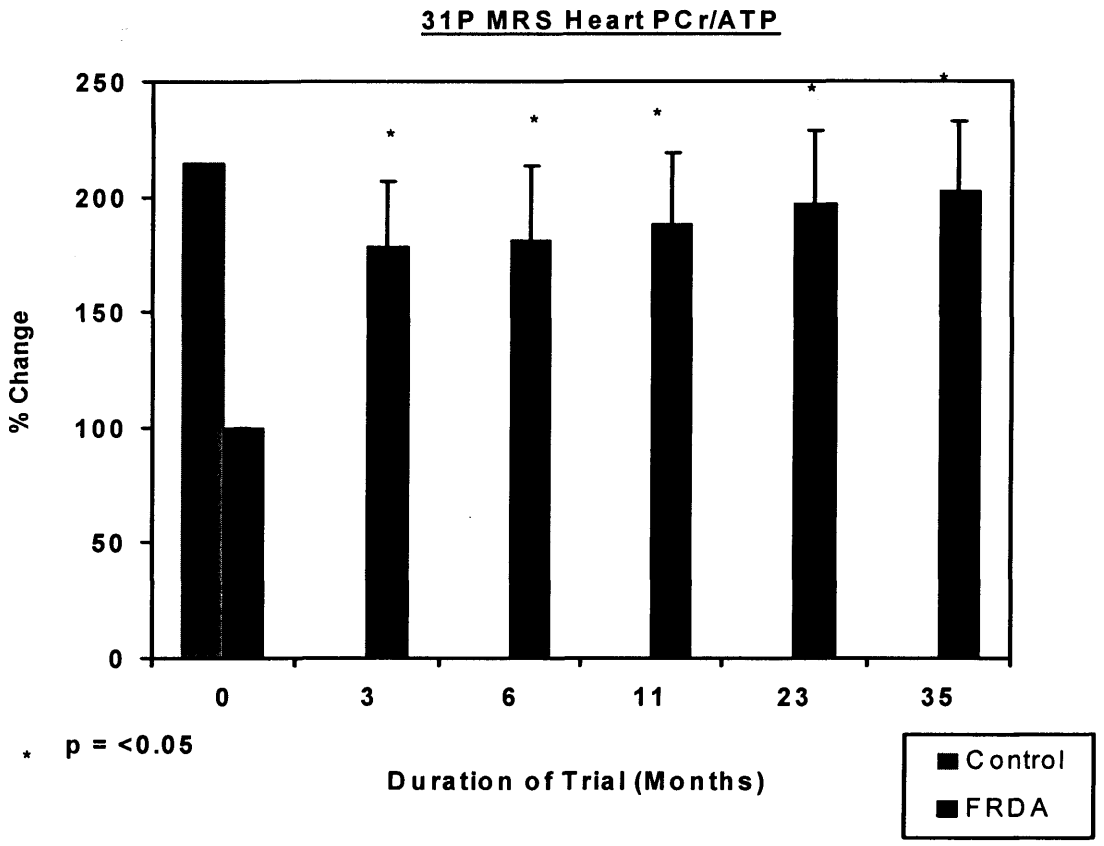

Figure 6.5 Percentage change (where 100% = baseline level in FRDA patients) and standard error in 31P MRS heart PCr/ATP (upper graph) and 31P skeletal muscle Vmax (lower graph) over 35 months of combined coenzyme Q10 and Vitamin E therapy in 10 FRDA patients. (* = p <0.05)

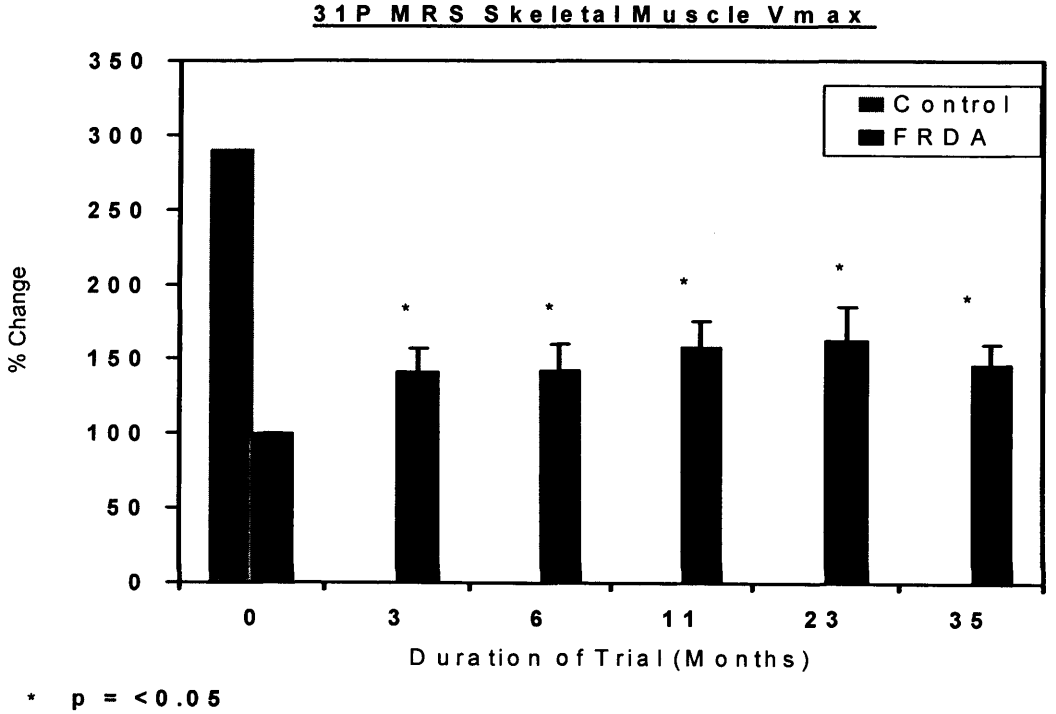

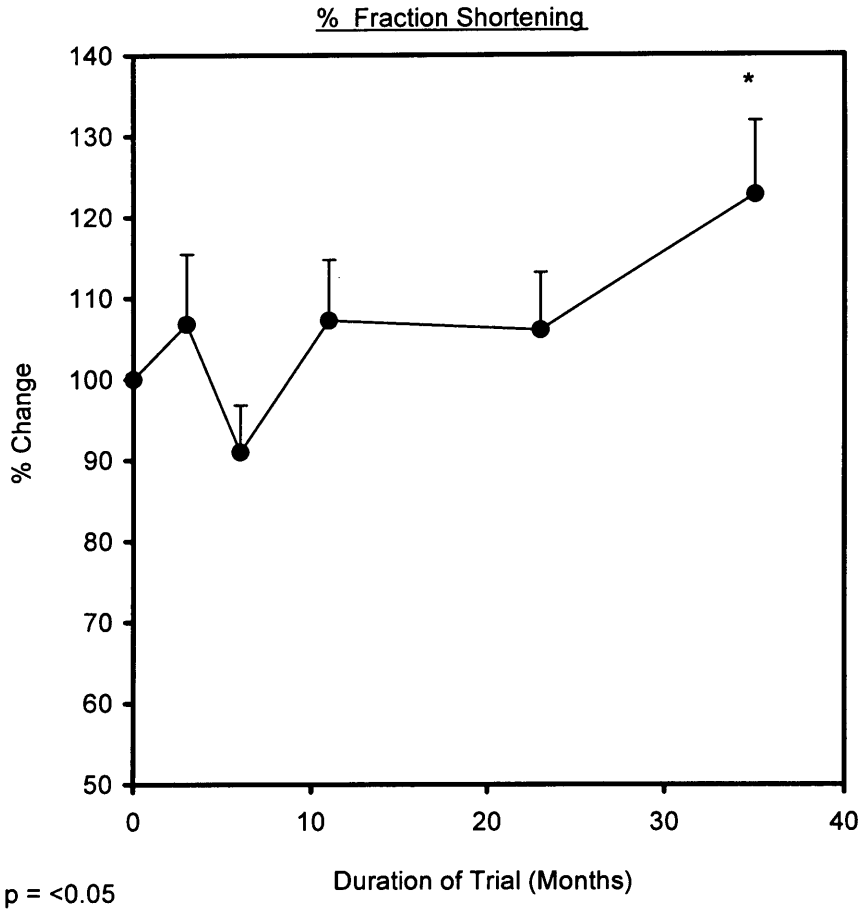

Figure 6.6

Percentage change (where 100% implies no change) and standard error in fraction shortening over 35 months of combined coenzyme Q10 and Vitamin E therapy in 10 FRDA patients. (* = p <0.05)

A
Total ICARS

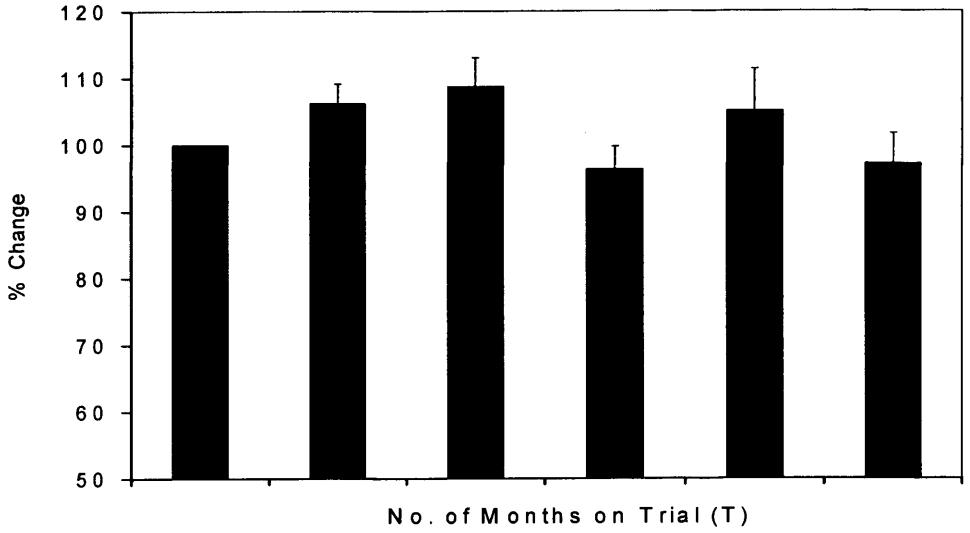

B
Posture
+ Gait

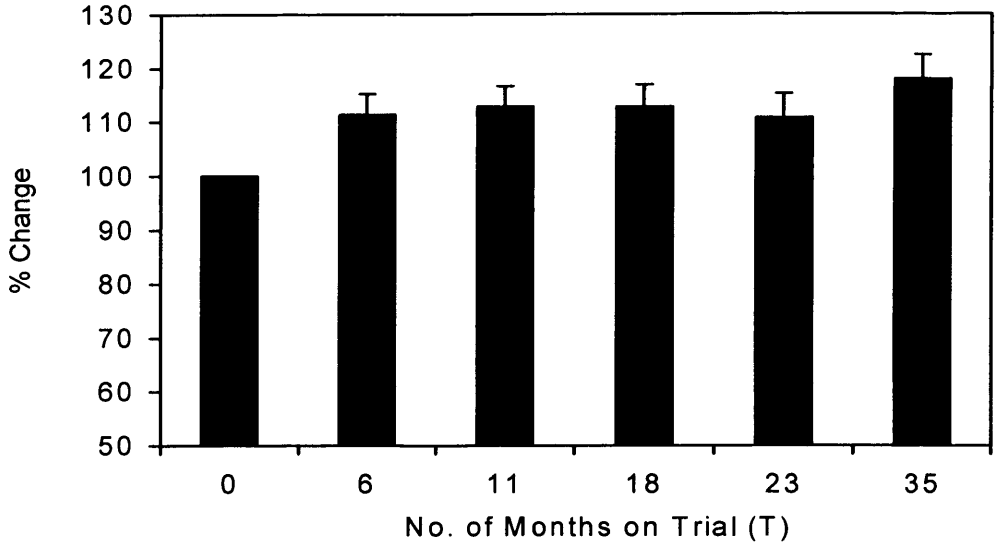

C
Kinetic

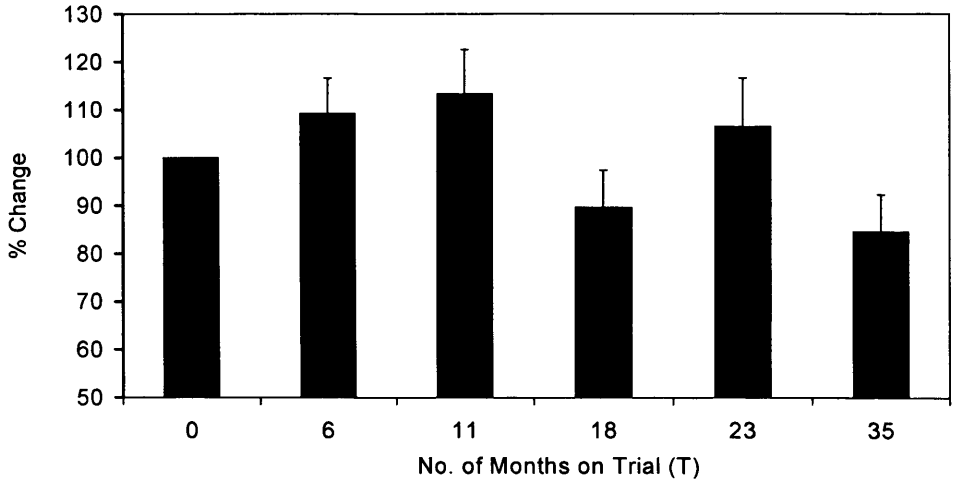

Figure 6.7 Percentage change (100% implies no change) and standard error in A) Total ICARS score, B) Posture and Gait component score, and C) Kinetic component score in 10 FRDA patients treated with combined coenzyme Q10 and Vitamin E therapy over 35 months.

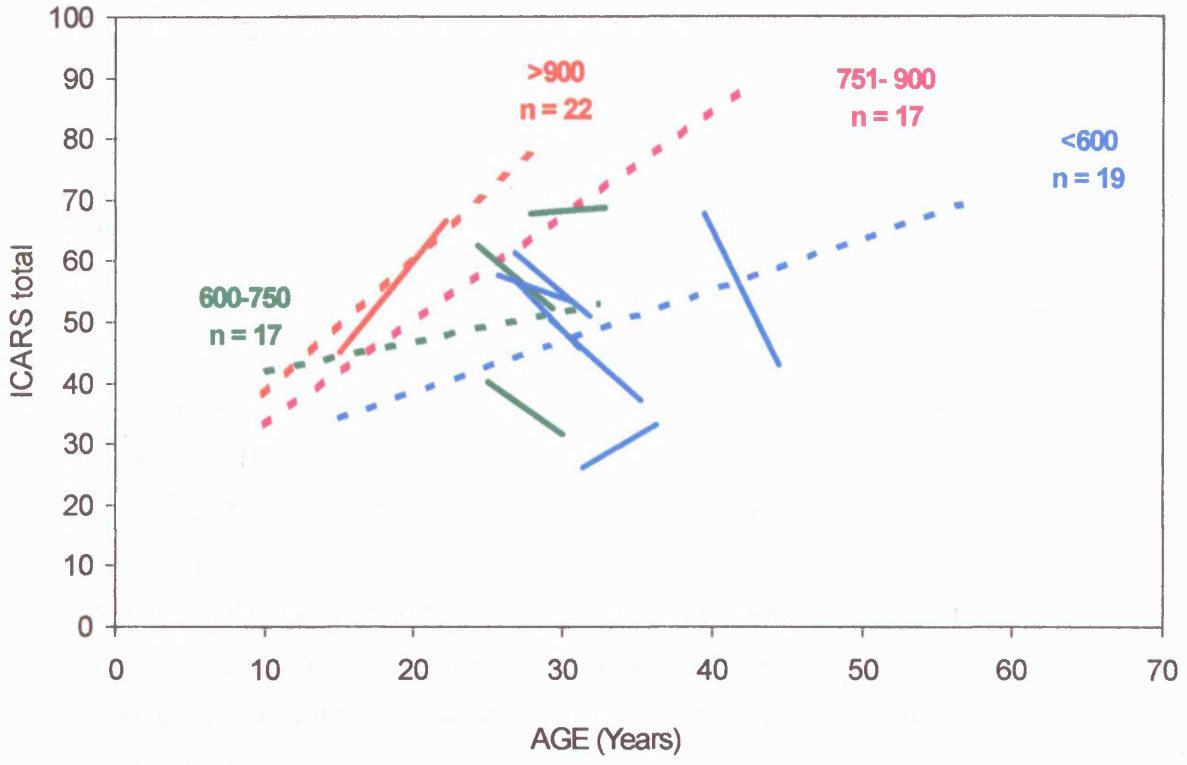

Figure 6.8

Comparison of the progression of the total ICARS score for 10 FRDA patients treated for 35 months with combined coenzyme Q10 and vitamin E, with cross-sectional data obtained from 75 untreated FRDA patients. Patients and cross-sectional groups ar clour coordinated according to GAA1 repeat size. (red = >900; purple = 751-900; green = 600-750; blue = < 600).

6.4.4 Discussion

The vitamin E and coenzyme Q_{10} doses used in this study were well tolerated, and are similar to those administered to patients with other neurodegenerative disorders where likewise no side effects were reported [709,710]. Both drugs localise to cellular membranes, including mitochondrial membranes, and act as free radical scavengers in addition to the role of coenzyme Q_{10} in electron transfer. The two antioxidants were combined to amplify their efficacy.

This pilot study demonstrated that antioxidant therapy in FRDA can improve surrogate bioenergetic parameters after six months therapy, and that this improvement is maintained over a prolonged period of time. The more marked bioenergetic improvement after therapy found in cardiac compared to skeletal muscle may reflect a higher dependence on frataxin and greater accumulation of iron and free radical mitochondrial damage in FRDA heart. The greater degree of PCr/ATP improvement in patients without LVH than those with LVH may indicate that the presence of LVH reduces the rate of bioenergetic recovery and that antioxidant therapy may be more effective if started before cardiomyopathy becomes established. Indeed, if the bioenergetic deficit precedes cardiac hypertrophy, then the early initiation of antioxidant therapy in FRDA may prevent the development of cardiac hypertrophy by reversing the bioenergetic abnormality. In addition to these improvements of surrogate markers, prolonged therapy was associated with a significant improvement in heart function as measured by fraction shortening. This latter finding is important because cardiac disease is often the life-limiting factor in FRDA.

Clinical progression of the disease however, as judged by ICARS and its component scores, did not change significantly over the course of the trial. It may be however that the treatment only served to slow the expected rate of progression of the disease rather than to cause improvement from baseline. In order to assess this the total ICARS score over 35 months for each of the ten individuals in the trial was compared with expected disease progression as generated by cross-sectional data. This analysis implied that eight

patients were deteriorating less rapidly than would have been expected. The validity of using cross sectional data to predict disease progression remains uncertain.

Based upon the results of this pilot study a double blind placebo controlled trial of combined coenzyme Q_{10} and vitamin E in FRDA is currently underway.

REFERENCE LIST

1. Anderson, S. *et al.* Sequence and organization of the human mitochondrial genome. *Nature* 290, 457-465 (1981).

2. Wolstenholme, D. R. Animal mitochondrial DNA: structure and evolution. *Int.Rev.Cytol.* 141, 173-216 (1992).

3. Mitchell, P. Keilin's respiratory chain concept and its chemiosmotic consequences. *Science* 206, 1148-1159 (1979).

4. Hatefi, Y. The mitochondrial electron transport and oxidative phosphorylation system. *Annu.Rev.Biochem.* 54, 1015-1069 (1985).

5. Herrmann, J. M. & Neupert, W. What fuels polypeptide translocation? An energetical view on mitochondrial protein sorting. *Biochim.Biophys.Acta* 1459, 331-338 (2000).

6. Stryer, L. Oxidative Phosphorylation in *Biochemistry* 529-558. Freeman, (1995).

7. Lenaz, G. *et al.* The function of coenzyme Q in mitochondria. *Clin.Investig.* 71, S66-S70 (1993).

8. Olson, R. E. & Rudney, H. Biosynthesis of ubiquinone. *Vitam.Horm.* 40, 1-43 (1983).

9. Taanman, J. W. & Williams, S. L. Structure and function of the mitochondrial oxidative phosphorylation system. in *Mitochondrial disorders in neurology 2.* 1-34. Butterworth-Heinemann, Boston (2002).

10. Boyer, P. D. A perspective of the binding change mechanism for ATP synthesis. *FASEB J.* 3, 2164-2178 (1989).

11. Schon, E. A., Hirano, M., & Di Mauro, S. Molecular genetic basis of the mitochondrial encephalomyopathies in *Mitochondrial disorders in neurology 2* 69-114. Butterworth-Heinemann, Boston (2002).

12. Chomyn, A. *et al.* Six unidentified reading frames of human mitochondrial DNA encode components of the respiratory-chain NADH dehydrogenase. *Nature* 314, 592-597 (1985).

13. Chomyn, A. *et al.* URF6, last unidentified reading frame of human mtDNA, codes for an NADH dehydrogenase subunit. *Science* 234, 614-618 (1986).

14. Ojala, D., Montoya, J., & Attardi, G. tRNA punctuation model of RNA processing in human mitochondria. *Nature* 290, 470-474 (1981).

15. Montoya, J., Christianson, T., Levens, D., Rabinowitz, M., & Attardi, G. Identification of initiation sites for heavy-strand and light-strand transcription in human mitochondrial DNA. *Proc.Natl.Acad.Sci.U.S.A* 79, 7195-7199 (1982).

16. Fisher, R. P., Topper, J. N., & Clayton, D. A. Promoter selection in human mitochondria involves binding of a transcription factor to orientation-independent upstream regulatory elements. *Cell* 50, 247-258 (1987).

17. Ghivizzani, S. C., Madsen, C. S., Nelen, M. R., Ammini, C. V., & Hauswirth, W. W. In organello footprint analysis of human mitochondrial DNA: human mitochondrial transcription factor A interactions at the origin of replication. *Mol.Cell Biol.* 14, 7717-7730 (1994).

18. Antoshechkin, I., Bogenhagen, D. F., & Mastrangelo, I. A. The HMG-box mitochondrial transcription factor xl-mtTFA binds DNA as a tetramer to activate bidirectional transcription. *EMBO J.* 16, 3198-3206 (1997).

19. Larsson, N. G. *et al.* Mitochondrial transcription factor A is necessary for mtDNA maintenance and embryogenesis in mice. *Nat.Genet.* 18, 231-236 (1998).

20. McCulloch, V., Seidel-Rogol, B. L., & Shadel, G. S. A human mitochondrial transcription factor is related to RNA adenine methyltransferases and binds S-adenosylmethionine. *Mol.Cell Biol.* 22, 1116-1125 (2002).

21. Murphy, W. I., Attardi, B., Tu, C., & Attardi, G. Evidence for complete symmetrical transcription in vivo of mitochondrial DNA in HeLa cells. *J.Mol.Biol.* 99, 809-814 (1975).

22. Shang, J. & Clayton, D. A. Human mitochondrial transcription termination exhibits RNA polymerase independence and biased bipolarity in vitro. *J.Biol.Chem.* 269, 29112-29120 (1994).

23. Fernandez-Silva, P., Martinez-Azorin, F., Micol, V., & Attardi, G. The human mitochondrial transcription termination factor (mTERF) is a multizipper protein but binds to DNA as a monomer, with evidence pointing to intramolecular leucine zipper interactions. *EMBO J.* 16, 1066-1079 (1997).

24. Christianson, T. W. & Clayton, D. A. In vitro transcription of human mitochondrial DNA: accurate termination requires a region of DNA sequence that can function bidirectionally. *Proc.Natl.Acad.Sci.U.S.A* 83, 6277-6281 (1986).

25. Van Etten, R. A., Bird, J. W., & Clayton, D. A. Identification of the 3'-ends of the two mouse mitochondrial ribosomal RNAs. The 3'-end of 16 S ribosomal RNA contains nucleotides encoded by the gene for transfer RNALeuUUR. *J.Biol.Chem.* 258, 10104-10110 (1983).

26. Levinger, L., Jacobs, O., & James, M. In vitro 3'-end endonucleolytic processing defect in a human mitochondrial tRNA(Ser(UCN)) precursor with the U7445C substitution, which causes non-syndromic deafness. *Nucleic Acids Res.* 29, 4334-4340 (2001).

27. Reichert, A., Rothbauer, U., & Morl, M. Processing and editing of overlapping tRNAs in human mitochondria. *J.Biol.Chem.* 273, 31977-31984 (1998).

28. Helm, M., Giege, R., & Florentz, C. A Watson-Crick base-pair-disrupting methyl group (m1A9) is sufficient for cloverleaf folding of human mitochondrial tRNALys. *Biochemistry* 38, 13338-13346 (1999).

29. Yasukawa, T., Suzuki, T., Ishii, N., Ohta, S., & Watanabe, K. Wobble modification defect in tRNA disturbs codon-anticodon interaction in a mitochondrial disease. *EMBO J.* 20, 4794-4802 (2001).

30. Nagaike, T. *et al.* Identification and characterization of mammalian mitochondrial tRNA nucleotidyltransferases. *J.Biol.Chem.* 276, 40041-40049 (2001).

31. Bullard, J. M., Cai, Y. C., & Spremulli, L. L. Expression and characterization of the human mitochondrial leucyl-tRNA synthetase. *Biochim.Biophys.Acta* 1490, 245-258 (2000).

32. Bonner, D. S., Wiley, J. E., & Farwell, M. A. Assignment1 of the mitochondrial translational initiation factor 2 gene (MTIF2) to human chromosome 2 bands p16->p14 by in situ hybridization and with somatic cell hybrids. *Cytogenet.Cell Genet.* 83, 80-81 (1998).

33. Ma, J. & Spremulli, L. L. Expression, purification, and mechanistic studies of bovine mitochondrial translational initiation factor 2. *J Biol.Chem.* 271, 5805-5811 (1996).

34. Liu, M. & Spremulli, L. Interaction of mammalian mitochondrial ribosomes with the inner membrane. *J.Biol.Chem.* 275, 29400-29406 (2000).

35. Koc, E. C. *et al.* Identification of four proteins from the small subunit of the mammalian mitochondrial ribosome using a proteomics approach. *Protein Sci.* 10, 471-481 (2001).

36. Koc, E. C. *et al.* The large subunit of the mammalian mitochondrial ribosome. Analysis of the complement of ribosomal proteins present. *J Biol.Chem.* 276, 43958-43969 (2001).

37. Cavdar, K. E. *et al.* A new face on apoptosis: death-associated protein 3 and PDCD9 are mitochondrial ribosomal proteins. *FEBS Lett.* 492, 166-170 (2001).

38. Suzuki, T. *et al.* Proteomic analysis of the mammalian mitochondrial ribosome. Identification of protein components in the 28 S small subunit. *J.Biol.Chem.* 276, 33181-33195 (2001).

39. Cantatore, P. *et al.* Synthesis and turnover rates of four rat liver mitochondrial RNA species. *FEBS Lett.* 213, 144-148 (1987).

40. Hammarsund, M. *et al.* Identification and characterization of two novel human mitochondrial elongation factor genes, hEFG2 and hEFG1, phylogenetically conserved through evolution. *Hum.Genet.* 109, 542-550 (2001).

41. Ling, M. *et al.* The human mitochondrial elongation factor tu (EF-Tu) gene: cDNA sequence, genomic localization, genomic structure, and identification of a pseudogene. *Gene* 197, 325-336 (1997).

42. Vernon, J. L., Burr, P. C., Wiley, J. E., & Farwell, M. A. Assignment of the mitochondrial translation elongation factor Ts gene (TSFM) to human chromosome 12 bands q13-->q14 by in situ hybridization and with somatic cell hybrids. *Cytogenet.Cell Genet.* 89, 145-146 (2000).

43. Nierhaus, K. H. Protein synthesis. An elongation factor turn-on. *Nature* 379, 491-492 (1996).

44. Nakamura, Y., Ito, K., & Isaksson, L. A. Emerging understanding of translation termination. *Cell* 87, 147-150 (1996).

45. Hansen, L. L., Jorgensen, R., & Justesen, J. Assignment of the human mitochondrial translational release factor 1 (MTRF1) to chromosome 13q14.1-->q14.3 and of the human mitochondrial ribosome recycling factor (MRRF) to chromosome 9q32-->q34.1 with radiation hybrid mapping. *Cytogenet.Cell Genet.* 88, 91-92 (2000).

46. Zhang, Y. & Spremulli, L. L. Identification and cloning of human mitochondrial translational release factor 1 and the ribosome recycling factor. *Biochim.Biophys.Acta* 1443, 245-250 (1998).

47. Sprinzl, M., Horn, C., Brown, M., Ioudovitch, A., & Steinberg, S. Compilation of tRNA sequences and sequences of tRNA genes. *Nucleic Acids Res.* 26, 148-153 (1998).

48. Dirheimer, G., Baranowski, W., & Keith, G. Variations in tRNA modifications, particularly of their queuine content in higher eukaryotes. Its relation to malignancy grading. *Biochimie* 77, 99-103 (1995).

49. Martin, F., Eriani, G., Reinbolt, J., Dirheimer, G., & Gangloff, J. Genetic selection for active E.coli amber tRNA(Asn) exclusively led to glutamine inserting suppressors. *Nucleic Acids Res.* 23, 779-784 (1995).

50. Holley, R. W. Structure of an alanine transfer ribonucleic acid. *JAMA* 194, 868-871 (1965).

51. Robertus, J. D. *et al.* Structure of yeast phenylalanine tRNA at 3 A resolution. *Nature* 250, 546-551 (1974).

52. Ryan, K. R. & Jensen, R. E. Protein translocation across mitochondrial membranes: what a long, strange trip it is. *Cell* 83, 517-519 (1995).

53. Paschen, S. A. & Neupert, W. Protein import into mitochondria. *IUBMB.Life* 52, 101-112 (2001).

54. Neupert, W. Protein import into mitochondria. *Annu.Rev.Biochem.* 66, 863-917 (1997).

55. Nass, M. M. Abnormal DNA patterns in animal mitochondria: ethidium bromide-induced breakdown of closed circular DNA and conditions leading to oligomer accumulation. *Proc.Natl.Acad.Sci.U.S.A* 67, 1926-1933 (1970).

56. Nass, M. M. Differential effects of ethidium bromide on mitochondrial and nuclear DNA synthesis in vivo in cultured mammalian cells. *Exp.Cell Res.* 72, 211-222 (1972).

57. Anderson, T. D. *et al.* Mitochondrial schwannopathy and peripheral myelinopathy in a rabbit model of dideoxycytidine neurotoxicity. *Lab Invest* 70, 724-739 (1994).

58. Wang, H. *et al.* Zidovudine and dideoxynucleosides deplete wild-type mitochondrial DNA levels and increase deleted mitochondrial DNA levels in cultured Kearns-Sayre syndrome fibroblasts. *Biochim.Biophys.Acta* 1316, 51-59 (1996).

59. King, M. P. & Attardi, G. Isolation of human cell lines lacking mitochondrial DNA. *Methods Enzymol.* 264, 304-313 (1996).

60. Gregoire, M., Morais, R., Quilliam, M. A., & Gravel, D. On auxotrophy for pyrimidines of respiration-deficient chick embryo cells. *Eur.J Biochem.* 142, 49-55 (1984).

61. King, M. P. & Attardi, G. Human cells lacking mtDNA: repopulation with exogenous mitochondria by complementation. *Science* 246, 500-503 (1989).

62. Poste, G. & Reeve, P. Formation of hybrid cells and heterokaryons by fusion of enucleated and nucleated cells. *Nat.New Biol.* 229, 123-125 (1971).

63. Poste, G. & Reeve, P. Enucleation of mammalian cells by cytochalasin B. II. Formation of hybrid cells and heterokaryons by fusion of anucleate and nucleated cells. *Exp.Cell Res.* 73, 287-294 (1972).

64. Veomett, G., Prescott, D. M., Shay, J., & Porter, K. R. Reconstruction of mammalian cells from nuclear and cytoplasmic components separated by treatment with cytochalasin B. *Proc.Natl.Acad.Sci.U.S.A* 71, 1999-2002 (1974).

65. Chomyn, A. *et al.* Platelet-mediated transformation of mtDNA-less human cells: analysis of phenotypic variability among clones from normal individuals--and complementation behavior of the tRNALys mutation causing myoclonic epilepsy and ragged red fibers. *Am.J Hum.Genet.* 54, 966-974 (1994).

66. King, M. P., Koga, Y., Davidson, M., & Schon, E. A. Defects in mitochondrial protein synthesis and respiratory chain activity segregate with the tRNA(Leu(UUR)) mutation associated with mitochondrial myopathy, encephalopathy, lactic acidosis, and strokelike episodes. *Mol.Cell Biol.* 12, 480-490 (1992).

67. Chomyn, A. *et al.* In vitro genetic transfer of protein synthesis and respiration defects to mitochondrial DNA-less cells with myopathy-patient mitochondria. *Mol.Cell Biol.* 11, 2236-2244 (1991).

68. Chomyn, A. *et al.* MELAS mutation in mtDNA binding site for transcription termination factor causes defects in protein synthesis and in respiration but no

change in levels of upstream and downstream mature transcripts. *Proc.Natl.Acad.Sci.U.S.A* 89, 4221-4225 (1992).

69. Dunbar, D. R., Moonie, P. A., Zeviani, M., & Holt, I. J. Complex I deficiency is associated with 3243G:C mitochondrial DNA in osteosarcoma cell cybrids. *Hum.Mol.Genet.* 5, 123-129 (1996).

70. Bodnar, A. G., Cooper, J. M., Holt, I. J., Leonard, J. V., & Schapira, A. H. Nuclear complementation restores mtDNA levels in cultured cells from a patient with mtDNA depletion. *Am.J.Hum.Genet.* 53, 663-669 (1993).

71. Tiranti, V. *et al.* Nuclear DNA origin of cytochrome c oxidase deficiency in Leigh's syndrome: genetic evidence based on patient's-derived rho degrees transformants. *Hum.Mol.Genet.* 4, 2017-2023 (1995).

72. DiMauro, S. & Schon, E. A. Mitochondrial respiratory-chain diseases. *N.Engl.J Med.* 348, 2656-2668 (2003).

73. Allen, J. F. & Raven, J. A. Free-radical-induced mutation vs redox regulation: costs and benefits of genes in organelles. *J Mol.Evol.* 42 , 482-492 (1996).

74. Pesole, G., Gissi, C., De Chirico, A., & Saccone, C. Nucleotide substitution rate of mammalian mitochondrial genomes. *J Mol.Evol.* 48, 427-434 (1999).

75. Loeffen, J. L. *et al.* Isolated complex I deficiency in children: clinical, biochemical and genetic aspects. *Hum.Mutat.* 15, 123-134 (2000).

76. Shoffner, J. M. Maternal inheritance and the evaluation of oxidative phosphorylation diseases. *Lancet* 348, 1283-1288 (1996).

77. Bourgeron, T. *et al.* Mutation of a nuclear succinate dehydrogenase gene results in mitochondrial respiratory chain deficiency. *Nat.Genet.* 11, 144-149 (1995).

78. Benit, P. *et al.* Large-scale deletion and point mutations of the nuclear NDUFV1 and NDUFS1 genes in mitochondrial complex I deficiency. *Am.J.Hum.Genet.* 68, 1344-1352 (2001).

79. Budde, S. M. *et al.* Combined enzymatic complex I and III deficiency associated with mutations in the nuclear encoded NDUFS4 gene. *Biochem.Biophys.Res.Commun.* 275, 63-68 (2000).

80. Loeffen, J. *et al.* The first nuclear-encoded complex I mutation in a patient with Leigh syndrome. *Am.J.Hum.Genet.* 63, 1598-1608 (1998).

81. Loeffen, J. *et al.* Mutations in the complex I NDUFS2 gene of patients with cardiomyopathy and encephalomyopathy. *Ann.Neurol.* 49, 195-201 (2001).

82. Petruzzella, V. *et al.* A nonsense mutation in the NDUFS4 gene encoding the 18 kDa (AQDQ) subunit of complex I abolishes assembly and activity of the complex in a patient with Leigh-like syndrome. *Hum.Mol.Genet.* 10, 529-535 (2001).

83. Schuelke, M. *et al.* Mutant NDUFV1 subunit of mitochondrial complex I causes leukodystrophy and myoclonic epilepsy. *Nat.Genet.* 21, 260-261 (1999).

84. Triepels, R. H. *et al.* Leigh syndrome associated with a mutation in the NDUFS7 (PSST) nuclear encoded subunit of complex I. *Ann.Neurol.* 45, 787-790 (1999).

85. van den, H. L. *et al.* Demonstration of a new pathogenic mutation in human complex I deficiency: a 5-bp duplication in the nuclear gene encoding the 18-kD (AQDQ) subunit. *Am.J.Hum.Genet.* 62, 262-268 (1998).

86. Birch-Machin, M. A., Taylor, R. W., Cochran, B., Ackrell, B. A., & Turnbull, D. M. Late-onset optic atrophy, ataxia, and myopathy associated with a mutation of a complex II gene. *Ann.Neurol.* 48, 330-335 (2000).

87. Parfait, B. *et al.* Compound heterozygous mutations in the flavoprotein gene of the respiratory chain complex II in a patient with Leigh syndrome. *Hum.Genet.* 106, 236-243 (2000).

88. Baysal, B. E. *et al.* Mutations in SDHD, a mitochondrial complex II gene, in hereditary paraganglioma. *Science* 287, 848-851 (2000).

89. Niemann, S. & Muller, U. Mutations in SDHC cause autosomal dominant paraganglioma, type 3. *Nat.Genet.* 26, 268-270 (2000).

90. Gimm, O., Armanios, M., Dziema, H., Neumann, H. P., & Eng, C. Somatic and occult germ-line mutations in SDHD, a mitochondrial complex II gene, in nonfamilial pheochromocytoma. *Cancer Res.* 60, 6822-6825 (2000).

91. Ogasahara, S., Engel, A. G., Frens, D., & Mack, D. Muscle coenzyme Q deficiency in familial mitochondrial encephalomyopathy. *Proc.Natl.Acad.Sci.U.S.A* 86, 2379-2382 (1989).

92. Boitier, E. *et al.* A case of mitochondrial encephalomyopathy associated with a muscle coenzyme Q10 deficiency. *J.Neurol.Sci.* 156, 41-46 (1998).

93. Musumeci, O. *et al.* Familial cerebellar ataxia with muscle coenzyme Q10 deficiency. *Neurology* 56, 849-855 (2001).

94. Sobreira, C. *et al.* Mitochondrial encephalomyopathy with coenzyme Q10 deficiency. *Neurology* 48, 1238-1243 (1997).

95. Grivell, L. A. *et al.* Mitochondrial assembly in yeast. *FEBS Lett.* 452, 57-60 (1999).

96. Koehler, C. M. *et al.* Human deafness dystonia syndrome is a mitochondrial disease. *Proc.Natl.Acad.Sci.U.S.A* 96, 2141-2146 (1999).

97. Shoubridge, E. A. Mitochondrial DNA segregation in the developing embryo. *Hum.Reprod.* 15 Suppl 2, 229-234 (2000).

98. Birky, C. W., Jr. The inheritance of genes in mitochondria and chloroplasts: laws, mechanisms, and models. *Annu.Rev.Genet.* 35, 125-148 (2001).

99. Hutchison, C. A., III, Newbold, J. E., Potter, S. S., & Edgell, M. H. Maternal inheritance of mammalian mitochondrial DNA. *Nature* 251, 536-538 (1974).

100. Shoubridge, E. A. Mitochondrial DNA segregation in the developing embryo. *Hum.Reprod.* 15 Suppl 2, 229-234 (2000).

101. Gyllensten, U., Wharton, D., Josefsson, A., & Wilson, A. C. Paternal inheritance of mitochondrial DNA in mice see comments]. *Nature* 352 , 255-257 (1991).

102. Robin, E. D. & Wong, R. Mitochondrial DNA molecules and virtual number of mitochondria per cell in mammalian cells. *J.Cell Physiol* 136, 507-513 (1988).

103. Man, P. Y., Turnbull, D. M., & Chinnery, P. F. Leber hereditary optic neuropathy. *J Med.Genet.* 39, 162-169 (2002).

104. McFarland, R. *et al.* Multiple neonatal deaths due to a homoplasmic mitochondrial DNA mutation. *Nat.Genet.* 30 , 145-146 (2002).

105. Boulet, L., Karpati, G., & Shoubridge, E. A. Distribution and threshold expression of the tRNA(Lys) mutation in skeletal muscle of patients with myoclonic epilepsy and ragged-red fibers (MERRF). *Am.J Hum.Genet.* 51, 1187-1200 (1992).

106. Chomyn, A. *et al.* In vitro genetic transfer of protein synthesis and respiration defects to mitochondrial DNA-less cells with myopathy-patient mitochondria. *Mol.Cell Biol.* 11, 2236-2244 (1991).

107. Kobayashi, Y. *et al.* The mutant mitochondrial genes in mitochondrial myopathy, encephalopathy, lactic acidosis and stroke-like episodes (MELAS) were selectively amplified through generations. *J.Inherit.Metab Dis.* 15, 803-808 (1992).

108. Ciafaloni, E. *et al.* Widespread tissue distribution of a tRNALeu(UUR) mutation in the mitochondrial DNA of a patient with MELAS syndrome. *Neurology* 41, 1663-1664 (1991).

109. Holt, I. J., Harding, A. E., Petty, R. K., & Morgan-Hughes, J. A. A new mitochondrial disease associated with mitochondrial DNA heteroplasmy. *Am.J.Hum.Genet.* 46, 428-433 (1990).

110. Macmillan, C., Lach, B., & Shoubridge, E. A. Variable distribution of mutanT mitochondrial DNAs (tRNA(Leu[3243])) in tissues of symptomatic relatives with MELAS: the role of mitotic segregation. *Neurology* 43, 1586-1590 (1993).

111. Campos, Y. *et al.* Clinical heterogeneity in two pedigrees with the 3243 bp tRNA(Leu(UUR)) mutation of mitochondrial DNA. *Acta Neurol Scand.* 91, 62-65 (1995).

112. Liou, C. W. *et al.* MELAS syndrome: correlation between clinical features and molecular genetic analysis. *Acta Neurol.Scand.* 90, 354-359 (1994).

113. Martinuzzi, A. *et al.* Correlation between clinical and molecular features in two MELAS families. *J.Neurol.Sci.* 113, 222-229 (1992).

114. Shiraiwa, N. *et al.* Content of mutant mitochondrial DNA and organ dysfunction in a patient with a MELAS subgroup of mitochondrial encephalomyopathies. *J.Neurol.Sci.* 120, 174-179 (1993).

115. Hammans, S. R. *et al.* The mitochondrial DNA transfer RNALeu(UUR) A-->G(3243) mutation. A clinical and genetic study. *Brain* 118 (Pt 3), 721-734 (1995).

116. Sparaco, M., Bonilla, E., DiMauro, S., & Powers, J. M. Neuropathology of mitochondrial encephalomyopathies due to mitochondrial DNA defects. *J Neuropathol.Exp.Neurol* 52, 1-10 (1993).

117. Tanno, Y. *et al.* Uniform tissue distribution of tRNA(Lys) mutation in mitochondrial DNA in MERRF patients. *Neurology* 43, 1198-1200 (1993).

118. Schon, E. A., Bonilla, E., & DiMauro, S. Mitochondrial DNA mutations and pathogenesis. *J.Bioenerg.Biomembr.* 29, 131-149 (1997).

119. Chen, X. *et al.* Rearranged mitochondrial genomes are present in human oocytes. *Am.J.Hum.Genet.* 57, 239-247 (1995).

120. Ashley, M. V., Laipis, P. J., & Hauswirth, W. W. Rapid segregation of heteroplasmic bovine mitochondria. *Nucleic Acids Res.* 17, 7325-7331 (1989).

121. Pulkes, T., Sweeney, M. G., & Hanna, M. G. Increased risk of stroke in patients with the A12308G polymorphism in mitochondria. *Lancet* 356, 2068-2069 (2000).

122. El Meziane, A. *et al.* A tRNA suppressor mutation in human mitochondria. *Nat.Genet.* 18, 350-353 (1998).

123. Leonard, J. V. & Schapira, A. H. Mitochondrial respiratory chain disorders I: mitochondrial DNA defects. *Lancet* 355, 299-304 (2000).

124. Leonard, J. V. & Schapira, A. H. Mitochondrial respiratory chain disorders II: neurodegenerative disorders and nuclear gene defects. *Lancet* 355, 389-394 (2000).

125. Majamaa, K. *et al.* Epidemiology of A3243G, the mutation for mitochondrial encephalomyopathy, lactic acidosis, and strokelike episodes: prevalence of the mutation in an adult population. *Am.J.Hum.Genet.* 63, 447-454 (1998).

126. Chinnery, P. F. *et al.* The epidemiology of pathogenic mitochondrial DNA mutations. *Ann.Neurol.* 48, 188-193 (2000).

127. Gerbitz, K. D., van Den Ouweland, J. M., Maassen, J. A., & Jaksch, M. Mitochondrial diabetes mellitus: a review. *Biochim.Biophys.Acta* 1271, 253-260 (1995).

128. Maassen, J. A. & Kadowaki, T. Maternally inherited diabetes and deafness: a new diabetes subtype. *Diabetologia* 39, 375-382 (1996).

129. Luft, R., Ikkos, D., Palmieri, G., & et al. A case of severe hypermetabolism of nonthyroid origin with a defect in the maintenance of mitochondrial respiratory control; a correlated clinical, biochemical, and morphological study. *J Clin Invest* 41, 1776-1804 (1962).

130. DiMauro, S. *et al.* Luft's disease. Further biochemical and ultrastructural studies of skeletal muscle in the second case. *J.Neurol.Sci.* 27, 217-232 (1976).

131. Morgan-Hughes, J. A. *et al.* Mitochondrial encephalomyopathies: biochemical studies in two cases revealing defects in the respiratory chain. *Brain* 105 (Pt 3), 553-582 (1982).

132. Morgan-Hughes, J. A. & Mair, W. G. Atypical muscle mitochondria in oculoskeletal myopathy. *Brain* 96, 215-224 (1973).

133. Olson, W., Engel, W. K., Walsh, G. O., & Einaugler, R. Oculocraniosomatic neuromuscular disease with "ragged-red" fibers. *Arch Neurol.* 26, 193-211 (1972).

134. DiMauro, S., Bonilla, E., Zeviani, M., Nakagawa, M., & DeVivo, D. C. Mitochondrial myopathies. *Ann.Neurol.* 17, 521-538 (1985).

135. Fukuhara, N., Tokiguchi, S., Shirakawa, K., & Tsubaki, T. Myoclonus epilepsy associated with ragged-red fibres (mitochondrial abnormalities): disease entity or a syndrome? Light-and electron-microscopic studies of two cases and review of literature. *J.Neurol.Sci.* 47, 117-133 (1980).

136. Shapira, Y., Harel, S., & Russell, A. Mitochondrial encephalomyopathies: a group of neuromuscular disorders with defects in oxidative metabolism. *Isr.J.Med.Sci.* 13, 161-164 (1977).

137. Berenberg, R. A. *et al.* Lumping or splitting? "Ophthalmoplegia-plus" or Kearns-Sayre syndrome? *Ann.Neurol.* 1, 37-54 (1977).

138. Roberts, N. K., Perloff, J. K., & Kark, R. A. Cardiac conduction in the Kearns-Sayre syndrome (a neuromuscular disorder associated with progressive external ophthalmoplegia and pigmentary retinopathy). Report of 2 cases and review of 17 published cases. *Am.J.Cardiol.* 44, 1396-1400 (1979).

139. Petty, R. K., Harding, A. E., & Morgan-Hughes, J. A. The clinical features of mitochondrial myopathy. *Brain* 109 (Pt 5), 915-938 (1986).

140. Hammans, S. R., Sweeney, M. G., Brockington, M., Morgan-Hughes, J. A., & Harding, A. E. Mitochondrial encephalopathies: molecular genetic diagnosis from blood samples. *Lancet* 337, 1311-1313 (1991).

141. Rowland, L. P. *et al.* Clinical syndromes associated with ragged red fibers. *Rev.Neurol.(Paris)* 147, 467-473 (1991).

142. Truong, D. D. *et al.* Movement disorders in mitochondrial myopathies. A study of nine cases with two autopsy studies. *Mov Disord.* 5, 109-117 (1990).

143. Harvey, J. N. & Barnett, D. Endocrine dysfunction in Kearns-Sayre syndrome. *Clin.Endocrinol.(Oxf)* 37, 97-103 (1992).

144. Quade, A., Zierz, S., & Klingmuller, D. Endocrine abnormalities in mitochondrial myopathy with external ophthalmoplegia. *Clin.Investig.* 70, 396-402 (1992).

145. Holt, I. J., Harding, A. E., & Morgan-Hughes, J. A. Deletions of muscle mitochondrial DNA in patients with mitochondrial myopathies. *Nature* 331, 717-719 (1988).

146. Zeviani, M. *et al.* An autosomal dominant disorder with multiple deletions of mitochondrial DNA starting at the D-loop region. *Nature* 339, 309-311 (1989).

147. Moslemi, A. R., Melberg, A., Holme, E., & Oldfors, A. Clonal expansion of mitochondrial DNA with multiple deletions in autosomal dominant progressive external ophthalmoplegia. *Ann.Neurol.* 40, 707-713 (1996).

148. Schon, E. A. *et al.* A direct repeat is a hotspot for large-scale deletion of human mitochondrial DNA. *Science* 244, 346-349 (1989).

149. Moraes, C. T. *et al.* Mitochondrial DNA deletions in progressive external ophthalmoplegia and Kearns-Sayre syndrome. *N.Engl.J.Med.* 320, 1293-1299 (1989).

150. Ballinger, S. W. *et al.* Maternally transmitted diabetes and deafness associated with a 10.4 kb mitochondrial DNA deletion. *Nat.Genet.* 1, 11-15 (1992).

151. Bresolin, N. *et al.* Muscle mitochondrial DNA deletion and 31P-NMR spectroscopy alterations in a migraine patient. *J.Neurol.Sci.* 104, 182-189 (1991).

152. Zeviani, M. *et al.* Deletions of mitochondrial DNA in Kearns-Sayre syndrome. 1988. *Neurology* 51, 1525 (1998).

153. Mariotti, C. *et al.* Genotype to phenotype correlations in mitochondrial encephalomyopathies associated with the A3243G mutation of mitochondrial DNA. *J.Neurol.* 242, 304-312 (1995).

154. Servidei, S. *et al.* Dominantly inherited mitochondrial myopathy with multiple deletions of mitochondrial DNA: clinical, morphologic, and biochemical studies. *Neurology* 41, 1053-1059 (1991).

155. Kaukonen, J. *et al.* A third locus predisposing to multiple deletions of mtDNA in autosomal dominant progressive external ophthalmoplegia. *Am.J.Hum.Genet.* 65, 256-261 (1999).

156. Li, F. Y. *et al.* Mapping of autosomal dominant progressive external ophthalmoplegia to a 7-cM critical region on 10q24. *Neurology* 53, 1265-1271 (1999).

157. Suomalainen, A. *et al.* An autosomal locus predisposing to deletions of mitochondrial DNA. *Nat.Genet.* 9, 146-151 (1995).

158. Van Goethem, G., Dermaut, B., Lofgren, A., Martin, J. J., & Van Broeckhoven, C. Mutation of POLG is associated with progressive external ophthalmoplegia characterized by mtDNA deletions. *Nat.Genet.* 28, 211-212 (2001).

159. Kaukonen, J. *et al.* Role of adenine nucleotide translocator 1 in mtDNA maintenance. *Science* 289, 782-785 (2000).

160. Spelbrink, J. N. *et al.* Human mitochondrial DNA deletions associated with mutations in the gene encoding Twinkle, a phage T7 gene 4-like protein localized in mitochondria. *Nat.Genet.* 28, 223-231 (2001).

161. Van Goethem, G., Dermaut, B., Lofgren, A., Martin, J. J., & Van Broeckhoven, C. Mutation of POLG is associated with progressive external ophthalmoplegia characterized by mtDNA deletions. *Nat.Genet.* 28, 211-212 (2001).

162. Washington, M. T., Rosenberg, A. H., Griffin, K., Studier, F. W., & Patel, S. S. Biochemical analysis of mutant T7 primase/helicase proteins defective in DNA binding, nucleotide hydrolysis, and the coupling of hydrolysis with DNA unwinding. *J.Biol.Chem.* 271, 26825-26834 (1996).

163. Buroker, N. E. *et al.* Length heteroplasmy of sturgeon mitochondrial DNA: an illegitimate elongation model. *Genetics* 124, 157-163 (1990).

164. Shoffner, J. M. *et al.* Spontaneous Kearns-Sayre/chronic external ophthalmoplegia plus syndrome associated with a mitochondrial DNA deletion: a slip-replication model and metabolic therapy. *Proc.Natl.Acad.Sci.U.S.A* 86, 7952-7956 (1989).

165. Ohno, K. *et al.* Mitochondrial DNA deletions in inherited recurrent myoglobinuria. *Ann.Neurol.* 29, 364-369 (1991).

166. Blumenthal, D. T. *et al.* Myoclonus epilepsy with ragged red fibers and multiple mtDNA deletions. *Neurology* 50, 524-525 (1998).

167. Oldfors, A., Larsson, N. G., Lindberg, C., & Holme, E. Mitochondrial DNA deletions in inclusion body myositis. *Brain* 116 (Pt 2), 325-336 (1993).

168. Bohlega, S. *et al.* Multiple mitochondrial DNA deletions associated with autosomal recessive ophthalmoplegia and severe cardiomyopathy. *Neurology* 46, 1329-1334 (1996).

169. Fadic, R. *et al.* Sensory ataxic neuropathy as the presenting feature of a novel mitochondrial disease. *Neurology* 49, 239-245 (1997).

170. van Domburg, P. H. *et al.* Mitochondrial cytopathy presenting as hereditary sensory neuropathy with progressive external ophthalmoplegia, ataxia and fatal myoclonic epileptic status. *Brain* 119 (Pt 3), 997-1010 (1996).

171. Pavlakis, S. G., Phillips, P. C., DiMauro, S., De Vivo, D. C., & Rowland, L. P. Mitochondrial myopathy, encephalopathy, lactic acidosis, and strokelike episodes: a distinctive clinical syndrome. *Ann.Neurol.* 16, 481-488 (1984).

172. Koo, B. *et al.* Mitochondrial encephalomyopathy, lactic acidosis, stroke-like episodes (MELAS): clinical, radiological, pathological, and genetic observations. *Ann.Neurol.* 34, 25-32 (1993).

173. Sharfstein, S. R., Gordon, M. F., Libman, R. B., & Malkin, E. S. Adult-onset MELAS presenting as herpes encephalitis. *Arch Neurol.* 56, 241-243 (1999).

174. Truong, D. D. *et al.* Movement disorders in mitochondrial myopathies. A study of nine cases with two autopsy studies. *Mov Disord.* 5, 109-117 (1990).

175. Allard, J. C., Tilak, S., & Carter, A. P. CT and MR of MELAS syndrome. *AJNR Am.J.Neuroradiol.* 9, 1234-1238 (1988).

176. Hanna, M. G., Nelson, I. P., Morgan-Hughes, J. A., & Wood, N. W. MELAS: a new disease associated mitochondrial DNA mutation and evidence for further genetic heterogeneity. *J.Neurol.Neurosurg.Psychiatry* 65, 512-517 (1998).

177. Majamaa, K., Turkka, J., Karppa, M., Winqvist, S., & Hassinen, I. E. The common MELAS mutation A3243G in mitochondrial DNA among young patients with an occipital brain infarct. *Neurology* 49, 1331-1334 (1997).

178. Bogousslavsky, J., Regli, F., Maeder, P., Meuli, R., & Nader, J. The etiology of posterior circulation infarcts: a prospective study using magnetic resonance imaging and magnetic resonance angiography. *Neurology* 43, 1528-1533 (1993).

179. Ohama, E. *et al.* Mitochondrial angiopathy in cerebral blood vessels of mitochondrial encephalomyopathy. *Acta Neuropathol.(Berl)* 74, 226-233 (1987).

180. Kuriyama, M. *et al.* Mitochondrial encephalomyopathy with lactate-pyruvate elevation and brain infarctions. *Neurology* 34, 72-77 (1984).

181. Schlaug, G., Siewert, B., Benfield, A., Edelman, R. R., & Warach, S. Time course of the apparent diffusion coefficient (ADC) abnormality in human stroke. *Neurology* 49, 113-119 (1997).

182. Peng, N. J. *et al.* Increased cerebral blood flow in MELAS shown by Tc-99m HMPAO brain SPECT. *Neuroradiology* 42, 26-29 (2000).

183. Takahashi, S., Tohgi, H., Yonezawa, H., Obara, S., & Nagane, Y. Cerebral blood flow and oxygen metabolism before and after a stroke-like episode in patients with mitochondrial myopathy, encephalopathy, lactic acidosis and stroke-like episodes (MELAS). *J.Neurol.Sci.* 158, 58-64 (1998).

184. Love, S., Nicoll, J. A., & Kinrade, E. Sequencing and quantitative assessment of mutant and wild-type mitochondrial DNA in paraffin sections from cases of MELAS. *J.Pathol* 170, 9-14 (1993).

185. Shoji, Y., Sato, W., Hayasaka, K., & Takada, G. Tissue distribution of mutant mitochondrial DNA in mitochondrial myopathy, encephalopathy, lactic acidosis and stroke-like episodes (MELAS). *J.Inherit.Metab Dis.* 16, 27-30 (1993).

186. Chinnery, P. F., Howell, N., Lightowlers, R. N., & Turnbull, D. M. Molecular pathology of MELAS and MERRF. The relationship between mutation load and clinical phenotypes. *Brain* 120 (Pt 10), 1713-1721 (1997).

187. Shimomura, T. *et al.* Point mutation in platelet mitochondrial tRNA(Leu(UUR)) in patient with cluster headache. *Lancet* 344, 625 (1994).

188. Kishnani, P. S. *et al.* Acute pancreatitis in an infant with lactic acidosis and a mutation at nucleotide 3243 in the mitochondrial DNA tRNALeu(UUR) gene. *Eur.J.Pediatr.* 155, 898-903 (1996).

189. Kuroiwa, T. *et al.* Mitochondrial encephalomyopathy showing prominent microvacuolation and necrosis of intestinal smooth muscle cells: a case diagnosed by rectal biopsy. *Acta Neuropathol.(Berl)* 96, 86-90 (1998).

190. Vilarinho, L., Maia, C., Coelho, T., Coutinho, P., & Santorelli, F. M. Heterogeneous presentation in Leigh syndrome. *J.Inherit.Metab Dis.* 20, 704-705 (1997).

191. Karvonen, S. L. *et al.* Increased prevalence of vitiligo, but no evidence of premature ageing, in the skin of patients with bp 3243 mutation in mitochondrial DNA in the mitochondrial encephalomyopathy, lactic acidosis and stroke-like episodes syndrome (MELAS). *Br.J.Dermatol.* 140, 634-639 (1999).

192. Thomeer, E. C., Verhoeven, W. M., van de Vlasakker, C. J., & Klompenhouwer, J. L. Psychiatric symptoms in MELAS; a case report. *J.Neurol.Neurosurg.Psychiatry* 64, 692-693 (1998).

193. Sue, C. M. *et al.* Pigmentary retinopathy associated with the mitochondrial DNA 3243 point mutation. *Neurology* 49, 1013-1017 (1997).

194. Bird, A. C. *et al.* An international classification and grading system for age-related maculopathy and age-related macular degeneration. The International ARM Epidemiological Study Group. *Surv.Ophthalmol.* 39, 367-374 (1995).

195. Sue, C. M. *et al.* Neuroradiological features of six kindreds with MELAS tRNA(Leu) A2343G point mutation: implications for pathogenesis. *J.Neurol.Neurosurg.Psychiatry* 65, 233-240 (1998).

196. Anan, R. *et al.* Cardiac involvement in mitochondrial diseases. A study on 17 patients with documented mitochondrial DNA defects. *Circulation* 91, 955-961 (1995).

197. Okajima, Y., Tanabe, Y., Takayanagi, M., & Aotsuka, H. A follow up study of myocardial involvement in patients with mitochondrial encephalomyopathy, lactic acidosis, and stroke-like episodes (MELAS). *Heart* 80, 292-295 (1998).

198. Klopstock, T., Jaksch, M., & Gasser, T. Age and cause of death in mitochondrial diseases. *Neurology* 53, 855-857 (1999).

199. Goto, Y., Nonaka, I., & Horai, S. A mutation in the tRNA(Leu)(UUR) gene associated with the MELAS subgroup of mitochondrial encephalomyopathies. *Nature* 348, 651-653 (1990).

200. Kobayashi, Y. *et al.* A point mutation in the mitochondrial tRNA(Leu)(UUR) gene in MELAS (mitochondrial myopathy, encephalopathy, lactic acidosis and stroke-like episodes). *Biochem.Biophys.Res.Commun.* 173, 816-822 (1990).

201. Penisson-Besnier, I. *et al.* Recurrent brain hematomas in MELAS associated with an ND5 gene mitochondrial mutation. *Neurology* 55, 317-318 (2000).

202. Manfredi, G. *et al.* A new mutation associated with MELAS is located in a mitochondrial DNA polypeptide-coding gene. *Neuromuscul.Disord.* 5, 391-398 (1995).

203. Pulkes, T. *et al.* The mitochondrial DNA G13513A transition in ND5 is associated with a LHON/MELAS overlap syndrome and may be a frequent cause of MELAS. *Ann.Neurol* 46, 916-919 (1999).

204. Santorelli, F. M. *et al.* Identification of a novel mutation in the mtDNA ND5 gene associated with MELAS. *Biochem.Biophys.Res.Commun.* 238, 326-328 (1997).

205. Tsairis, P., Engel, W. K., & Kark, P. Familial myoclonic epilepsy syndrome associated with skeletal muscle mitochondrial abnormalities. *Neurology* 23, 408-408 (1973).

206. Shoffner, J. M. *et al.* Myoclonic epilepsy and ragged-red fiber disease (MERRF) is associated with a mitochondrial DNA tRNA(Lys) mutation. *Cell* 61, 931-937 (1990).

207. Berkovic, S. F. *et al.* Myoclonus epilepsy and ragged-red fibres (MERRF). 1. A clinical, pathological, biochemical, magnetic resonance spectrographic and positron emission tomographic study. *Brain* 112 (Pt 5), 1231-1260 (1989).

208. Tulinius, M. H., Holme, E., Kristiansson, B., Larsson, N. G., & Oldfors, A. Mitochondrial encephalomyopathies in childhood. II. Clinical manifestations and syndromes. *J.Pediatr.* 119, 251-259 (1991).

209. Geny, C. *et al.* Muscle mitochondrial DNA in encephalomyopathy and ragged red fibres: a Southern blot analysis and literature review. *J.Neurol.* 238, 171-176 (1991).

210. Hammans, S. R. *et al.* The mitochondrial DNA transfer RNA(Lys)A-->G(8344) mutation and the syndrome of myoclonic epilepsy with ragged red fibres (MERRF). Relationship of clinical phenotype to proportion of mutant mitochondrial DNA. *Brain* 116 (Pt 3), 617-632 (1993).

211. Graf, W. D. *et al.* Phenotypic heterogeneity in families with the myoclonic epilepsy and ragged-red fiber disease point mutation in mitochondrial DNA. *Ann.Neurol.* 33, 640-645 (1993).

212. Ozawa, M., Nishino, I., Horai, S., Nonaka, I., & Goto, Y. I. Myoclonus epilepsy associated with ragged-red fibers: a G-to-A mutation at nucleotide pair 8363 in mitochondrial tRNA(Lys) in two families. *Muscle Nerve* 20, 271-278 (1997).

213. Tiranti, V. *et al.* Maternally inherited hearing loss, ataxia and myoclonus associated with a novel point mutation in mitochondrial tRNASer(UCN) gene. *Hum.Mol.Genet.* 4, 1421-1427 (1995).

214. Rosing, H. S., Hopkins, L. C., Wallace, D. C., Epstein, C. M., & Weidenheim, K. Maternally inherited mitochondrial myopathy and myoclonic epilepsy. *Ann.Neurol.* 17, 228-237 (1985).

215. Shoffner, J. M., Lott, M. T., & Wallace, D. C. MERRF: a model disease for understanding the principles of mitochondrial genetics. *Rev.Neurol.(Paris)* 147, 431-435 (1991).

216. Kobayashi, Y. *et al.* Respiration-deficient cells are caused by a single point mutation in the mitochondrial tRNA-Leu (UUR) gene in mitochondrial myopathy, encephalopathy, lactic acidosis, and strokelike episodes (MELAS). *Am.J.Hum.Genet.* 49, 590-599 (1991).

217. Boulet, L., Karpati, G., & Shoubridge, E. A. Distribution and threshold expression of the tRNA(Lys) mutation in skeletal muscle of patients with myoclonic epilepsy and ragged-red fibers (MERRF). *Am.J.Hum.Genet.* 51, 1187-1200 (1992).

218. Chinnery, P. F., Howell, N., Lightowlers, R. N., & Turnbull, D. M. MELAS and MERRF. The relationship between maternal mutation load and the frequency of clinically affected offspring. *Brain* 121 (Pt 10), 1889-1894 (1998).

219. Holt, I. J., Harding, A. E., Petty, R. K., & Morgan-Hughes, J. A. A new mitochondrial disease associated with mitochondrial DNA heteroplasmy. *Am.J Hum.Genet.* 46, 428-433 (1990).

220. Ciafaloni, E. *et al.* Maternally inherited Leigh syndrome. *J.Pediatr.* 122, 419-422 (1993).

221. Santorelli, F. M., Shanske, S., Macaya, A., DeVivo, D. C., & DiMauro, S. The mutation at nt 8993 of mitochondrial DNA is a common cause of Leigh's syndrome. *Ann.Neurol.* 34, 827-834 (1993).

222. De Vries, D. D., van Engelen, B. G., Gabreels, F. J., Ruitenbeek, W., & van Oost, B. A. A second missense mutation in the mitochondrial ATPase 6 gene in Leigh's syndrome. *Ann.Neurol.* 34, 410-412 (1993).

223. Santorelli, F. M. *et al.* A T-->C mutation at nt 8993 of mitochondrial DNA in a child with Leigh syndrome. *Neurology* 44, 972-974 (1994).

224. Cox, G. B., Fimmel, A. L., Gibson, F., & Hatch, L. The mechanism of ATP synthase: a reassessment of the functions of the b and a subunits. *Biochim.Biophys.Acta* 849, 62-69 (1986).

225. Makela-Bengs, P. *et al.* Correlation between the clinical symptoms and the proportion of mitochondrial DNA carrying the 8993 point mutation in the NARP syndrome. *Pediatr.Res.* 37, 634-639 (1995).

226. Uziel, G. *et al.* Mitochondrial disease associated with the T8993G mutation of the mitochondrial ATPase 6 gene: a clinical, biochemical, and molecular study in six families. *J.Neurol.Neurosurg.Psychiatry* 63, 16-22 (1997).

227. Parfait, B. *et al.* The neurogenic weakness, ataxia and retinitis pigmentosa (NARP) syndrome mtDNA mutation (T8993G) triggers muscle ATPase deficiency and hypocitrullinaemia. *Eur.J.Pediatr.* 158, 55-58 (1999).

228. Leigh, D. Subacute necrotizing encephalomyelopathy in an infant. *J Neurol Neurosurg Psychiatry* 14, 216-221 (1951).

229. van Erven, P. M., Gabreels, F. J., Ruitenbeek, W., Renier, W. O., & Fischer, J. C. Mitochondrial encephalomyopathy. Association with an NADH dehydrogenase deficiency. *Arch Neurol.* 44, 775-778 (1987).

230. Willems, J. L. *et al.* Leigh's encephalomyelopathy in a patient with cytochrome c oxidase deficiency in muscle tissue. *Pediatrics* 60, 850-857 (1977).

231. Kretzschmar, H. A. *et al.* Pyruvate dehydrogenase complex deficiency as a cause of subacute necrotizing encephalopathy (Leigh disease). *Pediatrics* 79, 370-373 (1987).

232. Baumgartner, E. R. *et al.* Biotinidase deficiency: a cause of subacute necrotizing encephalomyelopathy (Leigh syndrome). Report of a case with lethal outcome. *Pediatr.Res.* 26, 260-266 (1989).

233. Matthews, P. M. *et al.* Molecular genetic characterization of an X-linked form of Leigh's syndrome. *Ann.Neurol.* 33, 652-655 (1993).

234. Rahman, S. *et al.* Leigh syndrome: clinical features and biochemical and DNA abnormalities. *Ann.Neurol.* 39, 343-351 (1996).

235. Tiranti, V. *et al.* Mutations of SURF-1 in Leigh disease associated with cytochrome c oxidase deficiency. *Am.J.Hum.Genet.* 63, 1609-1621 (1998).

236. Zhu, Z. *et al.* SURF1, encoding a factor involved in the biogenesis of cytochrome c oxidase, is mutated in Leigh syndrome. *Nat.Genet.* 20, 337-343 (1998).

237. Coenen, M. J. *et al.* SURFEIT-1 gene analysis and two-dimensional blue native gel electrophoresis in cytochrome c oxidase deficiency. *Biochem.Biophys.Res.Commun.* 265, 339-344 (1999).

238. Tiranti, V. *et al.* Characterization of SURF-1 expression and Surf-1p function in normal and disease conditions. *Hum.Mol.Genet.* 8, 2533-2540 (1999).

239. Yao, J. & Shoubridge, E. A. Expression and functional analysis of SURF1 in Leigh syndrome patients with cytochrome c oxidase deficiency. *Hum.Mol.Genet.* 8, 2541-2549 (1999).

240. Papadopoulou, L. C. *et al.* Fatal infantile cardioencephalomyopathy with COX deficiency and mutations in SCO2, a COX assembly gene. *Nat.Genet.* 23, 333-337 (1999).

241. Valnot, I. *et al.* A mutation in the human heme A:farnesyltransferase gene (COX10) causes cytochrome c oxidase deficiency. *Hum.Mol.Genet.* 9, 1245-1249 (2000).

242. Valnot, I. *et al.* Mutations of the SCO1 gene in mitochondrial cytochrome c oxidase deficiency with neonatal-onset hepatic failure and encephalopathy. *Am.J.Hum.Genet.* 67, 1104-1109 (2000).

243. Agsteribbe, E. *et al.* A fatal, systemic mitochondrial disease with decreased mitochondrial enzyme activities, abnormal ultrastructure of the mitochondria and deficiency of heat shock protein 60. *Biochem.Biophys.Res.Commun.* 193, 146-154 (1993).

244. Briones, P. *et al.* A new case of multiple mitochondrial enzyme deficiencies with decreased amount of heat shock protein 60. *J.Inherit.Metab Dis.* 20, 569-577 (1997).

245. de Lonlay, P. *et al.* A mutant mitochondrial respiratory chain assembly protein causes complex III deficiency in patients with tubulopathy, encephalopathy and liver failure. *Nat.Genet.* 29, 57-60 (2001).

246. Chalmers, R. M. *et al.* A mitochondrial DNA tRNA(Val) point mutation associated with adult-onset Leigh syndrome. *Neurology* 49, 589-592 (1997).

247. Yamamoto, M., Clemens, P. R., & Engel, A. G. Mitochondrial DNA deletions in mitochondrial cytopathies: observations in 19 patients. *Neurology* 41, 1822-1828 (1991).

248. Morris, A. A. *et al.* Liver failure associated with mitochondrial DNA depletion. *J.Hepatol.* 28, 556-563 (1998).

249. De Meirleir, L., Seneca, S., Lissens, W., Schoentjes, E., & Desprechins, B. Bilateral striatal necrosis with a novel point mutation in the mitochondrial ATPase 6 gene. *Pediatr.Neurol.* 13, 242-246 (1995).

250. Thyagarajan, D., Shanske, S., Vazquez-Memije, M., De Vivo, D., & DiMauro, S. A novel mitochondrial ATPase 6 point mutation in familial bilateral striatal necrosis. *Ann.Neurol.* 38, 468-472 (1995).

251. Moraes, C. T. *et al.* mtDNA depletion with variable tissue expression: a novel genetic abnormality in mitochondrial diseases. *Am.J.Hum.Genet.* 48, 492-501 (1991).

252. Taanman, J. W. *et al.* Molecular mechanisms in mitochondrial DNA depletion syndrome. *Hum.Mol.Genet.* 6, 935-942 (1997).

253. Vu, T. H. *et al.* Clinical manifestations of mitochondrial DNA depletion. *Neurology* 50, 1783-1790 (1998).

254. Mandel, H. *et al.* The deoxyguanosine kinase gene is mutated in individuals with depleted hepatocerebral mitochondrial DNA. *Nat.Genet.* 29, 337-341 (2001).

255. Saada, A. *et al.* Mutant mitochondrial thymidine kinase in mitochondrial DNA depletion myopathy. *Nat.Genet.* 29 , 342-344 (2001).

256. Naviaux, R. K. *et al.* Mitochondrial DNA polymerase gamma deficiency and mtDNA depletion in a child with Alpers' syndrome. *Ann.Neurol.* 45, 54-58 (1999).

257. Vu, T. H. *et al.* Navajo neurohepatopathy: a mitochondrial DNA depletion syndrome? *Hepatology* 34, 116-120 (2001).

258. Bardosi, A. *et al.* Myo-, neuro-, gastrointestinal encephalopathy (MNGIE syndrome) due to partial deficiency of cytochrome-c-oxidase. A new mitochondrial multisystem disorder. *Acta Neuropathol.(Berl)* 74, 248-258 (1987).

259. Hirano, M. *et al.* Mitochondrial neurogastrointestinal encephalomyopathy (MNGIE): clinical, biochemical, and genetic features of an autosomal recessive mitochondrial disorder. *Neurology* 44, 721-727 (1994).

260. Papadimitriou, A. *et al.* Partial depletion and multiple deletions of muscle mtDNA in familial MNGIE syndrome. *Neurology* 51, 1086-1092 (1998).

261. Nishino, I., Spinazzola, A., & Hirano, M. Thymidine phosphorylase gene mutations in MNGIE, a human mitochondrial disorder. *Science* 283, 689-692 (1999).

262. Harding, A. E. & Sweeney, M. G. Leber's hereditary optic neuropathy. in *Mitochondrial Disorders in Neurology* 181-198. Butterworth-Heinemann, Oxford (1994).

263. Mackey, D. & Howell, N. A variant of Leber hereditary optic neuropathy characterized by recovery of vision and by an unusual mitochondrial genetic etiology. *Am.J.Hum.Genet.* 51, 1218-1228 (1992).

264. Howell, N. Leber hereditary optic neuropathy: how do mitochondrial DNA mutations cause degeneration of the optic nerve? *J.Bioenerg.Biomembr.* 29, 165-173 (1997).

265. Larsson, N. G., Andersen, O., Holme, E., Oldfors, A., & Wahlstrom, J. Leber's hereditary optic neuropathy and complex I deficiency in muscle. *Ann.Neurol.* 30, 701-708 (1991).

266. Oostra, R. J., Van Galen, M. J., Bolhuis, P. A., Bleeker-Wagemakers, E. M., & Van den, B. C. The mitochondrial DNA mutation ND6*14,484C associated with leber hereditary optic neuropathy, leads to deficiency of complex I of the respiratory chain. *Biochem.Biophys.Res.Commun.* 215, 1001-1005 (1995).

267. Bu, X. D. & Rotter, J. I. X chromosome-linked and mitochondrial gene control of Leber hereditary optic neuropathy: evidence from segregation analysis for dependence on X chromosome inactivation. *Proc.Natl.Acad.Sci.U.S.A* 88, 8198-8202 (1991).

268. Chalmers, R. M., Davis, M. B., Sweeney, M. G., Wood, N. W., & Harding, A. E. Evidence against an X-linked visual loss susceptibility locus in Leber hereditary optic neuropathy. *Am.J.Hum.Genet.* 59, 103-108 (1996).

269. Smith, P. R. *et al.* Antibodies to human optic nerve in Leber's hereditary optic neuropathy. *J.Neurol.Sci.* 130 , 134-138 (1995).

270. Harding, A. E. *et al.* Occurrence of a multiple sclerosis-like illness in women who have a Leber's hereditary optic neuropathy mitochondrial DNA mutation. *Brain* 115 (Pt 4), 979-989 (1992).

271. De Vries, D. D. *et al.* Genetic and biochemical impairment of mitochondrial complex I activity in a family with Leber hereditary optic neuropathy and hereditary spastic dystonia. *Am.J.Hum.Genet.* 58, 703-711 (1996).

272. Jun, A. S., Brown, M. D., & Wallace, D. C. A mitochondrial DNA mutation at nucleotide pair 14459 of the NADH dehydrogenase subunit 6 gene associated with maternally inherited Leber hereditary optic neuropathy and dystonia. *Proc.Natl.Acad.Sci.U.S.A* 91, 6206-6210 (1994).

273. Nikoskelainen, E., Wanne, O., & Dahl, M. Pre-excitation syndrome and Leber's hereditary optic neuroretinopathy. *Lancet* 1, 696 (1985).

274. Hudgson, P., Bradley, W. G., & Jenkison, M. Familial "mitochondrial" myopathy. A myopathy associated with disordered oxidative metabolism in muscle fibres. 1. Clinical, electrophysiological and pathological findings. *J.Neurol.Sci.* 16, 343-370 (1972).

275. Kamieniecka, Z. Myopathies with abnormal mitochondria. A clinical, histological, and electrophysiological study. *Acta Neurol.Scand.* 55, 57-75 (1977).

276. Koga, Y., Nonaka, I., Kobayashi, M., Tojyo, M., & Nihei, K. Findings in muscle in complex I (NADH coenzyme Q reductase) deficiency. *Ann.Neurol.* 24, 749-756 (1988).

277. Morgan-Hughes, J. A., Cooper, J. M., & Schapira, A. H. The mitochondrial myopathies. Defects of the respiratory chain and oxidative phosphorylation system. in *The London Symposia* 103-114. Elsevier, Amsterdam (1987).

278. Dalakas, M. C. *et al.* Mitochondrial myopathy caused by long-term zidovudine therapy. *N.Engl.J.Med.* 322, 1098-1105 (1990).

279. Dalakas, M. C., Leon-Monzon, M. E., Bernardini, I., Gahl, W. A., & Jay, C. A. Zidovudine-induced mitochondrial myopathy is associated with muscle carnitine deficiency and lipid storage. *Ann.Neurol.* 35, 482-487 (1994).

280. Lai, K. K., Gang, D. L., Zawacki, J. K., & Cooley, T. P. Fulminant hepatic failure associated with 2',3'-dideoxyinosine (ddI). *Ann.Intern.Med.* 115, 283-284 (1991).

281. Carr, A. & Cooper, D. A. Adverse effects of antiretroviral therapy. *Lancet* 356, 1423-1430 (2000).

282. Zupanc, M. L. *et al.* Deletion of mitochondrial DNA in patients with combined features of Kearns-Sayre and MELAS syndromes. *Ann.Neurol.* 29, 680-683 (1991).

283. Byrne, E. *et al.* Progression from MERRF to MELAS phenotype in a patient with combined respiratory complex I and IV deficiencies. *J.Neurol.Sci.* 88, 327-337 (1988).

284. Di Mauro, S. & Bonilla, E. Mitochondrial Encephalomyopathies in *The molecular and genetic basis of neurological disease* 201-235. Butterworth-Heinemann, Boston (1997).

285. Prezant, T. R. *et al.* Mitochondrial ribosomal RNA mutation associated with both antibiotic-induced and non-syndromic deafness. *Nat.Genet.* 4, 289-294 (1993).

286. Estivill, X. *et al.* Familial progressive sensorineural deafness is mainly due to the mtDNA A1555G mutation and is enhanced by treatment of aminoglycosides. *Am.J.Hum.Genet.* 62, 27-35 (1998).

287. Bykhovskaya, Y. *et al.* Candidate locus for a nuclear modifier gene for maternally inherited deafness. *Am.J.Hum.Genet.* 66, 1905-1910 (2000).

288. Guan, M. X., Fischel-Ghodsian, N., & Attardi, G. Biochemical evidence for nuclear gene involvement in phenotype of non-syndromic deafness associated with mitochondrial 12S rRNA mutation. *Hum.Mol.Genet.* 5, 963-971 (1996).

289. Munnich, A. *et al.* Clinical presentations and laboratory investigations in respiratory chain deficiency. *Eur.J.Pediatr.* 155, 262-274 (1996).

290. Turner, L. F. *et al.* Mitochondrial DNA in idiopathic cardiomyopathy. *Eur.Heart J.* 19, 1725-1729 (1998).

291. Sengers, R. C., Trijbels, J. M., Willems, J. L., Daniels, O., & Stadhouders, A. M. Congenital cataract and mitochondrial myopathy of skeletal and heart muscle associated with lactic acidosis after exercise. *J.Pediatr.* 86, 873-880 (1975).

292. Smeitink, J. A., Huizing, M., & Ruitenbeek, W. Adenine nucleotide translocator deficiency in a patientwith fatal congenital cardiomyopathy, cataract and mitochondrial myopathy. *J Inherit Metab Dis* 20, 7-7 (1997).

293. Kaukonen, J. *et al.* A third locus predisposing to multiple deletions of mtDNA in autosomal dominant progressive external ophthalmoplegia. *Am.J.Hum.Genet.* 65, 256-261 (1999).

294. Graham, B. H. *et al.* A mouse model for mitochondrial myopathy and cardiomyopathy resulting from a deficiency in the heart/muscle isoform of the adenine nucleotide translocator. *Nat.Genet.* 16, 226-234 (1997).

295. Pearson, H. A. *et al.* A new syndrome of refractory sideroblastic anemia with vacuolization of marrow precursors and exocrine pancreatic dysfunction. *J.Pediatr.* 95, 976-984 (1979).

296. Rotig, A. *et al.* Mitochondrial DNA deletion in Pearson's marrow/pancreas syndrome. *Lancet* 1, 902-903 (1989).

297. Bernes, S. M. *et al.* Identical mitochondrial DNA deletion in mother with progressive external ophthalmoplegia and son with Pearson marrow-pancreas syndrome. *J.Pediatr.* 123, 598-602 (1993).

298. Larsson, N. G., Holme, E., Kristiansson, B., Oldfors, A., & Tulinius, M. Progressive increase of the mutated mitochondrial DNA fraction in Kearns-Sayre syndrome. *Pediatr.Res.* 28, 131-136 (1990).

299. Gattermann, N. *et al.* A heteroplasmic point mutation of mitochondrial tRNALeu(CUN) in non-lymphoid haemopoietic cell lineages from a patient with acquired idiopathic sideroblastic anaemia. *Br.J.Haematol.* 93, 845-855 (1996).

300. Gattermann, N. *et al.* Heteroplasmic point mutations of mitochondrial DNA affecting subunit I of cytochrome c oxidase in two patients with acquired idiopathic sideroblastic anemia. *Blood* 90, 4961-4972 (1997).

301. Tuckfield, A., Ratnaike, S., Hussein, S., & Metz, J. A novel form of hereditary sideroblastic anaemia with macrocytosis. *Br.J.Haematol.* 97, 279-285 (1997).

302. Casademont, J. *et al.* Multiple deletions of mtDNA in two brothers with sideroblastic anemia and mitochondrial myopathy and in their asymptomatic mother. *Hum.Mol.Genet.* 3, 1945-1949 (1994).

303. Inbal, A. *et al.* Myopathy, lactic acidosis, and sideroblastic anemia: a new syndrome. *Am.J.Med.Genet.* 55, 372-378 (1995).

304. Kadowaki, H. *et al.* Mitochondrial gene mutation and insulin-deficient type of diabetes mellitus. *Lancet* 341, 893-894 (1993).

305. Rotig, A. *et al.* Deletion of mitochondrial DNA in a case of early-onset diabetes mellitus, optic atrophy, and deafness (Wolfram syndrome, MIM 222300). *J.Clin.Invest* 91, 1095-1098 (1993).

306. Barrientos, A. *et al.* A nuclear defect in the 4p16 region predisposes to multiple mitochondrial DNA deletions in families with Wolfram syndrome. *J.Clin.Invest* 97, 1570-1576 (1996).

307. Verma, A. *et al.* A novel mitochondrial G8313A mutation associated with prominent initial gastrointestinal symptoms and progressive encephaloneuropathy. *Pediatr.Res.* 42, 448-454 (1997).

308. Cormier-Daire, V. *et al.* Mitochondrial DNA rearrangements with onset as chronic diarrhea with villous atrophy. *J.Pediatr.* 124, 63-70 (1994).

309. Cormier-Daire, V. *et al.* Neonatal and delayed-onset liver involvement in disorders of oxidative phosphorylation. *J.Pediatr.* 130, 817-822 (1997).

310. Bindoff, L. A. *et al.* Multiple defects of the mitochondrial respiratory chain in a mitochondrial encephalopathy (MERRF): a clinical, biochemical and molecular study. *J.Neurol.Sci.* 102, 17-24 (1991).

311. Moraes, C. T., Ricci, E., Bonilla, E., DiMauro, S., & Schon, E. A. The mitochondrial tRNA(Leu(UUR)) mutation in mitochondrial encephalomyopathy, lactic acidosis, and strokelike episodes (MELAS): genetic, biochemical, and morphological correlations in skeletal muscle. *Am.J.Hum.Genet.* 50, 934-949 (1992).

312. Seibel, P. *et al.* Genetic biochemical and pathophysiological characterization of a familial mitochondrial encephalomyopathy (MERRF). *J.Neurol.Sci.* 105, 217-224 (1991).

313. Holt, I. J. *et al.* Mitochondrial myopathies: clinical and biochemical features of 30 patients with major deletions of muscle mitochondrial DNA. *Ann.Neurol.* 26, 699-708 (1989).

314. Kennaway, N. G. Defects in the cytochrome bc1 complex in mitochondrial diseases. *J.Bioenerg.Biomembr.* 20, 325-352 (1988).

315. DiMauro, S., Hirano, M., & Schon, E. A. Mitochondrial encephalomyopathies: therapeutic approaches. *Neurol.Sci.* 21, S901-S908 (2000).

316. Andreu, A. L. *et al.* Exercise intolerance due to mutations in the cytochrome b gene of mitochondrial DNA. *N.Engl.J Med.* 341, 1037-1044 (1999).

317. DiMauro, S. Exercise intolerance and the mitochondrial respiratory chain. *Ital.J Neurol Sci.* 20, 387-393 (1999).

318. Karadimas, C. L. *et al.* Recurrent myoglobinuria due to a nonsense mutation in the COX I gene of mitochondrial DNA. *Neurology* 55, 644-649 (2000).

319. Keightley, J. A. *et al.* A microdeletion in cytochrome c oxidase (COX) subunit III associated with COX deficiency and recurrent myoglobinuria. *Nat.Genet.* 12, 410-416 (1996).

320. Keightley, J. A. *et al.* Mitochondrial encephalomyopathy and complex III deficiency associated with a stop-codon mutation in the cytochrome b gene. *Am.J Hum.Genet.* 67, 1400-1410 (2000).

321. Musumeci, O. *et al.* Intragenic inversion of mtDNA: a new type of pathogenic mutation in a patient with mitochondrial myopathy. *Am.J Hum.Genet.* 66, 1900-1904 (2000).

322. Chinnery, P. F. *et al.* Very low levels of the mtDNA A3243G mutation associated with mitochondrial dysfunction in vivo. *Ann.Neurol* 47, 381-384 (2000).

323. Dubeau, F., De Stefano, N., Zifkin, B. G., Arnold, D. L., & Shoubridge, E. A. Oxidative phosphorylation defect in the brains of carriers of the tRNAleu(UUR) A3243G mutation in a MELAS pedigree. *Ann.Neurol* 47, 179-185 (2000).

324. Barrientos, A. & Moraes, C. T. Titrating the effects of mitochondrial complex I impairment in the cell physiology. *J.Biol.Chem.* 274, 16188-16197 (1999).

325. Chance, B., Sies, H., & Boveris, A. Hydroperoxide metabolism in mammalian organs. *Physiol Rev.* 59, 527-605 (1979).

326. Shigenaga, M. K., Hagen, T. M., & Ames, B. N. Oxidative damage and mitochondrial decay in aging. *Proc.Natl.Acad.Sci.U.S.A* 91, 10771-10778 (1994).

327. Boveris, A. & Chance, B. The mitochondrial generation of hydrogen peroxide. General properties and effect of hyperbaric oxygen. *Biochem.J.* 134, 707-716 (1973).

328. Nohl, H. & Hegner, D. Do mitochondria produce oxygen radicals in vivo? *Eur.J.Biochem.* 82, 563-567 (1978).

329. Esposito, L. A., Melov, S., Panov, A., Cottrell, B. A., & Wallace, D. C. Mitochondrial disease in mouse results in increased oxidative stress. *Proc.Natl.Acad.Sci.U.S.A* 96, 4820-4825 (1999).

330. Giulivi, C. Functional implications of nitric oxide produced by mitochondria in mitochondrial metabolism. *Biochem.J.* 332 (Pt 3), 673-679 (1998).

331. Giulivi, C., Poderoso, J. J., & Boveris, A. Production of nitric oxide by mitochondria. *J.Biol.Chem.* 273, 11038-11043 (1998).

332. Tatoyan, A. & Giulivi, C. Purification and characterization of a nitric-oxide synthase from rat liver mitochondria. *J.Biol.Chem.* 273, 11044-11048 (1998).

333. Brookes, P. S. *et al.* Concentration-dependent effects of nitric oxide on mitochondrial permeability transition and cytochrome c release. *J.Biol.Chem.* 275, 20474-20479 (2000).

334. Poderoso, J. J. *et al.* The regulation of mitochondrial oxygen uptake by redox reactions involving nitric oxide and ubiquinol. *J.Biol.Chem.* 274, 37709-37716 (1999).

335. Ischiropoulos, H. & al Mehdi, A. B. Peroxynitrite-mediated oxidative protein modifications. *FEBS Lett.* 364, 279-282 (1995).

336. Brown, G. C. Nitric oxide and mitochondrial respiration. *Biochim.Biophys.Acta* 1411, 351-369 (1999).

337. Yakes, F. M. & Van Houten, B. Mitochondrial DNA damage is more extensive and persists longer than nuclear DNA damage in human cells following oxidative stress. *Proc.Natl.Acad.Sci.U.S.A* 94, 514-519 (1997).

338. Tengan, C. H., Gabbai, A. A., Shanske, S., Zeviani, M., & Moraes, C. T. Oxidative phosphorylation dysfunction does not increase the rate of accumulation of age-related mtDNA deletions in skeletal muscle. *Mutat.Res.* 379, 1-11 (1997).

339. Wei, Y. H., Lu, C. Y., Wei, C. Y., Ma, Y. S., & Lee, H. C. Oxidative stress in human aging and mitochondrial disease-consequences of defective mitochondrial respiration and impaired antioxidant enzyme system. *Chin J.Physiol* 44, 1-11 (2001).

340. Tanaka, M. *et al.* Accumulation of deletions and point mutations in mitochondrial genome in degenerative diseases. *Ann.N.Y.Acad.Sci.* 786, 102-111 (1996).

341. Oexle, K. & Zwirner, A. Advanced telomere shortening in respiratory chain disorders. *Hum.Mol.Genet.* 6, 905-908 (1997).

342. Filla, A. *et al.* Prevalence of hereditary ataxias and spastic paraplegias in Molise, a region of Italy. *J.Neurol.* 239, 351-353 (1992).

343. Polo, J. M., Calleja, J., Combarros, O., & Berciano, J. Hereditary "pure" spastic paraplegia: a study of nine families. *J.Neurol.Neurosurg.Psychiatry* 56, 175-181 (1993).

344. Fink, J. K. Advances in hereditary spastic paraplegia. *Curr.Opin.Neurol.* 10, 313-318 (1997).

345. Lizcano-Gil, L. A., Garcia-Cruz, D., Pilar Bernal-Beltran, M., & Hernandez, A. Association of late onset spastic paraparesis and dementia: probably an autosomal dominant form of complicated paraplegia. *Am.J.Med.Genet.* 68, 1-6 (1997).

346. Casari, G. *et al.* Spastic paraplegia and OXPHOS impairment caused by mutations in paraplegin, a nuclear-encoded mitochondrial metalloprotease. *Cell* 93, 973-983 (1998).

347. McDermott, C. J. *et al.* Paraplegin gene analysis in hereditary spastic paraparesis (HSP) pedigrees in northeast England. *Neurology* 56, 467-471 (2001).

348. Hazan, J. *et al.* Spastin, a new AAA protein, is altered in the most frequent form of autosomal dominant spastic paraplegia. *Nat.Genet.* 23, 296-303 (1999).

349. Hedera, P., DiMauro, S., Bonilla, E., Wald, J. J., & Fink, J. K. Mitochondrial analysis in autosomal dominant hereditary spastic paraplegia. *Neurology* 55, 1591-1592 (2000).

350. Piemonte, F. *et al.* Respiratory chain defects in hereditary spastic paraplegias. *Neuromuscul.Disord.* 11, 565-569 (2001).

351. Sriram, K., Shankar, S. K., Boyd, M. R., & Ravindranath, V. Thiol oxidation and loss of mitochondrial complex I precede excitatory amino acid-mediated neurodegeneration. *J.Neurosci.* 18, 10287-10296 (1998).

352. Lutsenko, S. & Cooper, M. J. Localization of the Wilson's disease protein product to mitochondria. *Proc.Natl.Acad.Sci.U.S.A* 95, 6004-6009 (1998).

353. Murata, Y. *et al.* Failure of copper incorporation into ceruloplasmin in the Golgi apparatus of LEC rat hepatocytes. *Biochem.Biophys.Res.Commun.* 209, 349-355 (1995).

354. Buiakova, O. I. *et al.* Null mutation of the murine ATP7B (Wilson disease) gene results in intracellular copper accumulation and late-onset hepatic nodular transformation. *Hum.Mol.Genet.* 8, 1665-1671 (1999).

355. Hamza, I., Schaefer, M., Klomp, L. W., & Gitlin, J. D. Interaction of the copper chaperone HAH1 with the Wilson disease protein is essential for copper homeostasis. *Proc.Natl.Acad.Sci.U.S.A* 96, 13363-13368 (1999).

356. Schaefer, M. *et al.* Localization of the Wilson's disease protein in human liver. *Gastroenterology* 117, 1380-1385 (1999).

357. Sternlieb, I., Quintana, N., Volenberg, I., & Schilsky, M. L. An array of mitochondrial alterations in the hepatocytes of Long-Evans Cinnamon rats. *Hepatology* 22, 1782-1787 (1995).

358. Gu, M. *et al.* Oxidative-phosphorylation defects in liver of patients with Wilson's disease. *Lancet* 356, 469-474 (2000).

359. Sokol, R. J. *et al.* Oxidant injury to hepatic mitochondria in patients with Wilson's disease and Bedlington terriers with copper toxicosis. *Gastroenterology* 107, 1788-1798 (1994).

360. Gutteridge, J. M. & Halliwell, B. Iron toxicity and oxygen radicals. *Baillieres Clin.Haematol.* 2, 195-256 (1989).

361. Hung, I. H. *et al.* Biochemical characterization of the Wilson disease protein and functional expression in the yeast Saccharomyces cerevisiae. *J.Biol.Chem.* 272, 21461-21466 (1997).

362. Alexander, C. *et al.* OPA1, encoding a dynamin-related GTPase, is mutated in autosomal dominant optic atrophy linked to chromosome 3q28. *Nat.Genet.* 26, 211-215 (2000).

363. Delettre, C. *et al.* Nuclear gene OPA1, encoding a mitochondrial dynamin-related protein, is mutated in dominant optic atrophy. *Nat.Genet.* 26, 207-210 (2000).

364. Delettre, C., Lenaers, G., Pelloquin, L., Belenguer, P., & Hamel, C. P. OPA1 (Kjer type) dominant optic atrophy: a novel mitochondrial disease. *Mol.Genet.Metab* 75, 97-107 (2002).

365. Pelloquin, L., Belenguer, P., Menon, Y., & Ducommun, B. Identification of a fission yeast dynamin-related protein involved in mitochondrial DNA maintenance. *Biochem.Biophys.Res.Commun.* 251, 720-726 (1998).

366. Allikmets, R. *et al.* Mutation of a putative mitochondrial iron transporter gene (ABC7) in X-linked sideroblastic anemia and ataxia (XLSA/A). *Hum.Mol.Genet.* 8, 743-749 (1999).

367. Bekri, S. *et al.* Human ABC7 transporter: gene structure and mutation causing X-linked sideroblastic anemia with ataxia with disruption of cytosolic iron-sulfur protein maturation. *Blood* 96, 3256-3264 (2000).

368. Kispal, G., Csere, P., Prohl, C., & Lill, R. The mitochondrial proteins Atm1p and Nfs1p are essential for biogenesis of cytosolic Fe/S proteins. *EMBO J.* 18, 3981-3989 (1999).

369. Li, H., Li, S. H., Johnston, H., Shelbourne, P. F., & Li, X. J. Amino-terminal fragments of mutant huntingtin show selective accumulation in striatal neurons and synaptic toxicity. *Nat.Genet.* 25, 385-389 (2000).

370. Velier, J. *et al.* Wild-type and mutant huntingtins function in vesicle trafficking in the secretory and endocytic pathways. *Exp.Neurol.* 152, 34-40 (1998).

371. Tabrizi, S. J. *et al.* Biochemical abnormalities and excitotoxicity in Huntington's disease brain. *Ann.Neurol.* 45, 25-32 (1999).

372. Tabrizi, S. J. *et al.* Mitochondrial dysfunction and free radical damage in the Huntington R6/2 transgenic mouse. *Ann.Neurol.* 47, 80-86 (2000).

373. Swerdlow, R. H. *et al.* Characterization of cybrid cell lines containing mtDNA from Huntington's disease patients. *Biochem.Biophys.Res.Commun.* 261, 701-704 (1999).

374. Jenkins, B. G., Koroshetz, W. J., Beal, M. F., & Rosen, B. R. Evidence for impairment of energy metabolism in vivo in Huntington's disease using localized 1H NMR spectroscopy. *Neurology* 43, 2689-2695 (1993).

375. Koroshetz, W. J., Jenkins, B. G., Rosen, B. R., & Beal, M. F. Energy metabolism defects in Huntington's disease and effects of coenzyme Q10. *Ann.Neurol.* 41, 160-165 (1997).

376. Beal, M. F. *et al.* Age-dependent striatal excitotoxic lesions produced by the endogenous mitochondrial inhibitor malonate. *J.Neurochem.* 61, 1147-1150 (1993).

377. Brouillet, E. *et al.* Chronic mitochondrial energy impairment produces selective striatal degeneration and abnormal choreiform movements in primates. *Proc.Natl.Acad.Sci.U.S.A* 92, 7105-7109 (1995).

378. Bates, T. E. *et al.* Inhibition of N-acetylaspartate production: implications for 1H MRS studies in vivo. *Neuroreport* 7, 1397-1400 (1996).

379. Jenkins, B. G. *et al.* Nonlinear decrease over time in N-acetyl aspartate levels in the absence of neuronal loss and increases in glutamine and glucose in transgenic Huntington's disease mice. *J.Neurochem.* 74, 2108-2119 (2000).

380. Langston, J. W., Ballard, P., Tetrud, J. W., & Irwin, I. Chronic Parkinsonism in humans due to a product of meperidine-analog synthesis. *Science* 219, 979-980 (1983).

381. Singer, T. P., Castagnoli, N., Jr., Ramsay, R. R., & Trevor, A. J. Biochemical events in the development of parkinsonism induced by 1-methyl-4-phenyl-1,2,3,6-tetrahydropyridine. *J Neurochem.* 49, 1-8 (1987).

382. Mann, V. M. *et al.* Brain, skeletal muscle and platelet homogenate mitochondrial function in Parkinson's disease. *Brain* 115 (Pt 2), 333-342 (1992).

383. Hattori, N., Tanaka, M., Ozawa, T., & Mizuno, Y. Immunohistochemical studies on complexes I, II, III, and IV of mitochondria in Parkinson's disease. *Ann.Neurol* 30, 563-571 (1991).

384. Gu, M., Cooper, J. M., Taanman, J. W., & Schapira, A. H. Mitochondrial DNA transmission of the mitochondrial defect in Parkinson's disease. *Ann.Neurol* 44, 177-186 (1998).

385. Swerdlow, R. H. *et al.* Origin and functional consequences of the complex I defect in Parkinson's disease. *Ann.Neurol* 40, 663-671 (1996).

386. Sheehan, J. P., Palmer, P. E., Helm, G. A., & Tuttle, J. B. MPP+ induced apoptotic cell death in SH-SY5Y neuroblastoma cells: an electron microscope study. *J Neurosci.Res.* 48, 226-237 (1997).

387. Simon, D. K. *et al.* Familial multisystem degeneration with parkinsonism associated with the 11778 mitochondrial DNA mutation. *Neurology* 53, 1787-1793 (1999).

388. Simon, D. K. *et al.* Mitochondrial DNA mutations in complex I and tRNA genes in Parkinson's disease. *Neurology* 54, 703-709 (2000).

389. Parker, W. D., Jr. & Parks, J. K. Cytochrome c oxidase in Alzheimer's disease brain: purification and characterization. *Neurology* 45, 482-486 (1995).

390. Ojaimi, J. *et al.* Irregular distribution of cytochrome c oxidase protein subunits in aging and Alzheimer's disease. *Ann.Neurol* 46, 656-660 (1999).

391. Ito, S. *et al.* Functional integrity of mitochondrial genomes in human platelets and autopsied brain tissues from elderly patients with Alzheimer's disease. *Proc.Natl.Acad.Sci.U.S.A* 96, 2099-2103 (1999).

392. Davis, J. N. & Parker, W. D., Jr. Evidence that two reports of mtDNA cytochrome c oxidase "mutations" in Alzheimer's disease are based on nDNA pseudogenes of recent evolutionary origin. *Biochem.Biophys.Res.Commun.* 244, 877-883 (1998).

393. Hutchin, T. P., Heath, P. R., Pearson, R. C., & Sinclair, A. J. Mitochondrial DNA mutations in Alzheimer's disease. *Biochem.Biophys.Res.Commun.* 241, 221-225 (1997).

394. Mecocci, P., MacGarvey, U., & Beal, M. F. Oxidative damage to mitochondrial DNA is increased in Alzheimer's disease. *Ann.Neurol* 36, 747-751 (1994).

395. Nakano, Y., Hirayama, K., & Terao, K. Hepatic ultrastructural changes and liver dysfunction in amyotrophic lateral sclerosis. *Arch Neurol* 44, 103-106 (1987).

396. Sasaki, S., Maruyama, S., Yamane, K., Sakuma, H., & Takeishi, M. Ultrastructure of swollen proximal axons of anterior horn neurons in motor neuron disease. *J Neurol Sci.* 97, 233-240 (1990).

397. Wiedemann, F. R. *et al.* Impairment of mitochondrial function in skeletal muscle of patients with amyotrophic lateral sclerosis. *J Neurol Sci.* 156, 65-72 (1998).

398. Siklos, L. *et al.* Ultrastructural evidence for altered calcium in motor nerve terminals in amyotropic lateral sclerosis. *Ann.Neurol* 39, 203-216 (1996).

399. Swerdlow, R. H. *et al.* Mitochondria in sporadic amyotrophic lateral sclerosis. *Exp.Neurol.* 153, 135-142 (1998).

400. Comi, G. P. *et al.* Cytochrome c oxidase subunit I microdeletion in a patient with motor neuron disease. *Ann.Neurol* 43, 110-116 (1998).

401. Rosen, D. R. *et al.* Mutations in Cu/Zn superoxide dismutase gene are associated with familial amyotrophic lateral sclerosis. *Nature* 362, 59-62 (1993).

402. Carri, M. T. *et al.* Expression of a Cu,Zn superoxide dismutase typical of familial amyotrophic lateral sclerosis induces mitochondrial alteration and increase of cytosolic Ca2+ concentration in transfected neuroblastoma SH-SY5Y cells. *FEBS Lett.* 414, 365-368 (1997).

403. Kong, J. & Xu, Z. Massive mitochondrial degeneration in motor neurons triggers the onset of amyotrophic lateral sclerosis in mice expressing a mutant SOD1. *J Neurosci.* 18, 3241-3250 (1998).

404. Friedreich N. Uber degenerative Atrophie der spinalen Hinterstrange. Virchow's Arch Pathol Anat 27, 1-26. 1863.

405. Friedreich N. Uber degenerative Atrophie der spinalen Hinterstrange. Virchow's Arch Pathol Anat 26, 433-459. 1863.

406. Friedreich N. Uber degenerative Atrophie der spinalen Hinterstrange. Virchow's Arch Pathol Anat 26, 391-419. 1863.

407. Friedreich N. Uber ataxie mit besonderer berucksichtigung der heredtitaren formen. Virchow's Arch Pathol Anat 68, 145-245. 1876.

408. Friedreich N. Uber ataxie mit besonderer berucksichtigung der hereditaren formen. Virchow's Arch Pathol Anat 70, 140-152. 1877.

409. Harding, A. E. Friedreich's ataxia: a clinical and genetic study of 90 families with an analysis of early diagnostic criteria and intrafamilial clustering of clinical features. *Brain* 104, 589-620 (1981).

410. Cossee, M. *et al.* Evolution of the Friedreich's ataxia trinucleotide repeat expansion: founder effect and premutations. *Proc.Natl.Acad.Sci.U.S.A* 94, 7452-7457 (1997).

411. Epplen, C. *et al.* Differential stability of the (GAA)n tract in the Friedreich ataxia (STM7) gene. *Hum.Genet.* 99, 834-836 (1997).

412. Andermann, E. *et al.* Genetic and family studies in Friedreich's ataxia. *Can.J Neurol Sci.* 3, 287-301 (1976).

413. De Silva, R. *et al.* Molecular genetic diagnosis of Friedreich's ataxia in a pedigree with apparent autosomal dominant spinocerebellar degeneration. *J Neurol Neurosurg Psychiatry* 66, 117-118 (1999).

414. Harding, A. E. & Zilkha, K. J. 'Pseudo-dominant' inheritance in Friedreich's ataxia. *J Med.Genet.* 18, 285-287 (1981).

415. Geoffroy, G. *et al.* Clinical description and roentgenologic evaluation of patients with Friedreich's ataxia. *Can.J Neurol Sci.* 3, 279-286 (1976).

416. Chamberlain, S. *et al.* Genetic homogeneity at the Friedreich ataxia locus on chromosome 9. *Am.J Hum.Genet.* 44, 518-521 (1989).

417. De Michele, G. *et al.* Late onset Friedreich's disease: clinical features and mapping of mutation to the FRDA locus. *J Neurol Neurosurg Psychiatry* 57, 977-979 (1994).

418. Durr, A. *et al.* Clinical and genetic abnormalities in patients with Friedreich's ataxia. *N.Engl.J.Med.* 335, 1169-1175 (1996).

419. Filla, A. *et al.* The relationship between trinucleotide (GAA) repeat length and clinical features in Friedreich ataxia. *Am.J.Hum.Genet.* 59, 554-560 (1996).

420. Keats, B. J., Ward, L. J., Shaw, J., Wickremasinghe, A., & Chamberlain, S. "Acadian" and "classical" forms of Friedreich ataxia are most probably caused by mutations at the same locus. *Am.J Med.Genet.* 33, 266-268 (1989).

421. Klockgether, T. *et al.* Late-onset Friedreich's ataxia. Molecular genetics, clinical neurophysiology, and magnetic resonance imaging. *Arch Neurol.* 50, 803-806 (1993).

422. Klockgether, T. *et al.* Friedreich's ataxia with retained tendon reflexes: molecular genetics, clinical neurophysiology, and magnetic resonance imaging. *Neurology* 46, 118-121 (1996).

423. Montermini, L. *et al.* Phenotypic variability in Friedreich ataxia: role of the associated GAA triplet repeat expansion. *Ann.Neurol.* 41, 675-682 (1997).

424. Palau, F. *et al.* Early-onset ataxia with cardiomyopathy and retained tendon reflexes maps to the Friedreich's ataxia locus on chromosome 9q. *Ann.Neurol* 37, 359-362 (1995).

425. Gates, P. C., Paris, D., Forrest, S. M., Williamson, R., & Gardner, R. J. Friedreich's ataxia presenting as adult-onset spastic paraparesis. *Neurogenetics.* 1, 297-299 (1998).

426. Ragno, M. *et al.* Broadened Friedreich's ataxia phenotype after gene cloning. Minimal GAA expansion causes late-onset spastic ataxia. *Neurology* 49, 1617-1620 (1997).

427. Berciano, J., Combarros, O., De Castro, M., & Palau, F. Intronic GAA triplet repeat expansion in Friedreich's ataxia presenting with pure sensory ataxia. *J Neurol* 244, 390-391 (1997).

428. Hanna, M. G. *et al.* Generalized chorea in two patients harboring the Friedreich's ataxia gene trinucleotide repeat expansion. *Mov Disord.* 13, 339-340 (1998).

429. Klockgether, T. *et al.* The natural history of degenerative ataxia: a retrospective study in 466 patients. *Brain* 121 (Pt 4), 589-600 (1998).

430. Harding, A. E. The inherited ataxias. *Adv.Neurol* 48, 37-46 (1988).

431. Hughes, J. T., Brownell, B., & Hewer, R. L. The peripheral sensory pathway in friedreich's ataxia. An examination by light and electron microscopy of the posterior nerve roots, posterior root ganglia, and peripheral sensory nerves in cases of friedreich's ataxia. *Brain* 91, 803-818 (1968).

432. Jitpimolmard, S. *et al.* The sensory neuropathy of Friedreich's ataxia: an autopsy study of a case with prolonged survival. *Acta Neuropathol.(Berl)* 86, 29-35 (1993).

433. Lamarche, J. B., Lemieux, B., & Lieu, H. B. The neuropathology of "typical" Friedreich's ataxia in Quebec. *Can.J Neurol Sci.* 11, 592-600 (1984).

434. Eder, K., Kish, S. J., Kirchgessner, M., & Ross, B. M. Brain phospholipids and fatty acids in Friedreich's ataxia and spinocerebellar atrophy type-1. *Mov Disord.* 13, 813-819 (1998).

435. Cote, M. *et al.* Hemodynamic findings in Friedreich's ataxia. *Can.J Neurol Sci.* 3, 333-336 (1976).

436. Dutka, D. P., Donnelly, J. E., Nihoyannopoulos, P., Oakley, C. M., & Nunez, D. J. Marked variation in the cardiomyopathy associated with Friedreich's ataxia. *Heart* 81, 141-147 (1999).

437. Hewer, R. L. The heart in Friedreich's ataxia. *Br Heart J.* 31, 5-14 (1969).

438. Campuzano, V. *et al.* Frataxin is reduced in Friedreich ataxia patients and is associated with mitochondrial membranes. *Hum.Mol.Genet.* 6, 1771-1780 (1997).

439. Delatycki, M. B. *et al.* Clinical and genetic study of Friedreich ataxia in an Australian population. *Am.J.Med.Genet.* 87, 168-174 (1999).

440. De Michele, G. *et al.* Determinants of onset age in Friedreich's ataxia. *J.Neurol.* 245, 166-168 (1998).

441. Monros, E. *et al.* Phenotype correlation and intergenerational dynamics of the Friedreich ataxia GAA trinucleotide repeat. *Am.J.Hum.Genet.* 61, 101-110 (1997).

442. Lamont, P. J., Davis, M. B., & Wood, N. W. Identification and sizing of the GAA trinucleotide repeat expansion of Friedreich's ataxia in 56 patients. Clinical and genetic correlates. *Brain* 120 (Pt 4), 673-680 (1997).

443. Montermini, L., Kish, S. J., Jiralerspong, S., Lamarche, J. B., & Pandolfo, M. Somatic mosaicism for Friedreich's ataxia GAA triplet repeat expansions in the central nervous system. *Neurology* 49, 606-610 (1997).

444. Bidichandani, S. I. *et al.* Somatic sequence variation at the Friedreich ataxia locus includes complete contraction of the expanded GAA triplet repeat, significant length variation in serially passaged lymphoblasts and enhanced mutagenesis in the flanking sequence. *Hum.Mol.Genet.* 8, 2425-2436 (1999).

445. De Michele, G. *et al.* Parental gender, age at birth and expansion length influence GAA repeat intergenerational instability in the X25 gene: pedigree studies and analysis of sperm from patients with Friedreich's ataxia. *Hum.Mol.Genet.* 7, 1901-1906 (1998).

446. Machkhas, H., Bidichandani, S. I., Patel, P. I., & Harati, Y. A mild case of Friedreich ataxia: lymphocyte and sural nerve analysis for GAA repeat length reveals somatic mosaicism. *Muscle Nerve* 21, 390-393 (1998).

447. Kang, S., Wohlrab, F., & Wells, R. D. GC-rich flanking tracts decrease the kinetics of intramolecular DNA triplex formation. *J.Biol.Chem.* 267, 19435-19442 (1992).

448. Schols, L. *et al.* Friedreich's ataxia. Revision of the phenotype according to molecular genetics. *Brain* 120 (Pt 12), 2131-2140 (1997).

449. Chamberlain, S. *et al.* Mapping of mutation causing Friedreich's ataxia to human chromosome 9. *Nature* 334, 248-250 (1988).

450. Fujita, R. *et al.* Confirmation of linkage of Friedreich ataxia to chromosome 9 and identification of a new closely linked marker. *Genomics* 4, 110-111 (1989).

451. Hanauer, A. *et al.* The Friedreich ataxia gene is assigned to chromosome 9q13-q21 by mapping of tightly linked markers and shows linkage disequilibrium with D9S15. *Am.J Hum.Genet.* 46, 133-137 (1990).

452. Campuzano, V. *et al.* Friedreich's ataxia: autosomal recessive disease caused by an intronic GAA triplet repeat expansion. *Science* 271, 1423-1427 (1996).

453. Montermini, L. *et al.* The Friedreich ataxia GAA triplet repeat: premutation and normal alleles. *Hum.Mol.Genet.* 6, 1261-1266 (1997).

454. Pook, M. A. *et al.* Identification of three novel frameshift mutations in patients with Friedreich's ataxia. *J.Med.Genet.* 37, E38 (2000).

455. Cossee, M. *et al.* Friedreich's ataxia: point mutations and clinical presentation of compound heterozygotes. *Ann.Neurol.* 45, 200-206 (1999).

456. De Michele, G. *et al.* Atypical Friedreich ataxia phenotype associated with a novel missense mutation in the X25 gene. *Neurology* 54, 496-499 (2000).

457. McCabe, D. J. *et al.* Typical Friedreich's ataxia without GAA expansions and GAA expansion without typical Friedreich's ataxia. *J Neurol* 247, 346-355 (2000).

458. McCabe, D. J. *et al.* Intrafamilial phenotypic variability in Friedreich ataxia associated with a G130V mutation in the FRDA gene. *Arch Neurol* 59, 296-300 (2002).

459. Pandolfo, M. & Montermini, L. Prenatal diagnosis of Friedreich ataxia. *Prenat.Diagn.* 18, 831-833 (1998).

460. Kostrzewa, M., Klockgether, T., Damian, M. S., & Muller, U. Locus heterogeneity in Friedreich ataxia. *Neurogenetics.* 1, 43-47 (1997).

461. Cossee, M. *et al.* Inactivation of the Friedreich ataxia mouse gene leads to early embryonic lethality without iron accumulation. *Hum.Mol.Genet.* 9, 1219-1226 (2000).

462. Jiralerspong, S., Liu, Y., Montermini, L., Stifani, S., & Pandolfo, M. Frataxin shows developmentally regulated tissue-specific expression in the mouse embryo. *Neurobiol.Dis.* 4, 103-113 (1997).

463. Koutnikova, H. *et al.* Studies of human, mouse and yeast homologues indicate a mitochondrial function for frataxin. *Nat.Genet.* 16, 345-351 (1997).

464. Bidichandani, S. I., Ashizawa, T., & Patel, P. I. The GAA triplet-repeat expansion in Friedreich ataxia interferes with transcription and may be associated with an unusual DNA structure. *Am.J.Hum.Genet.* 62, 111-121 (1998).

465. Ohshima, K., Montermini, L., Wells, R. D., & Pandolfo, M. Inhibitory effects of expanded GAA.TTC triplet repeats from intron I of the Friedreich ataxia gene on transcription and replication in vivo. *J.Biol.Chem.* 273 , 14588-14595 (1998).

466. Patel, P. I. & Isaya, G. Friedreich ataxia: from GAA triplet-repeat expansion to frataxin deficiency. *Am.J.Hum.Genet.* 69, 15-24 (2001).

467. Koutnikova, H., Campuzano, V., & Koenig, M. Maturation of wild-type and mutated frataxin by the mitochondrial processing peptidase. *Hum.Mol.Genet.* 7, 1485-1489 (1998).

468. Dhe-Paganon, S., Shigeta, R., Chi, Y. I., Ristow, M., & Shoelson, S. E. Crystal structure of human frataxin. *J.Biol.Chem.* 275, 30753-30756 (2000).

469. Babcock, M. *et al.* Regulation of mitochondrial iron accumulation by Yfh1p, a putative homolog of frataxin. *Science* 276, 1709-1712 (1997).

470. Priller, J., Scherzer, C. R., Faber, P. W., MacDonald, M. E., & Young, A. B. Frataxin gene of Friedreich's ataxia is targeted to mitochondria. *Ann.Neurol.* 42, 265-269 (1997).

471. Branda, S. S., Yang, Z. Y., Chew, A., & Isaya, G. Mitochondrial intermediate peptidase and the yeast frataxin homolog together maintain mitochondrial iron homeostasis in Saccharomyces cerevisiae. *Hum.Mol.Genet.* 8, 1099-1110 (1999).

472. Cavalier, L. *et al.* Ataxia with isolated vitamin E deficiency: heterogeneity of mutations and phenotypic variability in a large number of families. *Am.J.Hum.Genet.* 62, 301-310 (1998).

473. Foury, F. & Cazzalini, O. Deletion of the yeast homologue of the human gene associated with Friedreich's ataxia elicits iron accumulation in mitochondria. *FEBS Lett.* 411, 373-377 (1997).

474. Bradley, J. L. *et al.* Clinical, biochemical and molecular genetic correlations in Friedreich's ataxia. *Hum.Mol.Genet.* 9, 275-282 (2000).

475. Hausladen, A. & Fridovich, I. Superoxide and peroxynitrite inactivate aconitases, but nitric oxide does not. *J Biol.Chem.* 269, 29405-29408 (1994).

476. Rotig, A. *et al.* Aconitase and mitochondrial iron-sulphur protein deficiency in Friedreich ataxia. *Nat.Genet.* 17, 215-217 (1997).

477. Waldvogel, D., van Gelderen, P., & Hallett, M. Increased iron in the dentate nucleus of patients with Friedrich's ataxia. *Ann.Neurol.* 46, 123-125 (1999).

478. Delatycki, M. B. *et al.* Direct evidence that mitochondrial iron accumulation occurs in Friedreich ataxia. *Ann.Neurol.* 45, 673-675 (1999).

479. Adamec, J. *et al.* Iron-dependent self-assembly of recombinant yeast frataxin: implications for Friedreich ataxia. *Am.J.Hum.Genet.* 67, 549-562 (2000).

480. Cavadini, P., O'Neill, H. A., Benada, O., & Isaya, G. Assembly and iron-binding properties of human frataxin, the protein deficient in Friedreich ataxia. *Hum.Mol.Genet.* 11, 217-227 (2002).

481. Levi, S. *et al.* A human mitochondrial ferritin encoded by an intronless gene. *J Biol.Chem.* 276, 24437-24440 (2001).

482. Rotig, A., Munnich, A., & Rustin, P. [Friedreich's ataxia and mitochondria: the puzzle reconstructed]. *Arch Pediatr.* 6 Suppl 2, 498s-499s (1999).

483. Schulz, J. B. *et al.* Oxidative stress in patients with Friedreich ataxia. *Neurology* 55, 1719-1721 (2000).

484. Emond, M., Lepage, G., Vanasse, M., & Pandolfo, M. Increased levels of plasma malondialdehyde in Friedreich ataxia. *Neurology* 55, 1752-1753 (2000).

485. Melov, S., Coskun, P. E., & Wallace, D. C. Mouse models of mitochondrial disease, oxidative stress, and senescence. *Mutat.Res.* 434, 233-242 (1999).

486. Melov, S. *et al.* Mitochondrial disease in superoxide dismutase 2 mutant mice. *Proc.Natl.Acad.Sci.U.S.A* 96, 846-851 (1999).

487. Huynen, M., Snel, B., Lathe, W., III, & Bork, P. Predicting protein function by genomic context: quantitative evaluation and qualitative inferences. *Genome Res.* 10, 1204-1210 (2000).

488. Huynen, M. A., Snel, B., Bork, P., & Gibson, T. J. The phylogenetic distribution of frataxin indicates a role in iron-sulfur cluster protein assembly. *Hum.Mol.Genet.* 10, 2463-2468 (2001).

489. Lill, R. *et al.* The essential role of mitochondria in the biogenesis of cellular iron-sulfur proteins. *Biol.Chem.* 380, 1157-1166 (1999).

490. Lodi, R. *et al.* Deficit of in vivo mitochondrial ATP production in patients with Friedreich ataxia. *Proc.Natl.Acad.Sci.U.S.A* 96, 11492-11495 (1999).

491. Lodi, R. *et al.* Cardiac energetics are abnormal in Friedreich ataxia patients in the absence of cardiac dysfunction and hypertrophy: An in vivo 31P magnetic resonance spectroscopy study. *Cardiovasc.Res.* 52, 111-119 (2001).

492. Vorgerd, M. *et al.* Mitochondrial impairment of human muscle in Friedreich ataxia in vivo. *Neuromuscul.Disord.* 10, 430-435 (2000).

493. Foury, F. Low iron concentration and aconitase deficiency in a yeast frataxin homologue deficient strain. *FEBS Lett.* 456, 281-284 (1999).

494. Li, D. S., Ohshima, K., Jiralerspong, S., Bojanowski, M. W., & Pandolfo, M. Knock-out of the cyaY gene in Escherichia coli does not affect cellular iron content and sensitivity to oxidants. *FEBS Lett.* 456, 13-16 (1999).

495. Puccio, H. *et al.* Mouse models for Friedreich ataxia exhibit cardiomyopathy, sensory nerve defect and Fe-S enzyme deficiency followed by intramitochondrial iron deposits. *Nat.Genet.* 27, 181-186 (2001).

496. Seeber, F. Biogenesis of iron-sulphur clusters in amitochondriate and apicomplexan protists. *Int.J Parasitol.* 32, 1207-1217 (2002).

497. Miranda, C. J. *et al.* Frataxin knockin mouse. *FEBS Lett.* 512, 291-297 (2002).

498. Hart, P. E. & Schapira, A. H. Mitochondria: Aspects for neuroprotection. *Drug Development Research* 46, 57-66 (1999).

499. Wallace, D. C. Mitochondrial diseases in man and mouse. *Science* 283, 1482-1488 (1999).

500. Raha, S. & Robinson, B. H. Mitochondria, oxygen free radicals, and apoptosis. *Am.J Med.Genet.* 106, 62-70 (2001).

501. Chinnery, P. F. & Turnbull, D. M. Epidemiology and treatment of mitochondrial disorders. *Am.J Med.Genet.* 106, 94-101 (2001).

502. Nagley, P. *et al.* Assembly of functional proton-translocating ATPase complex in yeast mitochondria with cytoplasmically synthesized subunit 8, a polypeptide normally encoded within the organelle. *Proc.Natl.Acad.Sci.U.S.A* 85, 2091-2095 (1988).

503. Sutherland, L., Davidson, J., & Jacobs, H. T. Nuclear expression of mitochondrial genes implicated in human encephalomyopathies. *Biochem.Soc.Trans.* 22, 413S (1994).

504. Seibel, P. *et al.* Transfection of mitochondria: strategy towards a gene therapy of mitochondrial DNA diseases. *Nucleic Acids Res.* 23, 10-17 (1995).

505. Kolesnikova, O. A. *et al.* Suppression of mutations in mitochondrial DNA by tRNAs imported from the cytoplasm. *Science* 289, 1931-1933 (2000).

506. Taylor, R. W., Chinnery, P. F., Turnbull, D. M., & Lightowlers, R. N. In-vitro genetic modification of mitochondrial function. *Hum.Reprod.* 15 Suppl 2, 79-85 (2000).

507. Manfredi, G. *et al.* Oligomycin induces a decrease in the cellular content of a pathogenic mutation in the human mitochondrial ATPase 6 gene. *J Biol.Chem.* 274, 9386-9391 (1999).

508. Taivassalo, T. *et al.* Gene shifting: a novel therapy for mitochondrial myopathy. *Hum.Mol.Genet.* 8, 1047-1052 (1999).

509. Sano, M. *et al.* A controlled trial of selegiline, alpha-tocopherol, or both as treatment for Alzheimer's disease. The Alzheimer's Disease Cooperative Study. *N.Engl.J.Med.* 336, 1216-1222 (1997).

510. Morris, M. C. *et al.* Vitamin E and vitamin C supplement use and risk of incident Alzheimer disease. *Alzheimer Dis.Assoc.Disord.* 12, 121-126 (1998).

511. Forsmark-Andree, P., Lee, C. P., Dallner, G., & Ernster, L. Lipid peroxidation and changes in the ubiquinone content and the respiratory chain enzymes of submitochondrial particles. *Free Radic.Biol.Med.* 22, 391-400 (1997).

512. Noack, H., Kube, U., & Augustin, W. Relations between tocopherol depletion and coenzyme Q during lipid peroxidation in rat liver mitochondria. *Free Radic.Res.* 20, 375-386 (1994).

513. Beyer, R. E. An analysis of the role of coenzyme Q in free radical generation and as an antioxidant. *Biochem.Cell Biol.* 70, 390-403 (1992).

514. Beal, M. F., Henshaw, D. R., Jenkins, B. G., Rosen, B. R., & Schulz, J. B. Coenzyme Q10 and nicotinamide block striatal lesions produced by the mitochondrial toxin malonate. *Ann.Neurol.* 36, 882-888 (1994).

515. Matthews, R. T., Yang, L., Browne, S., Baik, M., & Beal, M. F. Coenzyme Q10 administration increases brain mitochondrial concentrations and exerts neuroprotective effects. *Proc.Natl.Acad.Sci.U.S.A* 95, 8892-8897 (1998).

516. Muller, T., Buttner, T., Gholipour, A. F., & Kuhn, W. Coenzyme Q10 supplementation provides mild symptomatic benefit in patients with Parkinson's disease. *Neurosci.Lett.* 341, 201-204 (2003).

517. Shults, C. W. *et al.* Effects of coenzyme Q10 in early Parkinson disease: evidence of slowing of the functional decline. *Arch Neurol* 59, 1541-1550 (2002).

518. Hemmer, W. & Wallimann, T. Functional aspects of creatine kinase in brain. *Dev.Neurosci.* 15, 249-260 (1993).

519. O'Gorman, E., Beutner, G., Wallimann, T., & Brdiczka, D. Differential effects of creatine depletion on the regulation of enzyme activities and on creatine-stimulated mitochondrial respiration in skeletal muscle, heart, and brain. *Biochim.Biophys.Acta* 1276, 161-170 (1996).

520. Ferrante, R. J. *et al.* Neuroprotective effects of creatine in a transgenic mouse model of Huntington's disease. *J.Neurosci.* 20, 4389-4397 (2000).

521. Klivenyi, P. *et al.* Neuroprotective effects of creatine in a transgenic animal model of amyotrophic lateral sclerosis. *Nat.Med.* 5, 347-350 (1999).

522. Matthews, R. T. *et al.* Neuroprotective effects of creatine and cyclocreatine in animal models of Huntington's disease. *J.Neurosci.* 18, 156-163 (1998).

523. Matthews, R. T. *et al.* Creatine and cyclocreatine attenuate MPTP neurotoxicity. *Exp.Neurol.* 157, 142-149 (1999).

524. Botez, M. I. *et al.* The treatment of spinocerebellar ataxias: facts and hypotheses. *Med.Hypotheses* 51, 381-384 (1998).

525. De Smet, Y. *et al.* Effect of gamma-vinyl GABA in Friedreich's ataxia. *Can.J Neurol Sci.* 9, 171-173 (1982).

526. Filla, A. & Campanella, G. A six-month phosphatidylcholine trial in Friedreich's ataxia. *Can.J Neurol Sci.* 9, 147-150 (1982).

527. Filla, A. *et al.* A double-blind cross-over trial of amantadine hydrochloride in Friedreich's ataxia. *Can.J Neurol Sci.* 20, 52-55 (1993).

528. Livingstone, I. R., Mastaglia, F. L., Pennington, R. J., & Skilbeck, C. Choline chloride in the treatment of cerebellar and spinocerebellar ataxia. *J Neurol Sci.* 50, 161-174 (1981).

529. Melancon, S. B. *et al.* Oral lecithin and linoleic acid in Friedreich's ataxia: II. Clinical results. *Can.J Neurol Sci.* 9, 155-164 (1982).

530. Richards, C. L., Bouchard, J. P., Dumas, F., & Tardif, D. Quantitative evaluation of the effects of acetazolamide in Friedreich's ataxia: a pilot study. *Can.J Neurol Sci.* 11, 554-560 (1984).

531. Rohr, A., Eichler, K., & Hafezi-Moghadam, N. Citalopram, a selective serotonin reuptake inhibitor, improves symptoms of Friedreich's ataxia. *Pharmacopsychiatry* 32, 113-114 (1999).

532. Trouillas, P. Regression of cerebellar syndrome with long-term administration of 5-HTP or the combination 5-HTP-benserazide. *Ital.J Neurol Sci.* 5, 253-266 (1984).

533. Jin, Y., Baquet, A., Florence, A., Crichton, R. R., & Schneider, Y. J. Desferrithiocin and desferrioxamine B. Cellular pharmacology and storage iron mobilization. *Biochem.Pharmacol.* 38, 3233-3240 (1989).

534. Richardson, D. R., Mouralian, C., Ponka, P., & Becker, E. Development of potential iron chelators for the treatment of Friedreich's ataxia: ligands that mobilize mitochondrial iron. *Biochim.Biophys.Acta* 1536, 133-140 (2001).

535. Rustin, P. *et al.* Effect of idebenone on cardiomyopathy in Friedreich's ataxia: a preliminary study. *Lancet* 354, 477-479 (1999).

536. Wilson, R. B., Lynch, D. R., & Fischbeck, K. H. Normal serum iron and ferritin concentrations in patients with Friedreich's ataxia. *Ann.Neurol* 44, 132-134 (1998).

537. Hausse, A. O. *et al.* Idebenone and reduced cardiac hypertrophy in Friedreich's ataxia. *Heart* 87, 346-349 (2002).

538. Schols, L., Vorgerd, M., Schillings, M., Skipka, G., & Zange, J. Idebenone in patients with Friedreich ataxia. *Neurosci.Lett.* 306, 169-172 (2001).

539. Lodi, R. *et al.* Antioxidant treatment improves in vivo cardiac and skeletal muscle bioenergetics in patients with Friedreich's ataxia. *Ann.Neurol.* 49, 590-596 (2001).

540. Beyer, R. E. The function of Coenzyme Q in free radical production and as an antioxidant: a review. *Chemica Scripta* 27, 145-145 (1987).

541. Ernster, L. & Forsmark-Andree, P. Ubiquinol: an endogenous antioxidant in aerobic organisms. *Clin.Investig.* 71, S60-S65 (1993).

542. Crane, F. L., Hatefi, Y., Lester, R. L., Widmer, C. Isolation of a quinone from beef heart mitochondria. *Biochim.Biophys.Acta* 25, 220-221 (1957).

543. Lenaz, G. *et al.* The function of coenzyme Q in mitochondria. *Clin.Investig.* 71, S66-S70 (1993).

544. Folkers, K., Moesgaard, S., & Morita, M. A one year bioavailability study of coenzyme Q10 with 3 months withdrawal period. *Mol.Aspects Med.* 15 Suppl, s281-s285 (1994).

545. Nagai, Y., Yoshida, K., Narumi, S., Tanayama, S., & Nagaoka, A. Brain distribution of idebenone and its effect on local cerebral glucose utilization in rats. *Arch Gerontol.Geriatr.* 8, 257-272 (1989).

546. Zhang, Y., Turunen, M., & Appelkvist, E. L. Restricted uptake of dietary coenzyme Q is in contrast to the unrestricted uptake of alpha-tocopherol into rat organs and cells. *J Nutr.* 126, 2089-2097 (1996).

547. Bostick, R. M. *et al.* Reduced risk of colon cancer with high intake of vitamin E: the Iowa Women's Health Study. *Cancer Res.* 53, 4230-4237 (1993).

548. Shoulson, I. DATATOP: a decade of neuroprotective inquiry. Parkinson Study Group. Deprenyl And Tocopherol Antioxidative Therapy Of Parkinsonism. *Ann.Neurol* 44, S160-S166 (1998).

549. Stephens, N. G. *et al.* Randomised controlled trial of vitamin E in patients with coronary disease: Cambridge Heart Antioxidant Study (CHAOS). *Lancet* 347, 781-786 (1996).

550. Gabsi, S. *et al.* Effect of vitamin E supplementation in patients with ataxia with vitamin E deficiency. *Eur.J Neurol* 8, 477-481 (2001).

551. Kagan, V., Serbinova, E., & Packer, L. Antioxidant effects of ubiquinones in microsomes and mitochondria are mediated by tocopherol recycling. *Biochem.Biophys.Res.Commun.* 169, 851-857 (1990).

552. Stoyanovsky, D. A., Osipov, A. N., Quinn, P. J., & Kagan, V. E. Ubiquinone-dependent recycling of vitamin E radicals by superoxide. *Arch Biochem.Biophys.* 323, 343-351 (1995).

553. Rustin, P., Rotig, A., Munnich, A., & Sidi, D. Heart hypertrophy and function are improved by idebenone in Friedreich's ataxia. *Free Radic.Res.* 36, 467-469 (2002).

554. Hausse, A. O. *et al.* Idebenone and reduced cardiac hypertrophy in Friedreich's ataxia. *Heart* 87, 346-349 (2002).

555. Trouillas, P. *et al.* International Cooperative Ataxia Rating Scale for pharmacological assessment of the cerebellar syndrome. The Ataxia Neuropharmacology Committee of the World Federation of Neurology. *J.Neurol.Sci.* 145, 205-211 (1997).

556. Smith, R. A., Porteous, C. M., Coulter, C. V., & Murphy, M. P. Selective targeting of an antioxidant to mitochondria. *Eur.J Biochem.* 263, 709-716 (1999).

557. Desjardins, P., Frost, E., & Morais, R. Ethidium bromide-induced loss of mitochondrial DNA from primary chicken embryo fibroblasts. *Mol.Cell Biol.* 5, 1163-1169 (1985).

558. Pleasure, S. J. & Lee, V. M. NTera 2 cells: a human cell line which displays characteristics expected of a human committed neuronal progenitor cell. *J Neurosci.Res.* 35, 585-602 (1993).

559. Pleasure, S. J., Page, C., & Lee, V. M. Pure, postmitotic, polarized human neurons derived from NTera 2 cells provide a system for expressing exogenous proteins in terminally differentiated neurons. *J Neurosci.* 12, 1802-1815 (1992).

560. Scott, I. G., Akerman, K. E., Heikkila, J. E., Kaila, K., & Andersson, L. C. Development of a neural phenotype in differentiating ganglion cell-derived human neuroblastoma cells. *J Cell Physiol* 128, 285-292 (1986).

561. Ware, L. M. & Axelrad, A. A. Inherited resistance to N- and B-tropic murine leukemia viruses in vitro: evidence that congenic mouse strains SIM and SIM.R differ at the Fv-1 locus. *Virology* 50, 339-348 (1972).

562. Yasin, R. *et al.* A quantitative technique for growing human adult skeletal muscle in culture starting from mononucleated cells. *J Neurol Sci.* 32, 347-360 (1977).

563. Coore, H. G., Denton, R. M., Martin, B. R., & Randle, P. J. Regulation of adipose tissue pyruvate dehydrogenase by insulin and other hormones. *Biochem.J* 125, 115-127 (1971).

564. Ragan CI, Wilson MT, Darley-Usmar VM, & Lowe PN. Subfractionation of mitochondria, and isolation of the proteins of oxidative phosphorylation in *Mitochondria, a practical approach.* 79-112. IRL Press, (1987).

565. Redfearn ER. Isolation and determination of ubiquinone. *Methods Enzymol.* 10, 381-384 (1967).

566. King, D. L. Preparation of succinate cytochrome c reductase, and the cytochrome b-c1 particle, and the reconstitution of succinate cytochrome c reductase. *Methods Enzymol.* 10, 216-225 (2003).

567. Hatefi, Y. & Stiggall, D. L. Preparation and properties of NADH: cytochrome c oxidoreductase (complex I--III). *Methods Enzymol.* 53, 5-10 (1978).

568. Birch-Machin, M. A. *et al.* Fatal lactic acidosis in infancy with a defect of complex III of the respiratory chain. *Pediatr.Res.* 25, 553-559 (1989).

569. Wharton D & Tzagoloff, A. Cytochrome oxidase from beef heart mitochodria. *Methods Enzymol.* 10, 245-257 (1967).

570. Brazier, J. E. *et al.* Validating the SF-36 health survey questionnaire: new outcome measure for primary care. *BMJ* 305, 160-164 (1992).

571. Jenkinson, C., Coulter, A., & Wright, L. Short form 36 (SF36) health survey questionnaire: normative data for adults of working age. *BMJ* 306, 1437-1440 (1993).

572. Dittmar SS & Graham, G. *Functional assessment and outcome measures for the rehabilitation health professional.* Aspen Publishers inc., Maryland, Gaithesburg (1997).

573. Zilber, N., Inzelberg, R., Kahana, E., & Korczyn, A. D. Natural course of idiopathic torsion dystonia among Jews. *Neuroepidemiology* 13, 195-201 (1994).

574. Montoya, J., Gaines, G. L., & Attardi, G. The pattern of transcription of the human mitochondrial rRNA genes reveals two overlapping transcription units. *Cell* 34, 151-159 (1983).

575. Normanly, J. & Abelson, J. tRNA identity. *Annu.Rev.Biochem.* 58, 1029-1049 (1989).

576. Kaufmann, P. *et al.* Mitochondrial DNA and RNA processing in MELAS. *Ann.Neurol.* 40, 172-180 (1996).

577. Yasukawa, T., Suzuki, T., Ueda, T., Ohta, S., & Watanabe, K. Modification defect at anticodon wobble nucleotide of mitochondrial tRNAs(Leu)(UUR) with pathogenic mutations of mitochondrial myopathy, encephalopathy, lactic acidosis, and stroke-like episodes. *J.Biol.Chem.* 275, 4251-4257 (2000).

578. Flierl, A., Reichmann, H., & Seibel, P. Pathophysiology of the MELAS 3243 transition mutation. *J Biol.Chem.* 272, 27189-27196 (1997).

579. Schon, E. A., Koga, Y., Davidson, M., Moraes, C. T., & King, M. P. The mitochondrial tRNA(Leu)(UUR)) mutation in MELAS: a model for pathogenesis. *Biochim.Biophys.Acta* 1101, 206-209 (1992).

580. Jacobs, H. T. & Holt, I. J. The np 3243 MELAS mutation: damned if you aminoacylate, damned if you don't. *Hum.Mol.Genet.* 9, 463-465 (2000).

581. Janssen, G. M., Maassen, J. A., & van Den Ouweland, J. M. The diabetes-associated 3243 mutation in the mitochondrial tRNA(Leu(UUR)) gene causes severe mitochondrial dysfunction without a strong decrease in protein synthesis rate. *J.Biol.Chem.* 274, 29744-29748 (1999).

582. Borner, G. V. *et al.* Decreased aminoacylation of mutant tRNAs in MELAS but not in MERRF patients. *Hum.Mol.Genet.* 9, 467-475 (2000).

583. Camasamudram, V., Fang, J. K., & Avadhani, N. G. Transcription termination at the mouse mitochondrial H-strand promoter distal site requires an A/T rich sequence motif and sequence specific DNA binding proteins. *Eur.J Biochem.* 270, 1128-1140 (2003).

584. Folley, L. S. & Fox, T. D. Reduced dosage of genes encoding ribosomal protein S18 suppresses a mitochondrial initiation codon mutation in Saccharomyces cerevisiae. *Genetics* 137, 369-379 (1994).

585. Rinaldi, T., Lande, R., Bolotin-Fukuhara, M., & Frontali, L. Additional copies of the mitochondrial Ef-Tu and aspartyl-tRNA synthetase genes can compensate for a mutation affecting the maturation of the mitochondrial tRNAAsp. *Curr.Genet.* 31, 494-496 (1997).

586. Hao, H., Morrison, L. E., & Moraes, C. T. Suppression of a mitochondrial tRNA gene mutation phenotype associated with changes in the nuclear background. *Hum.Mol.Genet.* 8, 1117-1124 (1999).

587. Liolitsa, D. & Hanna, M. G. Models of mitochondrial disease. *Int.Rev.Neurobiol.* 53, 429-466 (2002).

588. Kenyon, L. & Moraes, C. T. Expanding the functional human mitochondrial DNA database by the establishment of primate xenomitochondrial cybrids. *Proc.Natl.Acad.Sci.U.S.A* 94, 9131-9135 (1997).

589. McKenzie, M. & Trounce, I. Expression of Rattus norvegicus mtDNA in Mus musculus cells results in multiple respiratory chain defects. *J.Biol.Chem.* 275, 31514-31519 (2000).

590. Brown, W. M. Polymorphism in mitochondrial DNA of humans as revealed by restriction endonuclease analysis. *Proc.Natl.Acad.Sci.U.S.A* 77, 3605-3609 (1980).

591. Horai, S., Hayasaka, K., Kondo, R., Tsugane, K., & Takahata, N. Recent African origin of modern humans revealed by complete sequences of hominoid mitochondrial DNAs. *Proc.Natl.Acad.Sci.U.S.A* 92, 532-536 (1995).

592. De Francesco, L., Attardi, G., & Croce, C. M. Uniparental propagation of mitochondrial DNA in mouse-human cell hybrids. *Proc.Natl.Acad.Sci.U.S.A* 77, 4079-4083 (1980).

593. Giles, R. E., Stroynowski, I., & Wallace, D. C. Characterization of mitochondrial DNA in chloramphenicol-resistant interspecific hybrids and a cybrid. *Somatic.Cell Genet.* 6, 543-554 (1980).

594. Ziegler, M. L. & Davidson, R. L. Elimination of mitochondrial elements and improved viability in hybrid cells. *Somatic.Cell Genet.* 7, 73-88 (1981).

595. Clayton, D. A., Teplitz, R. L., Nabholz, M., Dovey, H., & Bodmer, W. Mitochondrial DNA of human-mouse cell hybrids. *Nature* 234, 560-562 (1971).

596. Clayton, D. A. Structure and function of the mitochondrial genome. *J.Inherit.Metab Dis.* 15, 439-447 (1992).

597. Brown, W. M., George, M., Jr., & Wilson, A. C. Rapid evolution of animal mitochondrial DNA. *Proc.Natl.Acad.Sci.U.S.A* 76, 1967-1971 (1979).

598. She JX, Bonhomme F, Boursot P, Thaler L, & Catzeflis FM. Molecular phylogenies in the genus *Mus*: Comparative analysis of electrophoretic, scnDNA hybridization, and mtDNA RFLP data. *Biol.J.Linn.Soc.* 41, 83-103 (1990).

599. Solus, J. F. & Eisenstadt, J. M. Retention of mitochondrial DNA species in somatic cell hybrids using antibiotic selection. *Exp.Cell Res.* 151, 299-305 (1984).

600. Attardi, B. & Attardi, G. Fate of mitochondrial DNA in human-mouse somatic cell hybrids (density gradient centrifugation-ethidium bromide-karyotype). *Proc.Natl.Acad.Sci.U.S.A* 69, 129-133 (1972).

601. Graves, J. A. Chromosome segregation from cell hybrids. I. The effect of parent cell ploidy on segregation from mouse-Chinese hamster hybrids. *Can.J.Genet.Cytol.* 26, 557-563 (1984).

602. Shay, J. W. & Ishii, S. Unexpected nonrandom mitochondrial DNA segregation in human cell hybrids. *Anticancer Res.* 10, 279-284 (1990).

603. Moraes, C. T., Kenyon, L., & Hao, H. Mechanisms of human mitochondrial DNA maintenance: the determining role of primary sequence and length over function. *Mol.Biol.Cell* 10, 3345-3356 (1999).

604. Shoubridge, E. A. A debut for mito-mouse. *Nat.Genet.* 26 , 132-134 (2000).

605. Seibel, M. *et al.* Processing of artificial peptide-DNA-conjugates by the mitochondrial intermediate peptidase (MIP). *Biol.Chem.* 380, 961-967 (1999).

606. Kagawa, Y., Inoki, Y., & Endo, H. Gene therapy by mitochondrial transfer. *Adv.Drug Deliv.Rev.* 49, 107-119 (2001).

607. Inoue, K. *et al.* Generation of mice with mitochondrial dysfunction by introducing mouse mtDNA carrying a deletion into zygotes. *Nat.Genet.* 26, 176-181 (2000).

608. Kajander, O. A. *et al.* Human mtDNA sublimons resemble rearranged mitochondrial genoms found in pathological states. *Hum.Mol.Genet.* 9, 2821-2835 (2000).

609. Cummins, J. M. Fertilization and elimination of the paternal mitochondrial genome. *Hum.Reprod.* 15 Suppl 2, 92-101 (2000).

610. Shitara, H. *et al.* Selective and continuous elimination of mitochondria microinjected into mouse eggs from spermatids, but not from liver cells, occurs throughout embryogenesis. *Genetics* 156, 1277-1284 (2000).

611. Marchington, D. R., Barlow, D., & Poulton, J. Transmitochondrial mice carrying resistance to chloramphenicol on mitochondrial DNA: developing the first mouse model of mitochondrial DNA disease. *Nat.Med.* 5, 957-960 (1999).

612. Levy, S. E., Waymire, K. G., Kim, Y. L., MacGregor, G. R., & Wallace, D. C. Transfer of chloramphenicol-resistant mitochondrial DNA into the chimeric mouse. *Transgenic Res.* 8, 137-145 (1999).

613. Sligh, J. E. *et al.* Maternal germ-line transmission of mutant mtDNAs from embryonic stem cell-derived chimeric mice. *Proc.Natl.Acad.Sci.U.S.A* 97, 14461-14466 (2000).

614. Clark, K. M. *et al.* SCID mice containing muscle with human mitochondrial DNA mutations. An animal model for mitochondrial DNA defects. *J.Clin.Invest* 102, 2090-2095 (1998).

615. Parisi, M. A. & Clayton, D. A. Similarity of human mitochondrial transcription factor 1 to high mobility group proteins. *Science* 252, 965-969 (1991).

616. Wang, J. *et al.* Dilated cardiomyopathy and atrioventricular conduction blocks induced by heart-specific inactivation of mitochondrial DNA gene expression. *Nat.Genet.* 21, 133-137 (1999).

617. Silva, J. P. *et al.* Impaired insulin secretion and beta-cell loss in tissue-specific knockout mice with mitochondrial diabetes. *Nat.Genet.* 26, 336-340 (2000).

618. Giulivi, C., Boveris, A., & Cadenas, E. Hydroxyl radical generation during mitochondrial electron transfer and the formation of 8-hydroxydesoxyguanosine in mitochondrial DNA. *Arch Biochem.Biophys.* 316, 909-916 (1995).

619. Li, Y. *et al.* Dilated cardiomyopathy and neonatal lethality in mutant mice lacking manganese superoxide dismutase. *Nat.Genet.* 11, 376-381 (1995).

620. Melov, S. *et al.* A novel neurological phenotype in mice lacking mitochondrial manganese superoxide dismutase. *Nat.Genet.* 18, 159-163 (1998).

621. Esposito, L. A. *et al.* Mitochondrial oxidative stress in mice lacking the glutathione peroxidase-1 gene. *Free Radic.Biol.Med.* 28, 754-766 (2000).

622. Arsenijevic, D. *et al.* Disruption of the uncoupling protein-2 gene in mice reveals a role in immunity and reactive oxygen species production. *Nat.Genet.* 26, 435-439 (2000).

623. Vidal-Puig, A. J. *et al.* Energy metabolism in uncoupling protein 3 gene knockout mice. *J.Biol.Chem.* 275, 16258-16266 (2000).

624. Adachi,J. *et al.* Tempo and mode of mitochondrial DNA evolution in vertebrates at the amino acid sequence level: rapid evolution in warm-blooded vertebrates. *J.Mol.Evol.* 36, 270-281 (1993).

625. Hayashi, J. *et al.* Introduction of disease-related mitochondrial DNA deletions into HeLa cells lacking mitochondrial DNA results in mitochondrial dysfunction. *Proc. Natl. Acad. Sci. U.S.A.* 88, 10614-10618 (1991).

626. Manfredi, G. *et al.* Oligomycin induces a decrease in the cellular content of a pathogenic mutation in the human. *J. Biol. Chem.* 274, 9386-9391 (1999).

627. Holmes, E.C. *et al.* Different rates of substitution may produce different phylogenies of the eutherian mammals. *J. Mol. Evol.* 33,209-215 (1991).

628. Jukes, T.H. A comparison of mitochondrial tRNAs in five vertebrates *J. Mol. Evol.* 40,537-540 (1995).

629. Boulet, L. *et al.* Distribution and threshold expression of the tRNA(Lys) mutation in skeletal muscle of patients with myoclonic epilepsy and ragged-red fibers (MERRF) *Am. J. Hum. Genet.* 51,1187-1200 (1992).

630. Chaline, J., Cardoso, J., & Houssin, D. Organ xenografting between rodents: an evolutionary perspective. *Transpl.Int.* 7, 216-222 (1994).

631. Fahn, S. Systemic therapy of dystonia. *Can.J Neurol Sci.* 14, 528-532 (1987).

632. Fahn, S. Concept and classification of dystonia. *Adv.Neurol* 50, 1-8 (1988).

633. Duffey, P. O., Butler, A. G., Hawthorne, M. R., & Barnes, M. P. The epidemiology of the primary dystonias in the north of England. *Adv.Neurol.* 78, 121-125 (1998).

634. Nutt, J. G., Muenter, M. D., Melton, L. J., III, Aronson, A., & Kurland, L. T. Epidemiology of dystonia in Rochester, Minnesota. *Adv.Neurol.* 50, 361-365 (1988).

635. Marsden, C. D. & Quinn, N. P. The dystonias. *BMJ* 300, 139-144 (1990).

636. A prevalence study of primary dystonia in eight European countries. *J.Neurol.* 247, 787-792 (2000).

637. Duarte, J., Mendoza, A., & Garcia, M. T. [Epidemiology of primary dystonia]. *Rev.Neurol.* 29, 884-886 (1999).

638. Nakashima, K., Kusumi, M., Inoue, Y., & Takahashi, K. Prevalence of focal dystonias in the western area of Tottori Prefecture in Japan. *Mov Disord.* 10, 440-443 (1995).

639. Marsden, C. D., Harrison, M. J., & Bundey, S. Natural history of idiopathic torsion dystonia. *Adv.Neurol.* 14, 177-187 (1976).

640. Janavs, J. L. & Aminoff, M. J. Dystonia and chorea in acquired systemic disorders. *J.Neurol.Neurosurg.Psychiatry* 65, 436-445 (1998).

641. Bhatia, K. P. & Marsden, C. D. The behavioural and motor consequences of focal lesions of the basal ganglia in man. *Brain* 117 (Pt 4), 859-876 (1994).

642. Nemeth, A. H. The genetics of primary dystonias and related disorders. *Brain* 125, 695-721 (2002).

643. Ceballos-Baumann, A. O. & Brooks, D. J. Basal ganglia function and dysfunction revealed by PET activation studies. *Adv.Neurol* 74, 127-139 (1997).

644. Hornykiewicz, O., Kish, S. J., Becker, L. E., Farley, I., & Shannak, K. Brain neurotransmitters in dystonia musculorum deformans. *N.Engl.J.Med.* 315, 347-353 (1986).

645. Hornykiewicz, O., Kish, S. J., Becker, L. E., Farley, I., & Shannak, K. Biochemical evidence for brain neurotransmitter changes in idiopathic torsion dystonia (dystonia musculorum deformans). *Adv.Neurol.* 50, 157-165 (1988).

646. Karbe, H., Holthoff, V. A., Rudolf, J., Herholz, K., & Heiss, W. D. Positron emission tomography demonstrates frontal cortex and basal ganglia hypometabolism in dystonia. *Neurology* 42, 1540-1544 (1992).

647. Marsden, C. D., Obeso, J. A., Zarranz, J. J., & Lang, A. E. The anatomical basis of symptomatic hemidystonia. *Brain* 108 (Pt 2), 463-483 (1985).

648. Ceballos-Baumann, A. O. *et al.* Overactive prefrontal and underactive motor cortical areas in idiopathic dystonia. *Ann.Neurol.* 37, 363-372 (1995).

649. Ikoma, K., Samii, A., Mercuri, B., Wassermann, E. M., & Hallett, M. Abnormal cortical motor excitability in dystonia. *Neurology* 46, 1371-1376 (1996).

650. Bressman, S. B. *et al.* The DYT1 phenotype and guidelines for diagnostic testing. *Neurology* 54, 1746-1752 (2000).

651. Warner, T. T. & Jarman, P. The molecular genetics of the dystonias. *J.Neurol.Neurosurg.Psychiatry* 64, 427-429 (1998).

652. Risch, N. *et al.* Genetic analysis of idiopathic torsion dystonia in Ashkenazi Jews and their recent descent from a small founder population. *Nat.Genet.* 9, 152-159 (1995).

653. Greene, P., Kang, U. J., & Fahn, S. Spread of symptoms in idiopathic torsion dystonia. *Mov Disord.* 10, 143-152 (1995).

654. Ozelius, L. *et al.* Human gene for torsion dystonia located on chromosome 9q32-q34. *Neuron* 2, 1427-1434 (1989).

655. Kramer, P. L. *et al.* The DYT1 gene on 9q34 is responsible for most cases of early limb-onset idiopathic torsion dystonia in non-Jews. *Am.J.Hum.Genet.* 55, 468-475 (1994).

656. Ozelius, L. J. *et al.* The gene (DYT1) for early-onset torsion dystonia encodes a novel protein related to the Clp protease/heat shock family. *Adv.Neurol.* 78, 93-105 (1998).

657. Hewett, J. *et al.* Mutant torsinA, responsible for early-onset torsion dystonia, forms membrane inclusions in cultured neural cells. *Hum.Mol.Genet.* 9, 1403-1413 (2000).

658. Waddy, H. M., Fletcher, N. A., Harding, A. E., & Marsden, C. D. A genetic study of idiopathic focal dystonias. *Ann.Neurol.* 29, 320-324 (1991).

659. Micheli, S., Fernandez-Pardal, M., Quesada, P., Brannan, T., & Obeso, J. A. Variable onset of adult inherited focal dystonia: a problem for genetic studies. *Mov Disord.* 9, 64-68 (1994).

660. Munchau, A. *et al.* A Yorkshire family with adult-onset cranio-cervical primary torsion dystonia. *Mov Disord.* 15, 954-959 (2000).

661. Leube, B. *et al.* Idiopathic torsion dystonia: assignment of a gene to chromosome 18p in a German family with adult onset, autosomal dominant inheritance and purely focal distribution. *Hum.Mol.Genet.* 5, 1673-1677 (1996).

662. Nygaard, T. G. *et al.* Linkage mapping of dopa-responsive dystonia (DRD) to chromosome 14q. *Nat.Genet.* 5, 386-391 (1993).

663. Ichinose, H. *et al.* Hereditary progressive dystonia with marked diurnal fluctuation caused by mutations in the GTP cyclohydrolase I gene. *Nat.Genet.* 8, 236-242 (1994).

664. Steinberger, D. *et al.* High penetrance and pronounced variation in expressivity of GCH1 mutations in five families with dopa-responsive dystonia. *Ann.Neurol.* 43, 634-639 (1998).

665. Ludecke, B., Dworniczak, B., & Bartholome, K. A point mutation in the tyrosine hydroxylase gene associated with Segawa's syndrome. *Hum.Genet.* 95, 123-125 (1995).

666. Zimprich, A. *et al.* Mutations in the gene encoding epsilon-sarcoglycan cause myoclonus-dystonia syndrome. *Nat.Genet.* 29, 66-69 (2001).

667. Klein, C. *et al.* A major locus for myoclonus-dystonia maps to chromosome 7q in eight families. *Am.J.Hum.Genet.* 67, 1314-1319 (2000).

668. Novotny, E. J., Jr. *et al.* Leber's disease and dystonia: a mitochondrial disease. *Neurology* 36, 1053-1060 (1986).

669. Jun, A. S., Trounce, I. A., Brown, M. D., Shoffner, J. M., & Wallace, D. C. Use of transmitochondrial cybrids to assign a complex I defect to the mitochondrial DNA-encoded NADH dehydrogenase subunit 6 gene mutation at nucleotide pair 14459 that causes Leber hereditary optic neuropathy and dystonia. *Mol.Cell Biol.* 16, 771-777 (1996).

670. Jin, H. *et al.* A novel X-linked gene, DDP, shows mutations in families with deafness (DFN-1), dystonia, mental deficiency and blindness. *Nat.Genet.* 14, 177-180 (1996).

671. Hayes, M. W., Ouvrier, R. A., Evans, W., Somerville, E., & Morris, J. G. X-linked Dystonia-Deafness syndrome. *Mov Disord.* 13, 303-308 (1998).

672. Tranebjaerg, L. *et al.* Neuronal cell death in the visual cortex is a prominent feature of the X-linked recessive mitochondrial deafness-dystonia syndrome caused by mutations in the TIMM8a gene. *Ophthalmic Genet.* 22, 207-223 (2001).

673. Tranebjaerg, L. *et al.* A new X linked recessive deafness syndrome with blindness, dystonia, fractures, and mental deficiency is linked to Xq22. *J.Med.Genet.* 32, 257-263 (1995).

674. Tranebjaerg, L., Hamel, B. C., Gabreels, F. J., Renier, W. O., & Van Ghelue, M. A de novo missense mutation in a critical domain of the X-linked DDP gene causes the typical deafness-dystonia-optic atrophy syndrome. *Eur.J.Hum.Genet.* 8, 464-467 (2000).

675. Swerdlow, R. H., Juel, V. C., & Wooten, G. F. Dystonia with and without deafness is caused by TIMM8A mutation. *Adv.Neurol* 94, 147-154 (2004).

676. Paschen, S. A. *et al.* The role of the TIM8-13 complex in the import of Tim23 into mitochondria. *EMBO J.* 19, 6392-6400 (2000).

677. Roesch, K., Curran, S. P., Tranebjaerg, L., & Koehler, C. M. Human deafness dystonia syndrome is caused by a defect in assembly of the DDP1/TIMM8a-TIMM13 complex. *Hum.Mol.Genet.* 11, 477-486 (2002).

678. Palfi, S. *et al.* Delayed onset of progressive dystonia following subacute 3-nitropropionic acid treatment in Cebus apella monkeys. *Mov Disord.* 15, 524-530 (2000).

679. Benecke, R., Strumper, P., & Weiss, H. Electron transfer complex I defect in idiopathic dystonia. *Ann.Neurol.* 32, 683-686 (1992).

680. Schapira, A. H. *et al.* Complex I function in familial and sporadic dystonia. *Ann.Neurol.* 41, 556-559 (1997).

681. Tabrizi, S. J., Cooper, J. M., & Schapira, A. H. Mitochondrial DNA in focal dystonia: a cybrid analysis. *Ann.Neurol.* 44, 258-261 (1998).

682. Dubowitz V. *The muscle bipsy, a practical approach.*Balliere-Tindall,(1985).

683. Schapira, A. H. *et al.* Mitochondria in the etiology and pathogenesis of Parkinson's disease. *Ann.Neurol* 44, S89-S98 (1998).

684. Campanella, G. *et al.* Friedreich's ataxia in the south of Italy: a clinical and biochemical survey of 23 patients. *Can.J.Neurol.Sci.* 7, 351-357 (1980).

685. Hassin-Baer, S., Korczyn, A. D., & Giladi, N. An open trial of amantadine and buspirone for cerebellar ataxia: a disappointment. *J Neural Transm.* 107, 1187-1189 (2000).

686. Pourcher, E. & Barbeau, A. Field testing of an ataxia scoring and staging system. *Can.J Neurol Sci.* 7, 339-344 (1980).

687. Hobart, J. C., Freeman, J. A., & Lamping, D. L. Physician and patient-oriented outcomes in progressive neurological disease: which to measure? *Curr.Opin.Neurol* 9, 441-444 (1996).

688. Freeman, J. A., Hobart, J. C., Langdon, D. W., & Thompson, A. J. Clinical appropriateness: a key factor in outcome measure selection: the 36 item short form health survey in multiple sclerosis. *J Neurol Neurosurg Psychiatry* 68, 150-156 (2000).

689. Lezak, M. D. & O'Brien, K. P. Longitudinal study of emotional, social, and physical changes after traumatic brain injury. *J Learn.Disabil.* 21, 456-463 (1988).

690. Wade, D. T. Measurement in neurological rehabilitation. *Curr.Opin.Neurol Neurosurg* 5, 682-686 (1992).

691. Garratt, A., Schmidt, L., Mackintosh, A., & Fitzpatrick, R. Quality of life measurement: bibliographic study of patient assessed health outcome measures. *BMJ* 324, 1417 (2002).

692. Fischer, J. S. *et al.* Recent developments in the assessment of quality of life in multiple sclerosis (MS). *Mult.Scler.* 5, 251-259 (1999).

693. Jenkinson, C., Fitzpatrick, R., & Peto, V. Health-related quality-of-life measurement in patients with Parkinson's disease. *Pharmacoeconomics.* 15, 157-165 (1999).

694. Solomon, G. D. Evolution of the measurement of quality of life in migraine. *Neurology* 48, S10-S15 (1997).

695. Farcnik, K. & Persyko, M. S. Assessment, measures and approaches to easing caregiver burden in Alzheimer's disease. *Drugs Aging* 19, 203-215 (2002).

696. Jenkinson, C., Fitzpatrick, R., Swash, M., & Peto, V. The ALS Health Profile Study: quality of life of amyotrophic lateral sclerosis patients and carers in Europe. *J Neurol* 247, 835-840 (2000).

697. Delatycki, M. B., Williamson, R., & Forrest, S. M. Friedreich ataxia: an overview. *J.Med.Genet.* 37, 1-8 (2000).

698. Wessel, K., Moschner, C., Wandinger, K. P., Kompf, D., & Heide, W. Oculomotor testing in the differential diagnosis of degenerative ataxic disorders. *Arch Neurol* 55, 949-956 (1998).

699. Spieker, S. *et al.* Fixation instability and oculomotor abnormalities in Friedreich's ataxia. *J Neurol* 242, 517-521 (1995).

700. Arnold, D. L., Taylor, D. J., & Radda, G. K. Investigation of human mitochondrial myopathies by phosphorus magnetic resonance spectroscopy. *Ann.Neurol* 18, 189-196 (1985).

701. Ingwall, J. S. *et al.* The creatine kinase system in normal and diseased human myocardium. *N.Engl.J Med.* 313, 1050-1054 (1985).

702. Radda, G. K. The use of NMR spectroscopy for the understanding of disease. *Science* 233, 640-645 (1986).

703. Lodi, R. *et al.* Cardiac energetics are abnormal in Friedreich ataxia patients in the absence of cardiac dysfunction and hypertrophy: an in vivo 31P magnetic resonance spectroscopy study. *Cardiovasc.Res.* 52, 111-119 (2001).

704. Lodi, R., Kemp, G. J., Iotti, S., Radda, G. K., & Barbiroli, B. Influence of cytosolic pH on in vivo assessment of human muscle mitochondrial respiration by phosphorus magnetic resonance spectroscopy. *MAGMA.* 5, 165-171 (1997).

705. Blamire, A. M., Rajagopalan, B., & Radda, G. K. Measurement of myocardial pH by saturation transfer in man. *Magn Reson.Med.* 41, 198-203 (1999).

706. Lodi, R. *et al.* In vivo skeletal muscle mitochondrial function in Leber's hereditary optic neuropathy assessed by 31P magnetic resonance spectroscopy. *Ann.Neurol* 42, 573-579 (1997).

707. Kemp, G. J. *et al.* Quantitative analysis by 31P magnetic resonance spectroscopy of abnormal mitochondrial oxidation in skeletal muscle during recovery from exercise. *NMR Biomed.* 6, 302-310 (1993).

708. Henry, W. L. *et al.* Report of the American Society of Echocardiography Committee on Nomenclature and Standards in Two-dimensional Echocardiography. *Circulation* 62, 212-217 (1980).

709. Shults, C. W., Beal, M. F., Fontaine, D., Nakano, K., & Haas, R. H. Absorption, tolerability, and effects on mitochondrial activity of oral coenzyme Q10 in parkinsonian patients. *Neurology* 50, 793-795 (1998).

710. Vatassery, G. T., Fahn, S., & Kuskowski, M. A. Alpha tocopherol in CSF of subjects taking high-dose vitamin E in the DATATOP study. Parkinson Study Group. *Neurology* 50, 1900-1902 (1998).

711. El Meziane A, Lehtinen SK, Holt IJ, Jacobs HT. Mitochondrial tRNALeu isoforms in lung carcinoma cybrid cells containing the np 3243 mtDNA mutation. *Hum Mol Genet.* 1998 Dec;7(13):2141-7.

712. Helm M, Florentz C, Chomyn A, Attardi G. Search for differences in post-transcriptional modification patterns of mitochondrial DNA-encoded wild-type and mutant human tRNALys and tRNALeu(UUR). *Nucleis Acids Res.* 1999 27 (3):756-763.

713. Koga Y, Davidson M, Schon EA, King MP. Fine mapping of mitochondrial RNAsderived from the mtDNA region containing a point mutation associated with MELAS. *Nucleic Acids Res.* 1993 Feb 11;21(3):657-662.

714. Dunbar DR, Moonie PA, Jacobs HT, Holt IJ. Different cellular backgrounds confer a marked advantage to either mutant or wild-type mitochondrial genomes. *Proc Natl Acad Sci USA.* 1995 Jul 3;92(14):6562-6.

715. Silvestri G, Rana M, Odoardi F, Modoni A, Paris E, Papacci M, Tonali P, Servidei S. Single-fiber PCR in MELAS (3243) patients: correlations between

intratissue distribution and phenotypic expression of the mtDNA (3243) genotype. *Am J Med Genet.* 2000 Sep18;94(3):201-6.

716. Ozawa M, Nonaka I, Goto Y. Single muscle fiber analysis in patients with 3243 mutation in mitochondrial DNA: comparison with the phenotype and the proportion on mutant genome. *J Neurol Sci* 1998 Aug 14;159(2):170-5.

717. Chinnery PF, Zwijnenburg PJ, Walker M, Howell N, Taylor RW, Lightowlers RN, Bindoff L, Turnbull DM. Nonrandom tissue distribution of mutant mtDNA. *Am J Med Genet.* 1999 Aug 27;85(5):498-501.

718. Bakker A, Barthelemy C, Frachon P, Chateau D, Sternberg D, Mazat JP, Lombes A. Functional mitochondrial heterogeneityin heteroplasmic cells carrying the mitochondrial DNA mutation associated with the MELAS syndrome. *Pediatr Res.* 2000 Aug;48(2):143-50.

719. Laforet P, Ziegler F, Sternberg D, Rouche A, Franchon P, Fardeau M, Eymard B, Lombes A. 'MELAS' (A3243G) mutation of mitochondrial DNA: a study of the relationship between the clinical phenotype in 19 patients and morphological and molecular data. *Rev Neurol.* 2001;156:1136-47.

720. Jacobs HT. Pathological mutations affecting mitochondrial protein synthesis. In Genetics of mitochondrial diseases. Oxford University Press 2003

721. Vergani L, Prescott AR, Holt IJ. Rhabdomyosarcoma rho (0) cells: isolation and characterization of a mitochondrial depleted cell line with 'muscle-like' properties. *Neuromuscul Disord.* 2000 Aug;10(6):454-9.

722. Turner CJ, Granycome C, Hurst R, Pohler E, Juhola MK, Juhola MI, Jacobs HT, Sutherand L, Holt IJ. Systematic segregation to mutant mitochondrial DNA in human NT2 teratocarcinoma cybrids. *Genetics* 2005 Aug;170(4):1879-85.

723. Lehtinen Sk, Hance N, El Meziane A, Juhola MK, Juhola KM, Karhu R, Spelbrink JN, Holt IJ, Jacobs HT. Genotypic stability, segregation and selection in heteroplasmic human cell lines containing np3243 mutant mtDNA. *Genetics* 2000 Jan;154(1):363-80.

724. Lehtinen SK, Spelbrink JN, Jacobs HT. Heteroplasmic segregation associated with trisomy-9 in cultured human cells. *Somat Cell Mol Genet.* 1999 Nov;25(5-6):263-74.

APPENDIX

Homogenisation buffer

Sucrose	0.25M
Tris-HCl	10mM
EDTA-K_2	1mM

pH 7.4

Modified Tyrodes buffer

NaCl	150mM
NaH_2PO_4	0.55mM
$NaHCO_3$	7mM
KCl	2.7mM
Glucose	5.6mM
EDTA-K_2	1mM

pH 7.4

International Co-operative Ataxia Rating Scale (ICARS)

SPEECH

1. FLUENCY

("a mischievous spectacle in Czechoslovakia)
Repeated several times

0 Normal
1 Mild modification of fluency
2 Moderate modification of fluency
3 Considerably slow and dysarthric speech
4 No speech

2. DYSARTHRIA: clarity of speech

0 Normal
1 Suggestion of slurring
2 Definite slurring, most words understandable
3 Severe slurring, speech not understandable
4 No speech

POSTURE + GAIT

*****If patient cannot walk 10 metres even with support of someone score maximum points for 3 and 4 and go to 5**

3. WALKING CAPACITY

10 metre,
single step pivot half turn
1.5 m from wall
support from wall , 1 stick, 2 sticks / stroller, 1 arm, 2 arms
tandem walk distance ?

0 Normal (> 8 sequential steps in tandem).
1 Almost normal but can't tandem walk.(<4 sequential steps in tandem)
2 Walks without support, but clearly abnormal + irregular.
3 Walks without support but considerable staggering, difficulties with half turn.
4 Walking with autonomous support not possible episodic support of wall for 10 m walk
5 Walking only possible with one stick
6 Walking only possible with two special sticks or stroller
7 Walking only with accompanying person (one arm)
8 Walking impossible even with support from accompanying person

Can the patient RUN ☐ JUMP ☐

Time to walk 10 metres ☐ secs

4. GAIT SPEED
If 4 or greater in 3 above - score 4 in this test

0 Normal
1 Slightly reduced
2 Markedly reduced
3 Extremely slow
4 Walking with autonomous support no longer possible

5. SPREAD OF FEET (natural position, eyes open, no support).
Stand in natural position
Distance between medial malleoli

0 Normal <I0 cm
1 10 - 25 cm
2 25 - 35 cm
3 >35 cm
4 standing in natural position no longer possible

6. STANDING EYES OPEN
Ask the patient to proceed from one state to the next to obtain the maximum state possible. For times score best of 3 attempts

Stand in natural position (time) is support needed
Stand with feet together (time)
Stand with feet in tandem position
Stand on one foot (time)

0 Normal, able to stand on one foot for > I0 secs **[TIME_____sec , up to 1 min?]**
1 Able to stand with feet together, and in tandem(> 10 sec), but not 1 above
2 Able to stand with feet together, but not in tandem **[TIME ____sec, up to 1 min?]**
3 Stand in natural position with no or moderate sway **[TIME____ sec, up to 1 min?]**
4 Stand in natural position without support, with considerable sway + corrections
5 Needs strong support of one arm to stand in natural position
6 Unable to stand at all, even with strong support of 2 arms

*****If cannot stand unaided for 30 sec, score max points for 7 + 8 and go to 9**

7. BODY SWAY (feet together, eyes open)
Monitor over 30 secs

0 Normal
1 Slight oscillations (<1cm at level of head)
2 Moderate oscillations (1-10cm at level of head)
3 Severe oscillations (>10 cm at level of head) threatening upright position.
4 Immediate falling

8. BODY SWAY (feet together eyes closed)
Monitor over 30 secs

0 Normal
1 Slight oscillations (<1cm at level of head)
2 Moderate oscillations (1-I0 cm at level of head)
3 Severe oscillations (>I0 cm at level of head) threatening upright position.
4 Immediate falling

9. QUALITY OF SITTING POSITION
Monitor over 30 secs
Thighs together, feet on floor
Hard flat surface, standard chair with a back
Arms folded

0 Normal
1 With mild oscillations of the trunk
2 With moderate oscillations of the trunk and legs (intermittent contact with chair)
3 With severe dysequilibrium, (needs contact with chair back or sides)
4 Impossible (needs continuous contact with chair back and sides)

OCULOMOTOR

10. GAZE EVOKED NYSTAGMUS

0 Normal
1 Transient
2 Persistent but moderate
3 Persistent and severe

11. PURSUIT: saccadic

0 Normal
1 Slightly saccadic
2 Clearly saccadic

12. DYSMETRIA

0 Absent
1 Bilateral clear overshoot or undershoot of the saccade

KINETIC FUNCTIONS

13. FINGER-NOSE (decomposition + dysmetria)

Patient sitting on chair
Begin with hand on knee
3 times each arm

0 No trouble
1 Oscillating movement without decomposition of the movement
2 Segmental movement in 2 phases and / or moderate dysmetria in reaching nose
3 Segmental movement in more than 2 phases and / or considerable dysmetria in reaching nose / finger
4 Dysmetria preventing the patient from reaching the nose

R	L

14. FINGER-NOSE (intention tremor)
The studied tremor is that appearing during the ballistic phase of the movement

0 No trouble
1 Simple swerve of the movement
2 Moderate tremor with estimated amplitude < I0cm
3 Tremor with estimated amplitude between I0 and 40 cm
4 Severe tremor with estimated amplitude >40cm

R	L

15. FINGER - FINGER TEST (action tremor and / or instability)
Sitting
Maintain medially 2 index fingers pointing at each other I cm apart for 10 seconds at level of thorax

0 Normal
1 Mild instability
2 Moderate oscillations of finger with estimated amplitude <10cm
3 Considerable oscillations of finger with estimated amplitude 10-40cm
4 Jerky movements with estimated amplitude >40cm

R	L

16. PRONATION-SUPINATION
Sitting
Raise forearms vertically, elbows and shoulder 90° in front of body
pronate / supinate hand as fast as possible
Each arm assessed separately

0 Normal
1 Slightly irregular and slowed
2 Clearly irregular and slowed but without sway of the elbow
3 Extremely irregular and slowed movement, with sway of the elbow
4 Movement completely disorganised or impossible

R	L

17. KNEE - TIBIA (LOWERING OF HEEL)
Supine, visual control. Raise one leg place heel on knee and slide down anterior tibial surface to foot.
Note Decomposition of movement and intention tremor
3 times each leg

0 Normal
1 Lowering of heel in continuous axis, but the movement is decomposed in several phases, without real jerks, or abnormally slow
2 Lowering jerkily in the axis
3 Lowering jerkily with lateral movements (not falling off leg or outside width of leg)
4 Lowering jerkily with extremely strong lateral movements (falling off leg, failing to hit upper part of foot) or test impossible

R	L

18. ACTION TREMOR OF HEEL ON KNEE
Patient lifts foot onto knee and holds heel on knee for a few seconds

0 No trouble
1 Tremor stopping immediately when the heel reaches the knee
2 Tremor stopping in less than I0 secs after reaching the knee
3 Tremor continuing for more than 10 seconds after reaching the knee
4 Uninterrupted tremor or test impossible

R	L

19. ARCHIMEDES' SPIRAL

Sitting at table, Paper fixed ,Dominant hand
Move from centre to outside in a continuous movement

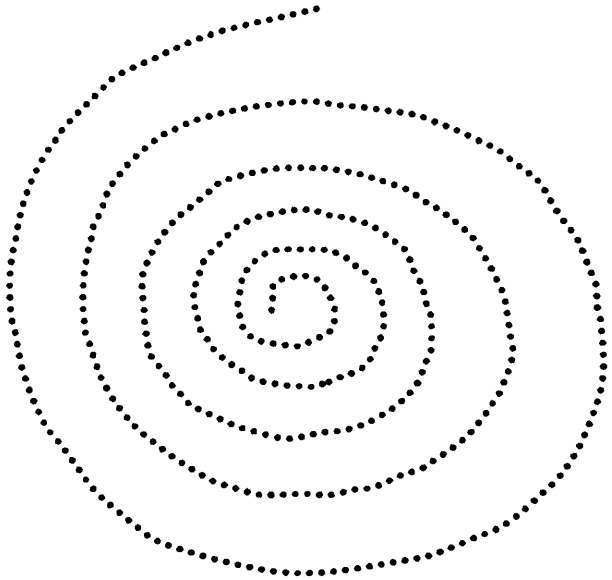

0	on the line
1	deviates from line in places
2	mostly off line but not crossing other neighbouring dotted line
3	crosses lines
4	incomplete and no resemblance to spiral

Non ICARS Clinical Assessments

20. HYPERTONIA

21. HYPOTONIA

22. INCREASED REFLEXES - upper limbs
Biceps, triceps, supinator deep tendon reflexes

0 normal
1 slight
2 very brisk (poly kinetic and/or presence of clonus)

23. INCREASED REFLEXES - lower limbs
Knee and ankle deep tendon reflexes

0 normal
1 slight
2 very brisk (poly kinetic and/or presence of clonus)

24. DECREASED REFLEXES - upper limb

0 normal
1 reduced
2 absent

25. DECREASED REFLEXES - lower limb

0 normal
1 reduced
2 absent

26. PLANTERS

0 normal
1 no response from big toe
2 Babinski

SUMMARY

	Biceps	Triceps	Supinator	Knee	Ankle	Planters
Right						
Left						

0 absent
+/- present with re-inforcement
+ normal
++ brisk but not pathologic
+++ pathologically brisk

27. VIBRATION
At styloid apophysis of ulnar bone
Tibial tuberosity
External malleolus

0 normal
1 decreased at lower limbs
2 decreased at upper and lower limbs
3 absent at lower limbs
4 absent at upper and lower limbs

General Health Questionnaire (GHQ-12)

- We would like to know if you have any medical complaints and how your helath has been, over the pat few weeks
- Please answer all the questions on the following pages simply by marking the answer which you think most nearly applies to you
- Remember that we want to know about present and recent complaints, not about those that you have had in the past

Have you recently:

1. Been able to concentrate on whatever you're doing?	Better than usual	Same as usual	Worse than usual	Much worse than usual
2. Lost much sleep over worry?	Not at all	No more than usual	Rather more than usual	Much more than usual
3. Felt that you are playing a useful part in things?	More so than usual	Same a s usual	Less useful than usual	Much less useful
4. Felt capable of making decisions about things?	More so than usual	Same as usual	Less so than usual	Much less capable
5. Felt constantly under strain	Not at all	No more than usual	Rather more than usual	Much more than usual
6. Felt you could'nt overcome your difficulties?	Not at all	No more than usual	Rather more than usual	Much more than usual
7. Been able to enjoy your normal day-to-day activities?	More so than usual	Same as usual	Less so than usual	Much less than usual
8. Been able to face up to your problems?	More so than usual	Same as usual	Less able than usual	Much less able
9. Been feeling unhappy and depressed?	Not at all	No more than usual	Rather more than usual	Much more than usual
10. Been losing confidence in yourself?	Not at all	No more than usual	Rather more than usual	Much more than usual
11. Been thinking of yourself as a worthless person?	Not at all	No more than usual	Rather more than usual	Much more than usual
12. Been feeling reasonably happy, all things considered?	More so than usual	About same as usual	Less so than usual	Much less than usual

Name: Town of Residence:

1. Are you
   1 female 2 Male

2. What is your age?..... (years) and date of birth? ... day ... month ...year

3. To which ethnic group do you belong?

   1 White
   2 Indian
   3 Black/Caribbean
   4 Pakistani
   5 Black/African
   6 Bangladeshi
   7 Black/Other (please specify)
   8 Chinese
   9 Any other ethnic group (please specify)

4. Roughly when did your Friedreichs ataxia start
5. Roughly when was your Friedreichs ataxia diagnosed
6. Concerning your mobility indoors, please tick the most appropriate box

   ☐ I walk unaided

   ☐ I use a stick or frame, or hold onto furniture or somebody when walking

   ☐ I use a wheelchair

7. Are you? (please circle one)

   1 Single
   2 Separated
   3 Married
   4 Divorced
   5 With a partner
   6 Widowed

8. Do you live? (please circle one):

   1 Alone
   2 With others (e.g. family, friends)

EUROQOL

By placing a tick in one box in each group below, please indicate which statement best indicates your own health state today.

Do not tick more than one box in each group

Mobility

I have no problems walking about	☐
I have some problems walking about	☐
I am confined to bed	☐

Self-Care

I have no problems with self-care	☐
I have some problems washing and dressing myself	☐
I am unable to wash and dress myself	☐

Usual activities (e.g. work, study, housework, family or leisure-activities)

I have no problems with performing my usual activities	☐
I have some problems with performing my usual activities	☐
I am unable to perform my usual activities	☐

Pain/Discomfort

I have no pain or discomfort	☐
I have moderate pain or discomfort	☐
I have extreme pain or discomfort	☐

Anxiety/Depression

I am not anxious or depressed	☐
I am moderately anxious or depressed	☐
I am extremely anxious or depressed	☐

To help people say how Good or bed a health state is, we have drawn a scale (rather like a thermometer) on which the best state you can imagine is marked 100 and the worst you can imagine is marked 0.

We would like you to indicate on this scale how good or bad your own health is today, in your opinion.
Please do this by drawing a line from the box below to whichever point on the scale indicates how good or bad your health state is.

Your own health state today

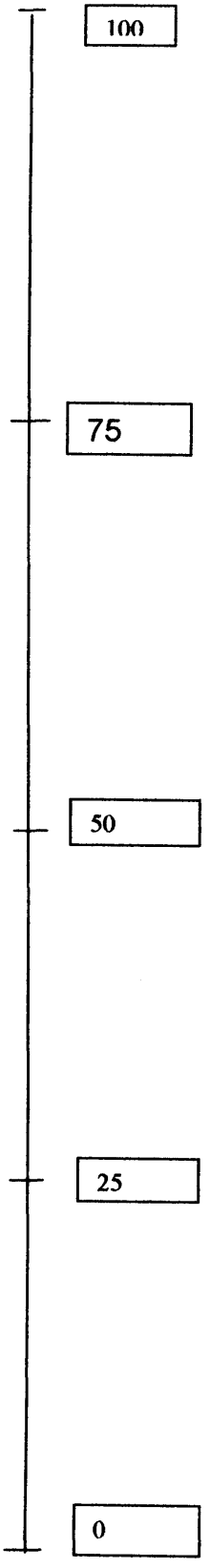

It will help us to understand your answers better if we have a little background data from everyone, as covered in the following questions

1. What is your age in years<

2. Are you
   male
   female

3. Are you
   a current smoker
   an ex-smoker
   a never smoker

4. Which of the following best describes your main activity
   In employment or self-employment
   Retired
   Housework
   Student
   Seeking work
   Other (please specify

5. Did your education continue after the minimum school leaving age?

   Yes
   No

6. Do you have a degree or equivalent professional qualification

   Yes
   No

7. If you know your postcode please write it here

Thank you for taking the time to complete this questionnaire.

POSTAL BARTHEL INDEX

- **These are some questions about your ability to look after yourself**
- **They may not seem to apply to you. Please answer them all.**
- **Tick one box in each section**

1. Bathing... In the bath or shower, do you:

- ☐ manage on your own? *(remember – tick one box only)*
- ☐ need help getting in or out?
- ☐ need other help?
- ☐ never have a bath or shower?
- ☐ need to be washed in bed?

2. Transfer... Do you move from bed to chair:

- ☐ on your own? *(remember – tick one box only)*
- ☐ with a little help from one person?
- ☐ with a lot of help from one or more person?
- ☐ not at all?

3. Dressing... Do you get dressed:

- ☐ without any help? *(remember – tick one box only)*
- ☐ just with help with buttons?
- ☐ with someone helping you most of the time?

4. Feeding... Do you eat food:

- ☐ without any help? *(remember – tick one box only)*
- ☐ with help cutting food or spreading butter?
- ☐ with more help?

5. Mobility... Do you walk indoors:

- ☐ without any help apart from a frame? *(remember – tick one box only)*
- ☐ with one person watching over you?
- ☐ with one person helping you?
- ☐ with more thanone person helping?
- ☐ not at all?
- ☐ or do you use a wheelchair independently (e.g. round corners)?

6. Stairs... Do you climb stairs at home:

- ☐ without any help? *(remember – tick one box only)*
- ☐ with someone carrying your frame?
- ☐ with someone encouraging you?
- ☐ with physical help?
- ☐ not at all?
- ☐ don't have stairs?

7. Toilet use... Do you use the toilet or commode:

- ☐ without any help? *(remember – tick one box only)*
- ☐ with some help but can do something?
- ☐ with quite a lot of help?

8. Grooming... Do you brush your hair and teeth, wash your face and shave:

- ☐ without help? *(remember – tick one box only)*
- ☐ with help?

9. Bladder... Are you incontinent of urine?

- ☐ never *(remember – tick one box only)*
- ☐ less than once a week
- ☐ less than once a day
- ☐ more often
- ☐ or do you have a catheter managed for you?

10. Bowels... Do you soil yourself?

- ☐ never *(remember – tick one box only)*
- ☐ occasional accident
- ☐ all the time
- ☐ or do you need someone to give you an enema?

Please check that you have answered all the questions. Thank you very much for your help.

Medical Outcomes Study Short-Form 36-Item Health Survey (SF-36)

- **This survey asks for your views about your health. This information will help keep track of how well you are able to do your usual activities.**
- **Answer every question by marking the answer as indicated**
- **If you are unsure about how to answer a question please give the best answer you can.**

1. **In general, would you say your health is:**

	Circle one
Excellent	1
Very good	2
Good	3
Fair	4
Poor	5

2. **Compared to one year ago, how would you rate your health in general now?**

	Circle one
Much better now than one year ago	1
Somewhat better now than one year ago	2
About the same as one year ago	3
Somewhat worse now than one year ago	4
Much worse now than one year ago	5

3. **The following questions are about activities you might do during a typical day. Does your health now limit you in these activities? If so, how much?**

ACTIVITIES	Circle one number Yes, limited a lot	Yes, limited a little	No, not limited at all
a) Vigorous activities, such as running, lifting heavy objects, participating in strenuous sports	1	2	3
b) Moderate activities, such as moving a table, pushing a vacuum cleaner, bowling, or playing golf	1	2	3
c) Lifting or carrying groceries	1	2	3
d) climbing several flights of stairs	1	2	3
e)climbing one flight of stairs	1	2	3
f)Bending, Kneeling, stooping	1	2	3
g) Walking more than a mile	1	2	3
h) Walking half a mile	1	2	3
i) Walking one hundred yards	1	2	3
j) Bathing or dressing yourself	1	2	3

4. During the past 4 weeks, have you had any of the fillowing problems with your work or other regular daily activities as a result of your physical helath?

Circle one number on each line	Yes	No
a) Cut down the amount of time you spent on work or other activities	1	2
b) Accomplished less than you would like	1	2
c) Were limited in the kind of work or other activities	1	2
d) Had difficulty performing the work or other activities (for example, it took extra effort)	1	2

5. **During the past four weeks, have you had any of the following problem with your work or other regular daily activities as a result of any emotional problems (such as feeling anxious or depressed)?**

Circle one number on each line	Yes	No
a) Cut down on the amount of time you spent on work or other activities	1	2
b) Accomplished less than you would like	1	2
c) Did'nt do work or activities as carefully as usual	1	2

6. **During the past four weeks, to what extent has youe physical helath or emotional problems interfered with your normal social activitieswith family, friends, neighbours, or groups?**

	Circle one
Not at all	1
Slightly	2
Moderately	3
Quite a bit	4
Extremely	5

7. **How much bodily pain have you had during the past four weeks?**

	Circle one
None	1
Very mild	2
Mild	3
Moderate	4
Severe	5
Very severe	6

8. **During the past 4 weeks, how much did pain interfere with your normal work (including both work outside the home and housework)**

	Circle one
Not at all	1
A little bit	2
Moderately	3
Quite a bit	4
Extremely	5

9. **These questions are about how you feel and how things have been with you during the past four weeks. For each question, please give the one answer that comes closest to the way you have been feeling. How much of the time during the past four weeks –**

Circle one number on each line	All of the time	Most of the time	A good bit of the time	Some of the time	A little of the time	None of the time
a) Did you feel full of life?	1	2	3	4	5	6
b) Have you been a very nervous person?	1	2	3	4	5	6
c) Have you felt so down in the dumps that nothing could cheer you up?	1	2	3	4	5	6
d) Have you felt calm and peaceful?	1	2	3	4	5	6
e) Did you have a lot of energy?	1	2	3	4	5	6
f) Have you felt downhearted and low?	1	2	3	4	5	6
g) Did you feel worn out	1	2	3	4	5	6
h) Have you been a happy person?	1	2	3	4	5	6
i) Did you feel tired?	1	2	3	4	5	6

10. **During the past four weeks, how much of the time has your physical health or emotional problems interfered with your social activities(like visiting with friends, relatives, etc.)?**

	Circle one
All of the time	1
Most of the time	2
Some of the time	3
A little of the time	4
None of the time	5

11. How TRUE or FALSE is each of the following statements for you?

Circle one number on each line	Definitely true	Mostly true	Don't know	Mostly false	Definitely false
a) I seem to get ill a little easier than other people	1	2	3	4	5
b) I am as healthy as anybody I know	1	2	3	4	5
c) I expect my health to get worse	1	2	3	4	5
d) My health is excellent	1	2	3	4	5

Thank you very much for your help.

Mitochondrial Dysfunction and Free Radical Damage in the Huntington R6/2 Transgenic Mouse

S. J. Tabrizi, MRCP,* J. Workman, BSc,* P. E. Hart, MRCP,* L. Mangiarini, PhD,† A. Mahal, PhD,† G. Bates, PhD,† J. M. Cooper, PhD,* and A. H. V. Schapira, MD, DSc*‡

Free Radical Research, 2002 Vol. 36 (4), pp. 461–466

Taylor & Francis
healthsciences

Mitochondrial Dysfunction in Friedreich's Ataxia: From Pathogenesis to Treatment Perspectives

R. LODI[a,*], B. RAJAGOPALAN[b], J.L. BRADLEY[c], D.J. TAYLOR[b], J.G. CRILLEY[b], P.E. HART[c], A.M. BLAMIRE[b], D. MANNERS[b], P. STYLES[b], A.H.V. SCHAPIRA[c,d] and J.M. COOPER[c]

ISSN 1071-5762 print/ISSN 1029-2470 online
DOI: 10.1080/10715760290021324

Neurochemical Research, Vol. 29, No. 3, March 2004 (© 2004), pp. 561–567

Role of Oxidative Damage in Friedreich's Ataxia*

J. L. Bradley,[1] S. Homayoun,[1] P. E. Hart,[1] A. H. V. Schapira,[1] and J. M. Cooper[1,2]

0364-3190/04/0300-0561/0

Movement Disorders
Vol. 20, No. 12, 2005, pp. 1585–1591

International Cooperative Ataxia Rating Scale (ICARS): Appropriate for Studies of Friedreich's Ataxia?

Stefan J. Cano, PhD,[1,2] Jeremy C. Hobart, PhD,[2,3]* Paul E. Hart, MD,[1] L.V. Prasad Korlipara, MD,[1] Anthony H.V. Schapira, MD,[1] and J. Mark Cooper, PhD[1]

ORIGINAL CONTRIBUTION

Antioxidant Treatment of Patients With Friedreich Ataxia

Four-Year Follow-up

Paul E. Hart, MRCP; Raffaele Lodi, MD; Bheeshma Rajagopalan, MD; Jane L. Bradley, PhD; Jenifer G. Crilley, MD; Christopher Turner, MRCP; Andrew M. Blamire, PhD; David Manners, DPhil; Peter Styles, DPhil; Anthony H. V. Schapira, MD, DSc; J. Mark Cooper, PhD